LEABHARLANN CHOLÁISTE NA TRÍONÓIDE, BAILE ÁTHA CLIATH | TRINITY COLLEGE LIBRARY DUBLIN
Ollscoil Átha Cliath | The University of Dublin

Terms and Conditions of Use of Digitised Theses from Trinity College Library Dublin

Copyright statement

All material supplied by Trinity College Library is protected by copyright (under the Copyright and Related Rights Act, 2000 as amended) and other relevant Intellectual Property Rights. By accessing and using a Digitised Thesis from Trinity College Library you acknowledge that all Intellectual Property Rights in any Works supplied are the sole and exclusive property of the copyright and/or other IPR holder. Specific copyright holders may not be explicitly identified. Use of materials from other sources within a thesis should not be construed as a claim over them.

A non-exclusive, non-transferable licence is hereby granted to those using or reproducing, in whole or in part, the material for valid purposes, providing the copyright owners are acknowledged using the normal conventions. Where specific permission to use material is required, this is identified and such permission must be sought from the copyright holder or agency cited.

Liability statement

By using a Digitised Thesis, I accept that Trinity College Dublin bears no legal responsibility for the accuracy, legality or comprehensiveness of materials contained within the thesis, and that Trinity College Dublin accepts no liability for indirect, consequential, or incidental, damages or losses arising from use of the thesis for whatever reason. Information located in a thesis may be subject to specific use constraints, details of which may not be explicitly described. It is the responsibility of potential and actual users to be aware of such constraints and to abide by them. By making use of material from a digitised thesis, you accept these copyright and disclaimer provisions. Where it is brought to the attention of Trinity College Library that there may be a breach of copyright or other restraint, it is the policy to withdraw or take down access to a thesis while the issue is being resolved.

Access Agreement

By using a Digitised Thesis from Trinity College Library you are bound by the following Terms & Conditions. Please read them carefully.

I have read and I understand the following statement: All material supplied via a Digitised Thesis from Trinity College Library is protected by copyright and other intellectual property rights, and duplication or sale of all or part of any of a thesis is not permitted, except that material may be duplicated by you for your research use or for educational purposes in electronic or print form providing the copyright owners are acknowledged using the normal conventions. You must obtain permission for any other use. Electronic or print copies may not be offered, whether for sale or otherwise to anyone. This copy has been supplied on the understanding that it is copyright material and that no quotation from the thesis may be published without proper acknowledgement.

The Influence of Scoliosis and Wheelchair Customisations in Rear Impact

Jennifer C. Walsh

A thesis submitted to the University of Dublin in partial fulfilment of the requirements for the degree of

Doctor in Philosophy

Trinity College Dublin

Supervisor

Dr. Ciaran Simms

Dr. David FitzPatrick

External Examiner **Internal Examiner**

October 2008

TRINITY COLLEGE
10 AUG 2009
LIBRARY DUBLIN
THOSIS
8844

Declaration

declare that I am the sole author of this thesis and that all the work presented in it, unless therwise referenced, is my own. I also declare that this work has not been submitted, in hole or in part, to any other university or college for any degree or other qualification.

I authorise the library of Trinity College Dublin to lend and copy this thesis.

Abstract

Considerable advances in wheelchair occupant frontal impact safety have been achieved, but further research in rear impact is required. Future analysis would benefit from more biofidelic representation of wheelchair occupants, including effects of postural deformities such as scoliosis. In this work, the development and validation of a Madymo baseline wheelchair and occupant model for rear impact analysis is presented. In the model, the BioRID rear impact dummy is seated in a rigid wheelchair without a headrest and subjected to a 10g rear impact pulse. Sled tests of this configuration were performed and used to provide validation data for the numerical model. A comparison of the kinematic model predictions with the high-speed video test data showed a good ability to reproduce the whiplash motion sequence. Furthermore, the model correlates with the experimental time histories with an average difference of 10%. The model is therefore considered a valid representation of a 50th percentile male occupant of a rigid wheelchair in rear impact.

This model was then adapted by implementing scoliosis and the influence of this was evaluated by comparison with the baseline model and based on this work there were the two major findings. Firstly it was found that the altered shape of the scoliotic spine introduces a point loading effect on the occupant. Secondly there is an associated stiffness introduced by the deformed shape of the spine. Both of theses factors lead to increased loading on the thoracic spine with the the largest increase in loading being on the apex of the scoliotic curve. The initial position of the occupant in the wheelchair was also found to have a significant effect on occupant loading, with initial proximity to the wheelchair reducing the loading. This has implications for seating clinics which adapt wheelchairs to suit the needs of the occupant. The wheelchair of the model was altered to represent these adaptations. It was found that the addition of postural supports can reduce the loading on the occupant as they mimic the close initial contact between occupant and the wheelchair. However the stiffness of the surfaces of such supports was also found to have a significant effect with softer foam surfaces bottoming out under crash loading which increases the forces on the occupant.

This work presents the first evaluation of wheelchair occupant loading in a rear impact on the whole spine. It also supports the hypothesis that alterations to the standard representative occupant and wheelchair models alter the loading on the spine in a rear impact.

Abstract

Considerable advances in wheelchair occupant frontal impact safety have been achieved, but further research in rear impact is required. Future analysis would benefit from more biofidelic representation of wheelchair occupants, including effects of postural deformities such as scoliosis. In this work, the development and validation of a Madymo baseline wheelchair and occupant model for rear impact analysis is presented. In the model, the BioRID rear impact dummy is seated in a rigid wheelchair without a headrest and subjected to a 10g rear impact pulse. Sled tests of this configuration were performed and used to provide validation data for the numerical model. A comparison of the kinematic model predictions with the high-speed video test data showed a good ability to reproduce the whiplash motion sequence. Furthermore, the model correlates with the experimental time histories with an average difference of 10%. The model is therefore considered a valid representation of a 50th percentile male occupant of a rigid wheelchair in rear impact.

This model was then adapted by implementing scoliosis and the influence of this was evaluated by comparison with the baseline model and based on this work there were the two major findings. Firstly it was found that the altered shape of the scoliotic spine introduces a point loading effect on the occupant. Secondly there is an associated stiffness introduced by the deformed shape of the spine. Both of theses factors lead to increased loading on the thoracic spine with the the largest increase in loading being on the apex of the scoliotic curve. The initial position of the occupant in the wheelchair was also found to have a significant effect on occupant loading, with initial proximity to the wheelchair reducing the loading. This has implications for seating clinics which adapt wheelchairs to suit the needs of the occupant. The wheelchair of the model was altered to represent these adaptations. It was found that the addition of postural supports can reduce the loading on the occupant as they mimic the close initial contact between occupant and the wheelchair. However the stiffness of the surfaces of such supports was also found to have a significant effect with softer foam surfaces bottoming out under crash loading which increases the forces on the occupant.

This work presents the first evaluation of wheelchair occupant loading in a rear impact on the whole spine. It also supports the hypothesis that alterations to the standard representative occupant and wheelchair models alter the loading on the spine in a rear impact.

Nomenclature

Symbol	Description	Units
NIC	Neck Injury Criterion	$[m^2/s^2]$
a_x^{T1}	Acceleration of first thoracic vertebra in X-direction	$[m/s^2]$
a_x^{Head}	Acceleration of Head in X-direction	$[m/s^2]$
Nkm	Neck injury criterion	$[-]$
$F_x(t)$	Shear force in upper neck	$[N]$
F_{int}	Shear force intercept value	$[N]$
$M_y(t)$	Moment at upper neck	$[Nm]$
M_{int}	Moment intercept value	$[Nm]$
PV	Peak Value	$[-]$
PT	Peak Time	$[ms]$
DUC	Difference Area under the Curve	$[-]$
R	Ratio of peak response of scoliosis model compared to baseline model	$[-]$

Acknowledgments

First of all I would like to thank Dr. Ciaran Simms for his encouragement throughout the course of this work. His guidance along the way has helped me greatly in this work. My co-supervisor, Dr. David FitzPatrick, has also played an important role in this work and I also wish to thank him for his scoliosis expertise. A special thank you also goes to John Tiernan in Enable Ireland who's clinical knowledge has helped to guide this work along its course. This project was possible due to the co-operation of these "three wise men" who each brought their own area of expertise to the project. I hope that this work is an accurate reflection of their valuable input, mentorship and integrity throughout this project.

I would also like to thank The Physically Challenged Irish And American Youth Team who opened my eyes initially to the area of assistive technology and the benefits it brings to people's lives. From working with them I knew I wanted to be involved in helping to further improve this technology. I hope my engineering endeavours will realise a real and lasting improvement to the quality of their lives.

Dr. Behnam Heidari also helped greatly with this work by providing me with the X-ray data I needed to create my models. I would also like to thank Brian Madden for his wheelchair and technical skills in the crash testing. The staff of the seating clinic of Enable Ireland also deserve a mention as they have opened the doors to their clinic to me and have been very supportive of my work. The staff of the Scoliosis Clinic in Crumlin Hospital have done likewise and have been very encouraging throughout. The support staff of MADYMO have also helped greatly. I would also like to thank the technical and administrative staff of the engineering department in Trinity College. Their assistance over the past few years has been invaluable.

I would also like to thank all of my fellow post-grads who have helped me along with this work. All of those from my office have been great support along the way.

Finally a big warm thank you to my family for their love and encouragement. I could never express how thankful I am to them and how much they have helped me along the way. I am forever grateful for all their support all the way through my student days. My friends too have always been very supportive and they deserve a big thanks as well.

Publications and presentations resulting from this study

Walsh, J, Simms, C, FitzPatrick D, Tiernan, J. Spinal Loading on Wheelchair Occupants with Postural Deformities in a Rear Impact during Surface Transport. In Proceedings of International Research Council on Biomechanics of Injury, p339-352, Bern, Switzerland

Walsh, J, Simms, C, FitzPatrick D, Tiernan, J. Investigation into Injury to Wheelchair Occupants with Postural Deformities in a Rear Impact. In Proceedings of European Society of Biomechanics, p37, Lucerne, Switzerland, 2008.

Walsh J, Simms C, FitzPatrick D, Tiernan J. Investigation into spinal injuries to wheelchair occupants with postural deformities in a rear impact. In Proceedings of Bio-Engineering in Ireland, p69, Sligo, Ireland, 2008.

Walsh J, Simms C, Heidari B, FitzPatrick D, Tiernan J. Towards improved crash safety for wheelchair occupants with scoliosis. In Proceedings of the European seating symposium, p21, Dublin, Ireland, 2007

Walsh J, Simms C, FitzPatrick D, Tiernan J. The effect of Lateral curvature of a scoliotic spine on whiplash injury risk. In Proceedings of Bio-Engineering in Ireland, pp 18, Fermanagh, Ireland, 2007

Walsh J, Simms C, FitzPatrick J, Tiernan J. Development of models of scoliosis for crash safety analysis of wheelchair occupants. In Proceedings of World Congress of Biomechanics, p60, Munich, Germany, 2006.

Walsh J, Simms C, FitzPatrick D, Tiernan J. Towards Development of Models of Scoliosis for Crash Safety Analysis of Wheelchair Occupants. In Proceedings of Bio-Engineering in Ireland, pp 136, Galway, Ireland, 2006

Walsh J, Simms C, Tiernan J. Improved Crash Safety for Wheelchair Occupants. In Proceedings of International Conference on Posture and Wheeled Mobility, p137-139 , Exeter, Uk, 2005.

Walsh J, Simms C, Tiernan J. Towards Improved Crash Safety for Wheelchair Occupants. In Proceedings of Bio-Engineering in Ireland p46, Dublin, Ireland 2005.

Contents

Nomenclature **1**

1 Introduction **1**

1.1 Rationale for the Study 1

1.2 Objectives of the Thesis 3

2 Literature Review **5**

2.1 Crash Safety Research 5

2.1.1 Crash Mechanics 5

2.1.2 Testing - Experimental Tests 7

2.1.3 Testing - Numerical Modelling 8

2.2 Rear Impact 9

2.3 Rear Impact Injury Mechanisms 10

2.4 Rear Impact Injury Criteria 11

2.4.1 Neck Injury Criterion - *NIC* 12

2.4.2 *Nkm* 12

2.5 Limitation of Representative Models 14

2.6 Crash Test Dummies 15

2.7 Rear Impact Protection 19

2.7.1 Seatbacks and head restraints 19

2.7.2 Occupant Restraints 20

2.8 Wheelchair transport 20

2.8.1 Wheelchair Impact Research 23

2.8.2 Numerical Modelling for a Frontal Impact 24

2.8.3 Component Testing 27

2.8.4 Rear Impact of Wheelchair and Occupant 30

2.9 Scoliosis 32

2.9.1 The Spine 32

2.10 Mechanical Testing of Vertebrae 36

2.10.1 Compressive Loading 37
2.10.2 Shear Loading 37
2.10.3 Types of Scoliosis 38
2.10.4 Severity of Scoliosis - Cobb Angle 40
2.11 Concluding Remarks 41

3 Methods 1: Physical Testing **45**
3.1 Introduction 45
3.2 Sled Testing 45
3.2.1 Wheelchair Occupant - BioRID II 45
3.2.2 Wheelchair - ISO Surrogate 46
3.3 Test Set-up 47
3.3.1 Wheelchair Tiedown 47
3.3.2 Occupant Restraint 48
3.3.3 Occupant 50
3.3.4 Crash Pulse 51
3.3.5 Outputs 51
3.3.6 Additional Information 52
3.4 Pre and Post Test Checks 53
3.5 Video Output from Sled Test 53
3.6 Variability between tests 54
3.6.1 Impact Pulse 55
3.6.2 Occupant Response 55
3.6.3 Wheelchair and WTORS Response 58

4 Methods 2: Numerical Modelling **59**
4.1 Introduction 59
4.2 Numerical Model 59
4.2.1 Multi-body Modelling 60
4.3 Kinematic Joints 61
4.4 Contacting Surfaces 62
4.5 BioRid II computational model 63
4.5.1 Thoracic and Lumbar Spine 63
4.5.2 Cervical Spine 64

5 Results 1: Validation of Model **66**
5.1 Introduction 66

5.2 BioRID II Occupant 67
5.3 Wheelchair 68
5.3.1 Wheelchair Contacting Surfaces 68
5.3.2 Wheelchair Contact Characteristic 69
5.3.3 Unloading Curve 70
5.3.4 Hysteresis slope 70
5.3.5 Coefficient of friction 71
5.3.6 Pelvis to Seat 72
5.4 Wheels to Sled Contact 73
5.5 Tie downs 74
5.5.1 Tie Down Characteristic 74
5.6 Modelling Parameters 74
5.6.1 Seatback to Occupant Interaction 74
5.6.2 Seat to Pelvis Interaction 75
5.6.3 Feet to Wheelchair Interaction 75
5.6.4 Additional Occupant to Wheelchair Contacts 76
5.6.5 Wheels to Sled Contact 76
5.6.6 Tiedowns 77
5.7 Time Step 77
5.8 Summary 78
5.9 Validation - Visual Comparison 79
5.10 Validation - Time History Comparison 82
5.11 Validation - Quantification of Discrepancy in the Model 86
5.12 Validation - Acceptance of Model 88
5.13 Injury Due to Rear Impact 88

6 Methods 3: Alterations to Occupant Model 90

6.1 Scoliosis Implementation 90
6.2 BioRID II Spine 94
6.3 Screw Axis Method - Application in MADYMO 97
6.4 Screw Axis Method - Validation 97
6.4.1 Positioning of Scoliosis Occupants 99
6.5 Neck Position 107
6.6 Joint Type 108

7 Results 2: Alterations to Occupant **111**

7.1 Kinematics . . . 112

7.1.1 Visual Difference . . . 112

7.1.2 Motion of the Spinal Column . . . 114

7.1.3 Vertebrae - Range of Motion . . . 115

7.2 Summary of Kinematics . . . 118

7.3 Point loading effect . . . 119

7.4 The Scoliotic Spine . . . 122

7.4.1 Quantification of the Effect of Scoliosis . . . 122

7.4.2 Local X Direction Forces . . . 124

7.4.3 Resultant Forces . . . 128

7.5 Summary . . . 128

7.6 Forces on the Vertebral Joints of Crash Simulation . . . 128

7.6.1 Contact Forces on the Spine . . . 129

7.6.2 Cervical . . . 130

7.6.3 Thoracic . . . 132

7.6.4 Lumbar . . . 138

7.7 Injury Criteria . . . 142

7.8 Summary of Investigation into Effect of Scoliosis . . . 147

7.9 Torques on the Body . . . 148

7.9.1 Forces . . . 149

7.9.2 Torques . . . 152

7.10 Summary of Investigation into Torques on the Body . . . 154

7.11 90-90-90 Seated Position . . . 155

7.11.1 Baseline Model . . . 155

7.11.2 Cervical Region . . . 156

7.11.3 Thoracic Region . . . 158

7.11.4 Lumbar Region . . . 159

7.11.5 Injury Criteria . . . 160

7.11.6 Scoliosis Models at 90-90-90 . . . 161

7.11.7 Cervical Region Forces . . . 161

7.11.8 Thoracic Region . . . 163

7.11.9 Lumbar Region . . . 165

7.12 Injury Criteria - *NIC* and *Nkm* . . . 166

7.12.1 Comparison of Baseline and Scoliosis Models at 90-90-90 . . . 166

7.13 Summary of Investigation in Occupants Seated at 90-90-90 169

8 Methods 4: Alterations to Wheelchair Model **171**

8.1 Introduction 171

8.2 Postural Supports 171

8.2.1 Implementation into Model 173

8.3 Cushioning 174

9 Results 3: Alterations to Wheelchair **176**

9.1 Introduction 176

9.2 Postural supports 176

9.3 Postural Supports added to Baseline Model 177

9.3.1 Cervical Region 177

9.3.2 Thoracic Region 178

9.3.3 Lumbar Region 179

9.3.4 Injury Criteria 180

9.4 Postural Supports added to Scoliosis Models 180

9.4.1 Forces on the Cervical Spine 180

9.4.2 Forces on the Thoracic Spine 181

9.4.3 Forces on the Lumbar Spine 182

9.5 Summary 183

9.6 Postural Supports without Cushioning 184

9.6.1 Baseline Model 185

9.7 Injury Criteria 187

9.7.1 Scoliosis Models 188

9.8 Injury Criteria 190

9.9 Summary 190

9.10 Seatback Height 191

9.10.1 Forces on the Spine 192

9.10.2 Injury Criteria 193

9.11 Summary 195

10 Discussion **196**

10.1 Limitations 196

10.2 Baseline Rear Impact 199

10.2.1 Baseline Evaluation - Injury Criteria 199

10.2.2 Baseline Rear Impact Evaluation - Spinal Loading 201

10.3 Scoliosis 202
10.3.1 Loading on the Scoliotic Spine 204
10.4 Injury Criteria 205
10.4.1 *NIC* 206
10.4.2 *Nkm* 206
10.5 More Vulnerable Occupants 207
10.6 Cobb Angle 208
10.7 Clinical Implications 209
10.7.1 Occupant Positioning 209
10.7.2 Wheelchair Seating Surface 210
10.7.3 Seatback Height 211

11 Conclusion **214**

11.1 Conclusion - Idealised Wheelchair and Occupant Interaction 214
11.2 Future Work 215
11.3 Concluding Statements 216
11.3.1 Recommendations for future standards 216

Bibliography **217**

List of Figures

1.1 Wheelchair Tiedown and Occupant Restraint (WTORS) 2

2.1 Family of Crash Test Dummies 7
2.2 Characteristic Reaction of an Occupant in a Rear Impact of 8km/hr 9
2.3 Phases of Whiplash 10
2.4 Thoracic Ramping in a Rear Impact 10
2.5 Neck of dummy 15
2.6 BioRID II 16
2.7 Head and T1 acceleration for BioRID II Compared to Volunteers 17
2.8 Upper Neck Moment and Shear Force for BioRID II Compared to Volunteers 17
2.9 Iliac Crest Displacement for BioRID II Compared to Volunteers 18
2.10 Wheelchair tiedowns 21
2.11 Wheelchair Add-on Components 22
2.12 ISO 10542 surrogate wheelchair 24
2.13 Drophooks 28
2.14 Postural head support 29
2.15 Types of seatback 30
2.16 Regions of the spine 33
2.17 Typical Vertebra 34
2.18 Facet Joints in Regions of Articulating Spine 35
2.19 Intervertebral Disc 36
2.20 Ligaments of the Spine 36
2.21 Scoliosis 39
2.22 Cobb Angle 41
2.23 Validation Process 44

3.1 BioRID II 46
3.2 ISO Surrogate Wheelchair 46
3.3 Front and rear securement point location zones 48

3.4 Position of Upper Anchorage Point 49
3.5 B-Pillar Position 49
3.6 Occupant restraint system 50
3.7 BioRID II Seated in Wheelchair 51
3.8 IIWPG Rear Impact Pulse 51
3.9 Head Stopper 52
3.10 20ms Snapshots of 10g Rear Impact Sled Test 54
3.11 IIWPG Crash Pulse for Tests 1, 2 and 3 55
3.12 X component of acceleration for sled tests 1, 2 and 3 56
3.13 Z component of acceleration for sled tests 1, 2 and 3 56
3.14 Lower Neck Shear and Axial Force and Sagittal Plane Bending Moment Responses for Sled Tests 1, 2 and 3 57
3.15 Upper Neck Shear and Axial Force and Sagittal Plane Bending Moment Responses for Sled Tests 1, 2 and 3 57
3.16 Madymo model of BioRID II wheelchair occupant showing coordinate system and location of armrest crossing point (A) for wheelchair displacement tracking. 58

4.1 Example of how MADYMO Works 61
4.2 BioRID II 64
4.3 BioRID II Muscle and Dampers 65

5.1 BioRID II 67
5.2 Computational Model of Wheelchair 68
5.3 Comparison of Characteristics used for Seatback; Model 1 Allows Excessive Penetration in the Seatback which is not Representative of the Sled Test . . 70
5.4 Comparison of Unloading Characteristic used for Seatback; Model 1 Results in Prolonged Contact with the Seatback which is not Representative of the Sled Test 70
5.5 Comparison of Response for Different Hysteresis Slope 71
5.6 Comparison of Response for Different Coefficient of Friction 72
5.7 Comparison of Characteristic used for Pelvis 73
5.8 Comparison of Unloading Characteristic used for Wheels; Model 1 Shows no Contact with Sled Surface at 140ms Whereas The Wheels in Model 2 are Deformed due to Contact between the Sled and Wheelchair 73
5.9 Tiedowns on Wheelchair in Computational Model 74
5.10 Seatback to Torso Interaction 75

5.11 Pelvis to Seat Characteristic 75
5.12 Severe Scoliosis Occupant in Wheelchair 76
5.13 Wheels to Sled Interaction 77
5.14 Tiedown Characteristic 77
5.15 Comparison of Simulation and Smaller Time Step 78
5.16 Comparison of Simulation and Larger Time Step 78
5.17 Comparison of Sled Test and Numerical Animation 81
5.18 Comparison of ouputs in X direction 83
5.19 Comparison of ouputs in Z direction 83
5.20 Comparison of outputs in upper neck 84
5.21 Comparison of outputs in lower neck 84
5.22 Wheelchair planar motion: angular and linear displacement of sled test and model compared 85
5.23 Injury Criteria 89

6.1 Mild Scoliosis X-rays 91
6.2 Moderate Scoliosis X-rays 91
6.3 Severe Scoliosis X-rays 92
6.4 Vertebra 93
6.5 3D Vector Overlayed on Vertebrae 94
6.6 BioRID II and Coordinate System 95
6.7 Implementation of Scoliosis Orientation 96
6.8 Mild, Moderate and Severe Scoliosis Spine 96
6.9 Validation of Vertebral Rotation 97
6.10 Comparison of Orientations in X-ray and Madymo Model 98
6.11 3D Comparison of Moderate Scoliosis Spine from X-rays and Numerical Model 99
6.12 Mild, Moderate and Severe Scoliosis Model in Wheelchair Seated at -26^o . . 100
6.13 BioRID II as Provided by MADYMO and Orientation by -26^o 100
6.14 Effect of -12^o 101
6.15 BioRID II Stripped to Show Spinal Column which has small Orientations between Vertebrae 101
6.16 Mild, Moderate and Severe Scoliosis Model in Wheelchair Seated at -26^o with -12^o Removed 102
6.17 Mild, Moderate and Severe Scoliosis Model in Wheelchair Seated at Baseline Position and Varied Orientation 102

6.18 Mild, Moderate and Severe Scoliosis Model in Wheelchair Seated at Baseline Position and $+12^o$ Orientation 103
6.19 Mild, Moderate and Severe Scoliosis Model in Wheelchair Seated at Baseline Position and $+12^o$ Orientation and Varied Position 103
6.20 Overlayed Images of Two Seating Postures 105
6.21 Comparison of Forces in Cervical Region of the Spine for Postures 1 and 2 . 106
6.22 Comparison of Forces in Thoracic Region of the Spine for Postures 1 and 2 . 106
6.23 Comparison of Forces in Lumbar Region of the Spine for Postures 1 and 2 . 107
6.24 Neck Correction Methods 107
6.25 Testing of Vertebrae 109
6.26 Cervical Vertebra 109
6.27 Thoracic Vertebra 110
6.28 Lumbar Vertebra 110

7.1 Altered Kinematics of Moderate Case of Scoliosis Compared to Baseline . . . 114
7.2 Spine of Baseline and Moderate Scoliosis in Contact with Seatback from Lateral and Frontal Views 115
7.3 Scoliotic Occupant in Wheelchair 116
7.4 Comparison of Local and Global Range of Motion for each Vertebra of Moderate Scoliosis compared to Baseline 118
7.5 Displaced Local Coordinate System of Vertebra for Moderate Scoliosis 118
7.6 Baseline Model with Kyphosis of Scoliosis Introduced and Original Baseline Occupant 119
7.7 Snapshots of baseline model with Scoliosis Kyphosis 121
7.8 Torso of Baseline and Moderate Scoliosis used for Isolating and Testing the Effect of Scoliosis 122
7.9 R Values of Local X Direction Force for Moderate Torso Compared to Baseline 124
7.10 Local X Direction Force on T10-T9 Joint 125
7.11 Local Y Direction Force for Moderate Torso Compared to Baseline 125
7.12 R Values of Local Z Direction Force for Moderate Scoliosis Torso Compared to Baseline 127
7.13 Comparison of Baseline Spine and Scoliotic Spine 127
7.14 Local Z Direction Force on T5-T6 and L2-L1 Joint 127
7.15 R Values of Resultant Force for Moderate Torso Compared to Baseline . . . 128

7.16 Contact Forces Between Occupant and Seatback for Moderate Scoliosis and Baseline Models 129
7.17 Interaction of Baseline Occupant and Wheelchair 130
7.18 Interaction of Moderate Scoliosis Occupant and Wheelchair 130
7.19 Time History Graphs of X-Direction Force in Cervical Joints for Baseline and Moderate Case of Scoliosis 131
7.20 *R* Values for Moderate Scoliosis in Cervical Region 132
7.21 Time History Graphs of X-Direction Forces in Thoracic Joints for Baseline and Moderate Case of Scoliosis 133
7.22 *R* Values for Moderate Scoliosis in the Thoracic Region 134
7.23 Seatback Height Relative to Torso for Baseline and Scoliosis Models 135
7.24 Postive and Negative Shear Forces on the Spine 136
7.25 Shear Forces on Severe Scoliosis - Effect of Initial Orientation of Upper Throacic Spine 137
7.26 *R* Values in the Thoracic Spine of Moderate Scoliosis and the Corresponding X-ray 138
7.27 Time History Graphs of X-Direction Forces in Lumbar Joints for Baseline and Moderate Case of Scoliosis 139
7.28 *R* Values for Moderate Scoliosis 139
7.29 Side View of Baseline and Mild Scoliosis Lumbar Regions at 40ms Intervals . 140
7.30 Time History Graphs of X-Direction Forces in Lumbar Joints for Baseline and Mild Case of Scoliosis 140
7.31 Lateral X-Ray of Severe Case of Scoliosis 141
7.32 Severe Case of Scoliosis in Wheelchair and Spine Joints of Severe Case of Scoliosis 141
7.33 Forces in Lumbar Spine of Mild Scoliosis 142
7.34 Side View of Baseline and Severe Scoliosis Lumbar Regions at 40ms Intervals 142
7.35 Predicted *NIC* values for Baseline and Moderate Scoliosis 143
7.36 Acceleration of Head and First Thoracic Vertebra in X direction 143
7.37 Predicted *NIC* values for Baseline, Mild, Moderate and Severe Cases of Scoliosis 144
7.38 Comparison of the Acceleration of the Occupant with Moderate and Severe Scoliosis 144
7.39 X-Direction Acceleration of T1 Vertebra in Moderate and Severe Scoliosis . . 145
7.40 Components of *Nkm* for Moderate Scoliosis 146
7.41 *Nkm* for Baseline and Moderate Scoliosis 146

7.42 *Nkm* scores for Baseline, Mild, Moderate and Severe Cases of Scoliosis 146
7.43 Local X Direction Forces on Thoracic Spine 150
7.44 Local Y Direction Forces on Thoracic Spine 151
7.45 Local Z Direction Forces on Thoracic Spine 152
7.46 Local Y Axis Torques on Thoracic Spine 153
7.47 Local X Axis Torques on Lumbar Spine 153
7.48 Local Z Axis Torques on Thoracic Spine 154
7.49 40 millisecond Snapshots from Animation of Baseline Model Positioned at 90 degrees 156
7.50 Contact Forces between Occupant and Seatback for Baseline and Baseline Seated at 90-90-90 156
7.51 Time History Plots of Forces on Cervical Spine of Validated Baseline and Baseline at 90 Degrees 157
7.52 R Values for Cervical Spine of Baseline at 90 Degrees and Validated Baseline 158
7.53 Time History Plots of Forces on Thoracic Spine of Baseline and Baseline at 90 Degrees 159
7.54 R Values for Thoracic Spine of Validated Baseline and Baseline at 90 Degrees 159
7.55 Time History Plots of Forces on Lumbar Spine of Baseline and Baseline at 90 Degrees 160
7.56 R Values for Lumbar Spine of Validated Baseline and Baseline at 90 Degrees 160
7.57 Injury Criteria 161
7.58 Mild, Moderate and Severe Cases of Scoliosis in 90-90-90 Seated Position . . 161
7.59 Forces on Cervical Region for Moderate Scoliosis Case Seated at 26 and 90 Degrees Orientation 162
7.60 R Values for Moderate Scoliosis Case Seated at 26 and 90 Degrees Orientation in Cervical Region 163
7.61 Forces on Thoracic Region for Moderate Scoliosis Case Seated at 26 and 90 Degrees Orientation 164
7.62 R Values for Moderate Scoliosis Case Seated at 26 and 90 Degrees Orientation in Thoracic Region 164
7.63 Forces on Lumbar Region for Moderate Scoliosis Case Seated at 26 and 90 Degrees Orientation 165
7.64 R Values for Moderate Scoliosis Case Seated at 26 and 90 Degrees Orientation in Lumbar Region 166
7.65 Local X Direction Forces for Baseline and Moderate Scoliosis in Cervical Region 167

7.66 Local X Direction Forces for Baseline and Moderate Scoliosis in Thoracic Region 168
7.67 Local X Direction Forces for Baseline and Moderate Scoliosis in Lumbar Region 169

8.1 Molded Seat 172
8.2 Adjustable Back Supports 172
8.3 Link System of Contoured Wheelchair 172
8.4 Deformed Surface of Occupants Torso 173
8.5 Moulded Seating System of Adapted Wheelchair 174
8.6 Headform Tested on Foam 174
8.7 Force Penetration Characteristic of Sunmate Foam 175
8.8 Force Penetration Characteristic of Sunmate Foam on the Surrogate Wheelchair 175

9.1 Forces in the Cervical Region for Baseline Occupant in Original Wheelchair and with Postural Supports 178
9.2 Forces in the Thoracic Region for Baseline Occupant in Original Wheelchair and with Postural Supports 179
9.3 Forces in the Lumbar Region for Baseline Occupant in Original Wheelchair and with Postural Supports 179
9.4 Mild Scoliosis X-rays 180
9.5 Forces on Cervical Region for Moderate Scoliosis Occupant with and without Postural Supports 181
9.6 Forces on Thoracic Region for Moderate Scoliosis Occupant with and without Postural Supports 182
9.7 Forces on Lumbar Region for Moderate Scoliosis Occupant with and without Postural Supports 183
9.8 Force Penetration Characteristic of Wheelchair with Cushioned Surface . . . 184
9.9 Forces on Cervical Region of Spine in Wheelchair without Supports and Wheelchair with Rigid Supports 185
9.10 Forces on Thoracic Region of Spine in Wheelchair without Supports and Wheelchair with Rigid Supports 186
9.11 Forces on Lumbar Region of Spine in Wheelchair without Supports and Wheelchair with Rigid Supports 187
9.12 Mild Scoliosis X-rays 187
9.13 Forces in the Cervical Region of the Spine for Moderate Scoliosis in Standard Wheelchair and in one with Rigid Postural Supports 188

9.14 Forces in the Thoracic Region of the Spine for Moderate Scoliosis in Standard Wheelchair and in one with Rigid Postural Supports 189
9.15 Forces in the Lumbar Region of the Spine for Moderate Scoliosis in Standard Wheelchair and in one with Rigid Postural Supports 190
9.16 Seatback Height Relative to Torso for Baseline and Scoliosis Models 191
9.17 Rear View of Models with Seatback Height at T5-T4 Joint 192
9.18 R Values for Mild, Moderate and Severe Scoliosis in Short Wheelchair Compared to Original 192
9.19 Time History Plots of Force on Mild, Moderate and Severe Scoliosis Models in Normal Wheelchair and Reduced Seatback Height 193
9.20 *NIC* for Mild, Moderate and Severe Case of Scoliosis in Wheelchair with Original Seatback Height and Reduced Height 194
9.21 *Nkm* for Mild, Moderate and Severe Case of Scoliosis in Wheelchair with Original Seatback Height and Reduced Height 194

10.1 Risk Probability of Injuries with Symptoms Lasting More Than One Month Associated with *NIC* and *Nkm* Scores 201
10.2 Displaced Axis of Rotation of Vertebra Compared to Global Coordinate System 202
10.3 Point Loading of Baseline Occupant Compared to Mild Case of Scoliosis . . 203
10.4 Severe Scoliosis Case and Moderate Scoliosis Case 206
10.5 Time History of Forces in Thoracic Spine of Baseline at 90-90-90, Moderate Scoliosis Model with Rigid Supports and Moderate Scoliosis Model with at 90-90-90 210
10.6 Baseline Occupant Seated at Validated 26^o and 90^o Orientation 212
10.7 Forces in Thoracic Region of Spine for Baseline and Baseline in 90-90-90 Seated Posture 212

List of Tables

2.1 Cut off Values for AIS Level 1 Injury using the *Nkm* 13

2.2 BioRID P3 compared to volunteer outputs 18

3.1 Filter Classes Used in Data Post-Processing 52

5.1 Duration of Contact Between Region of the Occupant and Wheelchair 82

5.2 Angle of Rotation of Head Relative to First Thoracic Vertebra (T1) 82

5.3 Comparison of PV, PT and DUC of Computational Model Compared to Sled Tests 87

5.4 Comparison of magnitude and timing of peak displacements of wheelchair with respect to the sled for the physical sled test and the model predictions . 88

5.5 *NIC* and *Nkm* Outputs from Numerical Model 89

6.1 Positioning of Scoliosis Models 104

7.1 Range of Motion of Baseline and Moderate Scoliosis Vertebrae Joints in Local Coordinates 116

7.2 Range of Motion of of Baseline and Moderate Scoliosis Vertebrae Joints in Global Coordinates 117

7.3 Range of Motion of Vertebral Joints of Baseline and Baseline with increased Ksyphosis in Local Coordinates 120

7.4 Range of Motion of Vertebral Joints of Baseline and Baseline with increased kyphosis in Global Coordinates 121

7.5 Range of Motion in Local Coordinate System of Vertebrae Joints of Baseline and Moderate Scoliosis reduced to Torso 123

7.6 Range of Motion in Global Coordinate System of Vertebrae Joints of Baseline and Moderate Scoliosis reduced to Torso 123

7.7 True Peak R Valeus for Mild, Moderate and Severe Case of Scoliosis 134

7.8 *NIC* peak Values for Baseline, Mild, Moderate and Severe Case of Scoliosis . 145

7.9 *Nkm* peak Values for Baseline, Mild, Moderate and Severe Case of Scoliosis . 147

9.1 Injury Criteria for Wheelchair Seatback at Original Height and at Reduced Seatback Height 194

10.1 Injury Criteria for Baseline Model 200

10.2 *NIC* peak Values for Baseline, Mild, Moderate and Severe Case of Scoliosis . 206

10.3 *Nkm* peak Values for Baseline, Mild, Moderate and Severe Case of Scoliosis . 207

Chapter 1

Introduction

1.1 Rationale for the Study

It is estimated that over 700,000 road journeys are undertaken by wheelchair occupants in Ireland each year [1]. This is growing number directly related to the increase and improvements in facilities and access. To transport these individuals in a safe and comfortable manner research has been conducted. This has established requirements for the retention of the wheelchair and occupant which have been used to develop transport safety legislation both in Europe and the U.S. [2] [3] [4] [5]. The improvement of the safety level for these occupants is a continuous process and is a focus of this work.

The research presented in this thesis was conducted in conjunction with Enable Ireland which is a state supported disability services provider. The senior clinical engineer of the seating clinic (John Tiernan) identified the need to address certain areas of concern for surface transport of wheelchair occupants and these are the focus of this work. In particular the disparity in the safety level for wheelchair occupants compared to automotive seated occupants was highlighted. One area of disparity is the use of head restraints which are not required for wheelchair transport however they are required for vehicle seated occupants which are a vital protective device in a rear impact [6]. Secondly the current voluntary standards focus on the frontal impact protection of wheelchairs and occupants, however common adaptations [1] of wheelchairs invalidates their safety certification [2].

Automotive seated passengers have inherent crash protection from the vehicle seat, through occupant restraint systems and crashworthy seat design [7]. However disabled people required to travel in their wheelchairs are not provided with the same safety features. Many of the characteristics which enhance wheelchair mobility, such as ease of collapse, are in conflict with those characteristics which promote safe use of the wheelchair as a vehicle seat. The use of a wheelchair as a vehicle seat introduces a number of new design requirements which the secured wheelchair must be capable of realising. Additionally, loads

are applied quasistatically during normal mobility use whereas crash forces associated with transportation are applied dynamically [8].

The voluntary standards created to provide guidelines for the safe transportation of wheelchair occupants, ISO 7176-19, ISO10542, SAE J2249 and WC-19, require a Wheelchair Tie down and Occupant Restraint System (WTORS),see figure 1.1 to retain the occupant and secure the wheelchair in a 48kph/20g frontal impact [2] [3]. While real world data on the effectiveness of the WTORS is lacking, staged tests and fundamental impact mechanics show that failure to restrain the wheelchair and occupant using a WTORS, results in very high injury potential due to impact with other vehicle structures. Therefore these standards have prevented and reduced injuries to occupants in a frontal impact.

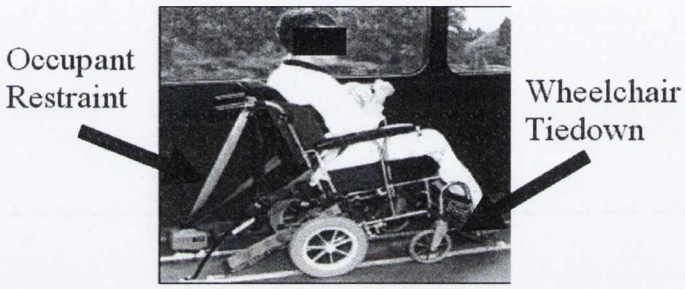


Figure 1.1: Wheelchair Tiedown and Occupant Restraint (WTORS)

However, although rear impact accounts for only 5% of fatalities [7] this crash mode results in 30% of automotive related trauma in the general population. Rear impact also accounts for more long term injury from low severity impact than any other crash mode [7]. While these are not severe injuries there is a large socioeconomic costs associated with them [7]. To further improve the level of safety, afforded to a wheelchair occupant in transit, rear impact must be addressed.

Crash safety standards for passenger vehicles (FMVSS 202, 208) [9] [10] require that injury thresholds assessed using crash test dummies representing the general population are not exceeded. In contrast, existing wheelchair safety standards do not refer to these injury criteria but rather focus on reducing injury by limiting occupant excursion. In a frontal impact, where the occupant is accelerated forward in the seat, these excursion limits help to prevent impact with the interior of the vehicle (secondary impact), and hence reduces the risk of serious injury. This is therefore the primary safety requirement for protecting the occupant in a frontal collision, however to improve the safety level to approach the level of an automotive seat occupant injury criteria need to be addressed.

However as noted by Bertocci et al these injury criteria thresholds are typically based on values at which 25% of the general population would experience serious injury, but the "levels of risk associated with the use of able-body population based injury criteria may actually result in higher risk in the disabled population" [11]. In general gender, age, height and weight all influence the risk of injury [12] and it is therefore likely that a disability and associated postural deformities will also significantly influence the likelihood of injury.

Another area of safety concern highlighted was the addition of postural supports as carried out in seating clinics as in Enable Ireland. These adapted wheelchairs better fit and suit the needs of the user and hold the occupant in a more upright posture and improve their functional range of motion. However, such adaptations invalidate the transport safety certification of the wheelchairs, [2] though the true effect of these alterations in a crash is unknown.

The area of wheelchair and occupant safety research is a relatively new area with a limited number of institutions carrying out investigations. To conduct this work the same methods, proven successful in the area of automotive crash safety, have been used. A combined physical and numerical approach which uses computational models validated against instrumented sled tests is common practice in the automotive industry. Such computational models can then be adapted to determine optimal parameters for safety, and the same can be applied to wheelchair crash safety.

1.2 Objectives of the Thesis

This work aims to evaluate a rear impact involving a wheelchair and occupant in transit. The specific aims of this work are therefore:

- To create and validate a baseline computational model of a rear impact sled test of a wheelchair and occupant. This model can then be used as an analysis tool to investigate the effect of alterations to the model.

- To create and investigate more realistic representations of wheelchair occupants by implementing scoliosis in the computational model.

- To investigate the influence that postural supports have in a rear impact.

- To determine occupant loading levels and predict the likelihood of injury for the baseline and altered models.

Each of these lead to the central hypothesis that alterations to the representative occupant and wheelchair models have a significant effect on occupant loading in a rear impact. This hypothesis will be assessed in this thesis.

Chapter 2

Literature Review

The aim of this literature review is to supply a concise description of the current state of knowledge of wheelchair user crash safety. This will highlight the gaps in the research which provides the impetus for this work. Crash mechanics and current crash safety methodology is explained. The current safety standards and research for wheelchair occupants during surface transport will be assessed and compared with that of automotive seat occupants.

Scoliosis is also introduced as this is a common postural deformity of found among wheelchair users [1] and its influence in a rear impact is investigated as part of this work. The normal configuration and mechanical properties of the spine are also presented.

2.1 Crash Safety Research

Crash safety research has improved the level of safety afforded to vehicle occupants by investigating crashes and applying fundamental mechanics to determine ways to improve safety. These investigations include crash reconstructions, instrumented laboratory crash tests, computational modelling and sub-injurious testing of volunteers. One such improvement that has been developed is occupant retention using restraints, which limits occupant excursion and it is estimated that these restraints have reduced the mortality rate due to a frontal impact by 9,500 lives per anumn in the U.S. [13].

One method of improving crash safety is to use a combined physical and numerical approach which uses data from instrumented crash tests to create and validate computational models. These numerical models can then be used to investigate how altering the parameters of the model effect the results of a crash. The loading associated with these alterations can then be assessed and these findings will lead to improvements in safety devices.

2.1.1 Crash Mechanics

Crash safety of vehicle occupants, whether seated in a vehicle seat or wheelchair, is based on the same fundamental principles of crash mechanics. The basis of crash mechanics is

that when a crash occurs there is a large deceleration of the vehicle and a related effect on the occupant. The displacement of an unbelted occupant is related to the velocity of the vehicle on impact as seen in equation 2.1. In this situation the initial velocity of a free flying occupant is constant, v_o. The acceleration therefore is zero ($a_o = 0$) and the free-flying displacement is $v_o t$ [14].

$$
\begin{aligned}
a' &= a(occupant) - a(vehicle) = 0 - a = -a \\
v' &= v_o - v = -\int_{t_o}^{t} a dt = \int_{t_o}^{t} a' dt \\
x' &= x_o - x = v_o t - x = -\int_{t_o}^{t}\int_{t_o}^{t} a dt dt = \int_{t_o}^{t}\int_{t_o}^{t} a' dt dt = \int_{t_o}^{t} v' dt
\end{aligned}
\tag{2.1}
$$

In this equation a', v' and x' are the acceleration, velocity and displacement of the unbelted occupant with respect to the vehicle. The variables a and v are the vehicle acceleration and velocity measured with respect to the ground. The displacement of the unbelted occupant is directly influenced by the vehicle speed on impact. In a high speed crash a large displacement of the occupant can result in ejection from the vehicle. Seat belts act as a restraining mechanisms on this displacement and reduce the velocity of the occupant relative to the vehicle to prevent secondary impact with the vehicle interior.

However, even if an occupant restraint is used injury can still occur. Rear impacts result in a greater incidence of moderate injury or greater at low severity than any other types of crash types and account for nearly 30% of all crash injuries [7]. These injuries are a result of the loading on the occupant, and will be deatailed in a later section.

In an impact the kinetic energy of the occupant can be related to the work done ($Force \times deformation$) on the body using the energy conservation principal so that:

$$F.d = \frac{1}{2}mv^2 \tag{2.2}$$

$$m.\overline{a}.d = \frac{1}{2}mv^2 \tag{2.3}$$

$$\overline{a} = \frac{1}{2}\frac{v^2}{d} \tag{2.4}$$

Therefore from equation 2.4 the injury level in the neck, which can be determined based on its mean acceleration, $\overline{a}$, [15], is directly related to the impact velocity and deformation of the body. Therefore reducing the velocity results in a reduced level of injury. Such a reduction can be achieved through energy management devices such as head restraints and seatbacks.

2.1.2 Testing - Experimental Tests

Crash testing of vehicles and occupants has lead to improvements in safety over the years [13]. The controlled tests conducted in laboratories provide information to manufacturers for the development and improvement of crash safety devices. Such tests are conducted by impacting the vehicle into a fixed structure at a known velocity. The outputs from such tests can be used to compare with real life cases for crash reconstruction or for comparison to other vehicles tested.

An essential component in the evaluation of impacts is the use of crash test dummies and their ability to replicate the kinematics of the human body. Much research has gone into the development of such representative occupants and a range of dummies have been created and specially designed for use in a given impact direction [16]. This includes a frontal impact, side impact and a rear impact dummy. This research has created representative dummies of different gender, size and age. These factors have been found to have a significant effect on the injury level due to a crash [12], [17]. Therefore a family of crash test dummies has been developed which represents a broad range of healthy occupants, see figure 2.1.

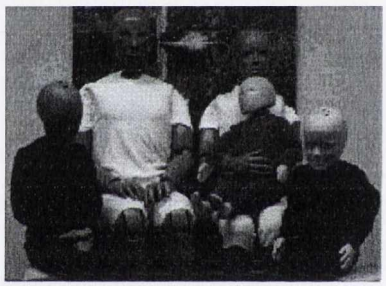


Figure 2.1: Family of Crash Test Dummies
[18]

These models have been created based on the height, weight and kinematic response to represent a given percentile of the general population. These include:

- The 50^{th} percentile male occupant
- The 95^{th} percentile male occupant
- The 5^{th} percentile female occupant
- A range of child occupants representing ages from newborn up to 10 years old

These occupant models have been validated against volunteer tests and cadavers tests [16] [19]. The BioRID II rear impact dummy is presented in detail in a later section of this chapter showing the creation and development of the physical dummy as well

as the validation of the computational model. These occupant models provide a valuable tool for improving rear impact protection as they have been found to match the response of volunteer and cadaver occupants in an impact [20].

2.1.3 Testing - Numerical Modelling

Crash simulation software provides a means to create numerical models of physical tests. There are many advantages associated with this, including reduced costs as destruction of numerous vehicles is not necessary to investigate the effect of varying a given parameter. Also more information on occupant and vehicle response can be obtained as force transducers and accelerometers can be positioned at any location in the numerical model. MADYMO is one such crash simulation software which is commonly used both in the automotive industry and in research facilities [21]. The applications of the software are varied and include vehicle to vehicle impacts, vehicle to pedestrian impacts, bicycling and motorcycling accidents [21] and more recently wheelchair crash safety investigations [22], [23] [24].

MADYMO uses both multi-body and finite element (FE) methods either combined or separately. These methods offer different levels of complexity to the model with the FE being more complex. A third modelling approach is the use of rigid surface elements which are 2D massless shell-type elements. These can be used for modelling more accurate geometric representation as they allow contours and smooth surfaces to be defined for more detailed contact interactions.

In multi body models the equations of motion of the modelled system are integrated using an explicit Euler integration procedure. Multi-bodies with assigned inertia properties are connected by kinematic joints, and idealized shapes (planes, cylinders and ellipsoids). Multi-body models predict kinematics and joint reactions without considering deformations. This limits the output data available from the models as deformations at the point of impact are not evaluated. Therefore injury caused by local stress-strain can not determined. Injury likelihood is assessed based on the forces, velocities and accelerations of the components instead.

Finite element models therefore have the advantage of allowing for more detailed contact interactions such as determining the deformation in a body as well as allowing for the creation of smooth arbitrary surfaces. This modelling approach can predict local deformations based on the stress-strain relationship assigned to the components. However, the detailed information required for such analysis is sometimes lacking and the non-linear, anisotropic, viscoelastic nature of biological tissue makes this process more complex [25]. Therefore,

research is on-going to characterise tissue responses due to impact so that accurate models can be created [25].

2.2 Rear Impact

Rear impact is the focus of this work with the overall aim being to raise the safety level afforded to a wheelchair seated occupant to that of a vehicle seated occupant. Much research has been conducted into the response of a vehicle seated occupant in a rear impact even though these injuries are not usually life threatening they do account for nearly 30% of all injuries due to impact [7]. These injuries are mostly minor however they have a large socio-economic cost associated with them [7]. The broad spectrum of injuries related to a low velocity rear impact are known as whiplash. Though the mechanisms of whiplash are still not fully understood [26], it is commonly believed that the relative motion of the head and neck influence the injury mechanism [27]. The reaction of an occupant in a rear impact has been a focus of rear impact analysis. It has been found that in a typical rear impact the seatback accelerates the torso relative to the head, resulting in neck bending and associated injury [26]. This characteristic reaction is detailed in figure 2.2 of a typical rear impact at 8km/hr in a rigid seat without a headrest.

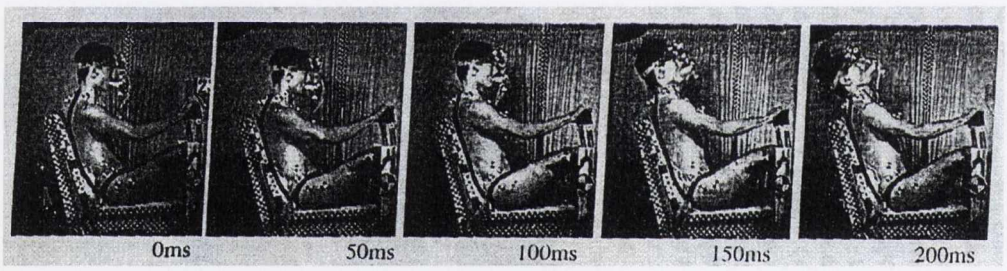


Figure 2.2: Characteristic Reaction of an Occupant in a Rear Impact of 8km/hr [28]

In a rear impact the neck is most likely to be injured [7] [26]. The motion of the neck in a typical rear impact is shown in figure 2.3. This figure shows the neck as it moves from the starting position and the head translates rearwards without any angular motion which creates the s-shaped curve. This phase is know as retraction and during this time the upper cervical spine is undergoing flexion whereas the lower cervical spine is undergoing an extension motion. After this phase the head rotates rearwards and a c-shaped curve is produced and the neck continues to maximum extension. Finally the neck retracts into flexion, known as retroflexion [29], [30], [31]. Each of these phases have an associated risk of injury due to the altered shape of the neck but there is still much unknown about the causes of whiplash [26].

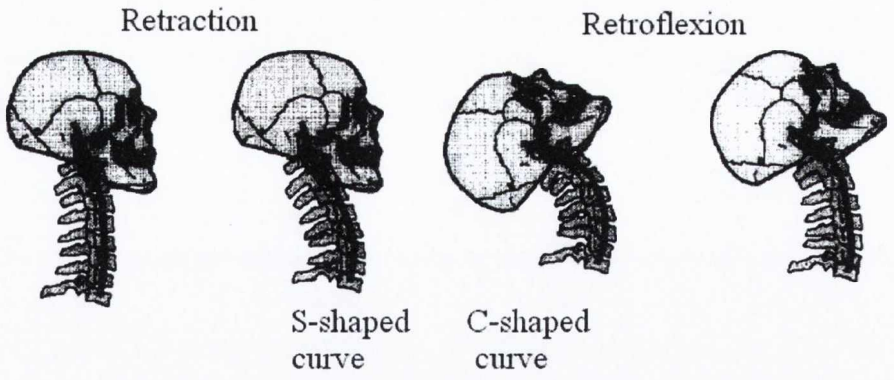


Figure 2.3: Phases of Whiplash [26]

Ono and Kaneoka [28] [29] [30] conducted rear impacts on healthy volunteers and captured the response on high speed video and by x-raying the neck response during the crash, see figure 2.2. Ramping of the thoracic region along the seatback and compressive loading of the cervical region was also apparent. This was also found in other volunteer studies [32]. Figure 2.4 shows the rearwards and upwards motion that is characteristic of the body's response in a rear impact.

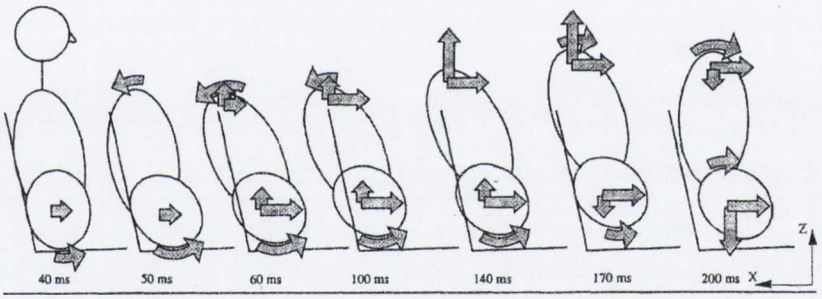


Figure 2.4: Thoracic Ramping in a Rear Impact [32]

2.3 Rear Impact Injury Mechanisms

The neck is the prevalent site of injury in a rear impact. The aetiology of these injuries is unknown [26], however many theories have been proposed. These include hyperextension of the neck [33], changes in the pressure gradient due to initial swift head motion [31], shear loading [27] and relative vertebrae motions [26]. However no one mechanism has been proven to be responsible for all symptoms associated with whiplash. The long term effects of whiplash including pain, numbness and a stiff neck have been found in patients up to 15 years after the accident [34].

It is thought that hyperextension of the neck leads to passive over stretching and tearing of innervated soft tissues surrounding the spine [33]. Damage to the innervated facet joints

which control the motion and interaction of the vertebrae is also thought to cause damage and pain [29]. The individual vertebral joints were also found to rotate to a much larger degree than for the normal range of motion which is a possible source of injury [26] [30].

The lumbar region of the spine has been found to be a site of pain in half of long term patients of whiplash injuries from a 15 year study [34]. Investigations into the effect of rear impact on the lumbar region using cadaver sled tests suggest that straining of the soft tissues surrounding the spinal column may be responsible for such long term pain. A case of vertebral fracture in the thoracic spine has also been found in real life accidents due to a rear impact [17].

However the main area of rear impact injury analysis remains the cervical region. This is due to the large socio-economic cost associated with injuries in this region of the spine [7]. Therefore until the aetiology of neck injury has been determined then injuries in other regions of the spine will remain a secondary consideration.

However this highlights the need to investigate the entire spine and assess the likelihood of injury which may occur due to a rear impact. The addition of postural deformities such as scoliosis may alter the response and so this is an important parameter to investigate. The effect of adapting the wheelchair to fit these occupants with scoliosis may also play a role in the predicted level of injury in the whole spine and this will also be investigated.

2.4 Rear Impact Injury Criteria

Rear impact injury criteria were created and developed using cadavers, volunteers and animal testing to provide a means to assess injury based on the loading in a rear impact. These focus on the force, moment, velocity and acceleration experienced by an occupant in a rear impact and use these to predict injury based on known biomechanical responses of human tissue.

Two examples of common neck injury criteria used for low velocity rear impact analysis are the *NIC* and *Nkm*. While other researchers have assessed a rear impact of paediatric wheelchair occupants using other criteria such as the *HIC* and *Nij* [35], these have been found to not be the most suitable for rear impact evaluation [27]. These injury criteria were developed for frontal impact in which the loading is due to direct impact whereas in a rear impact the body experiences inertial loading. It has also been noted that the axial component that is assessed in the *Nij* criterion are not appropriate for use as the BioRID II dummy cannot adequately represent this type of loading [27]. Due to these limitations only the *NIC* and *Nkm* will be presented in this work.

2.4.1 Neck Injury Criterion - *NIC*

The *NIC* was developed by Bostrom et al in 1996 [15]. This injury criterion is based on the relative velocity and acceleration of the head relative to the first thoracic vertebra (T1), as shown in Equation 2.5.

$$NIC = a_{relative} * 0.2 + v_{relative}^2 \tag{2.5}$$

$$a_{relative} = a_x^{T1} - a_x^{Head}$$

$$v_{relative} = \int (a_{relative}) \text{ [15]}$$

For this criterion injury is predicted for levels above $15m^2/s^2$. This is based on testing conducted on pigs which showed that injury can be due to changes in pressure in the spinal fluid. It was hypothesised that the rapid motion of the neck during a rear impact causes the length of the cervical spinal canal to alter in length while the cross sectional area remains constant. The flexion of the neck, figure 2.3, causes the size of the inner volume to change and since the inner tissues of the neck are considered incompressible the amount of fluid inside the canal must change. This fluid is transported across the tissues at a high velocity which increases the pressure in the fluid by up to 10 times the normal level in pigs. This causes large pressure gradients which it is thought lead to injury in the surrounding tissues. These changes in pressure are greatest at the retraction phase of a rear impact due to pressure increases caused by flexion of the upper neck and a reduction in pressure in the lower region of the neck due to extension, see figure 2.3. Based on this concept a mathematical model of fluid flow in the neck was developed based on porcine specimens. This is presented in equation 2.5. This is based on the relative velocity and acceleration of the head and neck. The 0.2 factor is based on the length of the cervical spinal canal. Further evaluation of the *NIC* using volunteers tested at 11km/hr and cadavers tested at 15km/hr showed that it predicted neck injury risk with acceptable accuracy [36].

2.4.2 *Nkm*

The *Nkm* was designed to investigate the reaction of the neck to a rear impact during its rearward and forward motion. This differs from the *NIC* which assesses injury in the retraction phase only of the crash. The combination of both criteria therefore provides a more detailed analysis of the effect of a rear impact on an occupant. The *Nkm* is based on a linear combination of shear forces and bending moments in the upper neck to calculate injury risk [27], eqution 2.6.

$$N_{km} = \frac{F_x(t)}{F_{int}} + \frac{M_y(t)}{M_{int}} \text{ [27]} \tag{2.6}$$

This criterion is based on the concept that shear forces in a rear impact may injure the facet joints in this region of the neck. The bending moment on this region is thought to amplify the strain on these joints. The level of injury predicted is based on human tolerance levels which cause an injury level 1, as marked on the Abbreviated Injury Scale (AIS) [27]. This scale is used as a marker of injury level with a level of 1 indicating minor injury. For this criterion the cut off values, table 2.1, are based on volunteer tests by Mertz and Patrick in 1993 in which Professor Patrick was the only volunteer in sled tests of 10g [37]. The 88.1Nm flexion bending moment limit is based on the level at which he experienced an immediate onset of pain and prolonged soreness after testing [37].

Load	Value
Extension	47.5Nm
Flexion	88.1Nm
Negative and Positive Shear	845N

Table 2.1: Cut off Values for AIS Level 1 Injury using the *Nkm*

It was found that the direction of the shear loading did not affect the outcome, however the direction of bending did. Therefore the flexion and extension bending moments are different. Using this information the criterion can be divided into four sections, the

- Neck extension anterior - Nea
- Neck extension posterior - Nep
- Neck flexion anterior - Nfa
- Neck flexion posterior - Nfp

The first index represents the bending moment - flexion or extension - and the second indicates the direction of the shear force - anterior or posterior. The sign convention is based on SAEJ211/2 and so positive values indicate the head is moved backwards relative to the uppermost cervical vertebra [38]. For the rear impact investigation presented in this work the Nea is used as it is composed of the predominant loading directions of the neck in a rear impact without a headrest [27]. The equation is given in equation 2.6. Injuries are predicted for *Nkm* scores above 1.

This criterion was validated using 37 sled tests of crash test dummies and the results found that different characteristics of seat design can be quantified with the different *Nkm* values such as the presence or absence of a head restraint [27].

More recent work has evaluated rear impact injuries from real world crashes. A correlation between rear impact injuries with symptoms lasting over a month and the *NIC* and *Nkm* score was found [39]. This adds to the validity of such criteria.

2.5 Limitation of Representative Models

These injury criteria have been developed based on the mechanical responses of cadaver and volunteers. These responses have then been developed to represent the risk of injury. Injury tolerance levels are difficult to determine because of physical differences between humans, as demonstrated in the validation of the BioRID II rear impact dummy [20], [19]. However levels have been determined which are typically based on values at which 25% of the general population would experience serious injury [11]. These values are based on indirect testing methods such as testing with volunteers below the injury level [19], cadaver testing [40] and animal testing [15]. Each of these indirect methods has limitations, but each provides valuable information regarding human tolerance levels.

Human volunteer testing has the obvious shortcoming that testing is done at sub-injurious exposure levels. It also poses problems in that instrumentation measurements must be obtained through non-invasive attachments, volunteers are often young and healthy and may not be representative of the average adult population, and the effects of muscle tension and involuntary reflexes are difficult to ascertain. While cadaver testing is essential to the development of human injury tolerances, it also has a number of inherent variables. Cardiopulmonary pressurization, post mortem tissue degradation, muscle tension, age, gender, anthropometry, and mass are all factors which produce considerable variability in test results. Animal testing also has this problem, along with the need to translate anatomy and injury to human physiology, but has the advantage of providing tolerance information under physiologic conditions. Crash reconstructions provide data on the injury resulting from an impact, however, the forces and accelerations which caused those injuries must be estimated. Computer simulation and testing with crash test dummies provide valuable information, but these methods are dependent upon response information obtained through the other methods [41]. However despite these drawbacks injury criteria provide valuable information on predicted levels of injury due to a crash. These same limitations apply to the development of

crash test dummies, however they have successfully been used in the development of safety devices such as airbags.

2.6 Crash Test Dummies

Anthropomorphic test devices (ATD) or crash test dummies are used in automotive testing to simulate an individual's kinetic response to an impact. These dummies are generally constructed from a steel skeleton and a rubber skin with sensing equipment in place. The head is made of aluminium with rubber flesh also covering this. The neck consists of steel disks separated by rubber to represent the cartilage between the articulating surfaces, as shown in figure 2.5

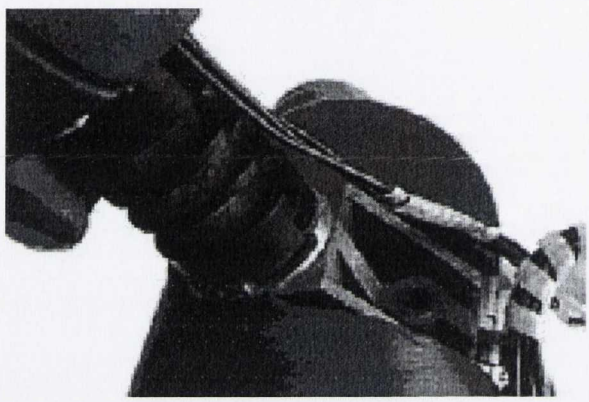


Figure 2.5: Neck of dummy

For rear impact investigations specialised models exist, the BioRID II, see figure 2.6. This has been specially designed and validated against volunteers and cadaver testing to simulate the reaction of the occupant in a rear impact [20], [16], [19]. The dummy is instrumented to provide detailed information about the neck and back which is used to predict the level of injury due to a crash. This 50^{th} percentile dummy is used to represent the size, weight and inertial properties of a 50^{th} percentile adult male.

The BioRID II has been found in comparative tests with volunteers and cadavers to have a more biofidelic neck motion in rear impact than other types of dummy, such as the Hybrid III [19]. The lumbar and thoracic region of the spine has also been validated against cadaver and volunteer tests [19]. The accelerations and displacements of these regions of the spine were found to correspond well in a rear impact. The seated posture that the BioRID II was validated in is 29^{o} orientation in space. Associated with this is the kyphosis of the thoracic region and straight lumbar region of the dummy which produces lordosis of the neck which represents the seated posture of volunteers [19], see figure 3.1.

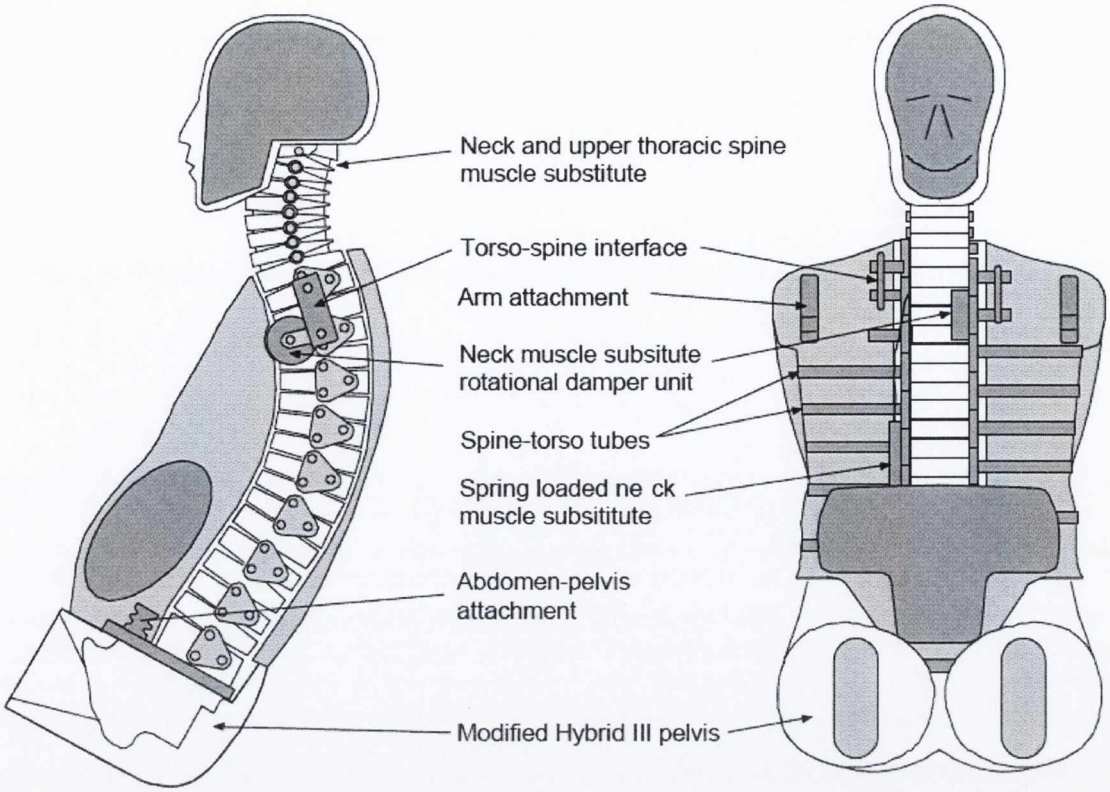


Figure 2.6: BioRID II [42]

The validation process of the BioRID II using data from human volunteers and post mortem human subjects (PMHS) showed good correlation with the response for the dummy. The BioRID P3 (predecessor of the BioRID II) was validated against volunteer tests that were subjected to a 9km/hr rear impact while seated in a rigid seat without a head rest [19]. The time histories comparing the acceleration of the head (angular) and T1, the displacement of the iliac crest in the X and Z directions and the upper neck moment and shear forces for the dummy and volunteers are shown in figures 2.7, 2.8, 2.9. From these graphs the variability in response of the volunteers is evident, due to factors such as weight and height of the volunteers. The BioRID II shows an average of 31% difference between the peak values of the dummy and the average of the volunteer test results, table 2.2. For these results the percentage difference was calculated as the difference between the average of the volunteer response corridors and the corresponding dummy response divided by the average volunteer response as shown in Equation 2.7. The time of occurance of the peak values showed no significant shift in the time of these peaks with an average difference of 16%, see table 2.2. The time shift was determined using equation 2.7 and should not be a large figure so that the peaks represent the same event in the dummy and volunteer tests. Based on these comparisons of the dummy with the volunteers the dummy was determined to be valid to represent an occupant in rear impact at speeds of 7km/hr to 15km/hr [20], [16], [19] [42].

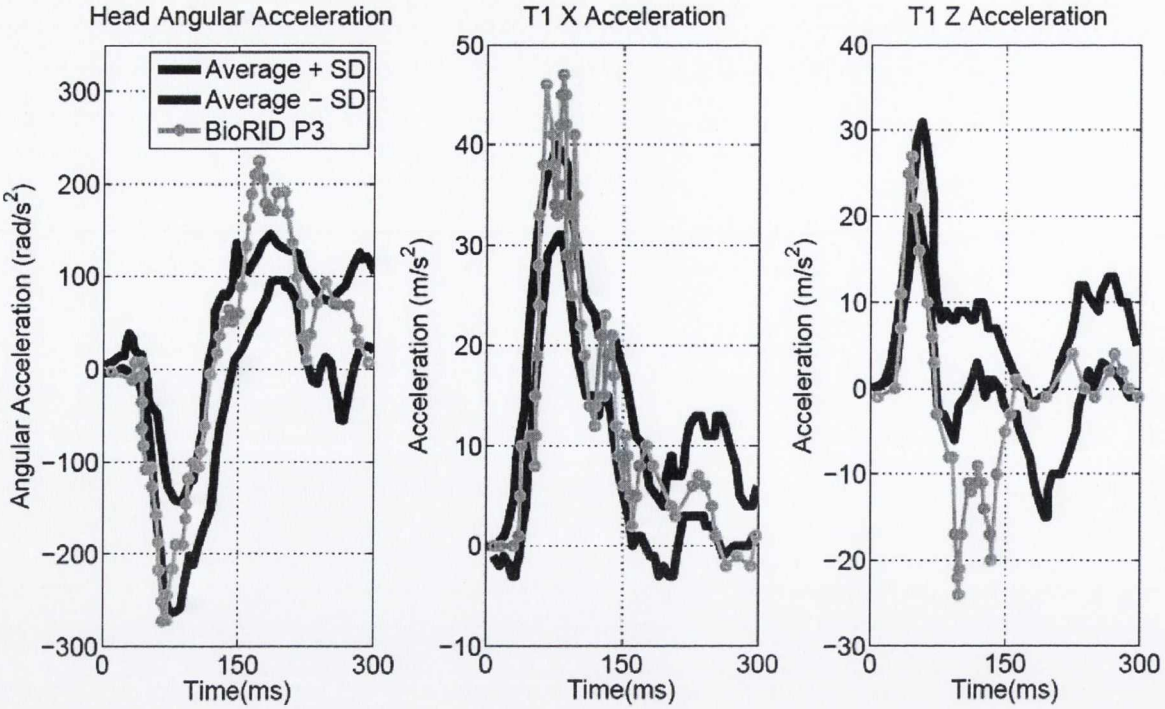


Figure 2.7: Head and T1 acceleration for BioRID II Compared to Volunteers

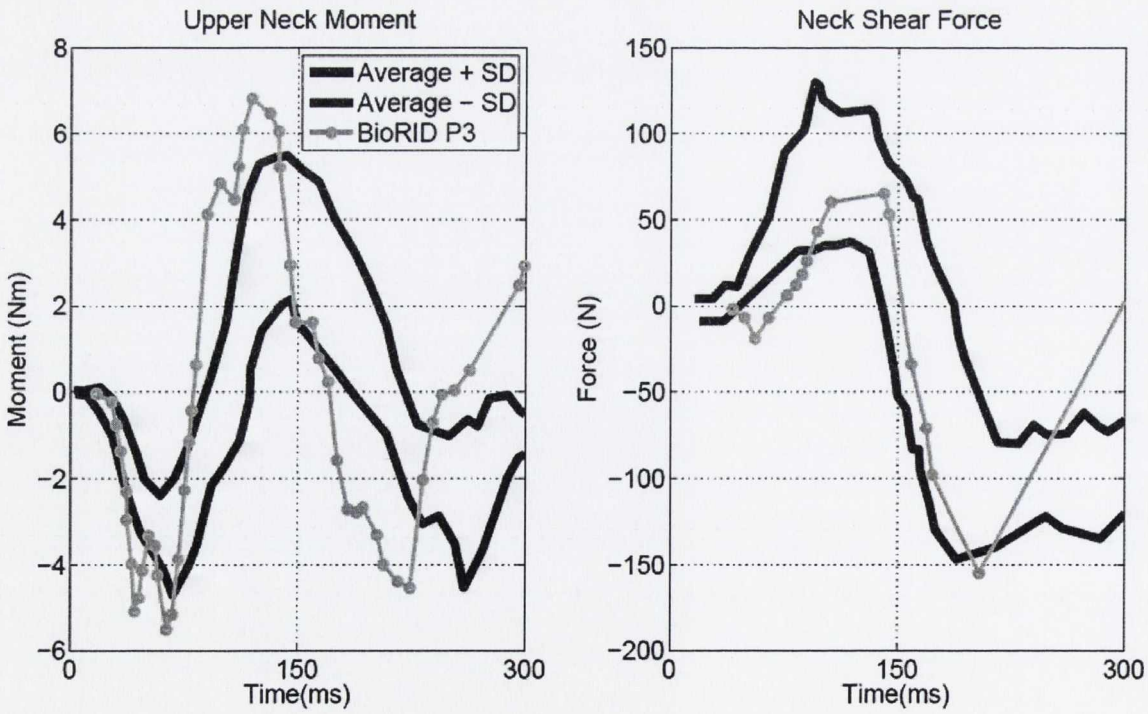


Figure 2.8: Upper Neck Moment and Shear Force for BioRID II Compared to Volunteers

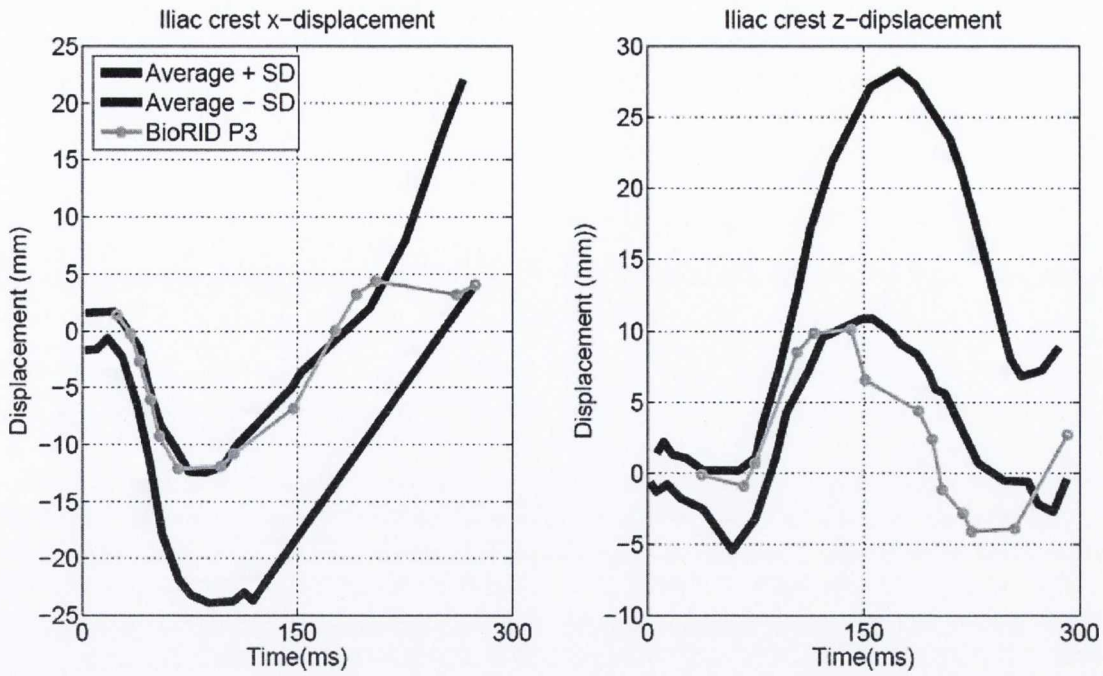


Figure 2.9: Iliac Crest Displacement for BioRID II Compared to Volunteers

$$Percentage\ Difference = \frac{average\ volunteer - dummy}{average\ volunteer} * 100 \tag{2.7}$$

	Value Percentage Difference	Time Percentage Difference
Head Angular Acceleration (rad/s^2)	34	16
T1 X Acceleration (m/s^2)	24	8
T1 Z Acceleration (m/s^2)	2	16
Neck Shear Force, Fx (N)	23	32
Neck Moment, My (Nm)	55	0
Iliac crest Z displacement (mm)	48	14
Iliac crest X dsiplacement (mm)	33	23
Average	31	16

Table 2.2: BioRID P3 compared to volunteer outputs

Validation of Numerical Dummy

For numerical models of a rear impact a MADYMO BioRID II was created [21]. The validation of the response of the numerical model of this crash test dummy was conducted by Chalmers University in Sweden. The model of the occupant uses the frontal impact dummy, the Hybrid III, as its basis. The head, arms and legs of the occupants are the same in both. The main area of change from the Hybrid III is the spine which control the reaction of the head and neck in a rear impact. This region of the spine is, as detailed

previously, the main area of injury in a rear impact and so its reaction in a rear impact is most important to replicate. The validation of the numerical model was based on tests of the components of the BioRID II - spine, head and pelvis - as well as sled testing the whole dummy. Testing of these components consisted of placing the torso and head on a sled which is then impacted at varying speeds to determine its response. The pelvis has also been testing to determine its reaction in a rear impact and to determine the stiffness of this component. The fully instrumented BioRID II was also sled tested using a 10g/16kph rear impact pulse [21]. Based on this work the model is presented by MADYMO as valid for in a rear impact of this velocity.

2.7 Rear Impact Protection

While the aetiology of a rear impact injury is unknown it is generally accepted that relative motion of the head and neck leads to injury. Therefore to prevent this motion head restraints have been developed and are mandatory on vehicle seats. The characteristic of the seatback also plays an important role in rear impact protection due to the loading it passes to the occupant in an impact [7]. In high speed rear crashes the occupant restraints also play an important role as they retain the occupant in the seat after rebounding from the seatback. This restraint therefore reduces the incidence of impact with the interior of the vehicle, known as secondary impact.

These passive safety devices do not require input from the occupant and provide automatic protection by limiting the loading passed to the occupant. This crash energy management is vital to reduce injuries to the vehicle occupant whether they are seated in a wheelchair or vehicle seat. Since the wheelchair occupant would be subjected to the same crash environment as a vehicle seat occupant it is important to provide them with the same level of protection.

The safety devices detailed in this section work to obtain the goal of reducing injury through energy management.

2.7.1 Seatbacks and head restraints

A rear impact results in relative motion of the head and neck which leads to injury [26]. Head restraints are a vital component used to reduce this motion and so prevent injury. However, they must be positioned correctly or else they can increase loading on the occupant [7]. If there is a gap between the occupant's head and the restraint the head is able to rotate so that headrest contacts the top of the skull. In this instance the loads are transmitted down

the vertical axis of the neck resulting in increased injury. However if positioned correctly head rests provide a great deal of protection in a rear impact [7].

The seatback, by providing support, also plays an important role in preventing injury due to a rear impact. Failure of the seat back can lead to increased injury to the cervical spine and ejection of the occupant from the seat which would lead to secondary impact. However, if the seatback is too stiff this can lead to increased loading on the spine as the occupant contacts the seatback. Therefore a balance must be struck to provide the most advantageous level of protection for a vehicle occupant [7].

2.7.2 Occupant Restraints

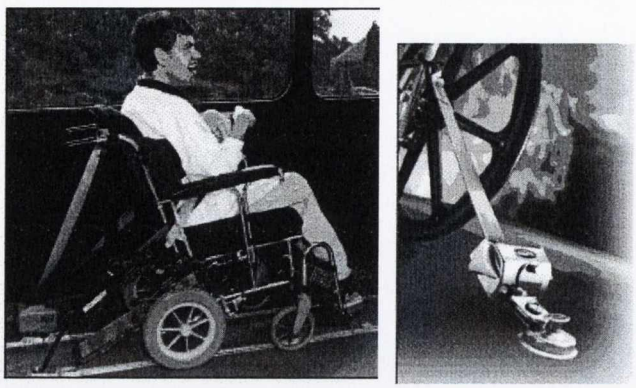
Occupant restraints play a role in crash protection as they work to reduce occupant excursion due to the elastic properties of the seatback. Without being restrained the occupant is free to move within the vehicle which can result in increased occupant injury due to secondary impact. Therefore occupant restraints are used to reduce the velocity of the occupant relative to the vehicle to zero before this secondary impact occurs. Seat belts are most effective in frontal impacts in which the occupant is accelerated forward and the restraints function to restrict this excursion. Occupant restraints play a secondary role in rear impact protection as the rebound of the occupant is controlled by the restraints again with the aim of preventing secondary impact. However to do this the restraints must be properly positioned over the bony structures of the abdominal area as opposed to the soft tissues as this can lead to injury to the internal organs [43] [44].

These principles of rear impact and the level of protection afforded to the occupant apply whether the occupant is seated in a vehicle seat or a wheelchair. However to date the same level of safety has not been achieved as head restraints are not mandatory for transport.

2.8 Wheelchair transport

The current best practice for transporting wheelchairs and occupants is based on frontal impact studies. These have found that the use of a wheelchair tiedown and occupant restraint system (WTORS) is necessary for protection as it secures the wheelchair in place in the event of a crash as well as restraining the occupant. Wheelchair securement is most commonly achieved using webbing attached to the vehicle and the wheelchair using a locking mechanism such as a hook or carabineer. The vehicle floor is specially adapted with tracking, as shown in figure 2.10, which is put in place to provide a locking point. Occupant restraint can also be achieved with a variety of other mechanisms. These are similar in design to restraints

used in vehicle seats using three point belts, however the positioning is different. Common arrangements can be a wheelchair integrated lap and/or shoulder belt. Inertia reels placed on the floor of the vehicle can be used for the lap and/or shoulder restraint, figure 2.10(a). Shoulder belts can also be mounted to the interior of the adapted vehicle.



(a)Track type locking system (b) Single locking point

Figure 2.10: Wheelchair tiedowns

Extensive research using a combined physical and numerical approach has led to the development of voluntary international standards to guide the transport of wheelchairs and occupants. Current wheelchair transport voluntary standards are split into two categories. The first grouping is wheelchair design and structural integrity when subjected to crash loading. The methodology used to test for structural integrity are also laid out in these standards. The voluntary standards are:

- ISO 10542 Technical Systems and Aids for Disabled or Handicapped Persons [2]
- ISO 7176 part 19 Wheeled mobility devices for use in motor vehicles [3]

The second aspect of wheelchair safety that is addressed in the standards is the requirement for the WTORS to be able to retain the occupant and secure the wheelchair in a 48kph/20g frontal impact. The relevant voluntary standards are:

- ANSI/RESNA (American National Standards Institute/Rehabilitation Engineering and Assistive Technology Society or North America) WC-19 Wheelchairs for Use in Motor Vehicles [4]
- SAE Recommended Practice J2249 Wheelchair Tiedown and Occupant Restraint Systems for Use in Motor Vehicles [5]

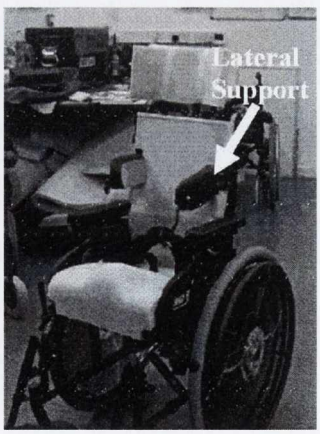
These standards focus on securement of the wheelchair in the vehicle and restraining the occupant within the wheelchair. They do not explicitly refer to occupant injury levels but

instead limit occupant excursion levels to prevent serious injuries due to contact with the vehicle interior. While real world data on the effectiveness of the WTORS is lacking, staged tests and fundamental impact mechanics show that failure to restrain the wheelchair and occupant using a WTORS results in very high injury potential due to impact with other vehicle structures.

Current standards state that occupant restraints are required which have both pelvic and upper torso belts designed to apply forces to the occupant's skeletal regions, they must also function independent of the wheelchair such that the restraint belts anchor to either the vehicle or wheelchair tiedown components so that occupant-restraint loads are not transmitted through the wheelchair. Also to be in accordance with these standards the occupant be positioned within the vehicle in the forward-facing orientation only [2] [3] [2] [4] [5].

Wheelchair transport - Future Safety Level

ISO 16840-4 is under development to bridge a major gap in the area of crashworthiness of wheelchairs and the after market add-ons that are commonly used to improve the fit of the wheelchair to the occupant who may need additional support due to a disability. These add-ons range from supporting structures such as lateral supports, see figure 2.11 to restraints such as a harnesses to keep the occupant seated upright 2.11. The effect of lateral supports in a rear impact may cause extra loading on the occupant and this needs to be evaluated. Harnesses are also a concern in a crash and these devices are currently a safety issue when used in day-to-day activities due to the possibility of the harnesses moving upwards and restricting the occupant's airway [45]. In a crash situation this risk may be further exaggerated.



(a)Lateral Supports



(b) Harness

Figure 2.11: Wheelchair Add-on Components

Research has previously been conducted into the performance of add-on components in isolation under impact loading and these tests have found that the components do not always

pass (the details of the testing is provided later in this chapter). However the results have found that the attachment hardware used as the bridging link between the wheelchair and the add-on components fail at 50% of the applied loading of 10kN. This would lead to the structures supporting the occupant - the seat and seatback - to fail. The seat and seatback are commonly adapted and replaced, as in figure 2.11, with only the frame of the wheelchair remaining of the original crash tested structure. The seatback's structure and integrity has special relevance for rear impact safety as they pass the loading to the occupant as well as provide the support required. Head restraints are also essential for rear impact protection, however previous research has found that these components failed under the predicted levels of loading associated with rear impact. These types of hardware failures in a rear impact could lead to increased loading as well as increased risk of injury. The introduction of voluntary standards can improve the safety level of these components through improved design, as it has for frontal impact.

2.8.1 Wheelchair Impact Research

The requirements for current standards have been based on a combined approach of physical testing and numerical simulation, this is common practice in the automotive industry and has been adapted for use in wheelchair occupant crash safety [46], [47], [48]. This method has proven particularly relevant as the securement of the wheelchair using tie downs imparts loading not normally associated with wheelchair use and these forces have been determined using this approach. The added forces include dynamic loading due to the tiedowns which are attached to the wheelchair, and the impingement of the occupant onto the wheelchair due to the occupant restraints. These extra loads can vary depending on the design of the wheelchair and the position of the tiedown anchors on the wheelchair frame [46]. However by investigating and understanding these, wheelchairs can be designed to be able to withstand them. The variability in wheelchair design can also be accounted for and the results from testing can help to develop wheelchairs that are safe for transportation of the occupant [23].

Surrogate Wheelchair

Due to the large variation of wheelchair types that are available which range in size, shape, weight and whether they are powered or manual a surrogate wheelchair was developed. This surrogate has the larger size and mass (85kg) of a powered wheelchair to increase the loading experienced on the components during the crash. The mass of the wheelchair was used as a representative case, however the prevalence of larger powered wheelchairs which weigh up

to 120kgs has become more common [1]. The design of the wheelchair is an annex to the ISO10542 standard, see figure 3.2.

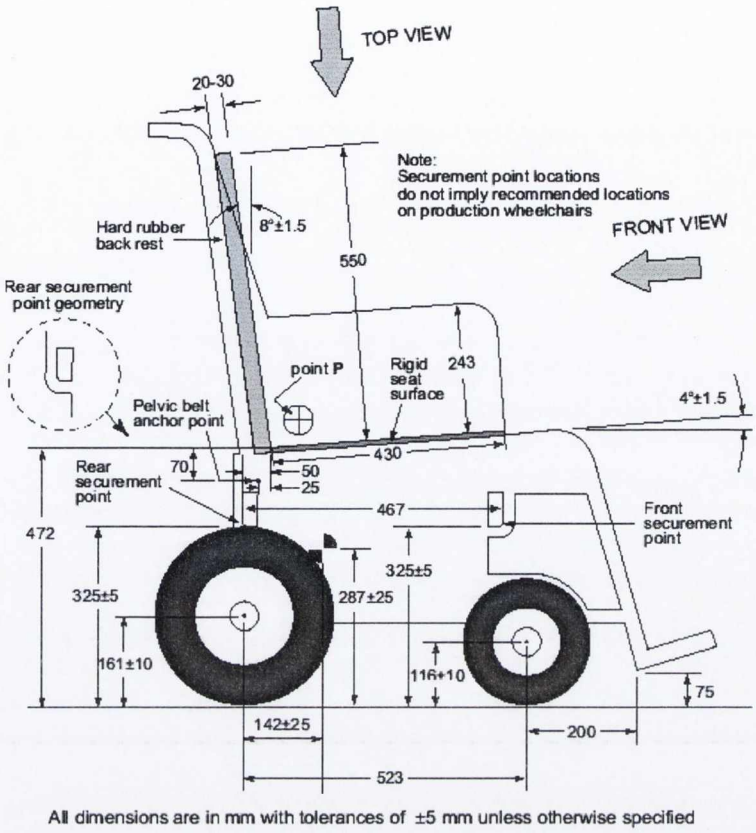


Figure 2.12: ISO 10542 surrogate wheelchair

2.8.2 Numerical Modelling for a Frontal Impact

Computational models of frontal impacts based on sled testing have been developed and validated based on a comparison of the kinetics and kinematics [11] [46] [48]. These models have then been used to determine optimal parameters for improved crash safety [44] [46] [49] which has guided the development of the aforementioned safety standards.

These computational models have developed and evolved with the developments in software and computational power. The modelling programmes used by Kang and Pilkey in 1998 [48] and Bertocci et al in 1996 [46] have improved in the intervening years, and so too have their modelling and predictive capabilities. However, these models were the first to investigate wheelchair safety which leads to improvements in the safety of wheelchair occupants in vehicles.

Wheelchair Tiedowns

In 1996 Bertocci et al created and validated a model of the ISO 10542 surrogate wheelchair with an occupant which was subjected to a frontal impact [46]. The tie down position

was altered to determine the location which was best capable of restraining the wheelchair. As expected the tiedowns placed near the centre of gravity of the wheelchair reduced the rotation of the wheelchair, which also reduces the chance of secondary impact with the interior of the vehicle. This arrangement also resulted in the loading imposed on the tie downs being more evenly distributed over the front and rear tie downs, which can reduce the strength requirements of the tie downs. However more recent research has found wheelchair structural failure at tie down attachment points when subjected to a rear impact [50] which highlights the need to look beyond frontal impact in order to properly assess the needs for crash protection.

A similar model was created in 1998 by Kang and Pilkey [48] of the surrogate wheelchair subjected to a frontal impact. This was used to investigate the sensitivity of the tie down and wheel characteristics. The influence of occupant position was also investigated. In 1999 by Bertocci et al [47] created and validated another frontal impact computational model using a commercially available power wheelchair rather than the surrogate wheelchair. The commercial wheelchair was used as the study aimed to more accurately represent a real life crash and it was felt that using a real wheelchair would better represent this.

Wheelchair Occupant Injury in a Frontal Impact

Evaluation of adult occupant injury in a frontal impact has been limited to date. The computational models created have focused on evaluating different configurations of the wheelchair, with the aim of improved wheelchair design [24] and hence reduce the likelihood of injury. Kang and Pilkey investigated the influence of altering the angle of tilt of the occupant seated in the wheelchair [48]. Bertocci et al investigated occupant loading and used this to predict injury based on the values found combined with the kinematics of the wheelchair [11]. The Combined Injury Criteria (CIC) index was developed which compares biomechanical loading to injury tolerances and sets limits of tolerable injury. The CIC index also accounts for the significance of injury to different body segments, the head being the most significant and the extremities being the least. The CIC index value is calculated using Equation 2.8.

$$CIC = 0.57\left[\frac{HIC}{HIC_t}\right]_{head} + 0.29\left[\frac{a}{a_t}\right]_{chest}$$
$$+0.144\left[\frac{F_{axial}}{F_{axial-t}} + \frac{F_{comp}}{F_{comp-t}} + \frac{F_{shear}}{F_{shear-t}} + \frac{M_{flex}}{M_{flex-t}}\right]_{neck} \tag{2.8}$$

In this equation HIC is the abbreviation for Head Injury Criterion which predicts head

injury based on the time history of the head acceleration. F_{axial}, F_{comp}, F_{shear} represent axial, compressive and shear forces acting on the neck. M_{flex} represents the flexion moment of the neck and a represents the acceleration of the chest. The subscript t stands for the injury tolerance levels. The values of 0.57, 0.29 and 0.144 sum to 1 and are the weightings based on the significance of injury to a body segment, the result is therefore a representation of the severity of the combination of the injuries. This research also established a Motion Criteria (MC) index based on evaluation of peak excursions of the head, wheelchair and knee compared to limits established by the SAE JJ2249 standard and is used to prevent secondary impact with the vehicle interior. Excursion limits are determined and assessed in the MC formula shown in Equation 2.9.

$$MC = 0.25\left[\frac{Exc_{Head}}{Exc_{Head-Limit}}\right] + 0.25\left[\frac{(Exc_{WC}/Exc_{knee})}{(Exc_{WC}/Exc_{knee})_{Limit}}\right]$$
$$+0.25\left[\frac{Exc_{Knee}}{Exc_{Knee-Limit}}\right] + 0.25\left[\frac{Exc_{WC}}{Exc_{WC-Limit}}\right] \tag{2.9}$$

In this equation the Exc represents the forward excursion of a body segment or wheelchair and the subscript *limit* is the SAE J22249 WTORS sled test performance limitation. When used together these indices are a useful tool to predict the performance of the wheelchair and occupant in a crash. However, to date neither of these have been widely adopted for researching injury due to a frontal impact, but have been used in determining the optimal seat belt position [44], [43].

Evaluation of loading on a child occupant subjected to a frontal impact while seated in a commercial wheelchair has been investigated by Ha et al using sled tests [51] and a computational model has been created and validated [22]. The occupant response was assessed using the occupant excursion limits as specified in the wheelchair standards (ANSI/RESNA WC-19) and the limits were not exceeded. Therefore this wheelchair and tiedown system would be deemed to be safe for transport. However, when the occupant was evaluated using automotive standards (FMVSS213 and FMVSS 208) injury was predicted in the neck and chest [22]. This disparity of results needs to be addressed.

The data suggests that while excursion limits prevent serious injury by reducing the risk of secondary impacts it does not address loading on the occupant in the primary phase of the crash which can also lead to injury.

Recent work by Dsouza et al has focused on occupant loading in a frontal impact [24]. Dsouza et al have developed a computational model based on sled testing of a commercial wheelchair and occupant. The model will be used in future parametric studies to reduce

occupant injury risk through improved wheelchair design by maximizing crash energy absorption while maintaining suitable occupant kinematics.

This method of investigating occupant excursion and loading in an impact needs to be further addressed for improved wheelchair transport safety.

2.8.3 Component Testing

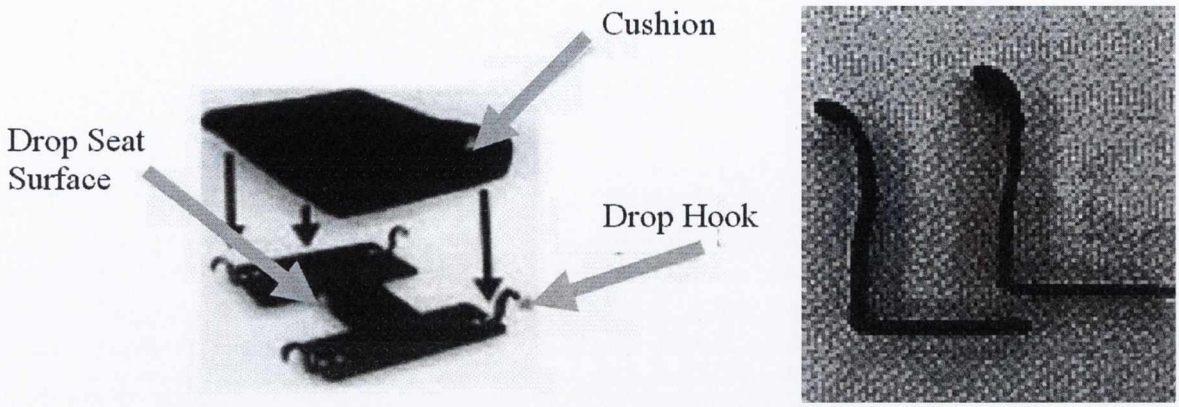
To understand more about the performance of a wheelchair in a crash and to determine design requirements for improved safety the components of the wheelchair have also been tested. These tests are generally based on the equivalent tests for automotive seats. The applied loads are based on automotive test values or values from numerical models of frontal impacts of wheelchairs, whichever is the larger. However due to the different nature and construction of vehicle seats and wheelchair seats these tests may not be the most applicable.

Impact performance of attachment hardware

Wheelchairs are commonly adapted to better fit the occupant and suit the needs of their disability. Attachment hardware is used to secure the additional wheelchair components to the frame, see figure 2.13. One of the most commonly used type of attachment hardware are drop hooks, see figure 2.13, which are typically used to secure a seating system to the wheelchair structure. They are usually mounted onto the rigid drop base (commonly plywood or hard plastic) with the hook portion of the hardware secured over the wheelchair frame tubing as seen in figure 2.13. A cushion is then placed on the drop base and attached with Velcro. These are also used to attach postural supports to improve the posture and functional ability of the occupant. However their response to crash loading is generally unknown.

To investigate this the performance of a wheelchair seatback attached to the wheelchair frame with drop hooks was investigated by Ha et al in 2000 [52]. The tests performed were based on testing procedure for automotive seatbacks and failure was found in all cases. Four out of the five products tested failed at less than 50% of the applied load of 10KN. In 2001 Bertocci et al [53] investigated the crashworthiness of different types of drop hooks by applying the force predicted in the seat from a validated computational model of a wheelchair subjected to a frontal impact. Three different material types of drop hook were investigated using a surrogate seating system and for all types of drop hook plastic deformation was found to occur at less than 50% of the applied force of 16.6KN. Further analysis was conducted into the combined performance of drop hooks and the attached seats by Bertocci et al in 2001 [54] and again the components were unable to withstand the applied load. For each of these investigations failure was due to straightening of the drop hook as shown in 2.13. Such

failures in all cases raises significant safety consideration for the crashworthiness of adapted wheelchairs.



(a)Drop hooks [53] (b) Failure of drop hook [53]

Figure 2.13: Drophooks

Seating system

Wheelchair adaptation can be extensive so that only the frame remains of the original wheelchair. The seat and seatback can be replaced with add-ons such as lateral supports and postural head rests being commonly added, see figure 2.11. The crash performance of this adapted seating system is generally unknown. Testing of the components is the first step in assessing this.

Rear impact protection components such as a head rest and seatbacks of a wheelchair have also been investigated and found to not always be unable to withstand crash loading. Postural head supports such as the one shown in figure 2.14 are commonly added to improve and maintain the posture of the occupant. However the crashworthiness of such items was investigated in 1996 and failure was found in most of the tests it was subjected to [6]. Failure occurred when the head restraint was at its maximum extension which resulted in a much larger moment arm.

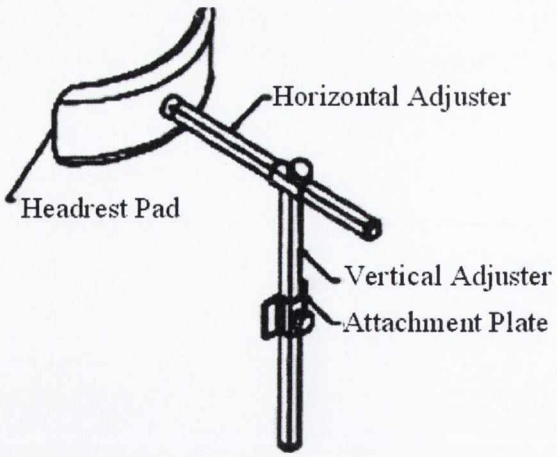


Figure 2.14: Postural head support [6]

More recently sled tests of a peadiatric occupant in a commercial wheelchair has found reduced levels of injury when a head rest is in place compared to when one is absent [35]. These supports were subjected to lower levels of loading due to the smaller mass of a child occupant and they were not positioned at their maximum extension and so moment arm acting on them was reduced and so they remained intact for the crash. The advantages of adequate support was shown by reductions in head and neck injury prediction ranging from 34% to 70%. Rear impact protection is also afforded to the occupant from the seatback and it has been found in the automotive industry that using a less stiff seat back reduces the loading on a head restraint as deformation of the seat back reduces the rearward acceleration of the head, the same is true for wheelchair seating [6]. However if the seat back is not stiff enough it can collapse under the loading of a crash which again would lead to increased injury [55].

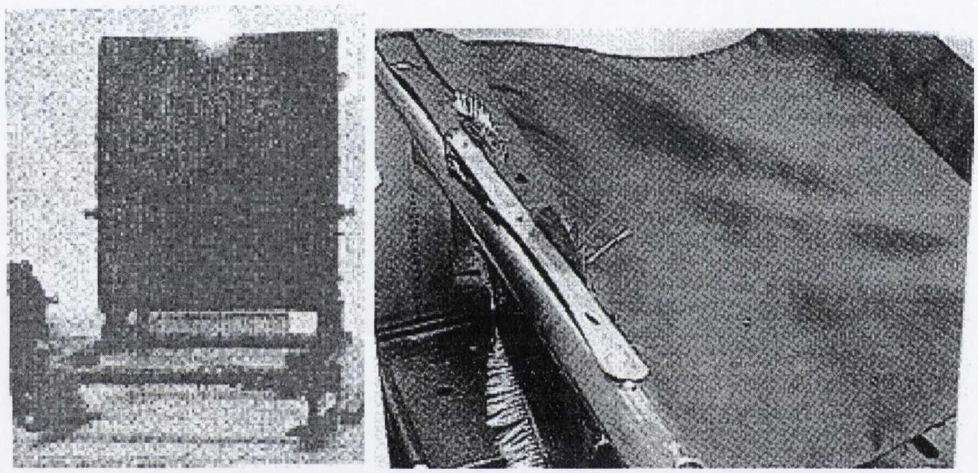
In 2000 to determine static test methods for such wheelchair seatbacks Van Roosmalen et al. [55] tested different brands of seatbacks, see figure 2.15, based on vehicle seat tests. The components tested were found to be able to withstand the maximum required loads of 20 times its own weight without significant deformation or failure. The seatbacks were also found to be stiffer than vehicle seats. The wheelchair seatbacks were found to have little permanent deformation therefore indicating that little energy would be absorbed in a crash. This implies that there may be excessive rebound loading on the occupant. However one issue that they noted is that the test method does not take into consideration loading due to the occupant, merely the weight of the seat. Therefore it is probably not adequate to reflect the strength needed to prevent seatback failure in a rear impact [56].

In 2002 Ha et al investigated another common type of seatback that is used, a fabric sling type as shown in figure 2.15 [56]. None of the components tested were capable of

withstanding the 10KN load applied for 5 seconds, with failures found at the seams of the fabric. The loading applied was based on frontal impact simulations which predicted higher levels of loading than the hypothesised level due to a rear impact [56].

Rear impact sled testing has also been used to investigate the performance of seatbacks when their stiffness was adjusted [57]. As expected significant rearward deflection of the seatback was found when the stiffness was reduced. Stiffer seatbacks deformed less than weaker ones but there was not a corresponding increase in loading on the occupant with the stiffer seatbacks.

Computational models of a frontal impact have also been used to investigate the influence of seat and seatback stiffness as well as seatback angle of recline [58]. All of these factors were found to influence the loading on the wheelchair as they lead to altered kinematics of the occupant.



(a)Rigid [55] (b) Sling [56]

Figure 2.15: Types of seatback

Research to date shows that the combination of head rest, seatback and seat will play an important role in protecting the wheelchair occupant in a rear impact. Due to the large variation of these components there is a great variation in response which greatly effects the level of protection afforded to the occupant.

2.8.4 Rear Impact of Wheelchair and Occupant

Research carried out to date has focused mainly on frontal impact whereas rear impact has not been investigated as extensively. The greatest risk of injury for wheelchair occupants in a rear impact is in the neck, however this can be reduced with the addition of head restraints and appropriate seatbacks, as detailed previously. While these restraints are standard in the automotive industry since 1960s they are not mandatory for wheelchairs when used for

transportation. Research has shown that in the U.S. wheelchair headrests are prescribed for over 60% of wheelchair users [35]. As such many wheelchair users are missing a fundamental safety system that plays a vital role in injury prevention for rear impacts.

Rear impact has started to be evaluated recently using sled tests to investigate the response of the wheelchair and tiedown system to determine design criteria for safer wheelchairs. Research by Fuhrman et al in 2006 of a child occupant in a 10g rear impact found deformation of the seatback as well as increased loading on the front tiedowns compared to a rear impact. The researchers highlighted the fact that front tiedowns generally have a less robust design than rear tiedowns [59]. More recent tests, by Manary et al, with an adult occupant have showed structural failures in all wheelchair and tie-down configurations subjected to the same rear impact pulse of 12-14g. Failure occurred due to breakages of wheelchair components at the front WTORS tie-downs due to the increased loading in a rear impact [50]. Similar investigations into rear impact of commercial wheelchairs by Salipur presented at the RESNA conference 2007 did not find such failures in the tests as the wheelchairs were reinforced. However, this research did find increased loading on the front tiedowns, compared to those on the rear tiedowns in a frontal impact [60]. These tests have been used to create and validate a computational model to design wheelchairs which are suitable for rear impact [23]. The impact pulse used in these studies is under development and will be incorporated as an informative annex to ISO 7176-19. While not the intended purpose of this standard, this annex may help protect rear facing wheelchair occupants in a frontal impact.

A less severe impact pulse (8g) was used by Senin et al to investigate the response of commercial wheelchairs in a rear impact. In this case breakages of the securement system were not found as the impact pulse was mostly absorbed by the backrest, which failed due to plastic deformation of the vertical supports [61].

While these investigations are beginning to address rear impact safety neither of these approaches has focused directly on evaluation of occupant spinal injury risk. Instead they provided occupant excursion levels and commented on the associated risk of secondary impact.

Rear impact injury risk has only been investigated for paediatric occupants using the Head Injury Criterion, *HIC*, and the *NIJ* for neck injury prediction [35], though these criteria are not commonly used for low speed rear impact assessment [27]. The work presented in this paper will focus on the more frequently used rear impact neck injury evaluation methods for adult occupants, the *NIC* and *Nkm* [15].

More recently rear impact investigations of an adult occupant were conducted by our collaborators [62]. This work assessed the *NIC* and *Nkm* resulting from a rear impact with and without a headrest attached to the wheelchair. The aim of this headrest study was to develop a headrest capable of withstanding impact loading. The headrest that was designed as part of that work was found to reduce the risk of injury. The study also showed the importance of the initial position of the headrest as a gap between the head and headrest was found to increase the predicted injury level.

2.9 Scoliosis

Scoliosis is defined as a lateral curvature of the spine [63], however there is commonly deviation in the other axes also [64]. This postural deformity is found among wheelchair users and in the ambulatory population [65] [66]. There may be no known cause for this abnormal growth and so it is referred to as idiopathic scoliosis. For many wheelchair users with scoliosis there is an underlying disability which causes it. For people with scoliosis commonly used injury criteria and injury indices (CIC and MC [11]) may not be applicable as these parameters were established for the 50^{th} percentile dummy which do not accurately represent many wheelchair occupants who have a disability. As noted by Bertocci et al the criteria tolerance levels are based on "a level at which 25% of the test population experience serious injury" [11] and the effect crash loading would have on a disabled person is unknown.

Scoliosis is a complex deformity of the spinal column, however to fully understand the deformity the undeformed spine must first be described.

2.9.1 The Spine

The spine is composed of bone and soft tissues such as muscles, tendons and ligaments which interact to give the body support while still allowing a large degree of flexibility.

The spine is composed of a column of vertebrae divided into five regions - cervical, thoracic, lumbar, sacral and coccyx see figure 2.16. The cervical region is comprised of 7 vertebrae and are the smallest of all the vertebrae in the spine. The joints in this region are the most flexible as they allows bending, flexion and rotation of the head. The thoracic area of the column has 12 vertebrae and are unique as they allow articulation with the ribs. The lower lumbar region is composed of the largest vertebrae which support most of the weight of the body. The sacral region beneath the lumbar region are fused into one single bone know as the sacrum and beneath this is the coccyx which again is a combination of fused vertebrae. This lower most regions of the body do not allow for relative motion as they are

fused, instead they provide stability to the pelvic region. The function of the spine is to provide support for the body, to protect the spinal cord and to allow motion of the torso.

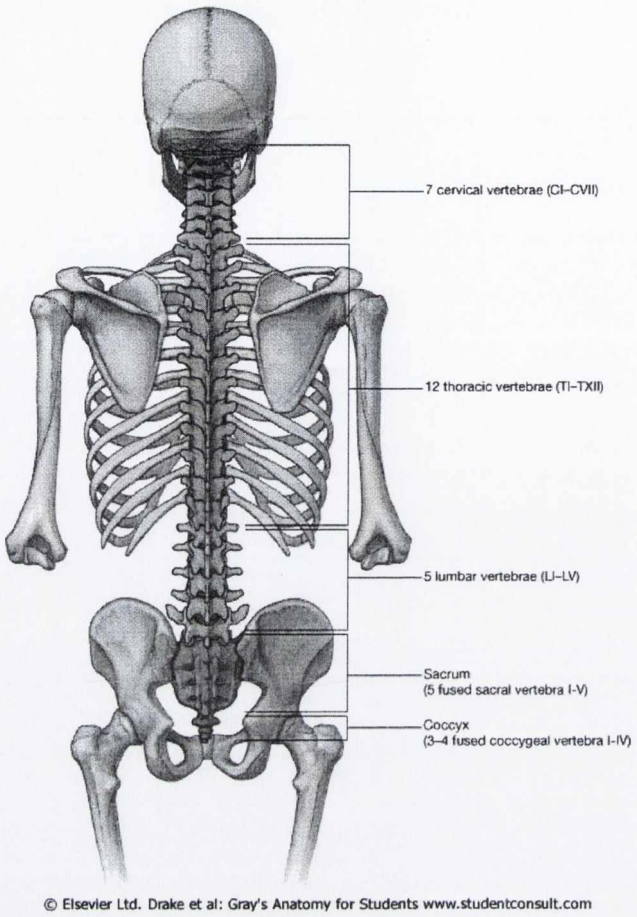


Figure 2.16: Regions of the spine
[63]

While there are some difference in the regions of the spine to allow a different degree of movement the basic structure of the vertebrae remains the same. The anatomy of a typical vertebra of the cervical, thoracic and lumbar vertebrae is shown in figure 2.17. This is seen to consist of a vertebral body and a vertebral arch. The vertebral body is anterior to the vertebral arch and is the major weight bearing component of the bone. The size of this body is seen to increase from the uppermost cercvical vertebrae down to the lower most lumbar vertebrae. Between the vertebral bodies are fibrocartilaginous discs. The vertebral arch is connected to the posterior of the vertebral body by two pedicles. These pedicles form the lateral pillars of the vertebral arch which is connected to the right and left lamina which fuse together at the midline. The vertebral arch forms a protective cover along the length of the spinal cord over the length of the spine. This arch also functions to allow attachment of muscles and ligaments and for the articulation with adjacent vertebrae. This articulation is allowed by the articular processes (facet joints) which stem from where a lamina meets a pedicle. Each vertebra has two of these processes one inferior and one superior to allow for

articulation with an adjacent vertebra. A spinous process is also found projecting posteriorly and generally inferiorly from the vertebral arch.

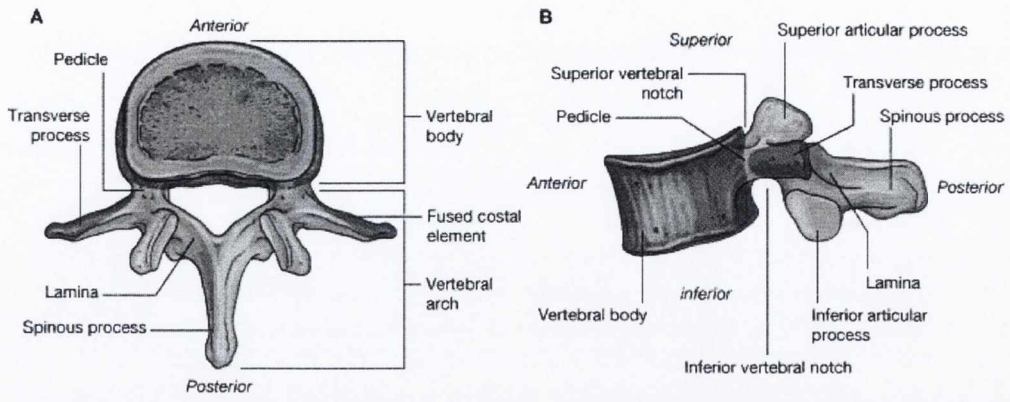
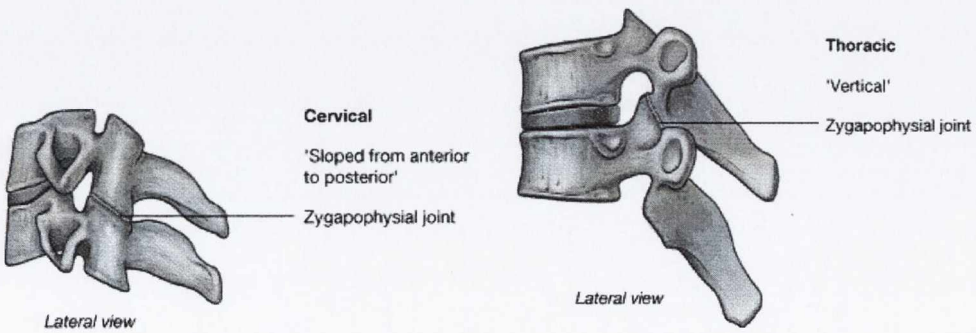
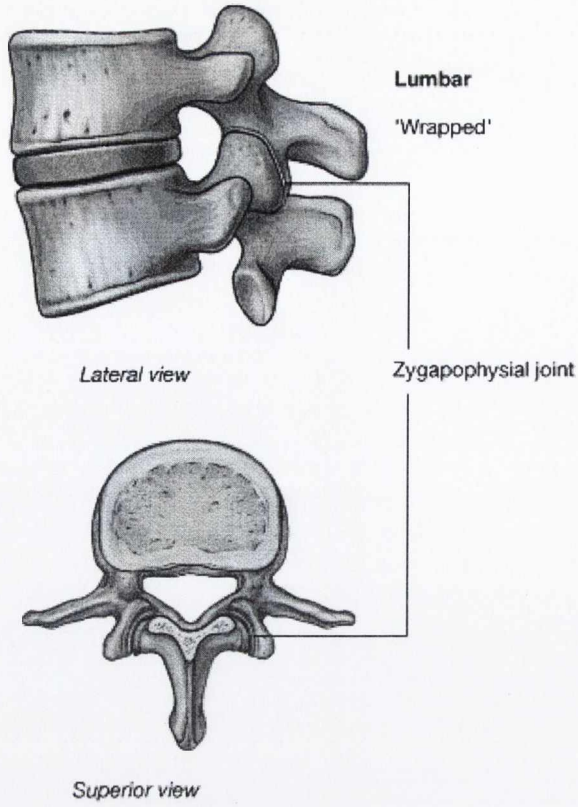


Figure 2.17: Typical Vertebra
[63]

The facet joints of the vertebra control the degree of motion allowable between the vertebra. The cervical, thoracic and lumbar regions of the spine all allow different degrees of motion and so in each of these regions the location of the facet joints is altered. In the cervical region the interacting surfaces slope inferiorly from anterior to posterior, figure 2.18(a). This configuration allows for the characteristic large range of relative motion between vertebrae. In the thoracic region of the spine the joints are orientated vertically and prevent a large degree of flexion and extension while still allowing rotation, figure 2.18(b). In the lower lumbar vertebrae the joints are curved and adjacent processes interlock which limits the range of movement allowing only flexion and extension, 2.18(c).



(a)Cervical (b)Thoracic



(c)Lumbar

Figure 2.18: Facet Joints in Regions of Articulating Spine [63]

The soft tissues surrounding these hard structures also play a vital role in the articulation of the spine. The intervertebral disc between adjacent vertebrae is composed of a nucleus pulposus with a surrounding anulus fibrosus, see figure 2.19. The anulus fibrous is a dual layer of an outer ring of collagen with an inner zone of fibrocartilage in a lamellar configuration. This arrangement of fibers limits rotation between vertebrae. The nucleus pulposus fills the center of the disc and is gelatinous and acts in compression to absorb the forces between the vertebrae.

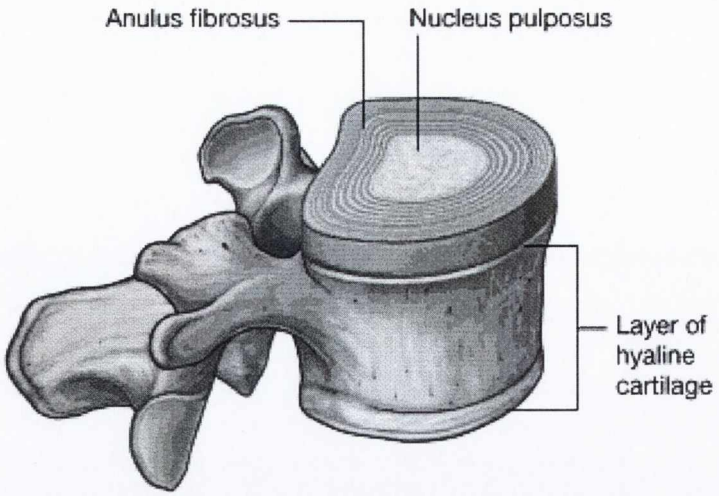


Figure 2.19: Intervertebral Disc
[63]

The ligaments surrounding the vertebrae are shown in figure 2.20. The posterior and anterior longitudinal ligaments both begin at the base of the skull and extend down to the sacrum while also connecting vertebral bodies and the intervertebral discs [63].

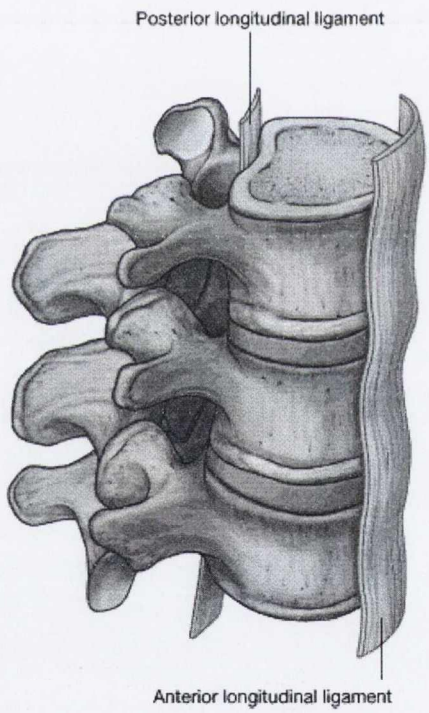


Figure 2.20: Ligaments of the Spine
[63]

2.10 Mechanical Testing of Vertebrae

To determine the mechanical properties of the spine testing has been conducted. Testing of the spine is reduced down to a single vertebral joint between two adjacent vertebrae. The information from such tests will be used to evaluate injury in a rear impact based on the levels

that have been found to cause damage to the vertebrae. This includes both compressive and shear testing.

2.10.1 Compressive Loading

The vertebrae have been determined to be well designed for compressive loading with large values of loading, at least 5kN, required to cause damage to the lumbar region of the spine [67], [68], [69]. The smaller thoracic vertebrae are as expected, less able to resist such loading with an average reduction in compressive strength of 0.17kN per vertebrae ranging from the lower most vertebra, L5, up to the uppermost T1 vertebra [69]. In the cervical region the head and neck have been investigated to determine their response to compressive loading and on average a force of 3kN was required to cause injury to the vertebrae [70].

Compression fractures of vertebrae were found to occur at substantially lower, 25%, values when the load is applied eccentrically to the vertebrae compared to when a purely axial load is applied [71].

This type of loading is apt for rear impact evaluation as in the cervical region of the spine there are compressive loads due to the straightening thoracic curve which passes loading upwards to the neck [29], [30].

2.10.2 Shear Loading

Shear loading of the vertebral regions of the spine of cadavers has also been conducted, and is particularly relevant for this analysis as it is the main type of loading on the spine in a rear impact due to contact with the seatback. Non-destructive testing is usually conducted to prevent damage to the structures of the spine. The testing is also usually conducted with the soft tissues such as the muscles removed [72].

Testing of vertebral pairs in shear has been limited to date and it has been noted that there is a "lack of fundamental data in shear" [73]. Therefore testing has been conducted at low force levels to characterise the response of the vertebrae under such loading [74], [72] [73], [68]. Testing below damage levels also prevents damage to the scarce specimens which can then be reused, for further testing. The scarcity of human vertebral tissue has led to the use of porcine vertebrae to provide information about the complex nature of the spine. These tests include fatigue failure due to cyclical loading of the lumbar vertebrae [75] as well as dynamic loading on the cervical region [76] and both types of testing have found the fracture site to be at the facet joints, at loads of approximately 2kN. The dynamic shear loading of the 6month old porcine specimens also found fractures at the end plates in two

instances - at higher loading rates and when the vertebrae are in a flexed position. These fractures have been attributed to the immature bone of the specimens [76].

The facet joints have been found to be the point of breakages in human specimens also at 2.8kN [77]. The facet joint has been found to be largely responsible for the shear loading response of the vertebrae. The intervertebral discs were found to be largely unloaded in shear until the facet joints break [77] or are removed for testing [76]. Testing of the facet joints by applying a load directly onto these regions of the spine were found to fail at 2kN [78]. Soft tissue injuries were investigated by Begeman and were determined that failures were likely to occur at loading of about 1.5kN in pure shear [77].

The applicability of these values to scoliotic spines is unknown as the altered alignment of the vertebrae and the facet joints may alter the vertebral response. While flexion of the vertebral pairs when tested under cyclical loading has not been found to alter the response, this is due to the fact that the facet joints can still make contact [75]. When vertebral pairs were subjected to dynamic loading in a flexed posture the ultimate load at failure was found to increase when compared to that at a neutral posture, this was attributed to realignment of the facets and lengthening of the moment arm on the joints [76]. However a 3D deformation due to scoliosis may alter this. It has been suggested that an altered posture may alter the injury mechanism when subjected to shear loading [76]. An altered range of motion and kinematic response of the scoliotic spine when compared to one without scoliosis has also been found [79], [80]. This suggests that the altered shape of the spine influences the structural properties of the spine. Therefore the response of a scoliotic spine in a rear impact as characteristed in a healthy spine by Ono [30] and Davidsson [32] may be altered.

2.10.3 Types of Scoliosis

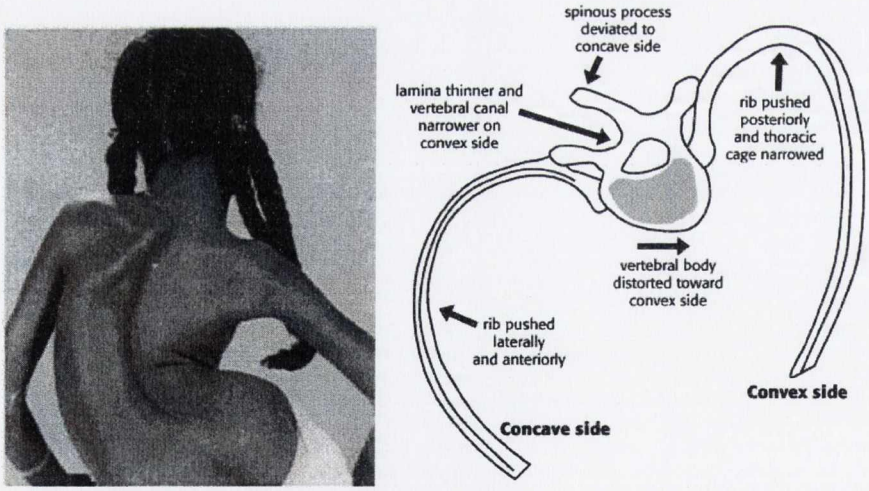
Scoliosis is found in a variety of forms depending on its underlying cuases. The groups of scoliosis include:

- Non structural scoliosis due to poor posture or postural compensation
- Transient structural scoliosis due to inflammation or problems with the hip bones
- Structural scoliosis due to structural deformity of the spinal column and the surrounding structures

Structural scoliosis is a permanent disability and without adequate medical intervention the degree of deformity can increase. The degree of spinal deformity varies for each individual as well as the region of the spine that is effected by the curve. A curve may be produced

in the lumbar or thoracic regions while it is rare in the cervical region [81], [82], figure 2.16, of the spine and may consist of a single or double curve. A single curve usually results in a c-shape of the spine whereas for a double curve this produces an s-shape. In a double curve there is a primary curve of deformity and a compensatory curve. Irrespective of the type of scoliosis the body tries to keep the head in the central line to allow the eyes to be horizontal. This is known as the ocular corrective reflex [66] [65].

A single thoracic curve is shown in figure 2.21(a), the deformation of the spine also deforms the surrounding structures such as the ribs resulting in a rib hump. Figure 2.21(b) shows a single deformed rib due to scoliosis in the spinal column to which it is attached. The axial rotation of the vertebrae causes the ribs to be forced anteriorly on one side and posteriorly on the other, thus forming the hump. There are associated medical problems with this condition including respiratory and digestive ailments due to pressure on the internal organs and hence medical intervention is required to relieve these problems and also to prevent the progression of the curve [83],[84]. For mild curvatures this intervention may be by supporting and holding the thorax in an upright position in a rigid brace. For more severe curvatures spinal fusion or the insertion of spinal rods may be required. This surgical procedure corrects the curvature and repositions the spine in an upright position. However, these procedures can also restrict the range of motion post surgery due to its rigidity and hence as small an area as possible is treated [82], [81].



(a)Scoliosis (b)Rib Hump [85]

Figure 2.21: Scoliosis

There are many types of structural scoliosis which are categorised by time of onset and the basis of the curve - bone or soft tissue. Scoliosis can be caused by a disability or there may be no known cause.

Scoliosis is found among 90% of patients with Duchenne Muscular Dystrophy (DMD) [86], the prevalence of which has grown in Denmark over the past 24 years from 3.1 to 5.5 per 10^5 males [87]. The majority of patients with DMD will be confined to a wheelchair by their mid-teens [86]. Scoliosis is associated with many other disorders such as cerebral palsy and the prevalence of this is also increasing [88]. One study of children with cerebral palsy has found scoliosis in 21% of the patients [89].

Scoliosis due to malformation of the spinal column often has no known cause and is referred to as idiopathic scoliosis, this is the most common type and accounts for 80-90% of cases [82]. This is sub-divided by the time of occurrence - early onset under the age of three, juvenile from the age of three to ten and the most common form - adolescent scoliosis.

The aetiology of this form of scoliosis is unknown however some factors have been suggested. These include the soft tissues structures such as the annulus fibrosus of the intervertebral disc [90], [91]. The soft tissues surrounding the spine have also been investigated as a cause of scoliosis as well as the interaction of the adjacent vertebrae as they grow [92], [93]. The time of growth and development in the adolescent years has been found to be the time of greatest progression of this type of scoliosis. Therefore the loading during this time of growth has been investigated as a possible cause of the deformity [94]. It is still unclear as to whether a lateral deviation or axial deviation from the normal curvature of the spine is responsible for the beginning of the scoliosis [82]. Therefore a general consensus on the causes of this type of scoliosis is still lacking. It is widely accepted that the effect of idiopathic scoliosis is to create a 3 dimensional curvature of the spine so that there is both a lateral and axial rotational element to the curve which have an effect on the overall shape of the back and the surrounding structures [95], [96], [64]. The deformity of the torso as a whole has an effect on the surrounding rib cage [83] to produce a rib hump as detailed previously and associated with this is a reduced respiratory capacity [84], [81]. Patients with idiopathic scoliosis have also been found to have a reduced flexibility [97] which correlates with the altered kinematics found by White [79] and Veldhuizen [80].

2.10.4 Severity of Scoliosis - Cobb Angle

The severity of the scoliosis is based on the degree of curvature as seen on a frontal plane x-ray and this information is used to determine whether surgery is appropriate. The most commonly used scale on which curvature is measured is the Cobb Angle which is based on the angle of the major apex as seen on an X-ray of the spine as shown in figure 2.22. This measurement is based on an AP X-ray and the apical vertebra is first identified and then the end vertebrae are identified. The end vertebra are the most superior and inferior

vertebra which are least displaced and rotated and have the maximally tilted end plate. A line is drawn along the superior end plate of the superior end vertebra and a second line drawn along the inferior end plate of the inferior end vertebra. The angle between these two lines (or lines drawn perpendicular to them as in figure 2.22) is measured as the Cobb angle. Because the Cobb angle reflects curvature only in a single plane and fails to account for vertebral rotation it may not accurately demonstrate the severity of three dimensional spinal deformity. A Cobb angle of 10 is regarded as a minimum angulation to define scoliosis [81].

Some problems exist with this method of classification as not only is the Cobb angle a 2D measurement of a 3D problem, a lack of repeatability and reproducibility has also been found [98]. However it is a widely used tool to aid in the treatment of scoliosis and used for comparisons pre- and post-surgery.

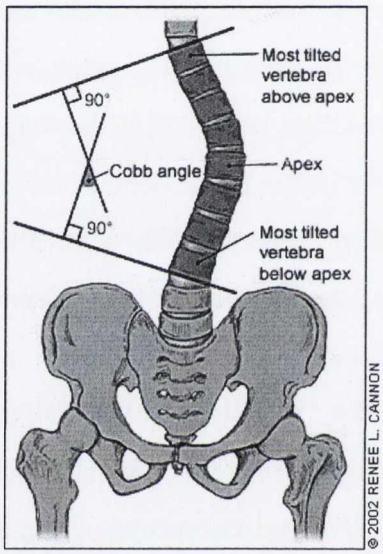


Figure 2.22: Cobb Angle [99]

2.11 Concluding Remarks

This literature review shows that considerable improvements have been made in frontal impact protection of wheelchair users, primarily through the provision of crashworthy wheelchairs and Wheelchair Tiedown and Occupant Restraint Systems that prevent secondary collisions with the vehicle interior. In contrast, there has been relatively little focus on wheelchair user rear impact protection. This project aims to address this inequality and increase the knowledge available about rear impact. Another shortcoming in wheelchair crash safety research has been a lack of injury assessment in impact, and this will be assessed in this work.

A combined multi-body and facet element approach that can predict the dynamic loading imposed on a wheelchair and occupant during an impact is an effective and efficient research

tool. This approach of assessing impact has been adopted in this work. It has been previously used to determine the effect of alterations to the wheelchair and WTORS in an impact. The work conducted for this study will build on this by investigating the following:

- The alteration of the numerical model of the occupant to represent scoliosis and its impact
- The effect of after market add-ons to wheelchairs
- Occupant loading will also be assessed and the influence that each of these adaptations have on the numerical model will be evaluated.

The crash test dummies and numerical models used in the literature to represent wheelchair occupants have been based on 50th percentile human anthropometrics. However, it is known that there can be significant variances in the geometry and stiffness of the musculoskeletal system for some wheelchair users compared to the healthy population. Idiopathic scoliosis is a common postural deformity found among wheelchair users and is a focus of this study. This type of scoliosis will be introduced to the occupant model used in this work, resulting in geometric alteration of the numerical model of the occupant. The effect of such a disability in a crash will be assessed in this study using these computational models.

Many wheelchair users with postural deformities use after market add-on devices as postural support, and the influence of these on rear impact injury is also assessed, as this is unknown. The validated wheelchair model will be adapted to reflect the addition of postural supports that is frequently conducted in seating clinics such as our collaborator, Enable Ireland.

The surface characteristic of the seatback of a wheelchair is an important consideration in rear impact protection. The surface characteristic will be investigated in this project to determine its effect in a rear impact. While the structural stiffness is not altered, as this is a validated part of the rigid wheelchair, the contacting surface will be altered to determine the effect this has on the outcome.

Current voluntary wheelchair standards do not assess injury, other than providing excursion limits, however they are necessary to provide information on the loading experienced by the occupant in a crash. The predicted level of injury based on commonly used injury criteria will be assessed in this work. These criteria can also be used to predict the effect a postural deformity has on the predicted level of injury.

As the literature shows, the traditional area of focus in investigating a rear impact is the neck as this is most likely to be injured. However, there is also an associated risk of injury in the thoracic and lumbar regions. The approach taken in this work is therefore to evaluate the loading on the three regions of the spine (cervical, thoracic and lumbar) and compare this to levels known to cause damage.

This work will therefore develop the area of wheelchair crash safety by analysing rear impact and also by investigating occupant loading. More realistic representative models of the occupant and wheelchair than the standard models (BioRID II and ISO surrogate wheelchair) will also be used as part of this study. The computational model of the standard baseline occupant in a rear impact is assessed through a validation process by comparing the kinematic outputs to the physical tests, producing a validated model.

The validated model is adapted to better reflect actual wheelchairs and the postural deformities of wheelchair users. The effect of such changes can then be investigated. A schematic showing this process and how it will be used to assess the influence of postural deformities on spinal loading is shown in figure 2.23.

In order to be considered as significant, comparisons between the baseline and the altered model must be greater than the differences found during the validation process. Values below this discrepancy may be due to a modelling artifact. Therefore the accepting or rejecting of the hypothesis depends on how well the computational model is validated, the limitations associated with this are discussed in Chapter 10.

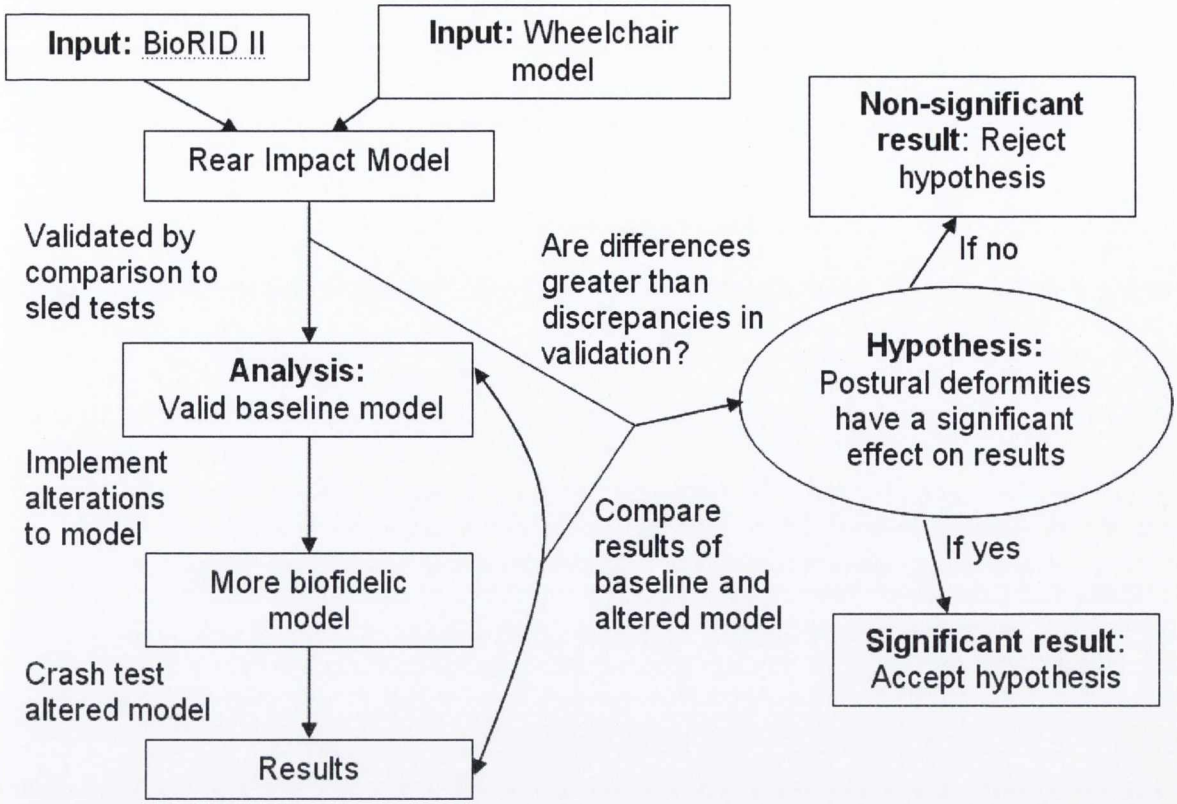


Figure 2.23: Validation Process

This resulting outcome will evaluate the hypothesis that alterations to the standard 50^{th} percentile occupant and wheelchair models have a significant effect on the results of a rear impact.

It is hypothesised in this thesis that the injury risk of wheelchair occupants in rear impact is significantly influenced by the presence of a postural deformity such as scoliosis. Considering the importance of rear impact for loading of the cervical spine, this hypothesis is evaluated using rear impact simulations modelled using multibody techniques. A simulation of a 50th percentile male wheelchair occupant (i.e. with no spinal deformity) seated in a rigid wheelchair subjected to a 10g rear impact pulse is used to provide a baseline for injury assessment. This model is validated by comparison with sled tests performed using a fully instrumented BIORID II crash dummy.

Scoliosis is then implemented in the multibody occupant model using X-ray data from patients with scoliosis. The wheelchair is also adapted to represent the processes conducted in seating clinics. The kinematics, joint loading and two complimentary neck injury criteria are evaluated for these altered models subjected to the same 10g rear impact pulse, and compared to the baseline injury predictions. These comparisons are used to evaluate the hypothesis that alterations to the standard representative wheelchair and occupant models influence wheelchair occupant injury risk. The focus is on the cervical spine, but potential injuries to the thoracic and lumbar region are also evaluated.

Chapter 3

Methods 1: Physical Testing

3.1 Introduction

A combined physical and numerical approach was adopted for use in this work. This chapter provides details of the physical testing that was conducted to provide the validation data for the numerical model.

3.2 Sled Testing

Sled testing of vehicles has been conducted extensively and has been adapted for use in safety testing of wheelchairs [100] [51] [60]. These wheelchair tests have been used to validate computational models [11], [22], [23]. The essential components are the wheelchair, tiedowns, occupant and restraints and so sled tests are conducted with these sections only. These are mounted on a sled and accelerated to a required level using an impactor ram which applies the required impulse. The fully instrumented test produces output data for use in the validation of the model.

3.2.1 Wheelchair Occupant - BioRID II

For rear impact investigations a specialised model exist, the BioRID II, see figure 3.1, see Chapter 2 for more details.

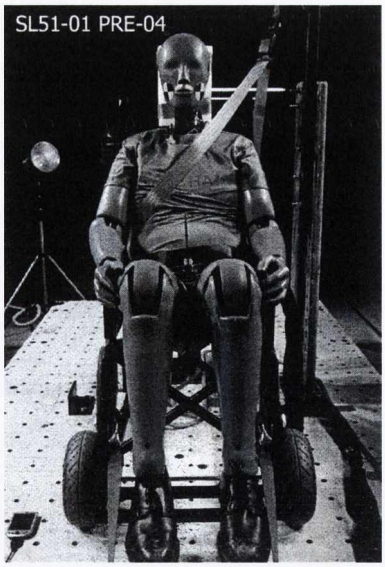


Figure 3.1: BioRID II

3.2.2 Wheelchair - ISO Surrogate

The surrogate wheelchair as specified in ISO10542 was developed based on a large powered wheelchair which is used as a representative model of the broad range of wheelchairs that are available, see Chapter 2 for details, an image of the wheelchair used is shown in figure 3.2.



Figure 3.2: ISO Surrogate Wheelchair

The surrogate wheelchair was chosen for testing as it has been extensively used for frontal impact evaluation and has been used to guide the design of the wheelchair tiedown and occupant restraint (WTORS) [48], [101], [46]. The seat and seatback of the wheelchair were constructed of plywood with a firm foam placed on the seatback. The rigidity of the seatback leads to increased loading on the spine. However, as the long term goal was to establish the influence of postural deformities on spinal loading, the confounding effects of wheelchair cushioning and structural deformation were avoided through the use of a rigid wheelchair.

Rigid seats have also been used to investigate injury and the kinematics of an occupant subjected to a rear impact [20] and in the evaluation of wheelchair headrests [6]. The same

approach was used for the validation of the BioRID II dummy comparing its response to that of volunteers in a rigid seat [19].

The wheelchair created for testing was made as part of a parallel project and is constructed approximately to the ISO standard [2]. The wheelchair deviated from the standard as a lower mass of 37kg was used instead of 85kg. The reduced mass was due to the materials and manner of construction. At the time of testing this was the only wheelchair available that approximates to the standard and as testing of the WTORS was not a goal of this work it would not affect the results. Also, due to availability constraints, a combination of pneumatic tyres on the front and solid wheels at the back were used instead of the required pneumatic tyres on the front and rear.

3.3 Test Set-up

At the time of testing a rear impact procedure for testing wheelchairs was not available and therefore a new test method was created by combining a wheelchair frontal impact procedure, ISO 7176-19, [3] with an automotive rear impact protocol - IIWPG Protocol for the Dynamic Testing of Motor Vehicle Seats for Neck Injury Prevention [102]. A detailed description of this new testing procedure is provided in Appendix A. A summary of these documents is presented in the following sections.

The wheelchair, tiedowns and occupant restraints were set up in accordance with ISO 7176-19 Annex - A Test method for frontal impact tests [3]. However, this frontal impact standard requires the use of the Hybrid III dummy for testing, which has been found not to be appropriate for rear impact evaluation [19]. Therefore the BioRID II which was created specially for rear impact evaluation was used. This is the occupant model required by IIWPG Protocol for the Dynamic Testing of Motor Vehicle Seats for Neck Injury Prevention [102] and therefore the position of the occupant was guided by the requirements of this protocol.

The sled had to be adapted for wheelchair testing as it had previously only been used for sled testing of vehicles and a protocol was drawn up for this also, see Appendix A.

3.3.1 Wheelchair Tiedown

In accordance with ISO 7176 a four point tie down system was used. This standard provides guidelines on the location of the front and rear tiedowns, as shown in figure 3.3. Accordingly an UNWINS four point tiedown with karabineer hooks (SWR/10) was used to secure the wheelchair within the location zones as required, 32^o for the front tiedowns and 44^o for the rear tiedowns. The tiedown positions on the wheelchair were created to be in the position

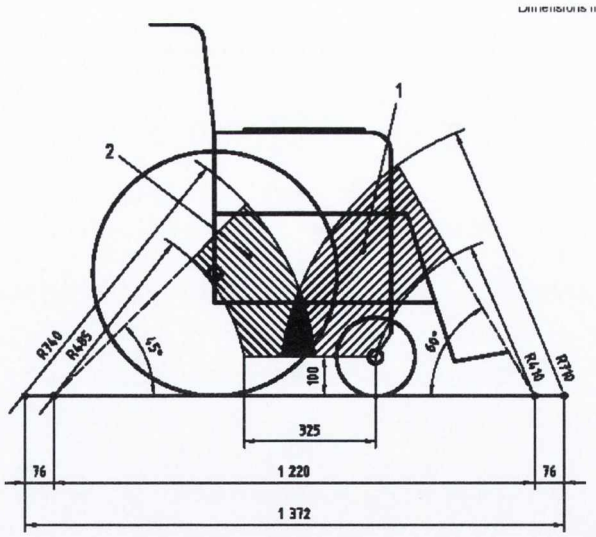


Figure 3.3: Front and rear securement point location zones [3]

designated by ISO 10542 [2], see drawings in Chapter 2 figure 3.2. The tiedowns were secured into the tiedown rail which were positioned 40cm apart, as specified by the manufacturers.

3.3.2 Occupant Restraint

The occupant restraint used was an UNWINS integrated lap and shoulder belt (QB20/2/1200) and the positioning of this was dictated by the ISO frontal impact standard. To position the restraint an upper anchor point location is required, see figure 3.4.

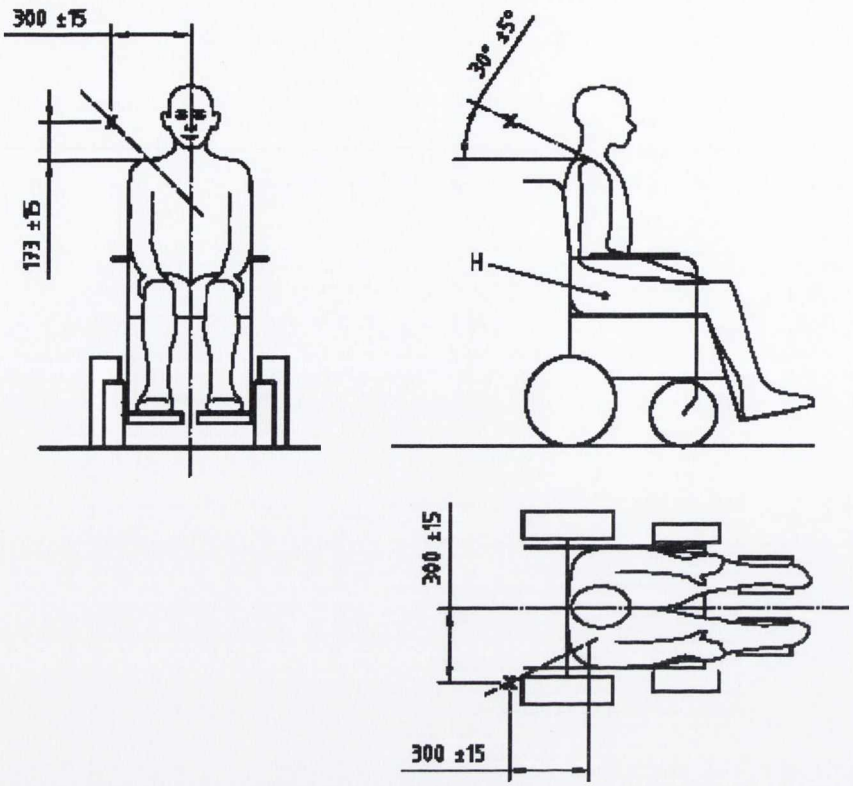


Figure 3.4: Position of Upper Anchorage Point

To achieve this location for the upper anchorage point as specified in the ISO standard, a B-pillar was constructed, see figure 3.5.

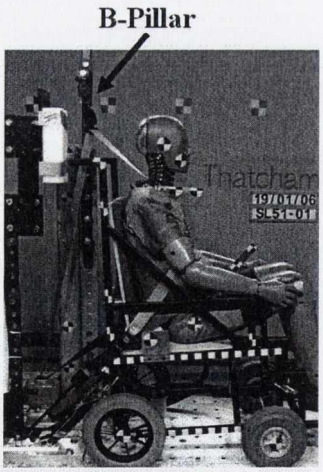
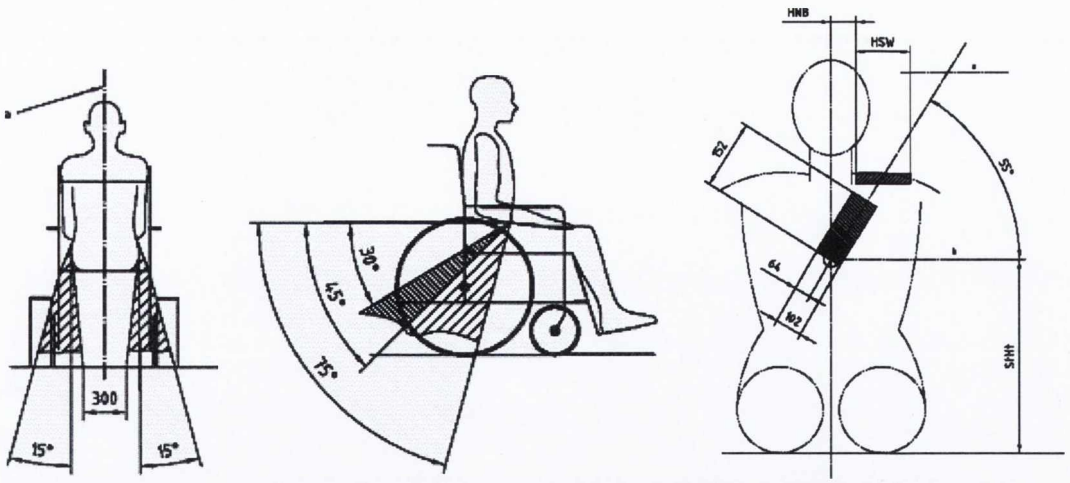


Figure 3.5: B-Pillar Position

The upper and lower restraints were then positioned on the dummy, figure 3.1, in accordance with the specified angles as show in figure 3.6.



(a)Range of angle for pelvic belt [3]

(b)Location of shoulder belt on occupant's torso [3]

Figure 3.6: Occupant restraint system

3.3.3 Occupant

The BioRID II used for testing has been found in comparative tests with volunteers and cadavers to have a more biofidelic neck, thoracic and lumbar motion in rear impact when compared to other types of dummy, cadavers and volunteer tests [19]. The seated posture that the BioRID II was validated in was 25-29^o orientation in space as this creates the kyphosis of the thoracic region, straight lumbar region and lordosis of the neck which represents the seated posture of volunteers [19]. For this series of testing the dummy was positioned in accordance with the IIWPG procedure with a 26^o pelvic tilt, see figure 3.7. This position creates a gap between the pelvis and the seatback which deviates from the idealised position of a wheelchair occupant, as the dummy is usually used in a contoured vehicle seat. However, this is the validated position of the occupant and the posture of the occupant used in these sled tests and it's limitations is discussed in further detail in Chapter 10. The head was positioned upright so that there was 0^o tilt. The knees were also positioned so that there was 200mm gap between the centrelines of the knees. The feet were then placed on the footrest. The occupant seated in the wheelchair is shown in figure 3.7.

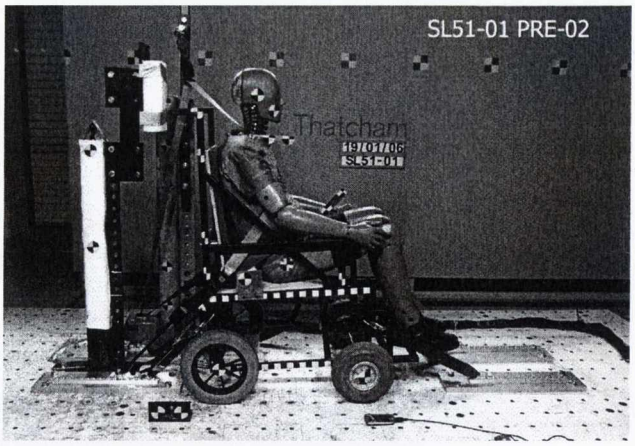


Figure 3.7: BioRID II Seated in Wheelchair

3.3.4 Crash Pulse

The pulse used in this test was proposed by the IIWPG for rear impact testing. The pulse is 10g/16kmph applied over 100ms, see figure 3.8, and is based on collision data which "indicates that the majority of whiplash injuries occur" at this speed [102].

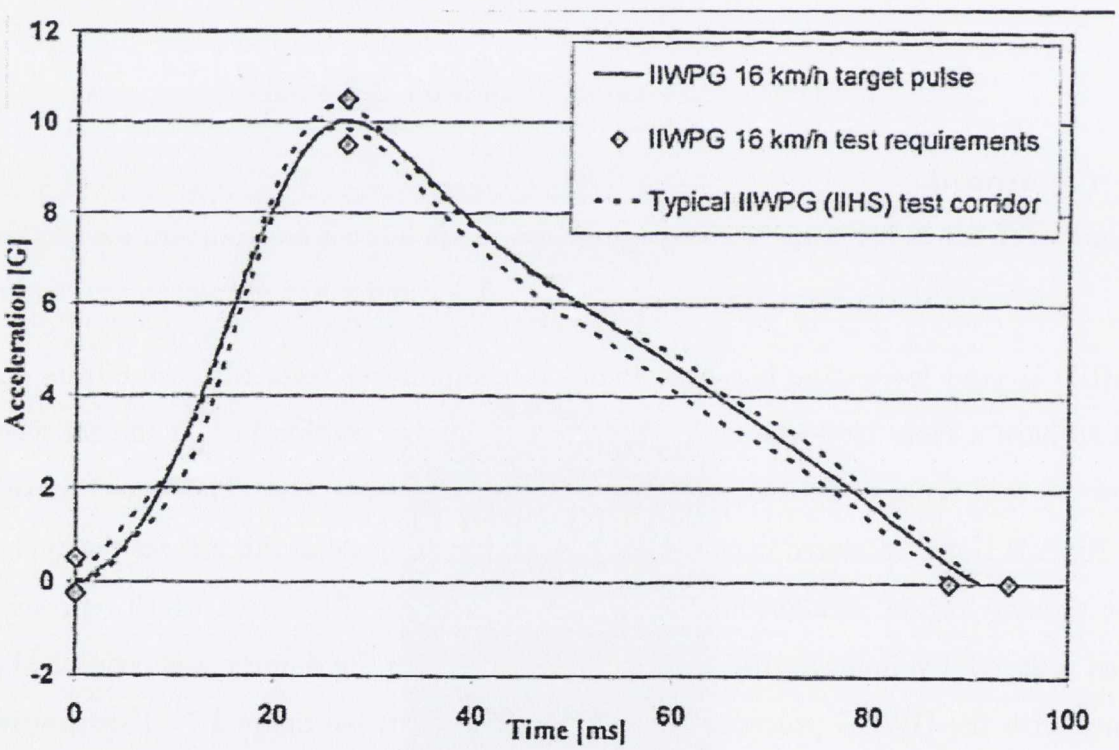


Figure 3.8: IIWPG Rear Impact Pulse

3.3.5 Outputs

Data was acquired at the sampling rate of 10kHz. The outputs from the sensors were filtered in accordance with SAE J211. The filter classes used for the sensor time histories are given in table 3.1.

Output	Filter
Head Acceleration	CFC 1000
Upper Neck Force	CFC 1000
Upper Neck Moment	CFC 600
Lower Neck Force	CFC 1000
Lower Neck Moment	CFC 600
C4 Acceleration	CFC 60
T1 Acceleration	CFC 60
T8 Acceleration	CFC 60
L1 Acceleration	CFC 60
Pelvis Acceleration	CFC 1000

Table 3.1: Filter Classes Used in Data Post-Processing

High speed video recording (1000Hz) of the crash was also conducted, these recordings can be used for comparison to the animation output from the simulation.

3.3.6 Additional Information

Three sled tests were performed. During testing a head stopper was put in place to prevent damage to the dummy neck after a significant hyperextension, as required by the Thatcham testing facility, see figure 3.9. However, for Test 1 the head stopper was fortuitously placed such that it made no contact with the head at all. In contrast, for tests 2 and 3, head contact occurred at around 70 to 80 ms. Test 1 was therefore used for the numerical validation of the computational model to investigate the effect of full hyperextension of the neck in a rear impact. The limitation of using a single test for validation purposes is detailed in Chapter 10. However, it was found that when the acceleration time histories for all three tests up to the time of head contact at about 80ms were compared, similar results were found and a response corridor from the three tests can be defined up to this time. This corridor will be used when presenting comparative graphs of the physical and numerical output data.

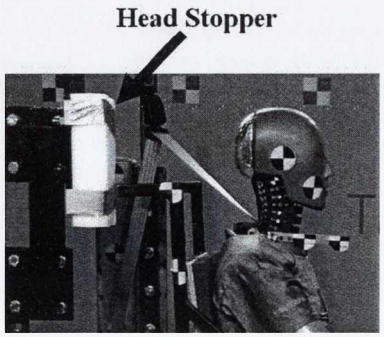


Figure 3.9: Head Stopper

3.4 Pre and Post Test Checks

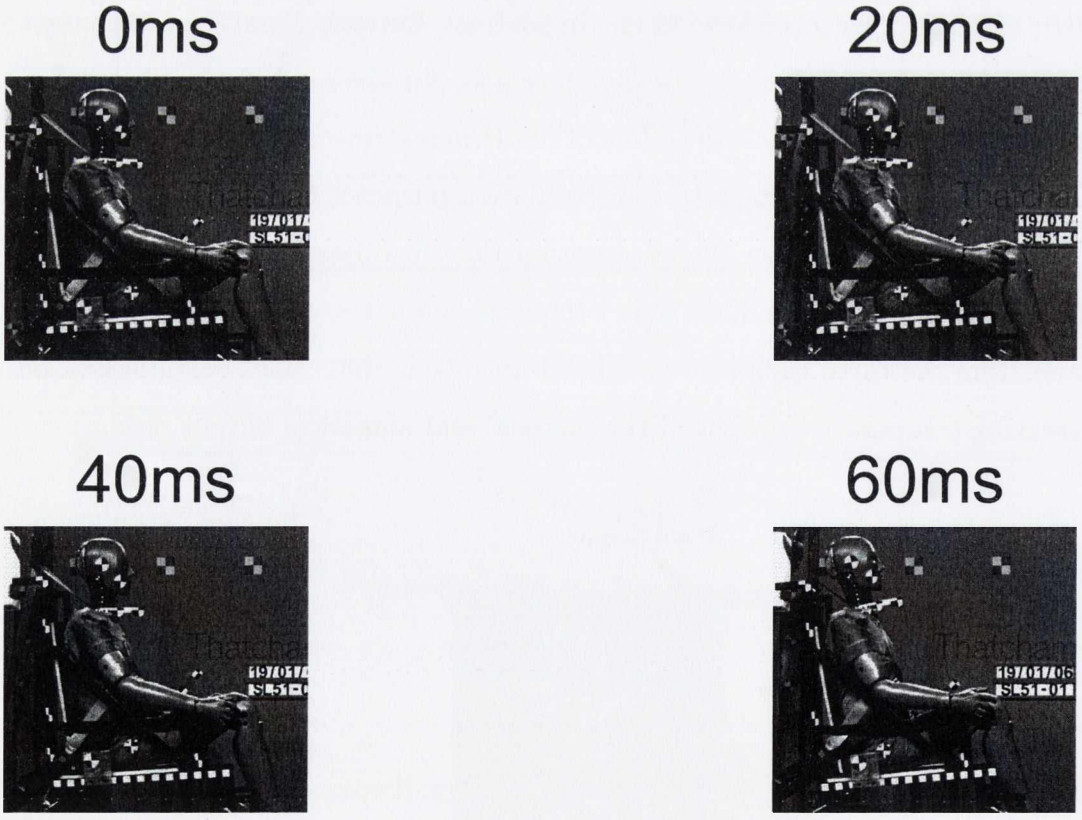
In the same manner as required for ISO7176 frontal impact procedure [3] pre and post tests examinations were conducted. A pretest checklist was created to check the angle of the tiedowns, and the tyres, seat, seatback and joints of the wheelchair which were inspected before each test to determine any damage, see Appendix A.

After the test was completed the items on the checklist, see Appendix A ,were investigated. This included evaluating the final position of the wheelchair and occupant and to check for damage caused by the testing.

Post test photos of the wheelchair and occupant also show no damage or breakages due to the test. This process found no unexpected events in each of the crash tests, which was also confirmed by analysing the video.

3.5 Video Output from Sled Test

High speed video recording (1000Hz) of the test was taken. The video of the sled test is shown in 20ms snapshots in figure 3.10.



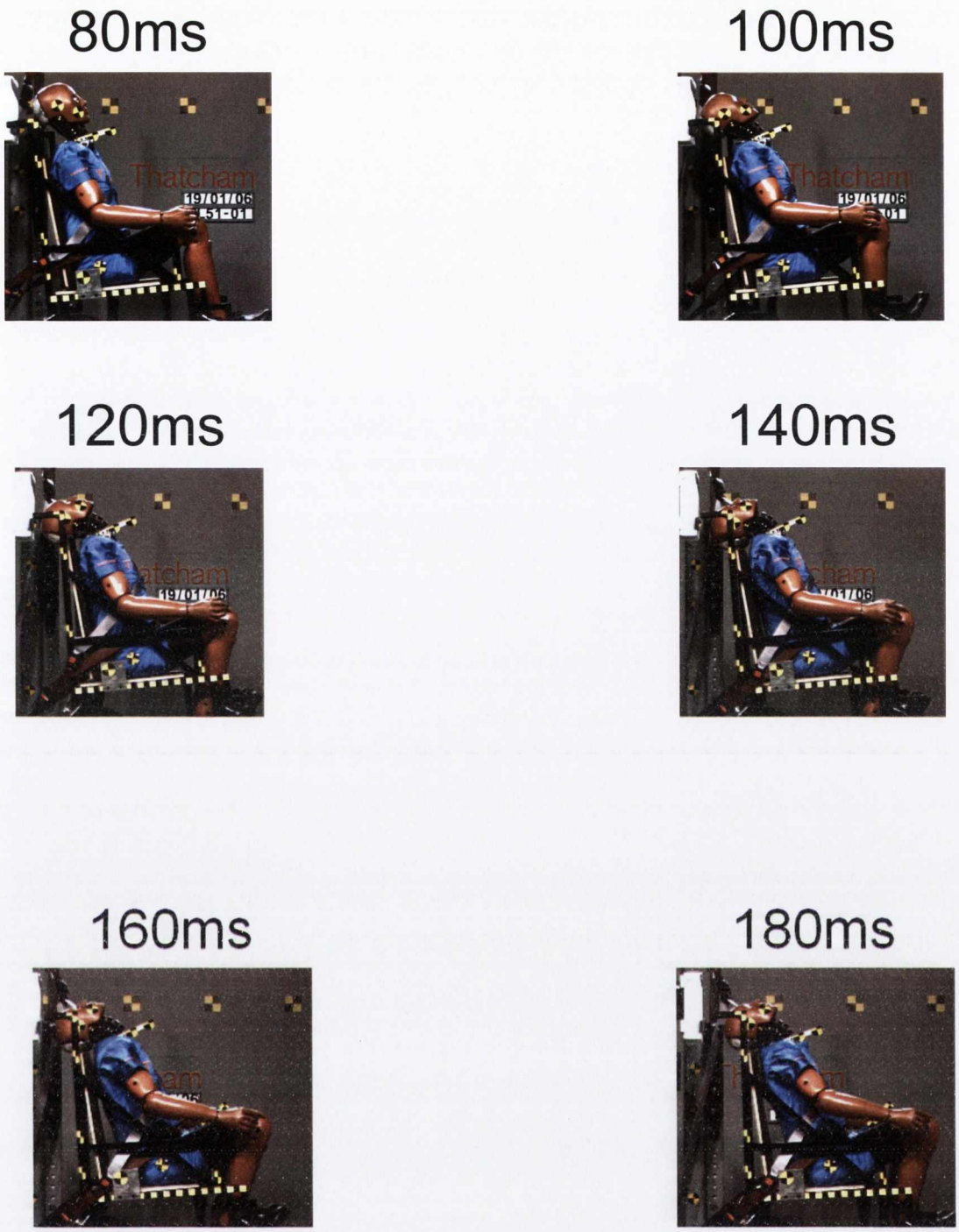


Figure 3.10: 20ms Snapshots of 10g Rear Impact Sled Test

3.6 Variability between tests

Three tests were conducted, which had a head stopper in place to prevent hyperextension of the neck. However in one test the the head stopper was positioned further from the occupant and so it did not stop hyperextension. The test method for all tests was the same and so the response should be the same for each test up to contact with the head stopper. This was evaluated and is presented in this section.

3.6.1 Impact Pulse

The impact pulse for each of the tests was compared to each other and the required IIWPG pulse 3.6.1. This graph shows that there was very little variation between the pulses for each of the tests.

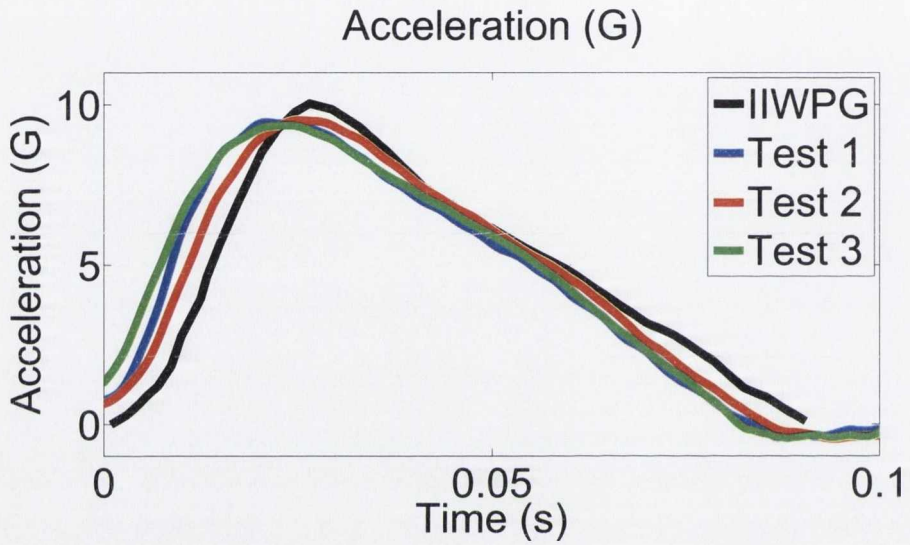


Figure 3.11: IIWPG Crash Pulse for Tests 1, 2 and 3

3.6.2 Occupant Response

The reaction of the dummy up to the time of contact with the head restraint (90ms) is expected to behave in the same manner for all tests and so this was evaluated. The acceleration outputs from these tests were found to correspond for the X component of acceleration, figure 3.12 and for the Z component, figure 3.13.

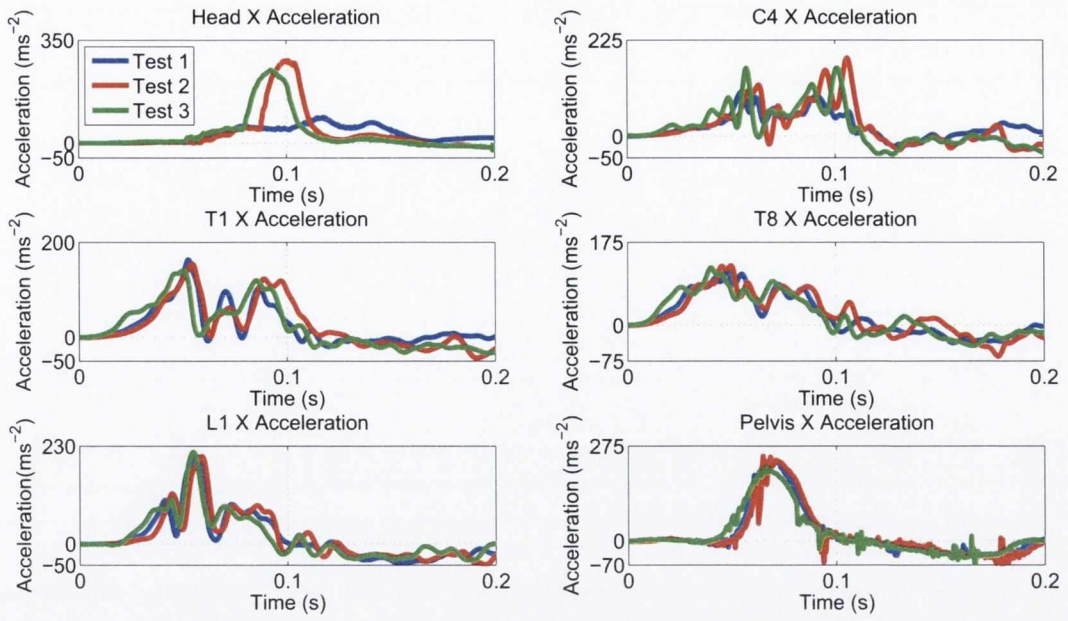


Figure 3.12: X component of acceleration for sled tests 1, 2 and 3

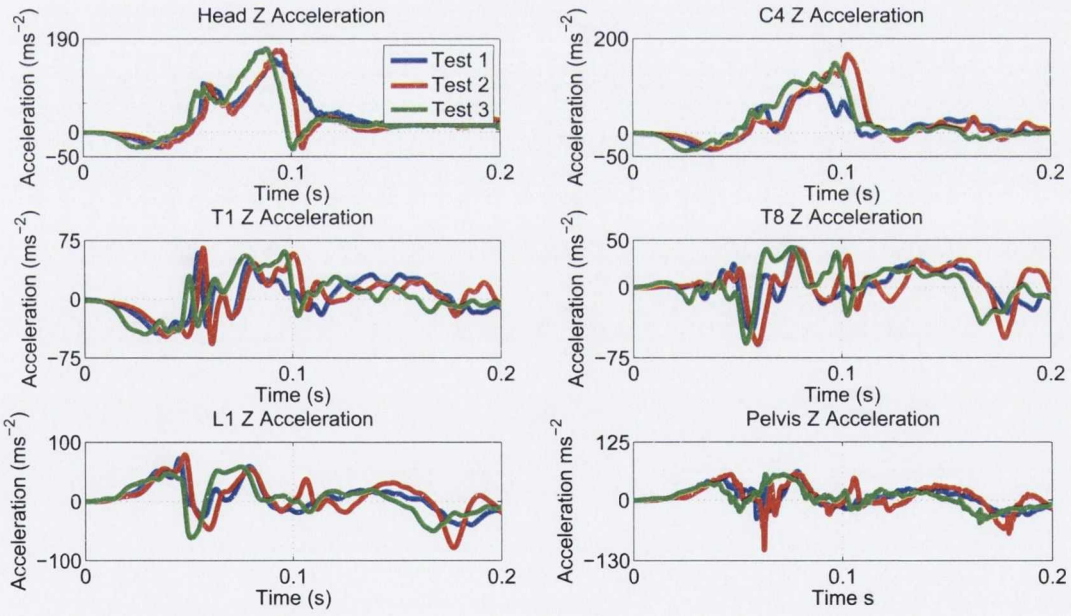


Figure 3.13: Z component of acceleration for sled tests 1, 2 and 3

The load cells in the lower and upper neck also produced similar outputs for the three tests 3.6.2 and 3.6.2 up to the time of contact with the head stopper.

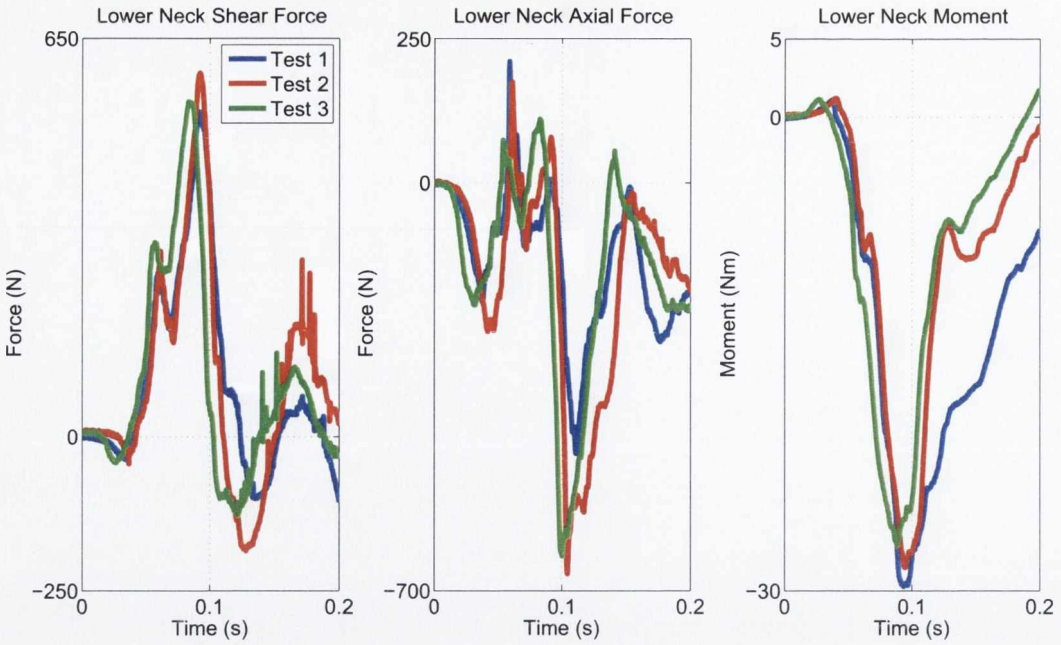


Figure 3.14: Lower Neck Shear and Axial Force and Sagittal Plane Bending Moment Responses for Sled Tests 1, 2 and 3

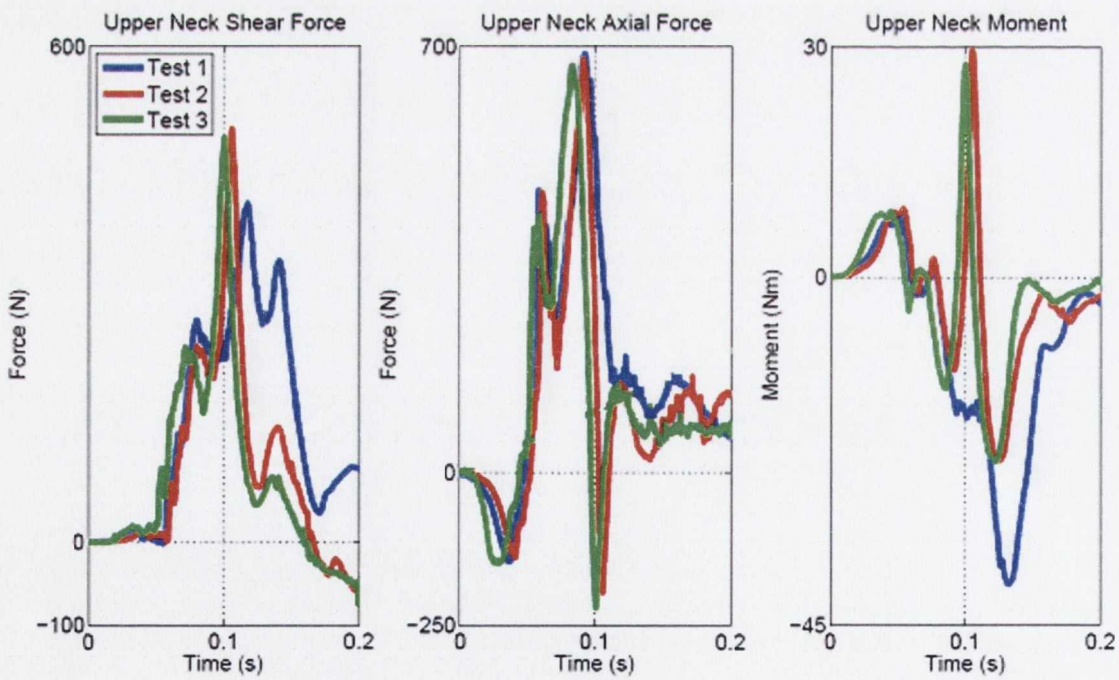


Figure 3.15: Upper Neck Shear and Axial Force and Sagittal Plane Bending Moment Responses for Sled Tests 1, 2 and 3

3.6.3 Wheelchair and WTORS Response

An accelerometer was placed on the wheelchair to trace its response in the crash, however it malfunctioned and this was only discovered after testing and therefore there is no data from this. To compare the displacement of the wheelchair in the physical and numerical tests the wheelchair angular and linear displacement was tracked on the video. To conduct this comparison the same point - A see figure 3.16 - was tracked. In the computational model a marker was placed at this point and it's linear and angular displacement was recorded over the duration of the test.

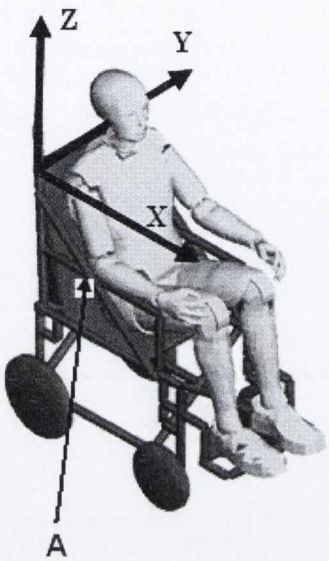


Figure 3.16: Madymo model of BioRID II wheelchair occupant showing coordinate system and location of armrest crossing point (A) for wheelchair displacement tracking.

The force-penetration characteristics of the wheelchair as well as its centre of gravity and moment of inertia were also required for the numerical model. These were determined from testing and the methods and results are presented in Appendix B.

The loading on the WTORS system was not recorded during the testing as this facility was not provided by the testing centre. However, the force-elongation response of the wheelchair tiedowns was determined, see Appendix B, and used to characterise the tiedowns used in the computational model. The tiedowns play a significant role in the controlling the displacement of the wheelchair, and so this measurement was also used to ensure that the tiedowns were modelled correctly. Due to the nature of a rear impact they are not loaded in the first 200ms of the crash and so their response was not modelled in this work.

The outputs from the test as presented in this Chapter provides information to validate the numerical model, which is presented in Chapter 5.

Chapter 4

Methods 2: Numerical Modelling

4.1 Introduction

This chapter details numerical modelling theory and how it is applied to create 3D models of crash tests. These models are an important tool that are broadly used in the automotive industry and wheelchair crash investigation. The computational models provide more information about a crash as extra outputs can be provided that might not be possible for sled tests as output sensors can be placed on any part of the model. They also provide a tool for investigating the effect that alterations to the vehicle or occupant would have on occupant response. These models are created using multi-bodies and/or finite elements and the fundamental mathematical principles upon which such complex models are based are provided and detailed in this chapter.

4.2 Numerical Model

To reproduce the test detailed in Chapter 3 the crash simulation software Madymo (Delft Inc. version 6.4.1 2007) was used in which the equations of motion of the modelled system are integrated using an explicit Euler integration procedure. Multi-bodies with assigned inertia properties are connected by kinematic joints, and idealized shapes (planes, cylinders and ellipsoids) as well as arbitrary surfaces using facet elements are available for visualisation and contact evaluation. Multi-body models predict kinematics and joint reactions without considering deformations.

A type of rigid surface element was used to model the outer skin of the dummy. These elements, known as facets, are a mesh of shell-type, massless contact elements and are connected to the rigid bodies of the model. They allow a more accurate geometric representation as they allow for contours and smooth surfaces.

Combined multi-body and facets can predict the dynamic loading imposed on a wheelchair and occupant during impact. The underlying methods of how this works is detailed in the following sections.

4.2.1 Multi-body Modelling

Investigations into complex models, such as the one presented in this work, reduce the components of the system to multibodies with assigned inertia properties which are connected by kinematic joints. The use of such representative components reduces the complexity of the model being investigated and can predict its kinematic response. The method used in this process is based on Newton's Second Law, equation 4.1, so that the acceleration of a body is based on its mass and the force applied to it.

$$F = ma \tag{4.1}$$

where, F is force, m is mass and a is acceleration.

The acceleration, a, in this equation can be replaced by the derivative of the velocity, v, which is denoted by $\frac{dv}{dt}$ to give:

$$F = m\frac{dv}{dt} \tag{4.2}$$

and since the mass of a body is constant

$$F = \frac{d}{dt}(mv) \tag{4.3}$$

MADYMO is based on Euler integration whereby the conditions of a body at a given time, t_2, is based on the conditions at the time previous t_1, and integrating equation 4.3 from time t_1 to t_2 produces:

$$\int_{t1}^{t2} F dt = mv_2 - mv_1 \tag{4.4}$$

or

$$mv_1 + \int_{t1}^{t2} F dt = mv_2 \tag{4.5}$$

The mv component of this equation is the linear momentum of the body. Equation 4.5 can be used to predict the momentum of a body at a time t_2, based on the momentum at t_1 combined with the resultant of all forces acting on the particle between the time t_1 and t_2. The total forces acting over the time interval between t_1 and t_2 which are denoted as Fdt is

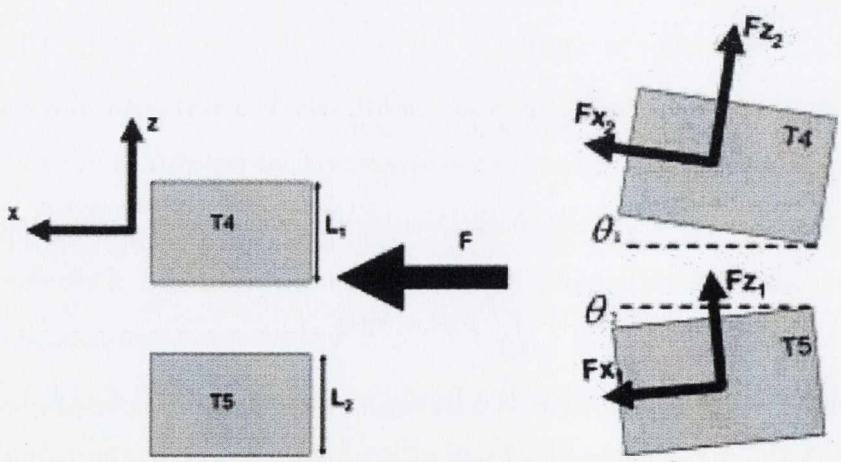
the impulse on the body. This is due to the interaction with other bodies and is based on the force penetration characteristics that are assigned to the contacting surfaces, which will be described in detail in a later section.

Time step

The time interval between integration points (t_1 to t_2) play an important role in determining the accuracy of the model. A smaller time interval produces more detailed results as the motion and interaction of the components of the model are determined at more frequent intervals, however this is more computationally expensive. Therefore there is a trade-off between precision of the model and the length of time to complete the simulation. However by investigating the outputs from the model accurate results can be obtained at a given time step, with little improvement found at a smaller time step. The chosen time step must produce non-significant differences when compared to the outputs from the simulation run at a smaller time step. This time step value is then said to be conditionally stable when this is achieved. In this manner a good compromise between accuracy and computational time can be established.

4.3 Kinematic Joints

For the joints connecting rigid bodies of a model there are related constraint forces and torques. As an example the forces and torques are calculated for a joint between two vertebrae in the spine. This is conducted for the fourth and fifth thoracic vertebrae, (T4 and T5), where T4 is impacted with a force, see figure 4.1(a). The applied force due to impact cases displacement and rotation of T4 and the connected vertebra T5, see figure 4.1(b).



(a) (b)

Figure 4.1: Example of how MADYMO Works

The force applied is in a single direction and in the numerical model of the spine the vertebra can rotate about a single axis. Therefore the constraint forces and torques, ignoring inertia, are:

$$Horizontal\ Forces: \ F_{x1}\cos\theta_1 + F_{x2}\cos\theta_2 = F \tag{4.6}$$

$$Vertical\ Forces: \ m_1 g + F_{z1}\sin\theta_1 + m_2 g + F_{z2}\sin\theta_1 = 0 \tag{4.7}$$

$$Torques: \ F_{x1}\cos\theta_1 \frac{L_1}{2} + F_{x2}\cos\theta_2 \frac{L_2}{2} \tag{4.8}$$

Where L_1 and L_2 are the heights of the vertebrae. The centre of gravity of the these bodies is positioned in their centres, and so the moment acts over $\frac{L_1}{2}$.

The inertia of the adjacent vertebra reduce the acceleration passed through the spine due to this point application of load, F. The force, F acting on the bodies is due to interaction with the contact surfaces, this process is detailed in the following section.

4.4 Contacting Surfaces

The contact interactions used are based on the force versus penetration characteristics assigned to the contacting pair. There are many modelling assumptions available as part of the MADYMO package to replicate the interaction of contacting surfaces.

The first assumption that has to be determined is which surface is the penetrated surface and which is the penetrating surface. The level of deformity of the more pliable material is modeled as penetration into that surface. The level of penetration is based on the force applied to the surface. This interaction can be based on the characteristic assigned to either contacting surfaces or a combination of the characteristic of the two interacting surfaces. The resulting force penetration characteristics are used to determine the penetration level associated with the applied force.

An unloading curve can also be assigned to the model which also allows for the inclusion of hysteresis. The energy dissipated during contact is modelled using hysteresis which can be defined using a hysteresis slope which connects the loading and unloading curves. The unloading of a material is based on the energy absorbance of the material. A coefficient of friction and damping can also be introduced based on testing. Friction is a velocity dependent characteristic. The resistance to movement is based on the mass and the materials that are

interacting. Damping can also be assigned and is used to model the restitution of the surfaces and high values reduce the "bounce" of the material.

4.5 BioRid II computational model

The computational model of the BioRID dummy was developed by Chalmers University of Technology. The physical dummy has been validated against volunteer and cadaver tests and the numerical model is a representation of this [16], [19]. The shoulder and hip joint are represented by spherical joints which allow 3 degrees of motion. The joints of the spine are represented by revolute joints which allow motion in the sagittal plane only. This corresponds to the physical dummy which was created to allow movement due to a zero offset rear impact which results in movement in the direction of the crash only.

The model of the BioRID II was created and validated by comparison to tests of the entire dummy as well as its components [21]. The articulation of the cervical, thoracic and lumbar spine as well as the force-penetration characteristics of the surface of the model was determined and modelled in MADYMO. These characteristics are encrypted due to the level of work required to determine them and are copyright of MADYMO. This can make the modelling process more complex as the response of the occupant is produced based on unknown parameters.

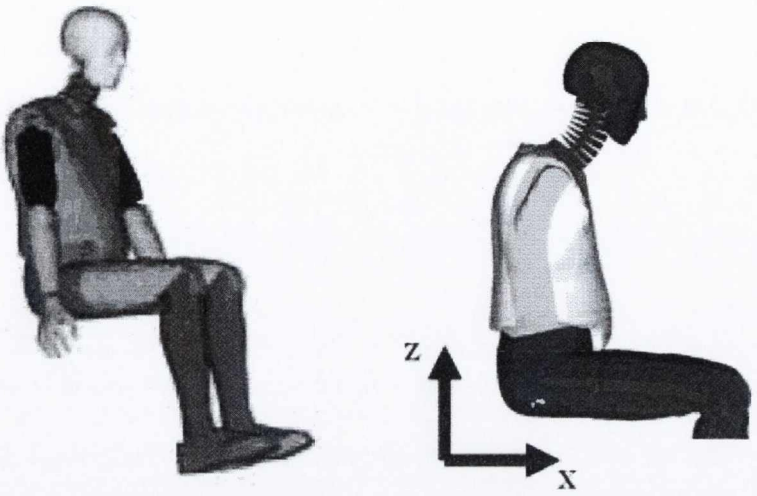
In this numerical model accelerometers and load cells can be placed on it at any specified point, the signal produced from which can be used to compare with those of the physical test and so can be used for validation of the simulation.

4.5.1 Thoracic and Lumbar Spine

In the BioRID II the spine is divided into cervical, thoracic and lumbar sections and the vertebrae of each region are of uniform size and shape. The lumbar vertebrae are the largest with the size reducing in the thoracic region and the smallest vertebrae are in the cervical spine. The joints of the spine are revolute joints which allow rotation only in the sagittal plane. While this is not anatomically correct the BioRID II was created and validated for investigating impacts with a 0^o offset which results in motion in this plane only.

The multi body model is covered with facet element skin which allows for better interaction with the surfaces. These facets are 2D rigid surface elements. These shell-type massless elements allow for better interaction with the contacting surfaces as well as smother graphical representation of the model. The skin is modelled as sections which cover different regions of the occupant these are the head, neck, torso, pelvis, arm, legs and shoes, see figure 4.2(a).

These sections can then be defined as interacting with other surfaces. The region of the skin covering the torso is referred to as the jacket.



(a)BioRID II Sections

(b)BioRID II Torso and Spine Interaction

Figure 4.2: BioRID II

This jacket is connected to the vertebrae using planar joints which restrict any out of plane motion of the torso. These planar joints allow motion in the sagittal plane only, figure 4.2(b). A stiffness is assigned to these joints to replicate the reaction of the physical BioRID II occupant to loading. When the torso makes contact with a surface the jacket is displaced according to its stiffness and this displacement is passed via the planar joints to the vertebrae which rotate about their axis to allow movement of the spine.

Facet Element Skin

The facet element skin used on the surface of the BioRID II occupant is used for visualisation purposes, whereas the contact interactions between the occupant and its surroundings is modelled as a mulitbody interaction rather than a finite element interaction. This reduces the complexity of the interaction as it does not take into account any deformation. The force passed from the jacket is based on the surface stiffness characteristics assigned to it.

4.5.2 Cervical Spine

The head and neck represent a complex physiological interaction as there are many soft tissues (muscles, tendons and ligaments) as well as hard tissues (facet joints of the vertebrae) which control its motion, see Chapter 2.

This complex motion is not only controlled by the characteristic assigned to the revolute joints of the neck but also by built in muscle substitutes which control the rotation of the

neck. These are modelled as belts which have been tuned to control the rotation of the neck and they extend from the thoracic region of the spine to the cervical region, see figure 4.3. These are modelled as belts and the response is based on a force-elongation characteristic which controls the movement of the head and neck.

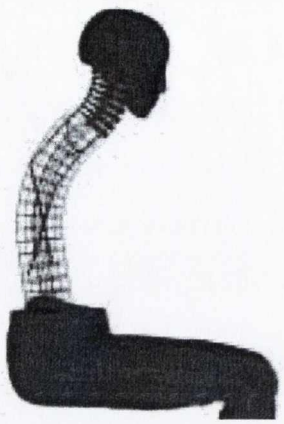


Figure 4.3: BioRID II Muscle and Dampers

This model has been validated for use in a rear impact, see Chapter 2. Its application in the wheelchair rear impact model created for this work is detailed in the following chapter.

Chapter 5

Results 1: Validation of Model

5.1 Introduction

The validation of the rear impact model is based on the kinematic and dynamic response comparisons of the model with the physical test. The numerical model was checked in terms of the animation output to ensure that the model behaves in the same way as the video of the sled test. An iterative process was conducted to correlate the kinematics of the numerical model with those of the sled testing. This process was based on a comparison of the video and animation outputs to ensure that they correspond, which is then followed by an analysis of the acceleration, force and moment outputs from the model and those of the sled tests.

For this type of comparative analysis apparent visual differences in the simulation video would correspond to large differences in the kinematic response and so the parameters which best represents the physical test can be easily identified. However, when the simulation video and the sled test video are similar the kinematics of the models are compared to those of the sled test. The accelerations, forces and moments of the occupant from the numerical and physical tests were compared for each variation of the parameters that were investigated with the aim of matching the numerical outputs to those of the sled tests. This process investigated which combination of parameters were best for use in the model to validate it against the sled test. This part of the study was motivated by the need to choose physically real parameters where possible. The initial values used for the unloading curves, hysteresis slopes and friction were based on those of the validated MADYMO models and literature [103] which investigated similar models, these values were then investigated to create the computational model which best represents the sled tests.

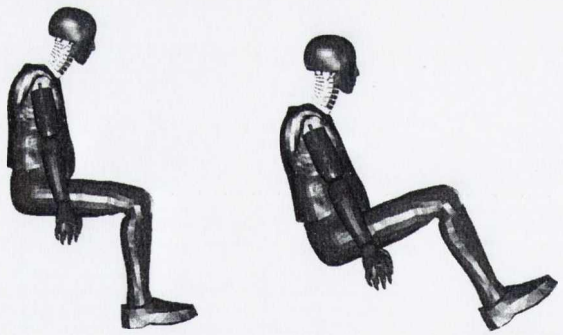
The acceptance of the validation of the model was based on the correlation of the graphs of the physical and numerical outputs. The percentage difference between the peak values and the timing of the peak values was determined. The differences found in this model were compared to other published work to ensure they were within an acceptable range.

A comparison was made with the validation of the BioRID II occupant [19] and other wheelchair computational models [22], [23],[47] and [48]. From these published works the upper limit of the acceptable difference in peak value is 20%. The difference in the timing of the peak values was found to be up to 16% and so this is the upper limit of difference that was deemed accpetable for the model presented in this work.

This process produced a valid model for a rear impact of a BioRID II occupant in a surrogate wheelchair subjected to the IIWPG 10g pulse [102]. The model was validated using the acceleration and force outputs from the occupant. These components can be used to predict the level of injury and therefore the rear impact model is validated for determining injury. The validation process of the model is presented in this chapter.

5.2 BioRID II Occupant

The BioRID II occupant was created by MADYMO in the seated posture which is slightly slumped forward, see figure 5.1(a). The dummy is then rotated to be in the required posture of a 26^o tilt in space, figure 5.1(b). This produces the straight lumbar spine, kyphosis of the thoracic region and the lordosis of the neck which was found to be representative of seated vehicle occupants [16].



(a)Original Position of BioRID II

(b)BioRID II orientated by 26^o

Figure 5.1: BioRID II

To position the dummy in the seat a drop simulation was conducted. This places the buttocks just above the seat of the wheelchair and the thoracic spine almost in contact with the seatback. The occupant is then dropped under gravity into the seat. This drop simulation dissipates the energy due to contact between the two to produce a force balanced system and the end position is that of a seated occupant at rest. The position of the joints from this pre-test simulation are used as the initial positions for the crash simulation.

5.3 Wheelchair

The wheelchair was created to replicate the ISO surrogate wheelchair that was used in crash testing. The video analysis of the crash test shows minimal deformation of the wheelchair and so it was modelled as a rigid structure. The computational model was created based on geometric, inertial and mass measurements taken of the wheelchair. The contact characteristics that were determined from testing of the components (see Appendix B for details) were assigned to the relevant parts. The outputs from the other physical tests of the wheelchair which were conducted - determination of centre of gravity and moments of inertia - were also assigned to the model (see Appendix B for details).

The model is composed of rigid bodies and related ellipsoids with geometry assigned to each. The ellipsoids represent each bar that was welded together to form the physical wheelchair. These sections were connected by bracket joints which do not allow any motion between the connected parts. To prevent a closed chain being created some sections of the wheelchair were connected by very stiff point restraints. The sections of the wheelchair were all then connected to a central body positioned at the centre of gravity. The mass and the inertia properties of the wheelchair, as determined from testing, was then assigned to the central body. This process created the rigid structure used for the sled tests, as shown in figure 5.2.



Figure 5.2: Computational Model of Wheelchair

5.3.1 Wheelchair Contacting Surfaces

Planes are used for contact interactions as they provide a better interaction with the facet surface of the occupant. The findings from testing the wheelchair were used to determine the interactions of the wheelchair and occupant as well as the wheelchair and the sled.

Within MADYMO there are many parameters that can be altered in the modelling process to represent the physical tests. The characteristics which have the greatest significance on the result are:

- Contact Characteristic
- Unloading Curve
- Hysteresis slope
- Coefficient of friction
- Time Step

Each of these parameters was investigated and this section details a sample comparison of the video and animation output. Also presented in this section is the effect that certain parameters have on the kinematic response of the occupant. The differences due to the different parameters are shown for the acceleration time history graphs of the head, first thoracic vertebra (T1), first lumbar vertebra (L1) and the pelvis. These are presented for the areas of investigation as they are a good representation of the kinematics of the model as a whole. The X direction was selected for presentation as it is the direction of the applied loading and this was found in the validation process to be of most significance as injury criteria are based on the loading in this direction [15] [27].

5.3.2 Wheelchair Contact Characteristic

Occupant to Seatback

The interaction of the occupant with the seatback is detailed in this section. The built in characteristic of the torso and pelvis were found to be too compliant to model the contact between them and the seatback, figure 5.3 model 1. These characteristics allowed for an increased level of deformation of the torso which did not replicate the reaction of the occupant in the sled tests. Therefore the characteristic of the seatback, model 2, was used, see figure 5.3.

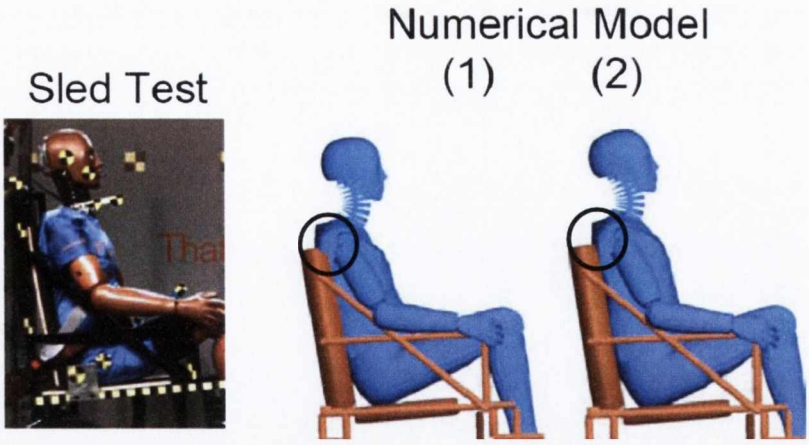


Figure 5.3: Comparison of Characteristics used for Seatback; Model 1 Allows Excessive Penetration in the Seatback which is not Representative of the Sled Test

5.3.3 Unloading Curve

The seatback unloading curve of one half of that of the loading curve was found to produce results that better matched the physical tests. The unloading curve was investigated and a value of one tenth of that of the loading curve was found to produce a response which has too much energy absorption. Figure 5.4 shows that model 1 resulted in a prolonged contact between the occupant and the seatback which did not match that of the physical tests. However the results for when the unloading curve is one half of that of the loading curve, model 2 in figure 5.4, was found to have a better correspondence of the results.

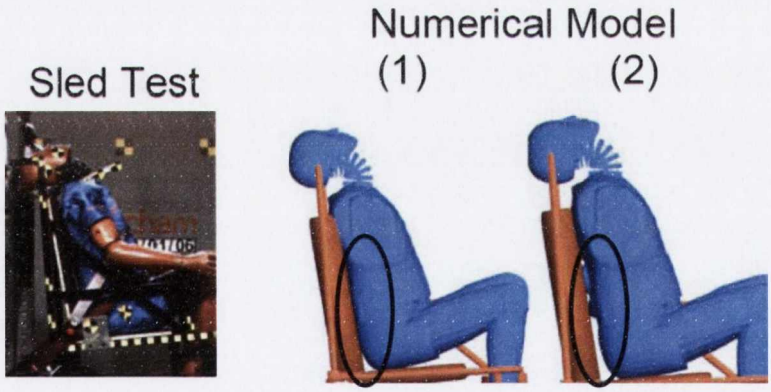


Figure 5.4: Comparison of Unloading Characteristic used for Seatback; Model 1 Results in Prolonged Contact with the Seatback which is not Representative of the Sled Test

5.3.4 Hysteresis slope

The comparison of 2 different hysteresis slopes, that were used in the contact characteristic of the seatback, are presented in figure 5.5. A slope of 1e6 was found to produces a better replication of the physical tests when compared to a slope value of 1e8. While both outputs

show similar trends in the graphs, the peak values are seen to be closer to the experimental values for the 1e6 hysteresis slope value.

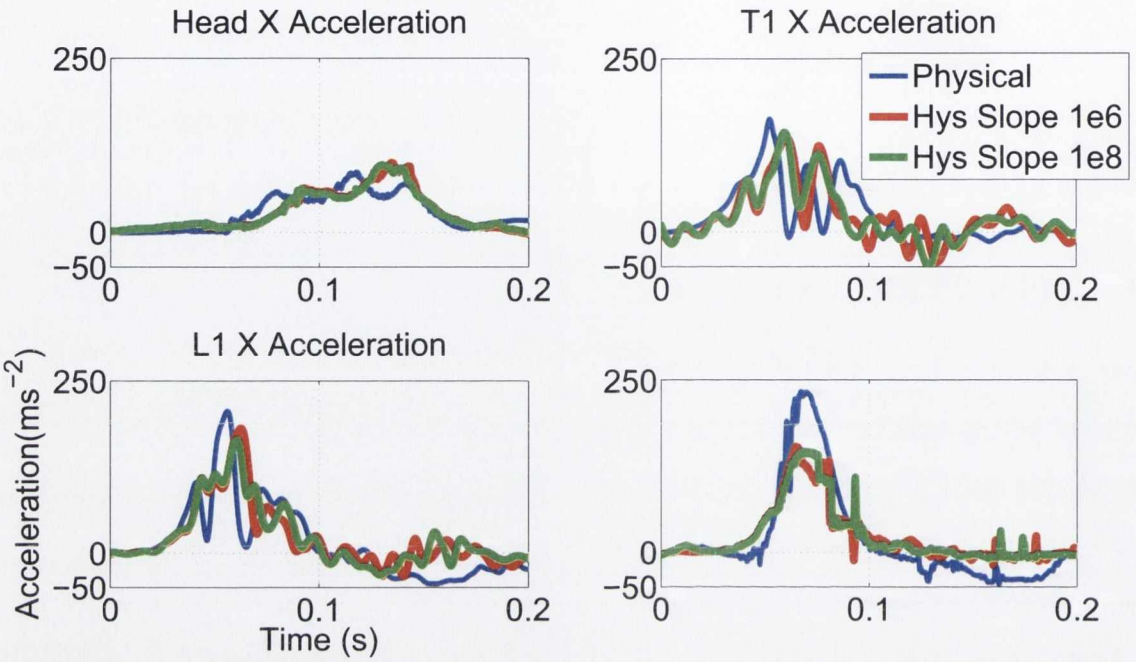


Figure 5.5: Comparison of Response for Different Hysteresis Slope

5.3.5 Coefficient of friction

The effect of altering friction is presented in the time history graphs of the occupant, figure 5.6. This figure shows the difference between the two models most clearly in the pelvis. This region is altered when a larger friction coefficient (0.7) is introduced and the response was seen not to correspond to the physical tests. However better results for a value of 0.4 were found when compared to the output from the physical test.

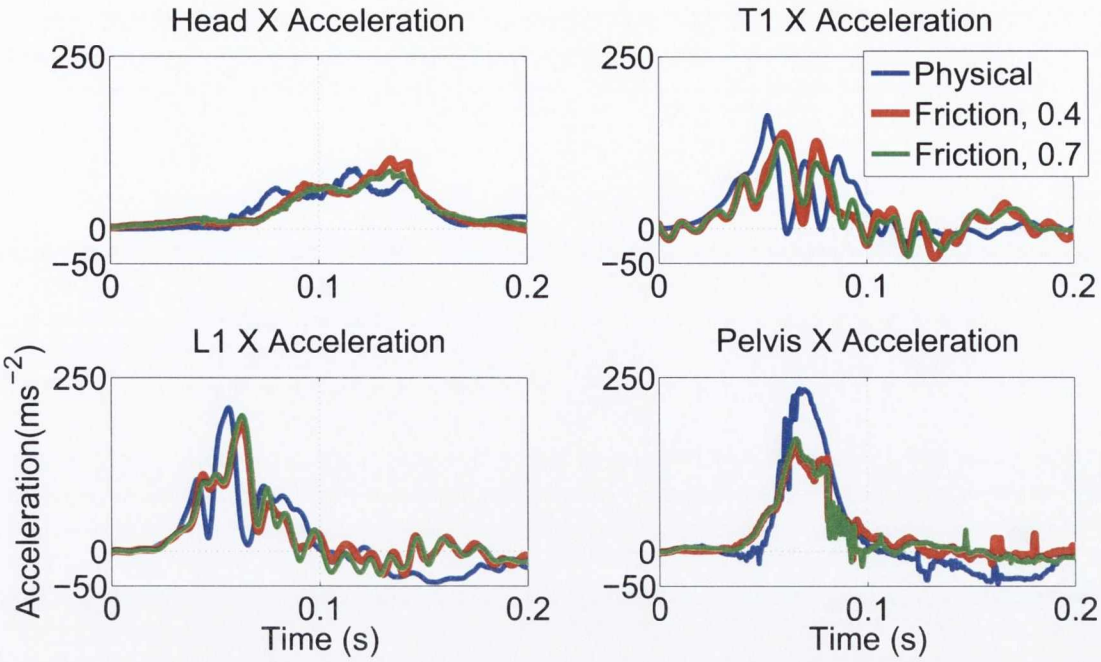


Figure 5.6: Comparison of Response for Different Coefficient of Friction

5.3.6 Pelvis to Seat

The interaction of the occupant and seat was found to be the most complex as in the physical tests the occupant's buttock was seen to move rearwards and realign under the lumbar spine as shown from the snapshot taken at 100ms, figure 5.7. This pattern of behaviour was found to be the most challenging aspect of the modelling process.

The characteristic of the seat, as determined from the force penetration tests, was used initially to model this interaction, however, this was found not to reproduce the required motion, see figure 5.7 model 1.

The characteristic assigned by MADYMO to the pelvis was found to more accurately reproduce the reaction of the pelvis as it slides along the seat to realign under the lumbar region of the spine, however there was still some large discrepancies between the physical and numerical model. To improve upon the response of the occupant the encrypted force penetration characteristic that was assigned by MADYMO was determined by reverse engineering. The output forces and penetration between the pelvis and seat were used as input into the characteristic of the contact and was found to produce the same kinematic result. Extensive testing of the response of the dummy when the pelvis to seat interaction was altered by adjusting different parameters improved upon the results. This iterative process involved investigating the unloading curve, hysteresis slope and friction. This produced the response of model 2 in figure 5.7 which was found to correspond to the reaction of the pelvis in the sled testing.

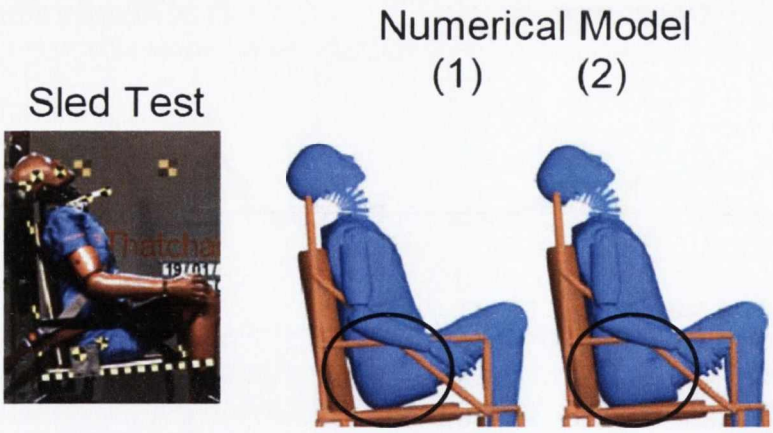


Figure 5.7: Comparison of Characteristic used for Pelvis

5.4 Wheels to Sled Contact

The interaction of the wheels and sled was also investigated. An example of a parameter that was investigated for this interaction is the unloading curve. The wheels of the wheelchair produced more accurate results when a one tenth unloading characteristic is used, figure 5.8 model 2. When a value of one half was used (model 1) a greater vertical displacement was found as shown in rear wheels which are no longer in contact with the sled surface at 140ms. This does not correspond to the physical tests, whereas the response of model 2 better replicates the reaction of the wheels as they are seen to be deformed as found in the sled tests.

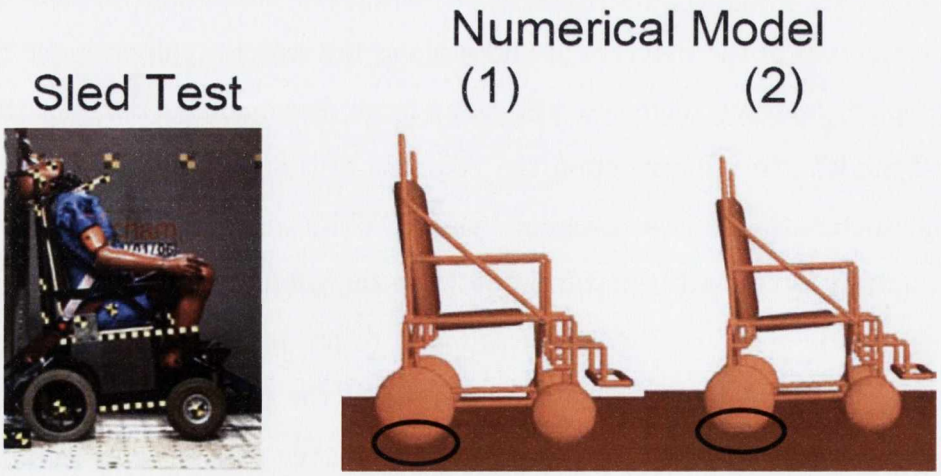


Figure 5.8: Comparison of Unloading Characteristic used for Wheels; Model 1 Shows no Contact with Sled Surface at 140ms Whereas The Wheels in Model 2 are Deformed due to Contact between the Sled and Wheelchair

5.5 Tie downs

The tie-downs were placed in the same position as that of the physical tests, see figure 5.9. These were also assigned the characteristics that were determined from the physical tests.

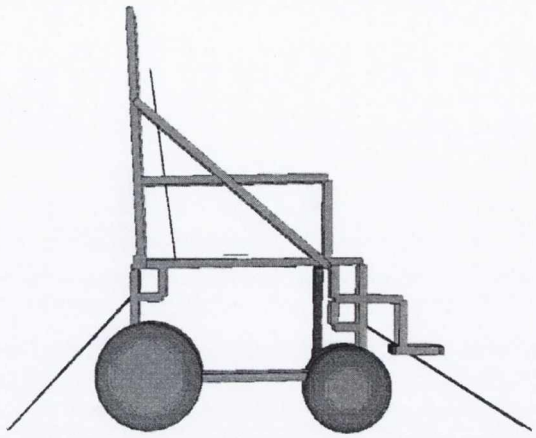


Figure 5.9: Tiedowns on Wheelchair in Computational Model

5.5.1 Tie Down Characteristic

In the same manner as for the contacting surfaces of the wheelchair the charactertisic of the tiedowns was investigated to determine the optimal parameters. The response due to an altered unloading curve and hysterseis slope were investigated and found to have minimal effect on the response of the model, this is due to the stiffness of the material. The influence of an altered unloading curve or hysteresis value is therefore not readily seen in their response.

5.6 Modelling Parameters

The results from these iterative processes determined the set of parameters which best replicated the response of the wheelchair and occupant in a rear impact. The characteristics assigned to each of the components are presented in the following sections.

5.6.1 Seatback to Occupant Interaction

The interaction between the torso and the seatback was modelled using the seatback response from testing with an unloading function that is one half of the loading curve and a hysteresis slope of 1e6, see figure 5.10.

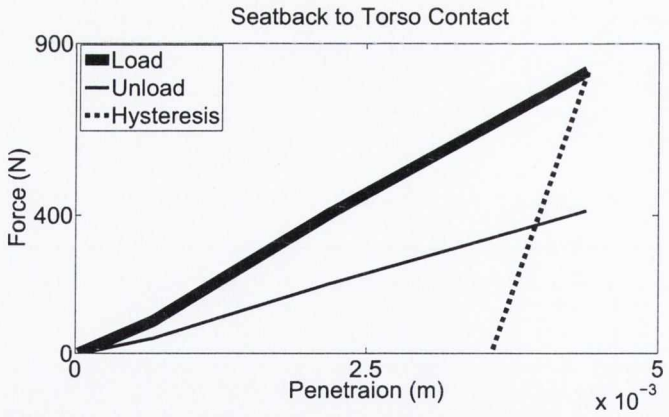


Figure 5.10: Seatback to Torso Interaction

The coefficient of friction in the interaction between the pelvis and the seatback was determined to be 0.4. Friction was also added to the interaction between the seatback and the torso of 0.7. The values of friction were different due to the material of construction under the clothes of the occupant which have an effect on the friction.

5.6.2 Seat to Pelvis Interaction

The reaction of the pelvis on the seat was found to be best represented when using the characteristic assigned to the pelvis group that is then slightly altered. An unloading curve of one half of that of the loading curve and a hysteresis slope of 2e6 was also implemented, see figure 5.11. Friction was also added to the interaction between the pelvis and the seat was assigned to be 0.4. A friction coefficient value of 0.4 was used for the pelvis to seat interaction based on experimental testing and computational models [103].

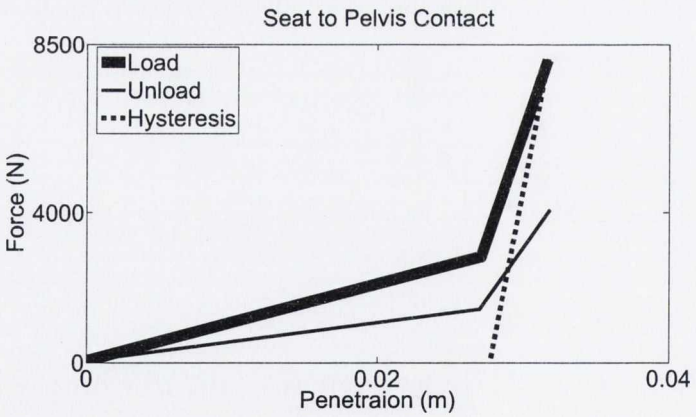


Figure 5.11: Pelvis to Seat Characteristic

5.6.3 Feet to Wheelchair Interaction

The feet contact the wheelchair and this was modelled using parameters based on a similar iterative process. There is initial contact between the feet and footrest and this was modelled

using the MADYMO defined characteristic of the shoe. A coefficient of friction of 0.2 was added to this encrypted characteristic to better replicate the behaviour of the feet in the rear impact. There is a second contact between the feet and the wheelchair as they move rearwards and connect with the cross members under the seat. This contact was defined by the characteristic of the rigid sections of the wheelchair.

5.6.4 Additional Occupant to Wheelchair Contacts

Contacts were also set up between the occupant's limbs and the sides of the wheelchair, to represent any contact that may occur. The interaction of the occupant with the wheelchair in these regions was found to be minimal and did not overall alter the kinematics of the occupant. Also the altered posture of the scoliotic occupants resulted in curvature of the spine in all three principle directions resulting in a wider occupant. This is seen for the severe scoliosis occupant model, figure 5.12. To accommodate for this wider occupant without altering the validated wheelchair model the contacts between the sides of the wheelchair and occupant were removed. The kinematics of the occupant (whether scoliosis was present or not) were largely unaffected by the presence or the absence of these contacts.

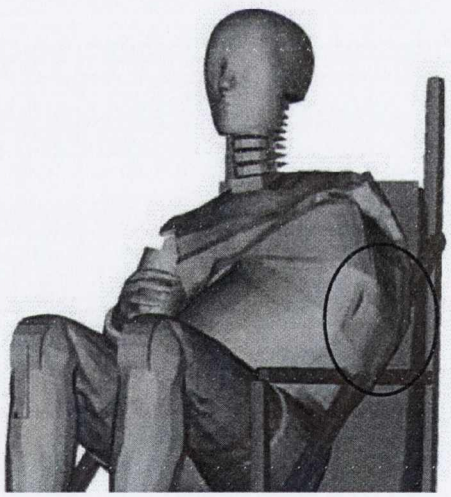
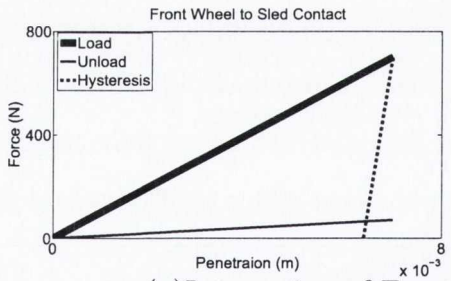


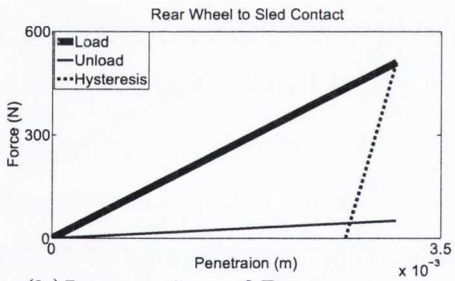
Figure 5.12: Severe Scoliosis Occupant in Wheelchair

5.6.5 Wheels to Sled Contact

The interaction of the wheels and the sled was created for the two different types of wheels which were used on the wheelchair. The front wheels were pneumatic whereas the rear ones were constructed of rubber. The interactions that were used for the front and rear tyres are presented in figures 5.13(a) and (b).



(a)Interaction of Front Wheels and Sled



(b)Interaction of Rear Wheels and Sled

Figure 5.13: Wheels to Sled Interaction

5.6.6 Tiedowns

The parameters for the tiedowns were determined to be one tenth of the loading curve for the unloading curve and a hysteresis slope of 1e8, see figure 5.14.

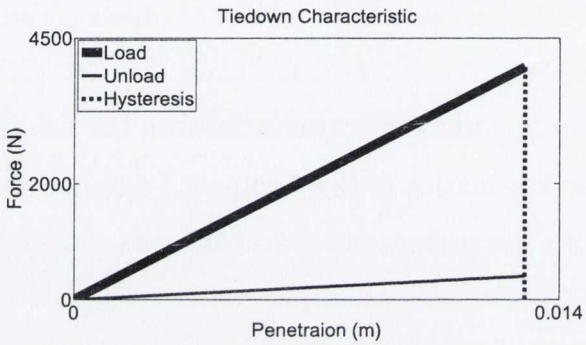


Figure 5.14: Tiedown Characteristic

5.7 Time Step

The time step used for the analysis plays an important role in reducing the integration error in the model and to prevent any data from being lost. A smaller time step produces more detailed results as the integration process is conducted in smaller intervals, however this is more computationally expensive. A parametric study of the time step for use in the model to determine the results and reduced computational time was conducted. This process determined the time step value of ($1e10^{-6}$) for use in this study. At this level there is little improvement found when a smaller time step ($5e10^{-7}$) is introduced. The $1e10^{-6}$ value is therefore a good compromise between accuracy and computational time. The comparison between the two different time step models is shown in figure 5.15.

The $1e10^{-6}$ time step was also compared to a larger time step to determine the influence this would have. The results are shown in figure 5.16 comparing the selected value to a larger time step ($5e10^{-5}$) and shows that there is variance in the results and that the larger time step is not suitable for use.

The $1e10^{-6}$ was therefore used as it was determined to produce accurate results with all peak values recorded and a smaller time step would not improve upon this. The simulation is therefore termed conditionally balanced.

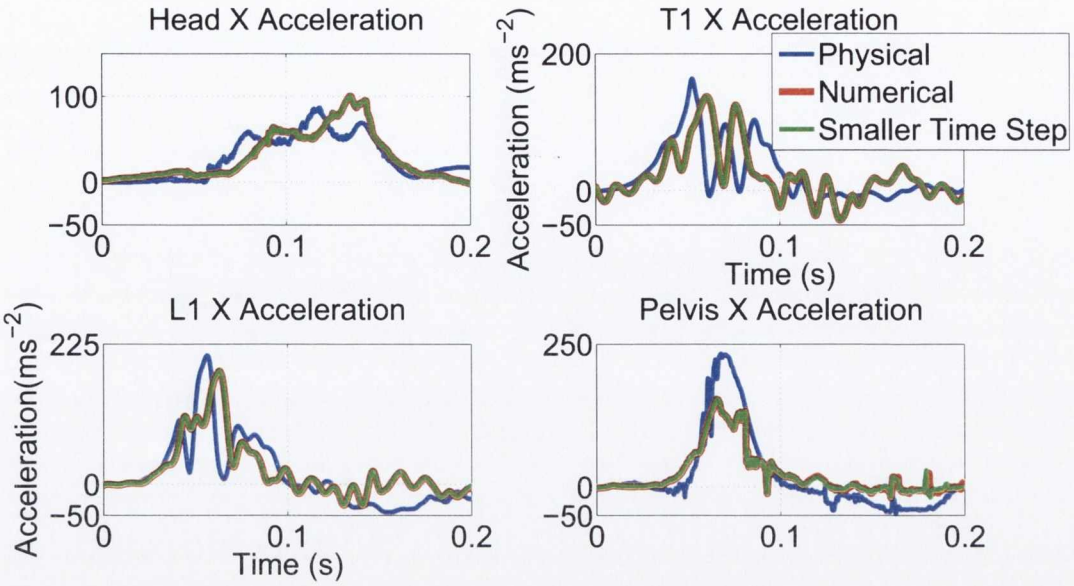


Figure 5.15: Comparison of Simulation and Smaller Time Step

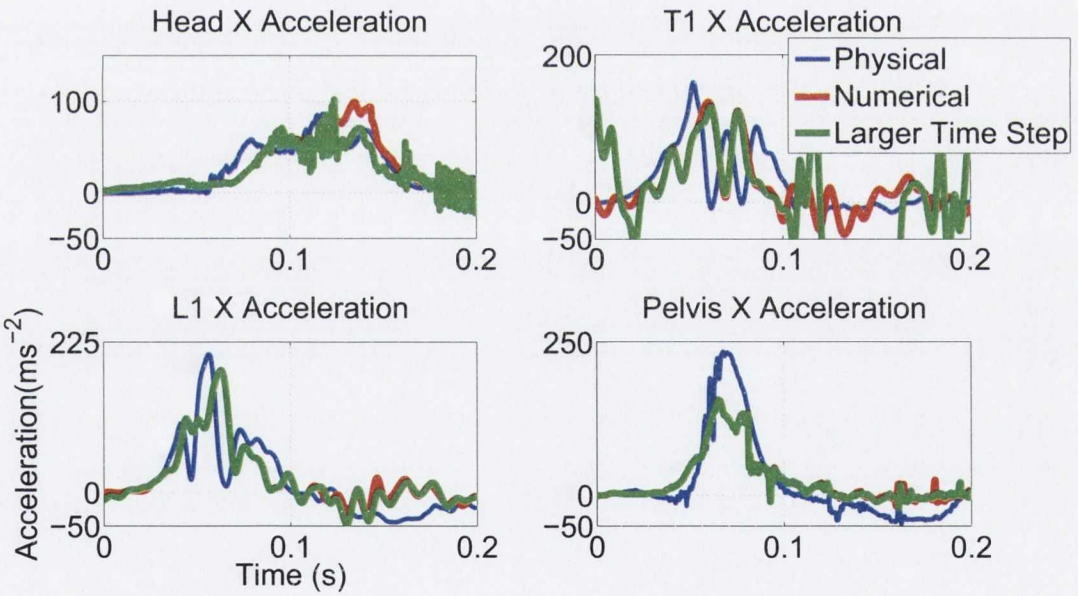


Figure 5.16: Comparison of Simulation and Larger Time Step

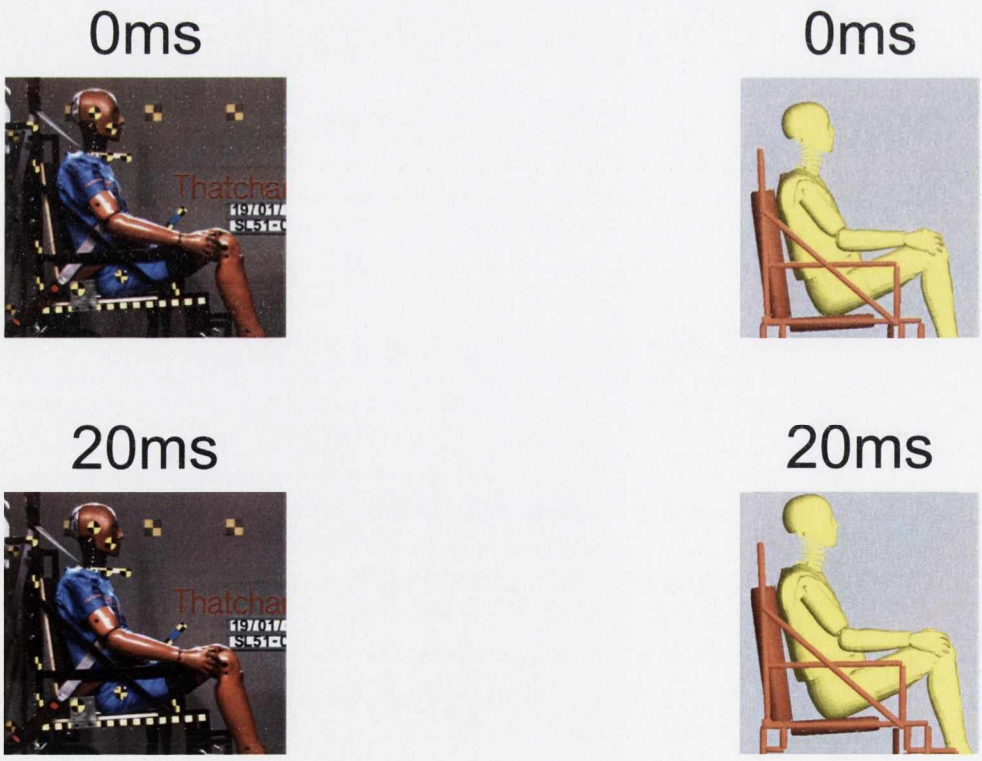
5.8 Summary

The combination of these parameters were determined to produce a model representative of the physical test. The quantification of the correlation between the model and experimental outputs is presented in the following section.

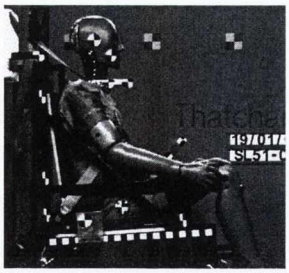
Since this process was conducted, work by Ha et al has been published on the development and validation of a frontal impact wheelchair model with a child occupant [22]. Ha's work shows a similar process in determining the parameters for use as the trends and peaks values of the output data as well as a visual comparison were used for developing the model.

5.9 Validation - Visual Comparison

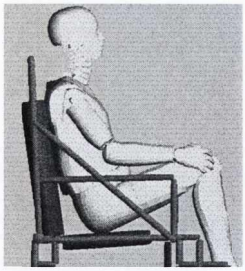
A visual comparison of the simulation and the physical rear impact sled test at 20ms time steps is given in 5.9. Good kinematic correspondence is in evidence in all stages of the test, with both the model and the dummy passing through the same range of motion. Key features such as duration of contact between the dummy's pelvis and lumbar region with the seatback were determined, table 5.1. The motion pattern of the dummy's pelvis also corresponded well which exhibited rotation and realigning under the lumbar spine.



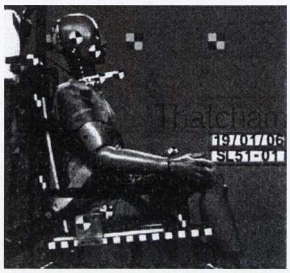
40ms



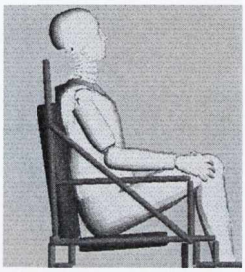
40ms



60ms



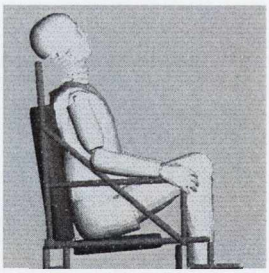
60ms



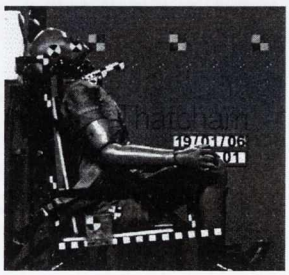
80ms



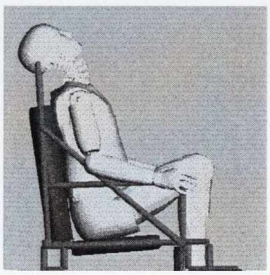
80ms



100ms



100ms



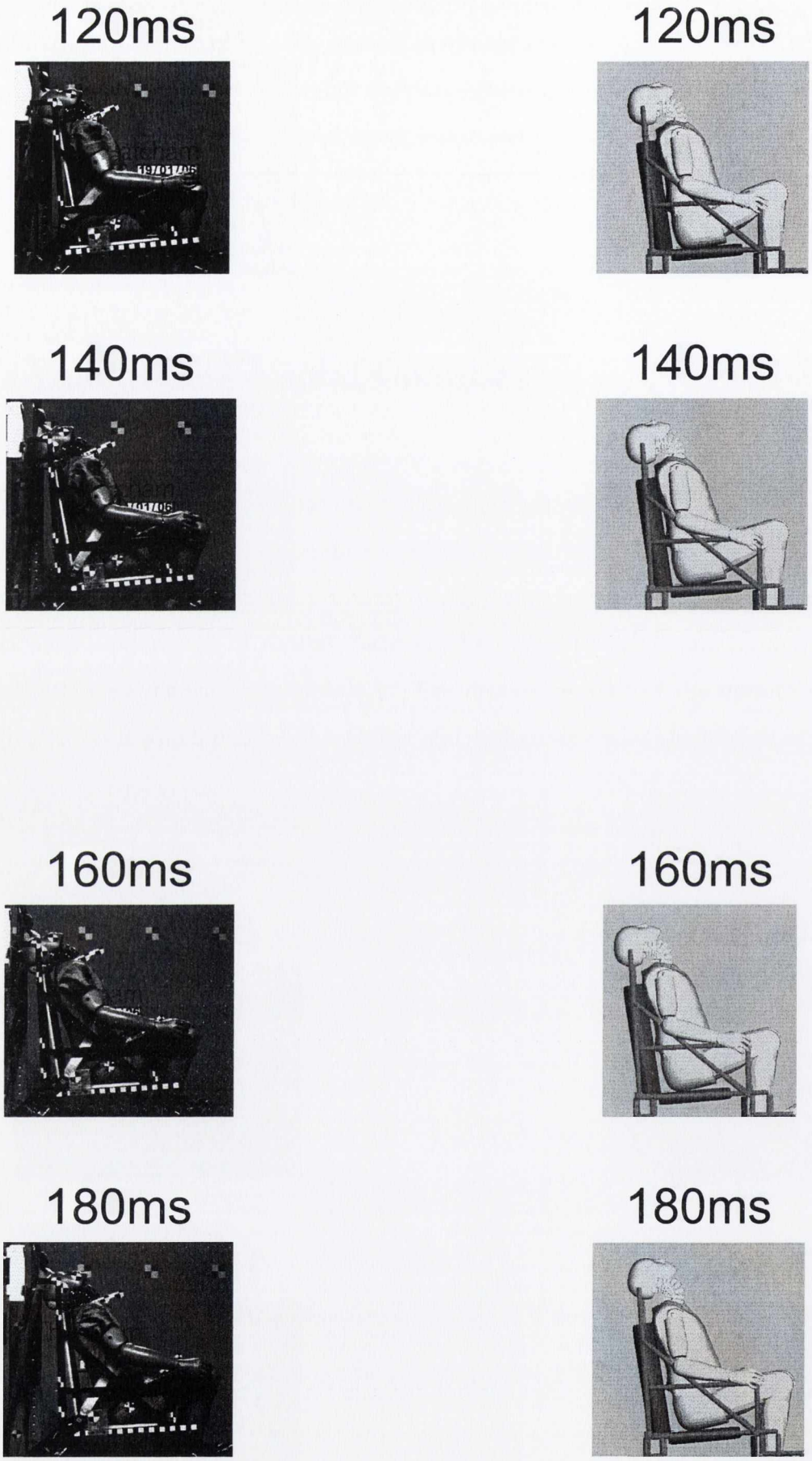


Figure 5.17: Comparison of Sled Test and Numerical Animation

	Sled Test Time (ms)	Numerical Model Time (ms)
Pelvis and Seatbak	70-114	76-116
Lumbar Region and Seatback	50-140	51-131

Table 5.1: Duration of Contact Between Region of the Occupant and Wheelchair

The hyperextension of the neck was also found to occur in both, as seen in figure 5.9. Maximum extension of the head and neck was found to occur at similar time, 140ms, in the physical and numerical tests. The angle that the head passes through relative to the first thoracic vertebra (T1) was also found to correspond well, table 5.2, with an average difference of 8%.

Time (ms)	Sled Test Angle (degrees)	Numerical Model Angle (degrees)	Percentage Difference
40	31	35	13
80	46	40	13
120	53	50	5
140	55	51	7
180	50	48	4
Average	47	45	8

Table 5.2: Angle of Rotation of Head Relative to First Thoracic Vertebra (T1)

5.10 Validation - Time History Comparison

In this section the simulation results are compared to sensor outputs from the physical tests to assess the validity of the model in more detail. The predicted values from the computational model are compared to the experimental corridors up to 80ms, after which only Test 1 is shown, since contact with the head stopper has occurred in the other two sled tests, as explained in Chapter 3.

Figure 5.18 shows the body local X (initially forward direction) accelerometer time histories from the physical test and the model for the head centre of gravity (cg), the fourth cervical vertebra (C4), the first and eighth thoracic vertebra (T1 and T8) and for the pelvis. Figure 5.19 shows the equivalent Z (initially vertical direction) accelerometer time history data.

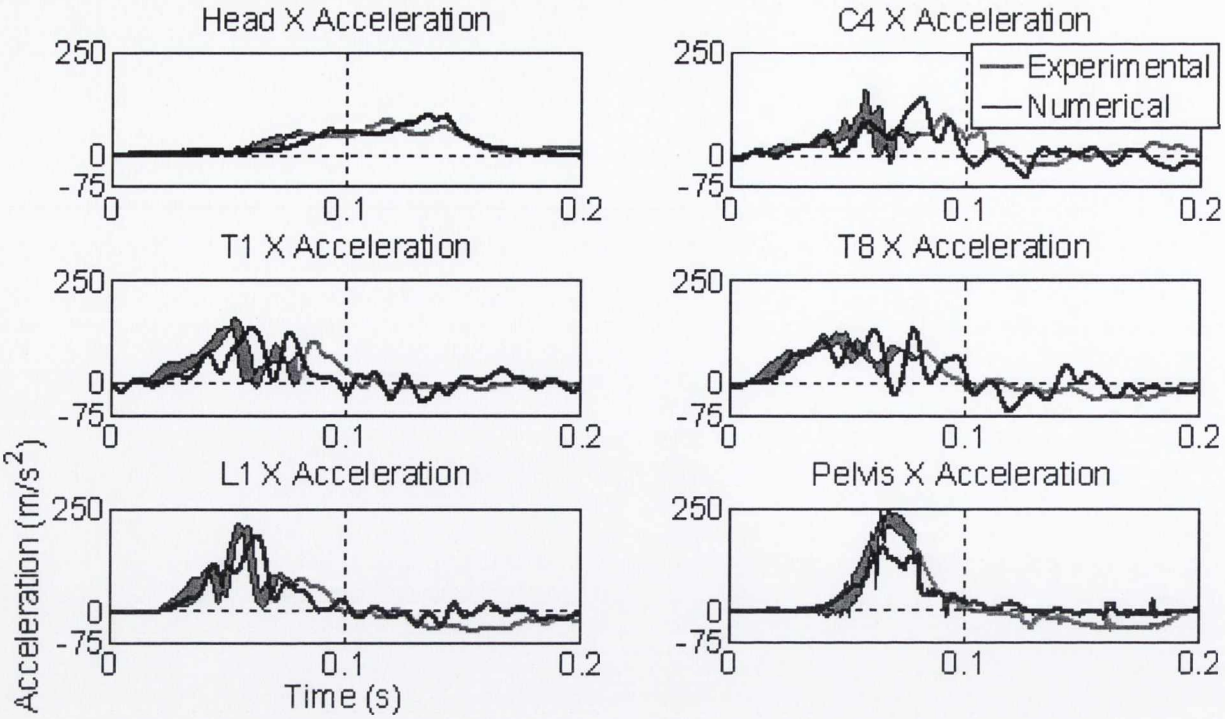


Figure 5.18: Comparison of ouputs in X direction

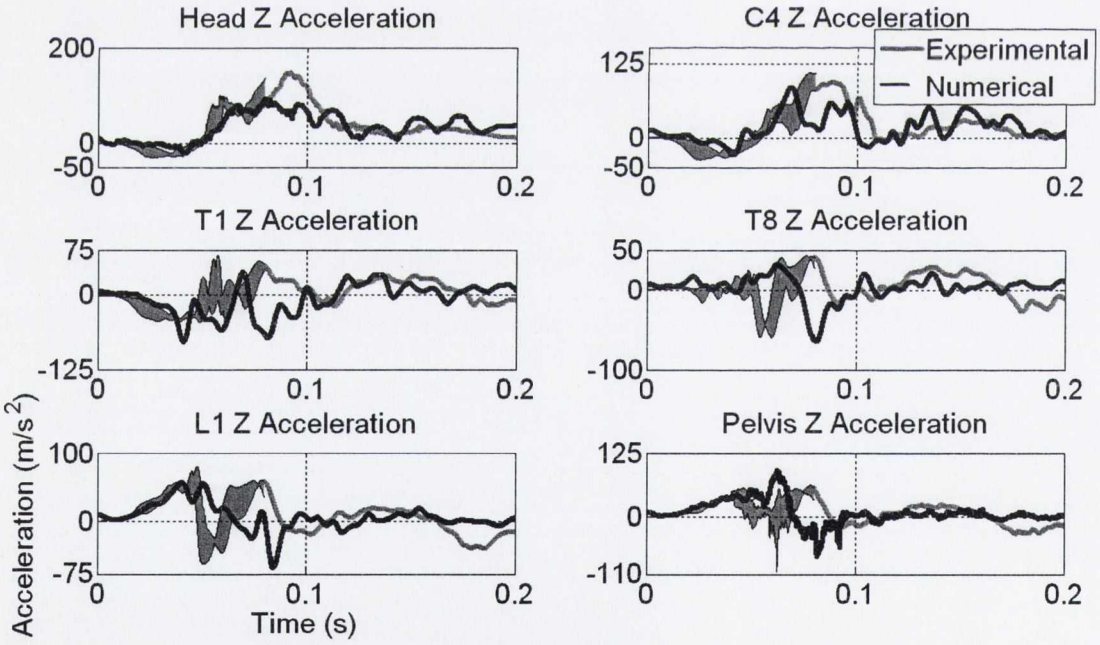


Figure 5.19: Comparison of ouputs in Z direction

For rear impact loading in the neck, the most important modes are X direction force (shear) and Y direction bending moment as these are used for predicting injury level [27] [15]. The comparison of these is given in figures 5.21 and 5.21 for the top and bottom of the neck.

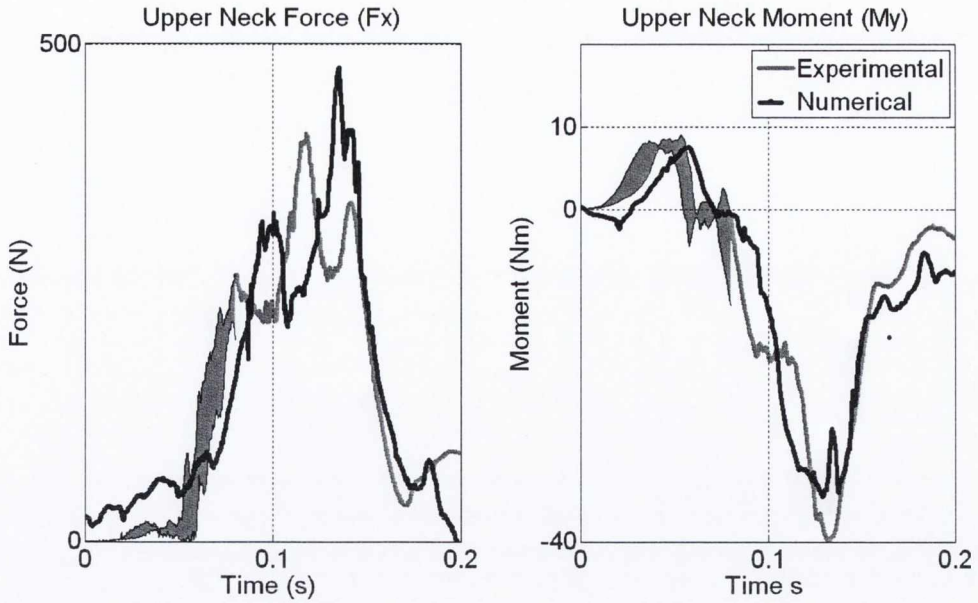


Figure 5.20: Comparison of outputs in upper neck

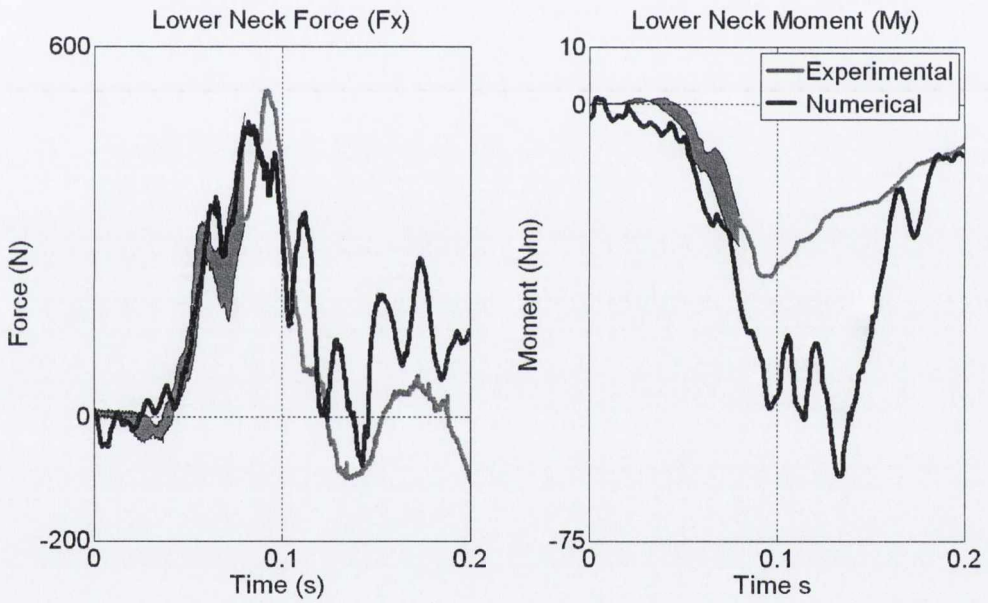


Figure 5.21: Comparison of outputs in lower neck

The validity of this model can be assessed by focusing separately on the X and Z components of the acceleration and load cell outputs. The time histories of the baseline model for the head, neck, thoracic and lumbar regions correspond very well to the BioRID sled test for the X direction, however, for the pelvis there are some differences. The Z component of acceleration was found to produce larger deviations from the physical tests.

However, the validation process conducted by other researchers focuses solely on the X component of acceleration and presents these and the forces in the upper neck as the validation of the model [104]. Similarly, Cormarkovic et al assessed the X direction acceler-

ation and the loading on the upper neck when evaluating the validity of their rear impact simulation of a vehicle occupant [105].

The predicted upper neck load cell response matches the experimental data very well for the shear forces and bending moments, figure 5.21, which was also found by other researchers. The lower neck responses are not presented in other validations and were found in this research to show good correlation for the shear force, but not for the bending moment, see figure 5.21.

As detailed in Chapter 3, the accelerometer on the wheelchair malfunctioned and so the displacement of the wheelchair was calculated from the video data. This was then compared to the displacement of the wheelchair in the numerical model.

A comparison of the planar motion of the wheelchair relative to the sled is shown in figure 5.22. The horizontal and vertical displacement of the armrest crossing point (see point A in figure 3.16 Chapter 3), and the angular displacement of the wheelchair with respect to the sled base for the simulation and Test 1 are presented. The comparison of the displacement of the wheelchair shows good overall correlation.

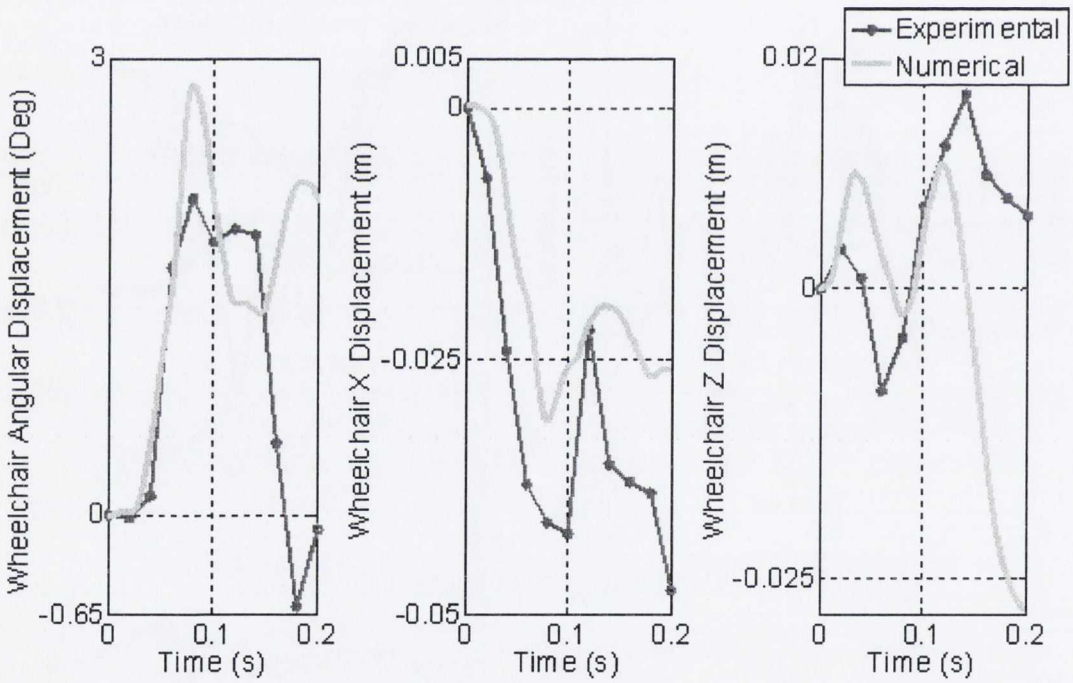


Figure 5.22: Wheelchair planar motion: angular and linear displacement of sled test and model compared

The percentage differences in the peak values and timing of these peaks for the wheelchair displacement in the physical and numerical tests were determined. This data was used as a guideline to ensure that the wheelchair reacted in the same manner in the computational model as in the sled tests. However, the differences found were not used to quantify the discrepancy in the validation of the model as the displacement of the wheelchair in the

physical tests is based on an estimated value, and so it would introduce errors. However, the good correlation found between the physical and numerical data shows that the wheelchair in the computational model behaved in a similar manner to that of the physical tests.

5.11 Validation - Quantification of Discrepancy in the Model

The validation of the rear impact model created in this work is based on kinematic and dynamic response comparisons of the occupant model with the occupant in the physical tests. This showed some differences compared to the experimental tests but overall the validation process showed good correlation for the acceleration, force and moment outputs.

The average percentage difference for the peak values (PV) of the dummy outputs used for comparison, figures 5.18, 5.19 and 5.21, was 17%, see table 5.3, which is calculated using equation 5.1. This value is within the established limits (based on other published models) to accept the model validation. Similarly the timiing of these peak values (PT) is within the limit of 16%.

$$PercentageDifference = \frac{Test - Simulation}{Test} x100 \tag{5.1}$$

The model was also assessed using the Difference Area under Curve (DUC) assessment. This method evaluates how well two outputs correlate based on the difference between the area under the both curves. This method is an inbuilt function within MADYMO and a DUC value greater than 75% is deemed to be an acceptable score and shows good correlation between data. For the rear impact model presented in this work the DUC method produced an average score of 90%, table 5.3, which indicates good correlation of the data.

The discrepancy in the model was therefore determined to be 10%.

Output	PV %	PT %	DUC %
Head X Acceleration	86	87	95
C4 X Acceleration	74	68	97
T1 X Acceleration	84	87	97
T8 X Acceleration	88	61	95
L1 X Acceleration	88	90	80
Pelvis X Acceleration	66	96	64
Upper Neck Shear Force	90	87	95
Upper Neck Moment	83	97	99
Total Average	**83**	**84**	**90**

Table 5.3: Comparison of PV, PT and DUC of Computational Model Compared to Sled Tests

A similar method of analysis was also used in the development of the BioRID II to asses its repeatability [19]. This analysis of the peak values has also been used to validate other wheelchair crash simulations [22], [23],[47] and [48]. The values found for the validation of this model are not dissimilar to the variation found in both of the sample cases mentioned. The frontal impact models of a wheelchair and occupant found differences ranging from 4.7% to 15.6%. The values are comparable to those found for this model, and below the limit of 20% difference.

As detailed in Chapter 2 for the validation process the response of the BioRID P3 dummy were compared to data from volunteer tests also subjected to a rear impact while seated in a rigid seat without a headrest [19]. This produced an average of 31% difference between the dummy and there was no significant shift in the time of these peak values with an average difference of 16%, which is not dissimiliar to the values found in this model.

The graphs comparing the wheelchair displacement, figure 5.22, shows a good overall correlation. A comparison of the peak value and timing of these peaks, table 5.4, shows good correspondence between the physical and numerical values. The peak values differ by 33% and the timing of these match well with a difference of 14%. Overall, the predicted and measured relative wheelchair displacements are both small: $\leq 3^o$ wheelchair rotation and $\leq 5cm$ linear displacement of point A with respect to the sled.

	Peak Value Percentage Difference	Peak Time Percentage Difference
Angular Displacement of Wheelchair	37	1
X direction Linear Displacement of point A	27	23
Z-direction Linear Displacement of point A	36	17
Average	**33**	**14**

Table 5.4: Comparison of magnitude and timing of peak displacements of wheelchair with respect to the sled for the physical sled test and the model predictions

5.12 Validation - Acceptance of Model

For the model created in this work the differences between the model predictions and the test measurements were deemed acceptable as they were less than the upper tolerance limits that were established based on other published models - 20% difference in peak value and 16% difference in timing of the peak values.

The main focus of the findings of this work, and others, are in the X direction as this is the direction of the crash and the injury criteria used focus on these components to predict injury. The predicted kinematics of the crash test corresponds well with the high speed video of the crash, with key events occurring at the same time. It was concluded from this analysis that the Madymo model is a good representation of the physical sled test.

This work presents the first computational model of a surrogate wheelchair and BioRID II occupant subjected to a 10g rear impact and validated through comparison to sled tests. This model focuses on the response of an adult wheelchair occupant in a rear impact which had not been evaluated previously. The forces and accelerations on the occupant were used for the validation process and so it is validated to predict these values which can be used to determine the level of injury due to a rear impact.

The MADYMO file of the baseline model is provided as part of the appendices with a description of the file provided in Appendix C.

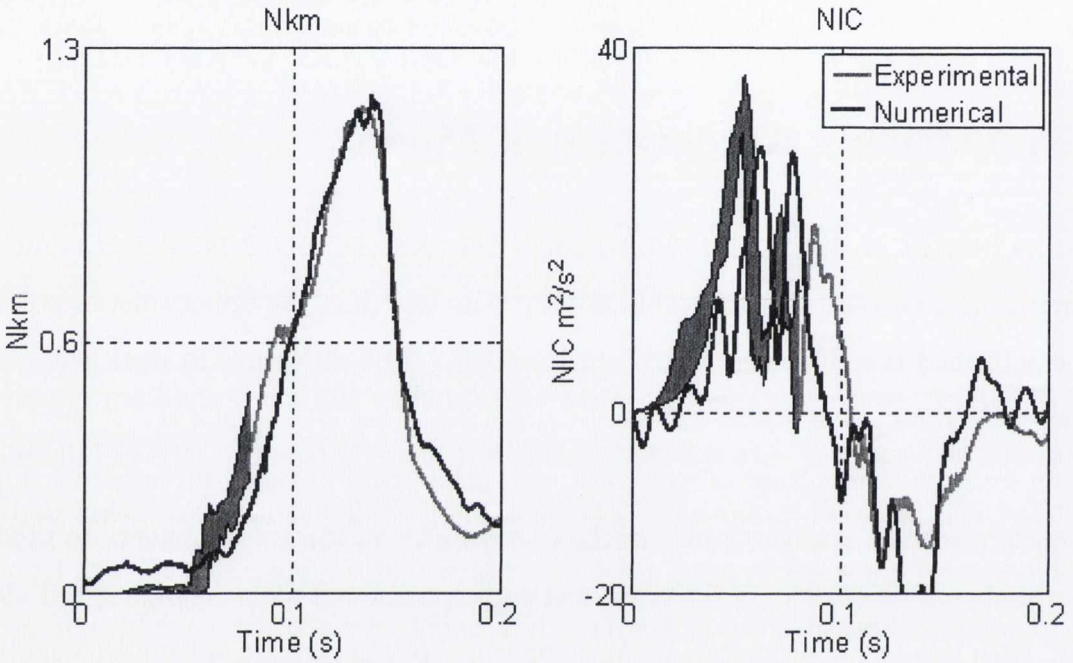
5.13 Injury Due to Rear Impact

The level of injury due to a rear impact was predicted in the computational model using standarised injury criteria, *NIC* and *Nkm*, see Chapter 2.

NIC and *Nkm*

The *NIC* and *Nkm* predicted in the computational model are compared to the outputs from the physical testsup to 80ms and to Test 1 only from 80ms to the end of the test.

The *Nkm* predicted a high risk of injury with a value of 1.2 which is above the cut off value of 1, figure 5.23(a). The NIC score predicts a high probability of injury with the peak value of $30m^2/s^2$ with the cut off limit being $15m^2/s^2$ above which injury is predicted. The graph of which is shown in figure 5.23(b). The peak values for each are compared to the cut off values, as shown in table 5.5



(a) *Nkm* from Computational Model

(b) *NIC* from Computational Model

Figure 5.23: Injury Criteria

	NIC (m^2/s^2)	*Nkm*
Cut off Value	15	1
Baseline Model	30	1.2

Table 5.5: *NIC* and *Nkm* Outputs from Numerical Model

These high levels of injury are, as expected, due to the absence of a headrest and the rigid wheelchair used. These values indicated a significant risk of neck injury for the baseline standardised occupant as used in this model. The predicted level of risk to the occupant when the occupant and wheelchair are altered are presented in Chapters 7 and 9.

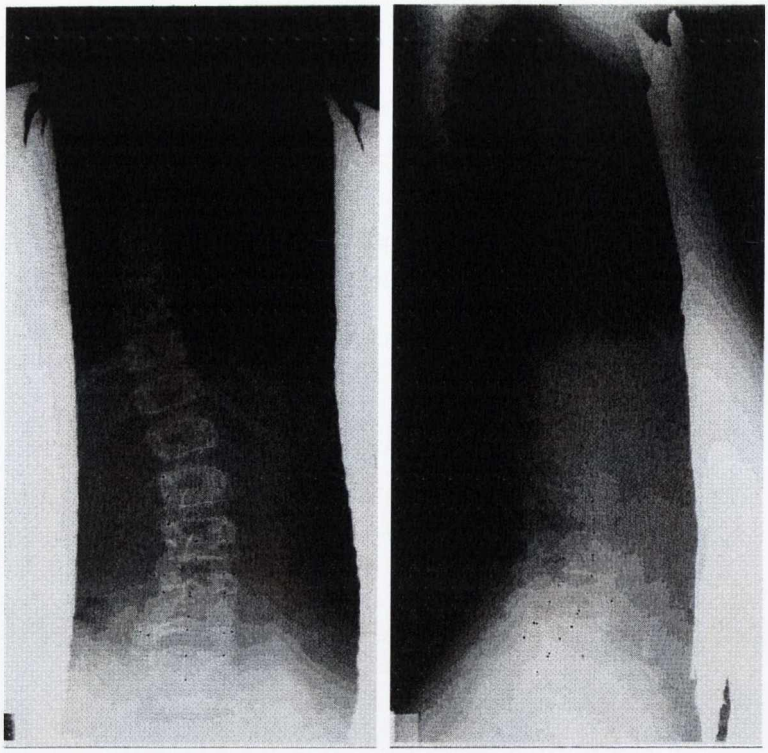
Chapter 6

Methods 3: Alterations to Occupant Model

6.1 Scoliosis Implementation

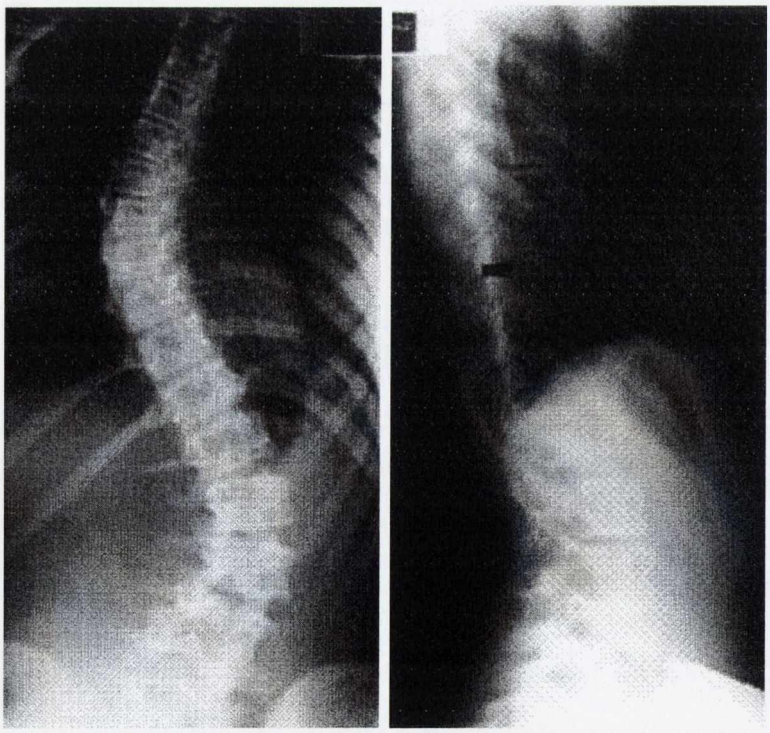
Scoliosis is a complex 3D deformation of the spine, which has many causes, and due to the degrees of freedom of spinal motion, each case of scoliosis is unique [81], [82]. Therefore, a parametric analysis to analyse the influence of different degrees of scoliosis was not feasible. Instead representative cases of a mild, moderate and severe case of scoliosis were identified in the scoliosis clinic by a clinician who provided the X-rays. The spine shapes are therefore based on real life cases of scoliosis and are presented in figures 6.1, 6.2 and 6.3. Limited patient information was provided with these X-rays and so each are implemented into the model as a fixed idiopathic scoliosis.

The Cobb Angle, see Chapter 2, was determined to be 25^o for the mild scoliosis, 56^o for the moderate case and 94^o for the severe case.



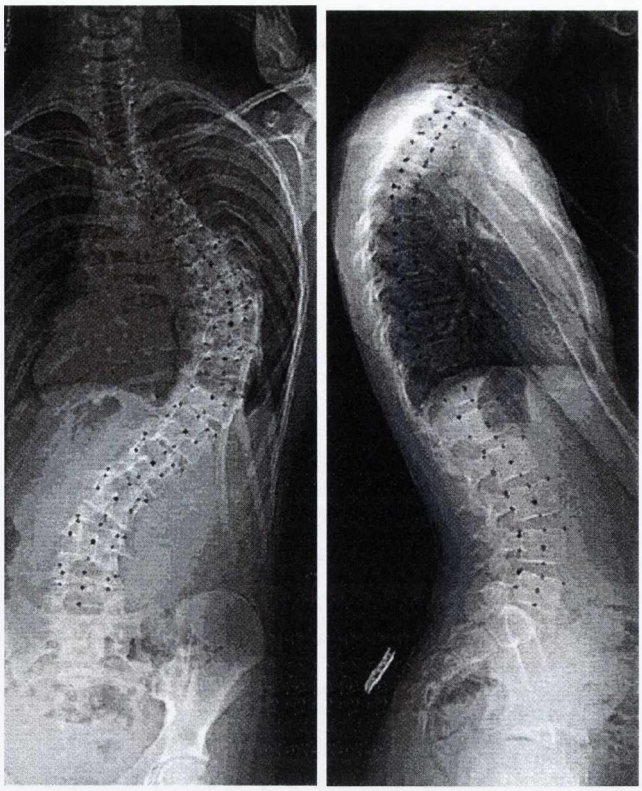
(a)Frontal View of mild scoliosis (b)Lateral View of mild scoliosis

Figure 6.1: Mild Scoliosis X-rays



(a)Frontal View of moderate scoliosis (b)Lateral View of moderate scoliosis

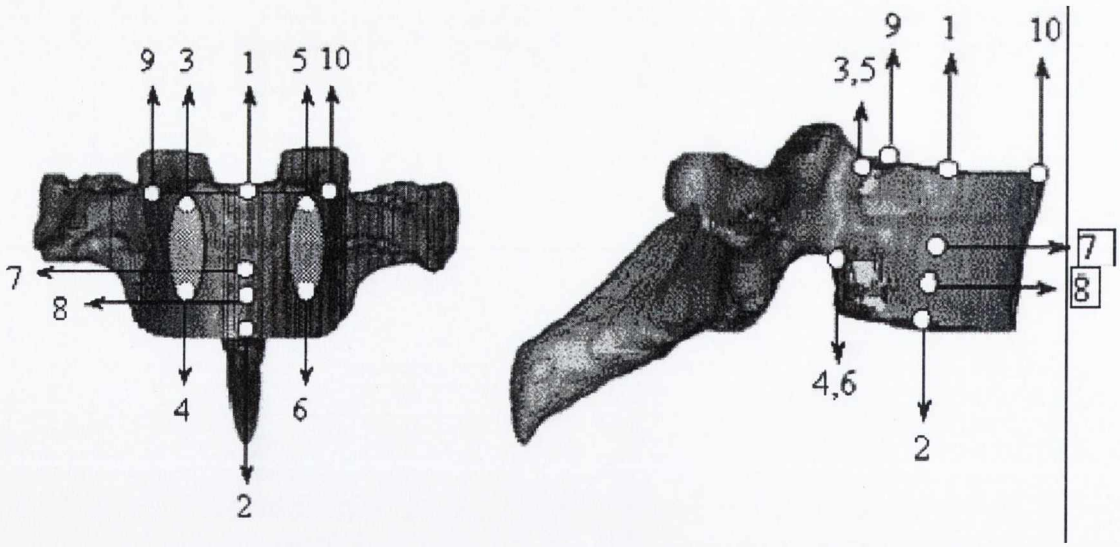
Figure 6.2: Moderate Scoliosis X-rays



(a)Frontal View of Severe Scoliosis (b)Lateral View of Severe Scoliosis

Figure 6.3: Severe Scoliosis X-rays

The X-rays were used to determine the position and orientation of the vertebra of the spine. The 2D X-ray images were converted into 3D representations of the spine using prominent bony features on the vertebrae, seen as the dots on the X-ray in figure 6.3. A total of 10 features were used to reconstruct the 3D spine, which are shown in figure 6.4. The points which these markers represent are detailed below the figure. The markers were defined as the upper and lower endplates of the vertebral bodies. The pedicles (marked as points 3,4,5,6), were also used to describe the vertebrae. These are features that are found on all vertebrae and can be used to describe the position and orientation of each vertebra within the global reference space.



(a)Frontal View (b)Lateral View

Figure 6.4: Vertebra

The markers represent the following landmarks on the vertebrae:

1. Centre of the upper endplate
2. Centre of the lower endplate
3. Upper point of left pedicle
4. Lower point of left pedicle
5. Upper point of the right pedicle
6. Lower point of the right pedicle
7. Centre of vertebral body
8. Intersection of the line connecting the centre of upper and lower endplates (points 1,2) with the line connecting the lower point of pedicles (points 4,6) in the frontal view which is perpendicular to point 4,6 in the lateral view
9. Edge of the upper endplate
10. Edge of the upper endplate

This method has previously been used to determine an aetiological factor in idiopathic scoliosis and to predict the progression of scoliosis [91], [90]. Using the information provided the centre point of the upper and lower endplates (points 1 and 2) of each of the vertebrae were used to create a vector which represented the vertebrae in 3D space, see figure 6.5. The sign convention used is also shown in this figure.

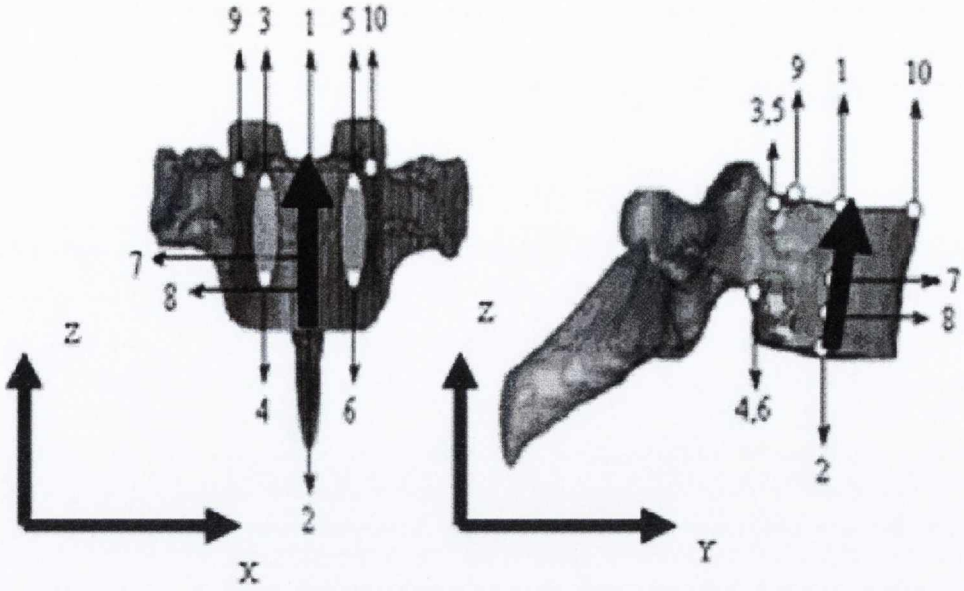


Figure 6.5: 3D Vector Overlayed on Vertebrae

The orientation of the vertebra as defined by these 3D vectors in the X-rays was then implemented into MADYMO. To create the scoliotic spine the joints which connect the vertebrae were altered. The coordinate systems of the vertebrae align with the coordinate systems of the joints. The orientation of the joints was therefore orientated in space. However this was a non-trivial process as the vertebrae are altered in 3D space and is made more complex by the single axis of rotation allowed by the BioRID II. This is detailed in the following section.

6.2 BioRID II Spine

The BioRID II was created and validated for use in zero offset rear impacts, and as such requires movement in the sagittal plane only with all other degrees of motion constrained. The spine of the physical model therefore rotates about the Y axis, see figure 6.6, however the computational model of this single axis of rotation (revolute joint) allows movement about the joint X axis only. To correct for this each joint must be rotated by 90^o about the Z axis. This rotation as well as that of the scoliosis must be implemented which adds complexity to the model. Added to this is the fact that in the spine of the BioRID II the MADYMO software creates each vertebra with reference to the coordinate system of the previous vertebra rather than the reference space as in the X-ray data.

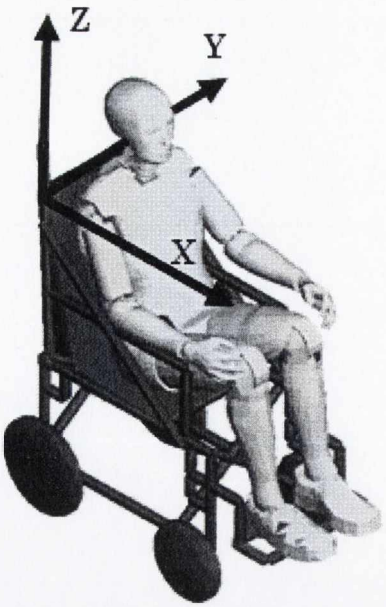


Figure 6.6: BioRID II and Coordinate System

To achieve both of the orientations required (scoliosis and 90^o about Z) and to have the rotation with respect to the correct coordinate system an extra "orientation" body was created between the vertebrae that did not alter the kinematics of the spine. This added body allows for the additional rotations to be introduced in this tree-like system. These orientation bodies have negligible mass and have no net kinematic influence, but provide a practical solution to developing the scoliotic spine.

The method to implement scoliosis that was adopted is shown graphically in figure 6.7. In the spine the lower vertebra is connected to the orientation body using a bracket joint which does not allow movement in any degree of freedom. The scoliosis orientation of the upper vertebra is applied to the orientation body and it is then also orientated by 90degrees about the Z axis to allow movement about the correct axis (global Y). The revolute joint which allows rotation about a single axis then allows the spine of the dummy to move in the sagittal plane. The upper vertebra is connected to this joint and then rotated back by 90 degrees to return the X and Y to be in the original configuration. The inverse of the scoliosis orientation is applied to return the next vertebra to align with the global coordinate system. The next scoliosis orientation is then applied, this process is continued throughout the entire spine and a scoliotic spine is created, as shown for the mild, moderate and severe scoliosis spines in figure 6.8.

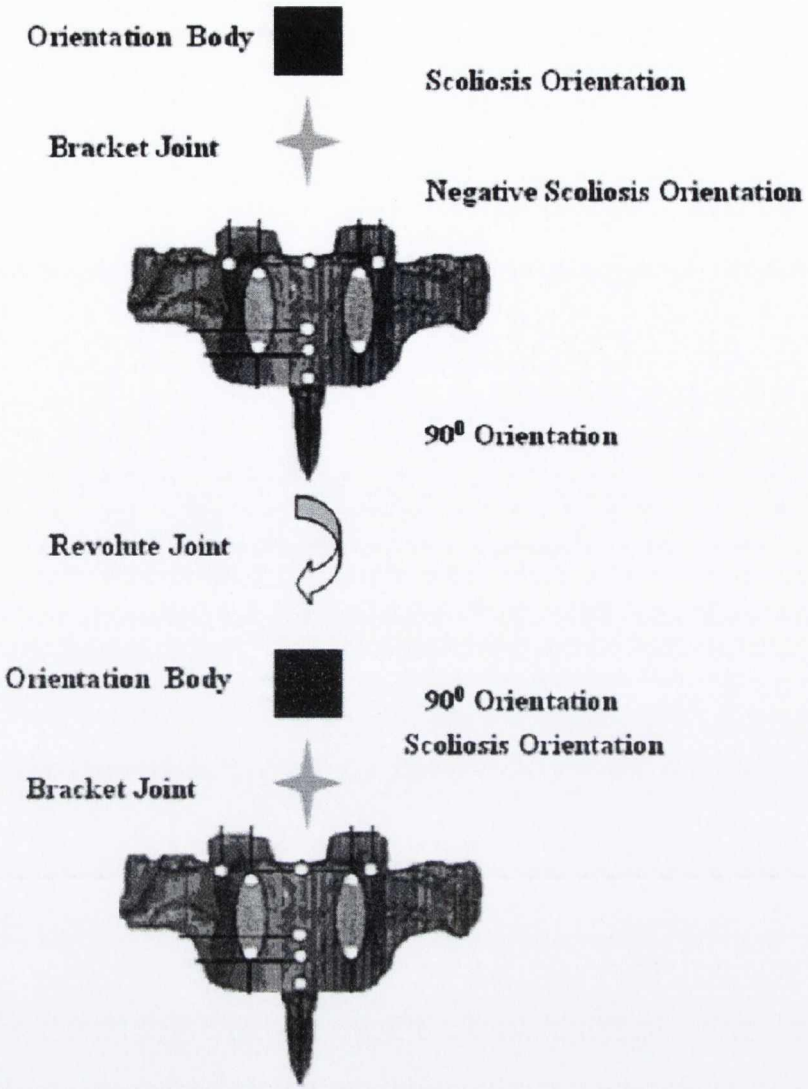


Figure 6.7: Implementation of Scoliosis Orientation

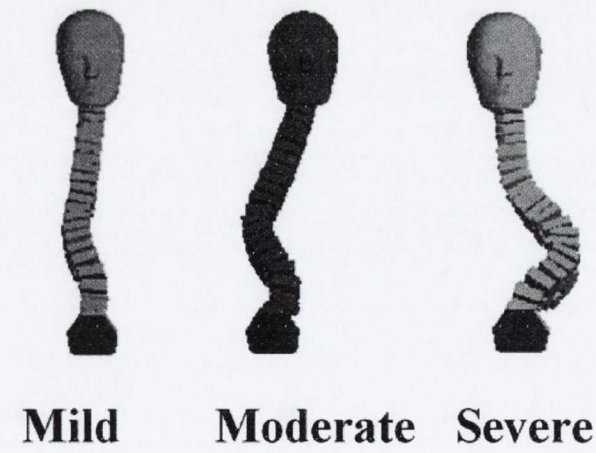


Figure 6.8: Mild, Moderate and Severe Scoliosis Spine

The addition of these orientation bodies was firstly assessed in the baseline model to ensure that they did not alter the kinematics of the spine. The animation outputs of the crash simulation showed the same response from each model. The acceleration outputs from

these models in the X and Z directions were also compared and are provided in Appendix D.

The addition of these orientation bodies was not found to alter the response of the occupant. Therefore they can be used in the creation of the scoliotic spine without altering its response.

The scoliosis rotation for these models was implemented in MADYMO using a method called the screw axis.

6.3 Screw Axis Method - Application in MADYMO

The rotation method used to introduce scoliosis is based on an axis and angle rotation and is named in MADYMO the screw axis rotation. The details of how this is implemented is provided in Appendix E. This method is carried out in the MADYMO software package and the user input required is simply the axis and angle of rotation. Therefore this was determined for each vertebra of the X-rays using the cross and dot product. To determine these values a Matlab script was written, see Appendix F.

To check the spines were rotated correctly using this procedure the rotation of each vertebra and the whole spine in the numerical model was determined and compared to the X-rays.

6.4 Screw Axis Method - Validation

To check the method used the orientation of each vertebra was related back to the global reference space as shown in figure 6.9. The orientation of the vertebra found in the X-ray was determined using points 1 and 2 and the centre point between them was found and this was translated back to the global 0,0,0 coordinate system.

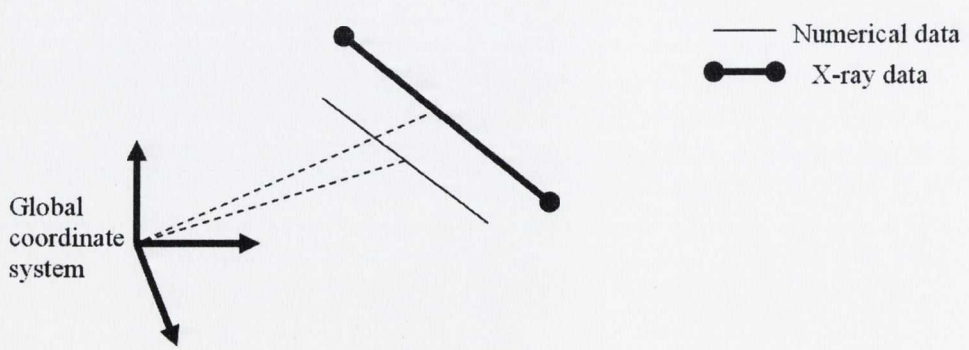
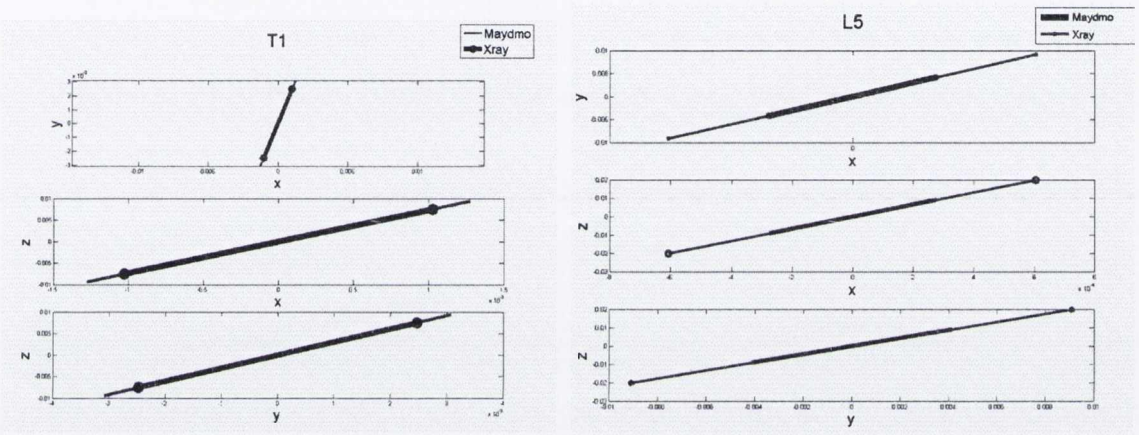


Figure 6.9: Validation of Vertebral Rotation

In the computational model the centre point of the vertebrae was determined in the local coordinate system and the relative position of the centre of the upper and lower endplates was determined. The corresponding rotation in the numerical model was also translated back to the global reference space.

When related to the global coordinate system, the orientation of the two was found to match. This was carried out in MATLAB for each of the vertebrae of all of the scoliosis models that were created. This method showed that the relative orientation of each vertebrae was seen to correspond exactly to that found in the X-ray when viewed from all directions. The samples shown in figure 6.10(a) and (b) of T1 and of the moderate scoliosis case are typical examples of the entire spine.



(a)Comparison of T1 (b)Comparison of L5

Figure 6.10: Comparison of Orientations in X-ray and Madymo Model

When comparing the entire spines it is important to note that the size of the vertebrae in the X-ray and the model are different as in the X-rays they are of different sizes and shapes. However, in the computational model all of the vertebra in the lumbar and thoracic region are of the same size therefore, when the two are compared there may be some differences. However it is the orientation of the individual vertebrae in the scoliotic spine which is being modelled and this has previously been shown to correspond to the X-rays. As a result, an overlay plot of the X-ray and model data shows small apparent differences, see figure 6.11. This difference in vertical height (Z) of the model of the spine and the spine in the X-ray accounts for these differences. However, the orientation of each of the vertebrae in the model are identical to the X-rays, as verified previously it is the altered scale that stretches and skews these comparisons.

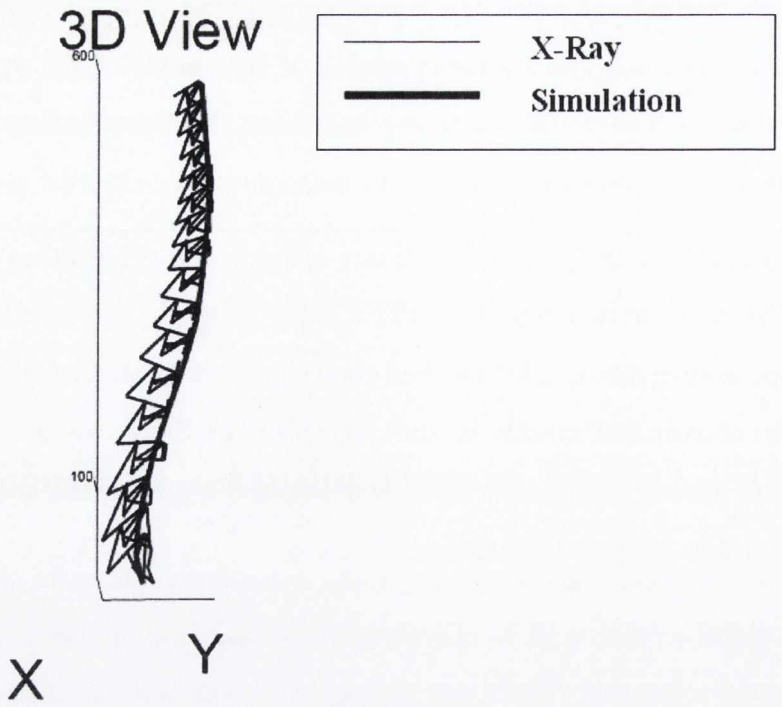


Figure 6.11: 3D Comparison of Moderate Scoliosis Spine from X-rays and Numerical Model

6.4.1 Positioning of Scoliosis Occupants

The X-rays provided were of scoliosis patients standing upright and the shape of the spine when seated is unknown, and therefore some assumptions were necessary. It was assumed that the scoliosis was fixed so that when seated or standing the shape remained the same. Also the orientation of the spine relative to the pelvis was unknown so it was assumed that the the lowermost lumbar vertebra (L5) was orientated relative to the pelvis when seated as shown in the X-ray. Therefore when scoliosis was implemented from L5 upwards the altered posture of the model increased the sitting length of the dummy. When this occupant was placed in the same position as the validated baseline model there was insufficient depth in the seat to accommodate the shoulders of the occupant, see figure 6.12. The position of the baseline occupant in the wheelchair is to allow a 26^o orientation of the occupant which is the validated posture of the BioRID II occupant [42] and is the required posture for use with the IIWPG 10g rear impact pulse [102].

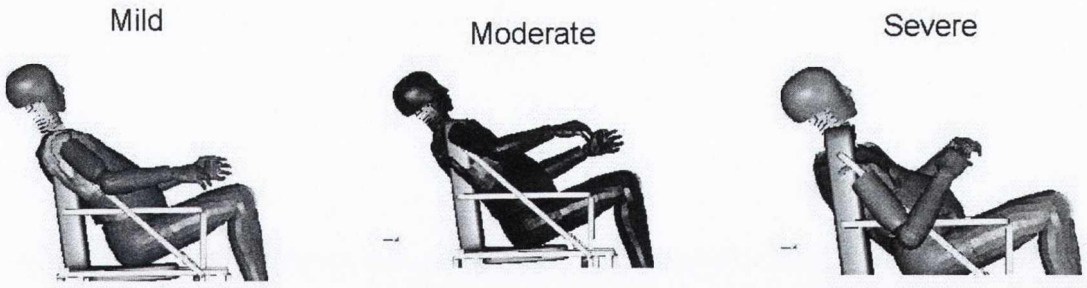


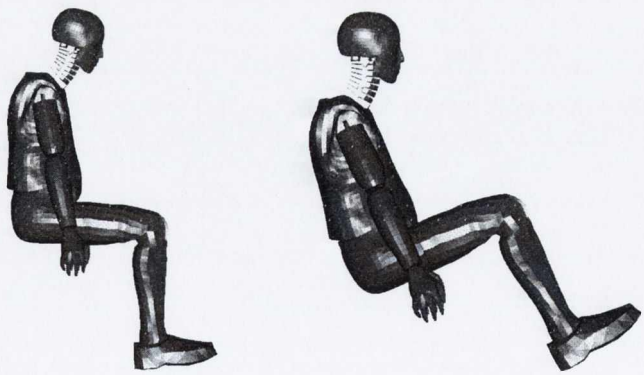
Figure 6.12: Mild, Moderate and Severe Scoliosis Model in Wheelchair Seated at -26^o

To position the scoliosis occupants in the wheelchair there were restrictions in the approach, these were:

- The wheelchair could not be altered as this is the validated model
- The BioRID II model is validated to be seated with an orientation of 20^o to 29^o and adjusting the occupant within this range would be insufficient to alter the occupant to fit into this wheelchair
- As this study was based on real life cases of scoliosis the shape of the spine was not to be altered

To determine an approach to altering the scoliotic occupant model the baseline model was investigated to determine the positioning of its spine.

The validated baseline occupant is provided by MADYMO, as shown in figure 6.13(a) [21]. This is then orientated by -26^o (counter clock wise) to be in the validated seated posture [42], see figure 6.13(b). When this same -26^o seated orientation was applied to the scoliosis models this resulted in the seated scoliotic occupants as shown previously, figure 6.12.

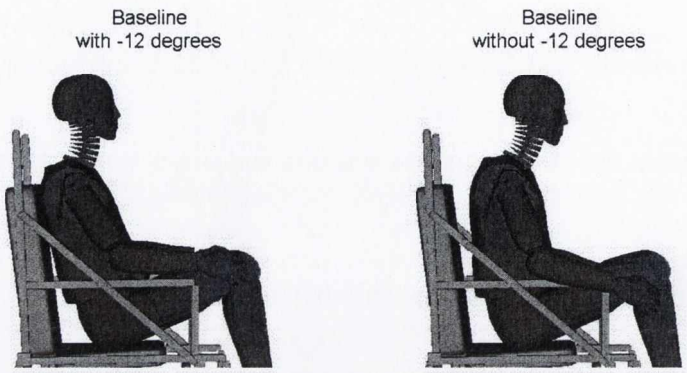


(a) (b)

Figure 6.13: BioRID II as Provided by MADYMO and Orientation by -26^o

The baseline occupant was further investigated and it was found that there is a -12^o orientation at the joint between the sacral spine and the lowermost lumbar vertebra (L5).

Without this additional -12^o orientation the occupant's seated position does not allow contact with the seatback as shown in figure 6.14(b). A translation of the occupant seated in the posture shown in figure 6.14(b) would not produce the correct posture of the head, neck and upper thoracic region as seen in part (a).



(a) (b)

Figure 6.14: Effect of -12^o

This -12^o orientation also allows for the joints from L5 up to the first thoracic vertebra (T1) to have a small orientation between the vertebrae to create the validated straight lumbar region and kyphotic thoracic region, as shown in the stripped down model in figure 6.15. This -12^o orientation is therefore required to create the correct seated position of the occupant.



Figure 6.15: BioRID II Stripped to Show Spinal Column which has small Orientations between Vertebrae

When this -12^o orientation is removed from the scoliosis models the seated posture is slightly improved, figure 6.16, however the occupant is still not seeated correctly in the wheelchair.

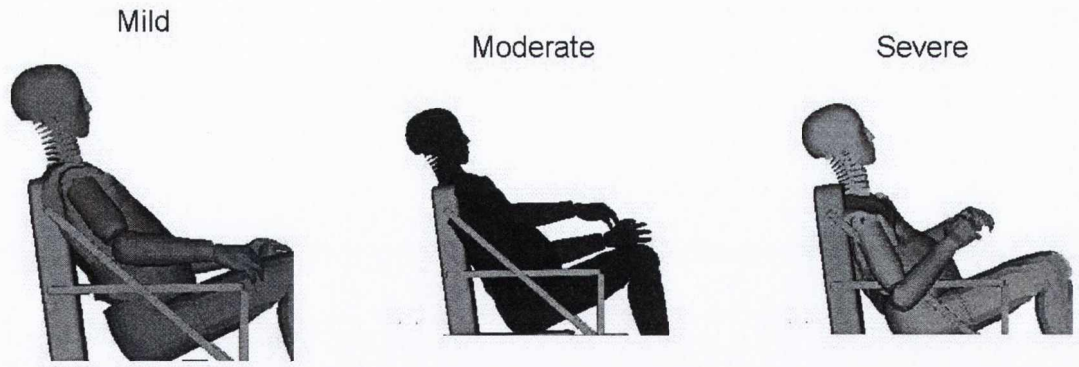


Figure 6.16: Mild, Moderate and Severe Scoliosis Model in Wheelchair Seated at -26^o with -12^o Removed

Therefore to fit the occupants in the wheelchair when placed at the same linear position as the baseline occupant a clockwise orientation between L5 and the pelvis is required. Due to the variation in the the postures of the mild, moderate and severe occupant a range of values, (14^o, 17^o, 21^o) is required to fit the occupants into the wheelchair. These pure rotational corrections produce the image in figure 6.17.

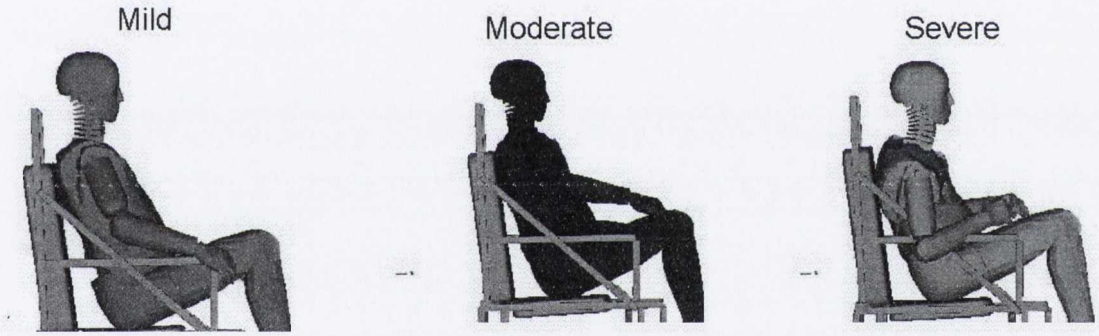


Figure 6.17: Mild, Moderate and Severe Scoliosis Model in Wheelchair Seated at Baseline Position and Varied Orientation

However the large rotation of up to 21^o between these vertebrae, required for the severe case, may not be possible. As detailed in Chapter 2 a spine with scoliosis is less flexible than one without scoliosis and this flexibility reduces with an increase in the curvature and so a 21^o orientation in the severe case of scoliosis may not be possible [97]. It has also been found that angular displacements of 20^o between lumbar vertebrae can lead to injury in non-scoliotic spines [71].

A pure translation of these occupants when orientated to the same degree as the baseline occupant (26^o and 12^o) would not result in the correct seating posture of the scoliosis occupants for two reasons. Firstly, the seat would not be long enough to accommodate the much increased sitting length. Secondly, the contact with the wheelchair would be on the shoulders

of the occupant. Therefore a combined translation and rotation approach to positioning the occupant was adopted.

For consistency a sub-injurous orientation of $+12^o$ was added to each of the scoliossis models. This improved the seated posture of the occupants however as seen in figure 6.18, this did not result in the correct seated posture of the scoliosis occupants when placed at the same position as the baseline occupant.

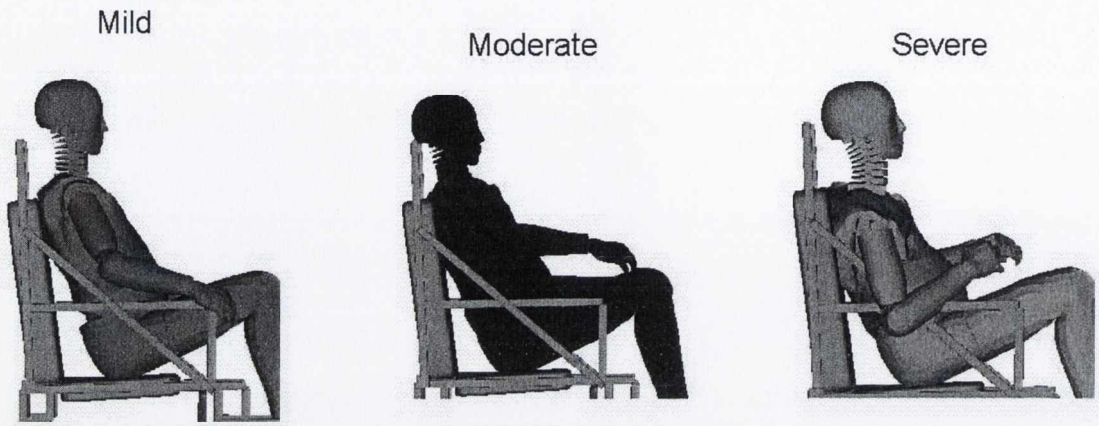


Figure 6.18: Mild, Moderate and Severe Scoliosis Model in Wheelchair Seated at Baseline Position and $+12^o$ Orientation

The position of the H-point (buttocks) was then also translated to accommodate this posture of the scoliotic occupants. This produces the seated postures as shown in figure 6.19.

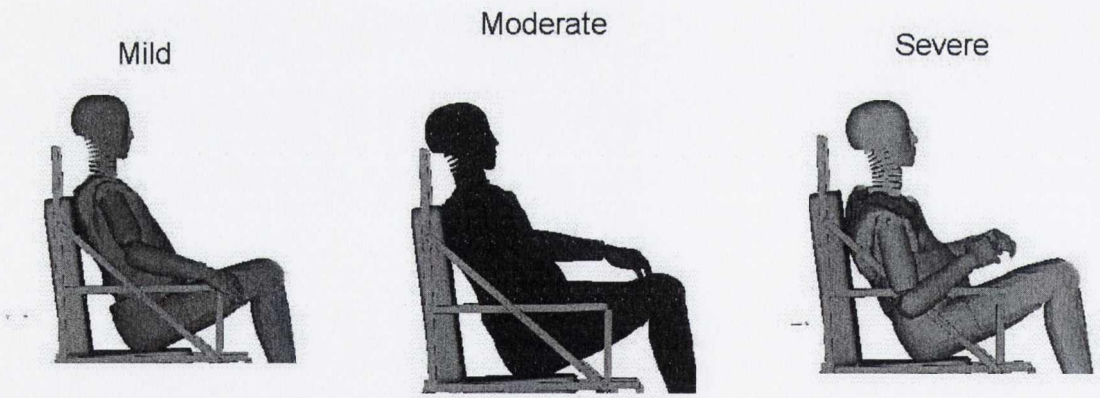


Figure 6.19: Mild, Moderate and Severe Scoliosis Model in Wheelchair Seated at Baseline Position and $+12^o$ Orientation and Varied Position

This combined translation and orientation approach was adopted as best practice for positioning the scoliotic occupant. This method is based on a consistent and relatively small orientation of 12^o between the L5 and sacral joint. It was felt that this consistency was necessary so that any effect it has on the results would be the same in all models.

This level orientation also meant that the level of translation required to fit the occupants was also relatively small, the level of adjustment is shown in table 6.1. An increase in this position moves the dummy forward in the seat and increases the distance between the lumbar region and the seatback.

Model	Position (m)	Difference (m)
Baseline	0.033	
Mild Scoliosis	0.045	0.015
Moderate Scoliosis	0.0625	0.0295
Severe Scoliosis	0.0735	0.0405

Table 6.1: Positioning of Scoliosis Models

Different levels of rotation and translation were also investigated and were found not to effect the results to any great extent. Therefore the decision to use the 12^o orientation is based on the need to have a chosen level of orientation to apply to all scoliosis models and as variations of this value did not alter the results.

However to ensure that this does not alter the response of the occupant in an impact when compared to a different approach this method of altering both the position and orientation was compared to altering the rotation only (figure 6.17). The images of the two different seated postures are overlaid in figure 6.20. This figure shows the occupants altered by pure rotation (Posture 2) overlaid on the occupants with an adjusted position and orientation (Posture 1). It is seen that there is not a large difference in the seated postures of the occupants. Both postures show that the surface of the back and its contact with the the wheelchair in the thoracic region is largely unchanged. The lumbar region has a more distinct variation as its displacement from the seatback is slightly increased for the occupants seated using the Posture 1 method.

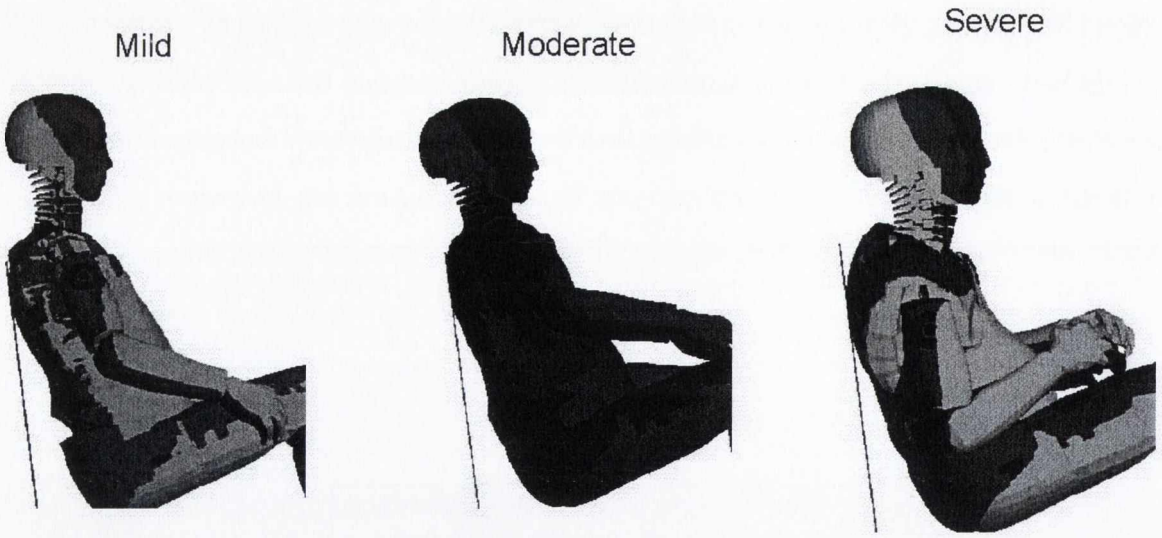
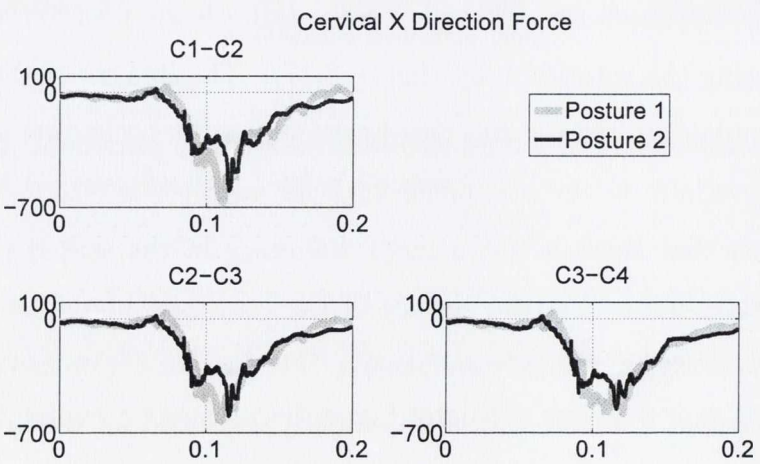


Figure 6.20: Overlayed Images of Two Seating Postures

To further evaluate this selection of seating position the outputs from the model seated in Posture 1 and Posture 2 were compared. These two types of model positioning showed that there was little variation between the two methods when looking at the loading on the spine,see figures 6.21, 6.22 and 6.23. These figures show the forces in the joints of the spine in the cervical, thoracic and lumbar regions in the direction of the crash (X-axis). The average differences between postures 1 and 2 for the mild, moderate and severe cases of scoliosis was 12%. The visual differences between the two models in the animation outputs were negligable.

Therefore the method adopted to position the occupant (Posture 1) was found to be consistent and more realistic as it reduces large angles between the vertebrae. Also the alternative methods, as discussed, were found not to greatly affect the kinematics from the model.



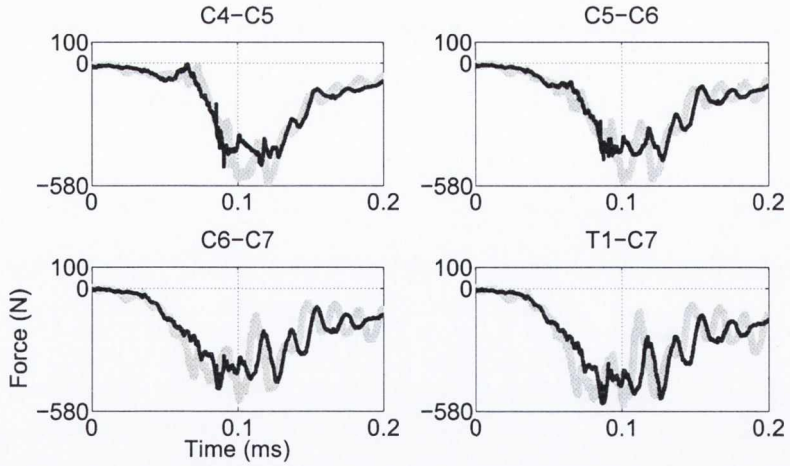


Figure 6.21: Comparison of Forces in Cervical Region of the Spine for Postures 1 and 2

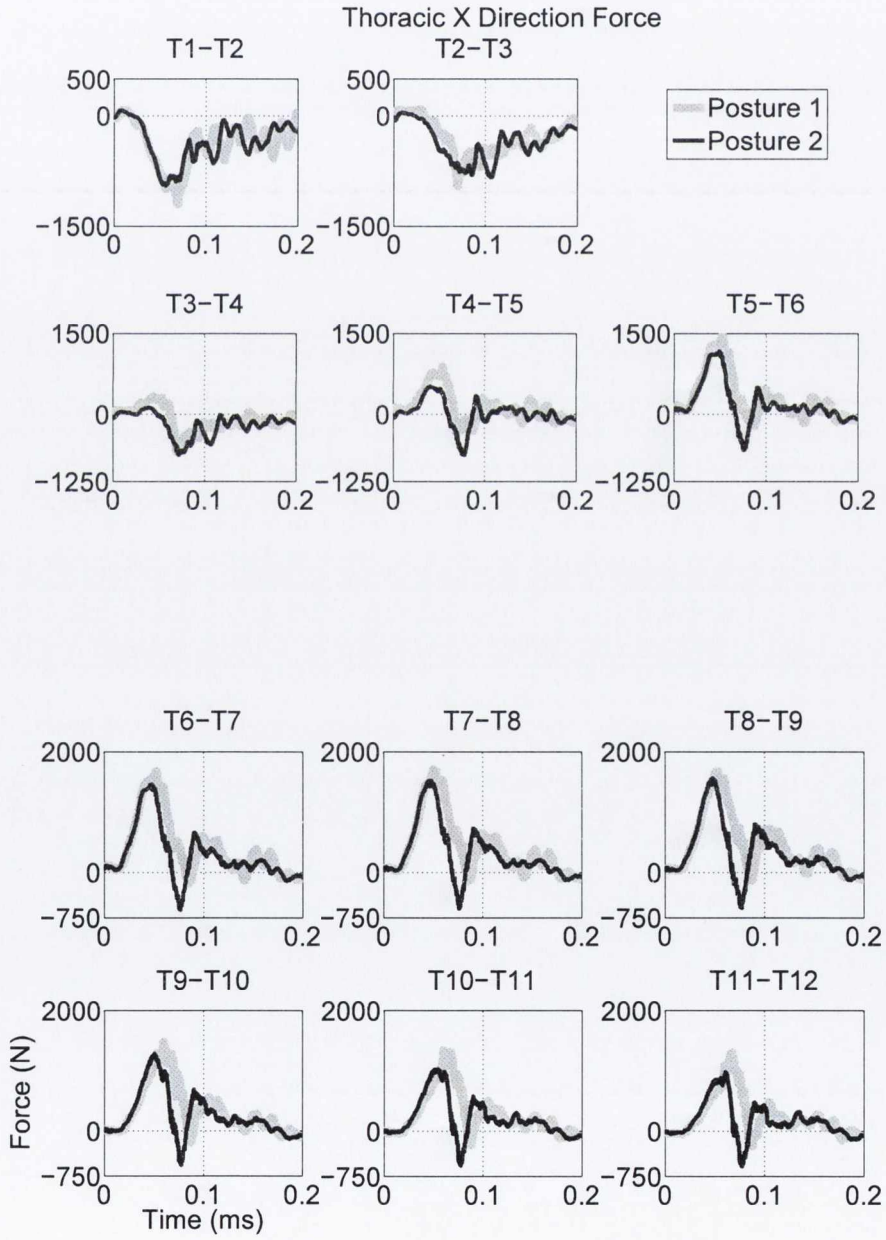


Figure 6.22: Comparison of Forces in Thoracic Region of the Spine for Postures 1 and 2

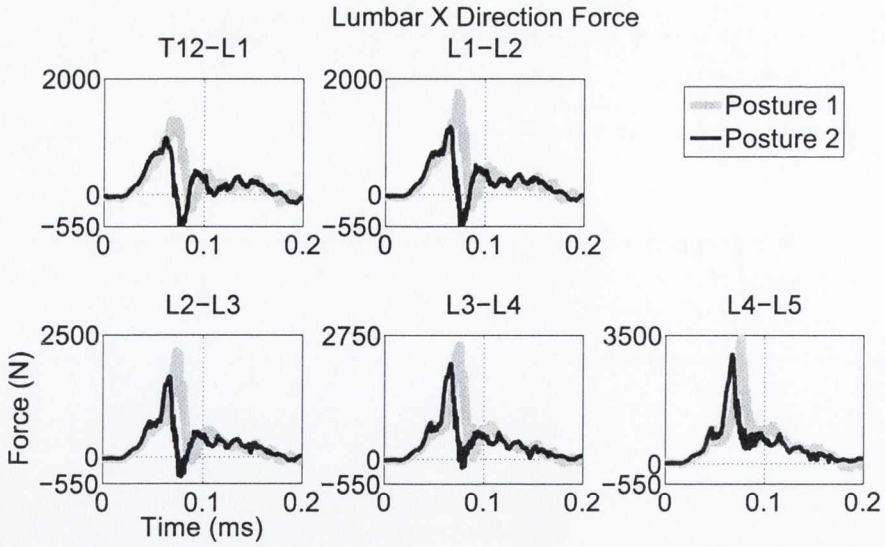


Figure 6.23: Comparison of Forces in Lumbar Region of the Spine for Postures 1 and 2

6.5 Neck Position

The position of the neck at the top of the scoliotic curve is not provided in the X-rays however it is known that the ocular corrective reflex causes the head to be straight and horizontal [65] [66]. This reflex is the reason for a compensatory curve as found in scoliotic spines. Also scoliosis is not generally found in the cervical spine [82] and so a correction of the neck to have the head horizontal is modeled. This is based on a study of clinical photographs of wheelchair occupants and the resting position of the head of wheelchair occupants who attend the Enable Ireland seating clinic.

Two methods of correcting the neck were investigated and the loading on the neck in terms of force and predicted level of injury were determined to be similar. The two methods are presented in figure 6.24. Method 1 in this figure shows the correction solely at the T1-C7 joint, whereas in Method 2 the correction of the head is spread throughout the joints of the neck. Method 2 was determined to be a more realistic representation of clinical findings [1] and was adopted for use in this work.

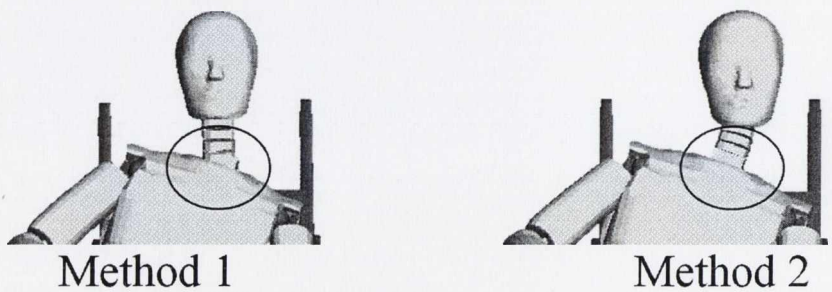


Figure 6.24: Neck Correction Methods

6.6 Joint Type

The joints of the BioRID II occupant allow movement in the sagittal plane only as the model was designed to represent the kinematics of a human occupant in a zero offset rear impact [42]. However, to investigate further the effects of a 3D deformation such as scoliosis these joints were altered to allow rotation about all three axes. In MADYMO different joint types are available to allow or constrain rotation about the principal axes. The original joints of the BioRID II are called Revolute Joints and allow rotation about one axis while constraining movement in all other directions. The axis which allows rotation is then assigned a torque-angle characteristic which controls the motion of the occupant. These were replaced with Spherical Joints which allow rotation about all 3 principal axes while constraining any translation. Torque-angle characteristics are again assigned to control the motion of these joints.

To begin this process of altering the joints, the revolute joints are replaced with spherical joints. These spherical joints are assigned the original characteristic from the revolute joints which controls sagittal plane motion. The other 2 axes of the spherical joints are assigned very stiff characteristics to constrain motion about these axes which recreates the revolute joint. These adapted spherical joints were applied in the baseline and the scoliosis models and compared to the original occupant models with revolute joints. This process ensures that changing the joint types does not alter the kinematics of the occupant. The animations and the acceleration time history outputs from these simulations were found to be unchanged with the different joints.

The next step in this process was to assign the lateral and axial characteristics of the cervical, thoracic and lumbar regions to the spherical joints. These characteristics were taken from research by Panjabi et al into torque-angle relationships of vertebral pairs in the three regions of the spine [106], [106], [107]. These stiffness characteristics are produced from tests conducted of the vertebrae, intervertebral discs and ligaments, see figure 6.25. The results from testing show that there is a coupled translation and rotation however this will not be modelled as part of this work. Only the main rotational motion of the vertebrae (dark solid line in figures 6.26, 6.27 and 6.28) will be assigned to the rear impact models. The axial and lateral characteristics of each of the models are shown in figures 6.26, 6.27 and 6.28.

The curves for the thoracic region of the spine were different to those of the lumbar and cervical region. While all testing was conducted by the same researcher the testing of the cervical and lumbar vertebrae was conducted 20 years after that of the thoracic region. The slightly different testing methods used meant that the neutral zone of the thoracic region,

where there is no displacement under an applied load, was not defined. However the results are used for this work due to the scarcity of such investigations and as the neutral zones are quite small and would not greatly effect the results.

The effect of altering these joints is detailed in Chapter 7.

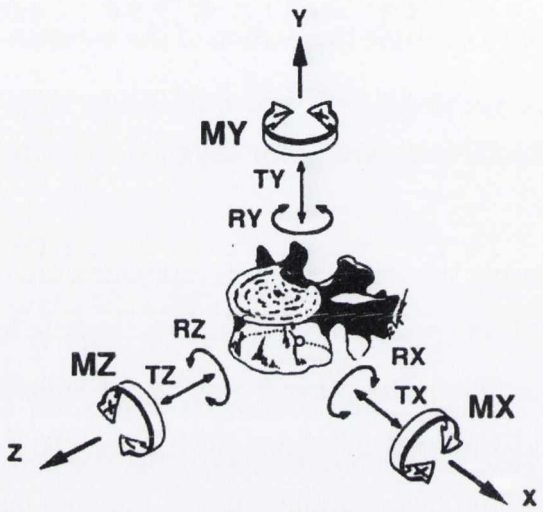
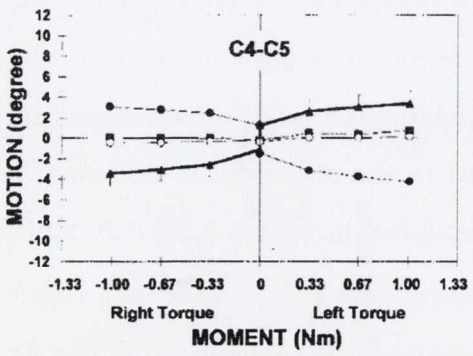
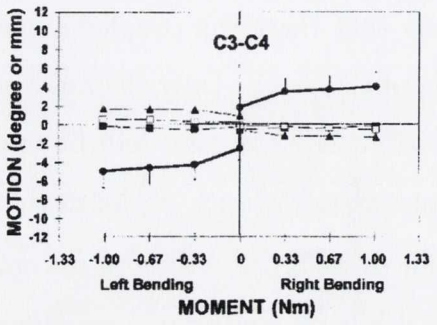


Figure 6.25: Testing of Vertebrae

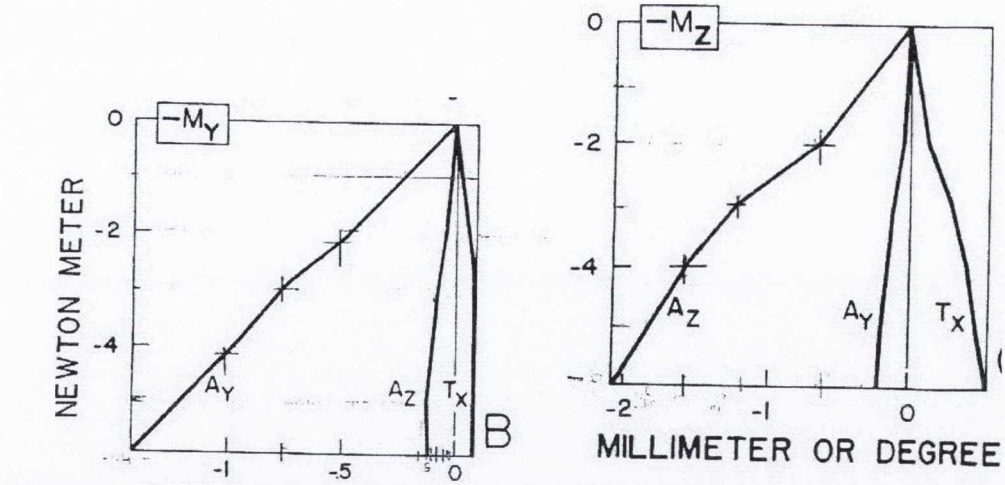


(a)Axial Characteristic of Cervical Vertebra



(b)Lateral Characteristic of Cervical Vertebra

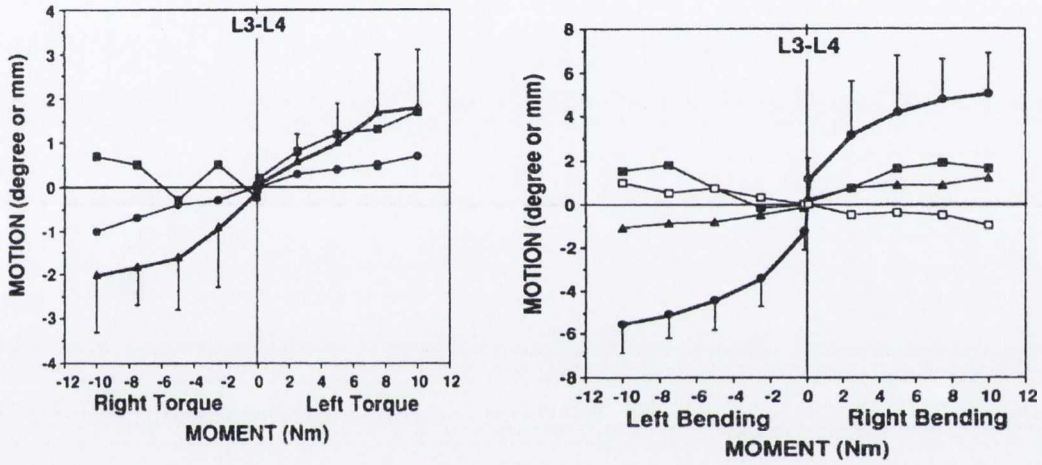
Figure 6.26: Cervical Vertebra



(a)Axial Characteristic of Thoracic Vertebra

(b)Lateral Characteristic of Thoracic Vertebra

Figure 6.27: Thoracic Vertebra



(a)Axial Characteristic of Lumbar Vertebra

(b)Lateral Characteristic of Lumbar Vertebra

Figure 6.28: Lumbar Vertebra

The MADYMO simulation models created using these methods are provided as part of the appendices. A description of each of the models is provided in Appendix C. These models were then used to investigate the effect of scoliosis in a rear impact, which is detailed in the following chapter.

Chapter 7

Results 2: Alterations to Occupant

The validated baseline model was altered by introducing scoliosis as detailed in Chapter 6 and the results of these altered modes are presented in this Chapter.

The results for the mild, moderate and severe scoliosis cases in a rear impact often show a similar pattern and therefore the moderate case is presented as a representative model. The results for the crash simulations of the mild and severe case are provided in Appendix G. However, any deviation from the pattern is presented and analysed in this chapter.

For each case comparisons with the baseline case are made to determine the effect of each degree of scoliosis. The first step in this process is to analyse the kinematics of the occupant and investigate any changes found. This is done by comparing the animations of the scoliosis models with the baseline models. The resulting loading on the occupant is also investigated. Differences in the loading conditions may lead to an increased risk of injury. The important parameters that will be investigated here are the forces, moments and the range of motion that the spine passes through. These are compared to levels which are known to cause damage. Particular emphasis is placed on the spine as this is where the loading is concentrated due to interaction with the seatback in a rear impact. The predicted level of neck injury is also evaluated using injury criteria (*NIC* and *Nkm*).

The predicted values of loading and injury are also assessed to quantify the relative increase or decrease in the scoliosis models compared to the baseline case. To to this an R value will be determined by comparing the peak output values of the scoliosis models with those of the baseline case, see Equation 7.1.

$$R = \frac{Scoliosis\ Response}{Baseline\ Response} \tag{7.1}$$

In accordance with the validation process of the model, see Chapter 2, the findings in the comparisons between the baseline and the scoliosis models have to be greater than the discrepancies found in the model validation process (10%) to be considered significant.

Values below this level are not considered to be sigificant as they may be due to a modelling artifact.

While the level of deformity of every case of scoliosis is unique, in order to understand the general influence of scoliosis the specific behavior of the models used in this study must first be determined. This analysis is presented here. An important part of this investigation is to determine trends in the responses and to understand these.

The positioning of these occupants in the wheelchair is also investigated in this analysis as it may play a key role in injury prevention.

The clinical significance of any findings is also highlighted in this Chapter and discussed in Chapter 10.

7.1 Kinematics

The models of the occupants with scoliosis produced an altered rear impact response. To investigate this the movement of the dummy from the spine upwards is analysed. The motion of the individual vertebrae are also analysed in this section.

7.1.1 Visual Difference

The simulations of the sled tests of the baseline and scoliotic occupants show a marked difference, see figure 7.1.1. These images show snapshots of the baseline and moderate scoliosis models at 40ms time steps. As seen from the animations the effect of scoliosis is to introduce assymetry while hyperextension of the neck is still found. This fundamental characteristics of hyperextension of the neck in a rear impact is unaffected and so injury in this area is expected.

Baseline
0ms



Moderate Scoliosis
0ms



40ms



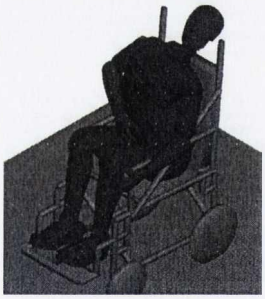
40ms



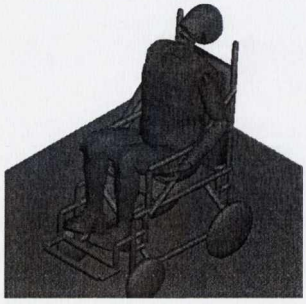
80ms



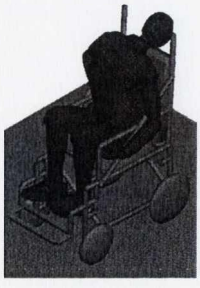
80ms



120ms



120ms



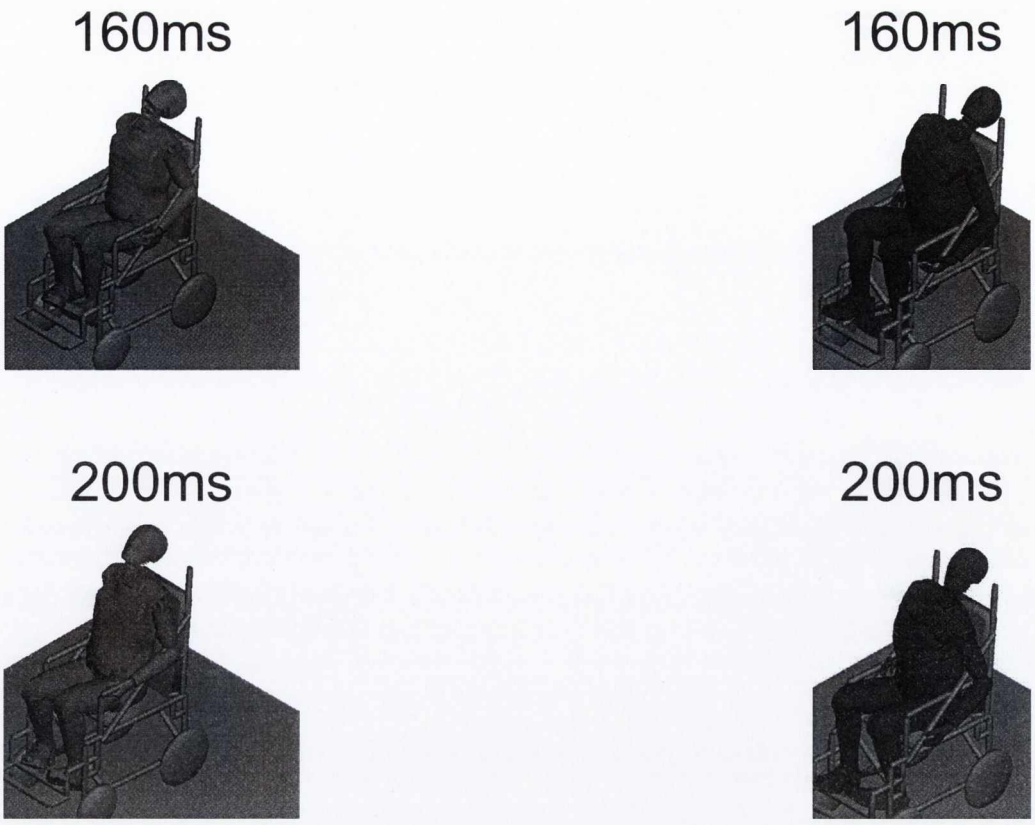


Figure 7.1: Altered Kinematics of Moderate Case of Scoliosis Compared to Baseline

7.1.2 Motion of the Spinal Column

The altered interaction of the spine with the seatback as the dummy moves backwards and makes contact with it at 85ms is shown in figure 7.2, with the models stripped down to the spinal column. This displays the altered reaction of the scoliotic spine compared to a non-scoliotic case subjected to the same loading environment. The spine does not fully straighten and align under the head in the moderate scoliosis case as it does for the baseline. This alters the transfer of force from the wheelchair to the occupant.

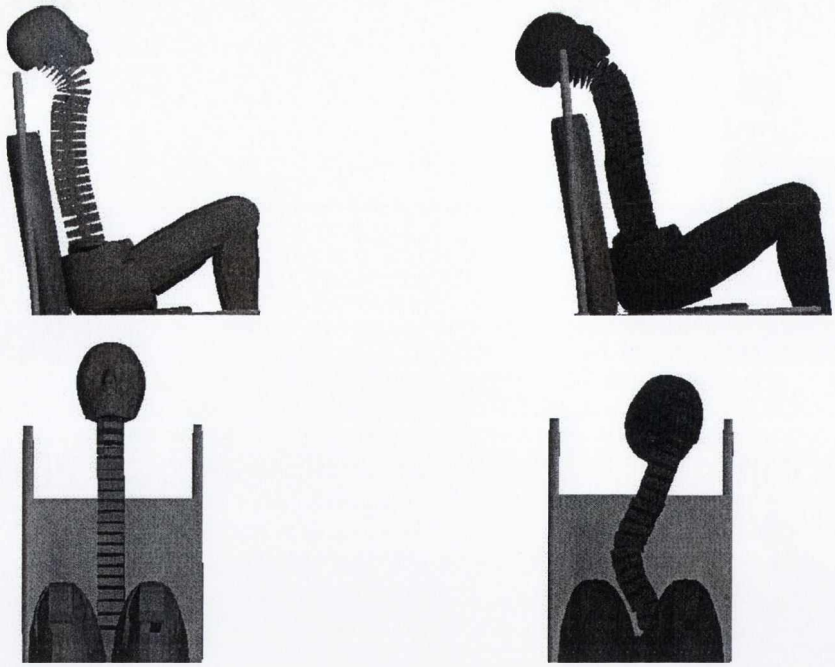


Figure 7.2: Spine of Baseline and Moderate Scoliosis in Contact with Seatback from Lateral and Frontal Views

7.1.3 Vertebrae - Range of Motion

The range of motion that the vertebrae move through is the difference between the maximum and minimum angular position. This was determined for each of the vertebrae of the spine both in the local and global coordinate system. The local coordinate system is that of the joint between the lower and upper vertebrae. This is orientated relative to the global coordinate system due to scoliosis. The gross motion of each of the vertebral bodies within the global reference space was also determined. The values for each coordinate system are presented here and compared to each other. This method of evaluation will provide more information about the reaction of a scoliotic spine in a rear impact compared to one without scoliosis.

Rotation of Vertebrae in Local Coordinate System

The motion of the vertebrae relative its parent (lower vertebra) for the moderate case of scoliosis model and the baseline case is presented in table 7.1. It was found that for the scoliosis case the vertebrae moved relative to the lower vertebrae to a greater extent than those of the baseline case. The peak value is seen to be 100% greater at the T9T8 joint and the adjacent joints also had large increases (highlighted in bold). As shown in figure 7.3 this area is where the kyphosis of the spine is in inital contact with the seatback. This contact zone is subjected to the largest force which causes motion of the vertebrae about their local axes.

Joint	Baseline	Moderate	Percentage Difference
T2T1	6	6	0
T3T2	5	6	20
T4T3	5	5	0
T5T4	5	5	0
T6T5	4	5	**25**
T7T6	3	5	**66**
T8T7	3	5	**66**
T9T8	3	6	**100**
T10T9	3	5	**66**
T11T10	3	5	**66**
T12T11	4	5	**25**
L1T12	5	5	0
L2L1	8	10	25
L3L2	7	9	29
L4L3	8	6	-25
L5L4	7	6	-14

Table 7.1: Range of Motion of Baseline and Moderate Scoliosis Vertebrae Joints in Local Coordinates

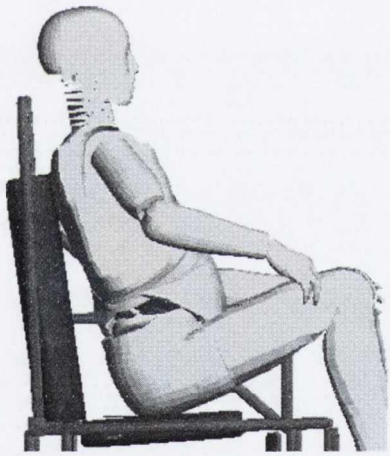


Figure 7.3: Scoliotic Occupant in Wheelchair

Motion of Vertebrae in Global Space

The angles that the vertebrea move through in the global coordinate system are presented in table 7.1.3. In this table the region of the scoliotic spine that was found to rotate to a greater extent than that of the baseline case are highlighted in bold. This area is again found at the contact area between the torso and seatback, see figure 7.3. Lower levels of rotation were found for some of the joints of the scoliosis models compared to the baseline as indicated by the negative values. These joints were furthest away from the contact area.

Joint	Baseline	Moderate	Percentage Difference
T1	21	21	0
T2	19	18	-5
T3	17	14	-18
T4	15	11	-27
T5	12	7	-42
T6	10	8	-20
T7	10	10	0
T8	11	13	**+18**
T9	13	15	**+15**
T10	15	16	**+6**
T11	16	19	**+19**
T12	16	22	**+38**
L1	16	19	**+19**
L2	14	17	**+21**
L3	19	15	-21
L4	24	14	-42
L5	21	18	-14

Table 7.2: Range of Motion of of Baseline and Moderate Scoliosis Vertebrae Joints in Global Coordinates

Translation of movement from Local to Global Coordinate System

The comparison of the percentage difference in the local and global coordinate system for the moderate case of scoliosis compared to the baseline spine is shown in figure 7.4. The difference in the results shows that the vertebrae of the scoliosis models are moving to a greater extent in the local coordinate system with values of up to 100%. However this does not translate to a corresponding increase in movement in the global coordinate system. In some cases the scoliotic spine is seen to move to a lesser extent in the global coordinate system, denoted as the neagtive values. This pattern of response was found for all levels of scoliosis.

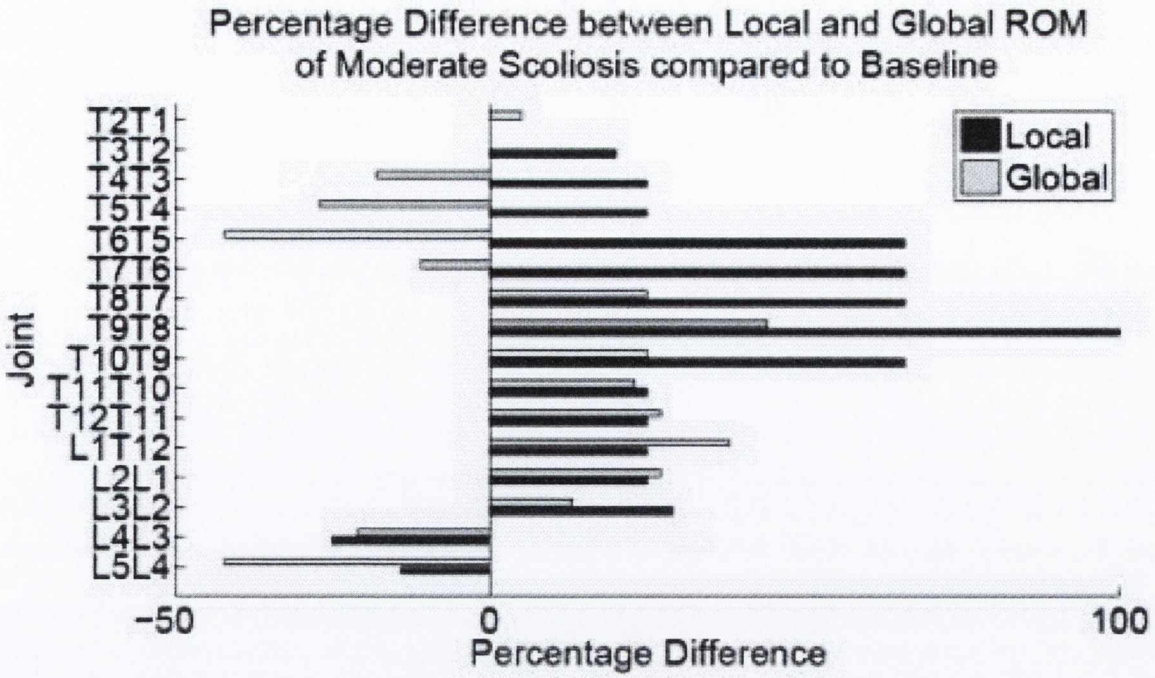


Figure 7.4: Comparison of Local and Global Range of Motion for each Vertebra of Moderate Scoliosis compared to Baseline

This disparity in the results is found as the joints rotate about their local Y axes which are displaced from the global Y axis by scoliosis. This is illustrated for one joint in figure 7.5, which shows the local coordinate system for the joint and the global coordinate system. The displaced local coordinate system can be clearly seen in this image. This pattern is found throughout all of the spine and in each level of scoliosis.

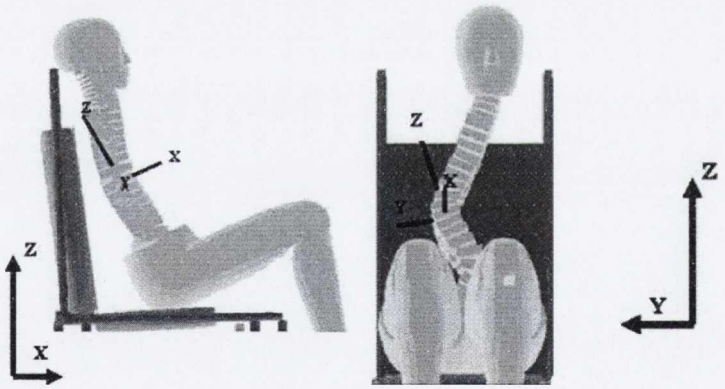


Figure 7.5: Displaced Local Coordinate System of Vertebra for Moderate Scoliosis

7.2 Summary of Kinematics

There is a marked change in the reaction of the spine when scoliosis is introduced and the interaction of the occupant with the wheelchair is also altered. There is a smaller contact zone between the torso and the seatback in the scoliosis cases than in the baseline case. The effect of scoliosis is to create a more pronounced kyphosis of the thoracic spine which results

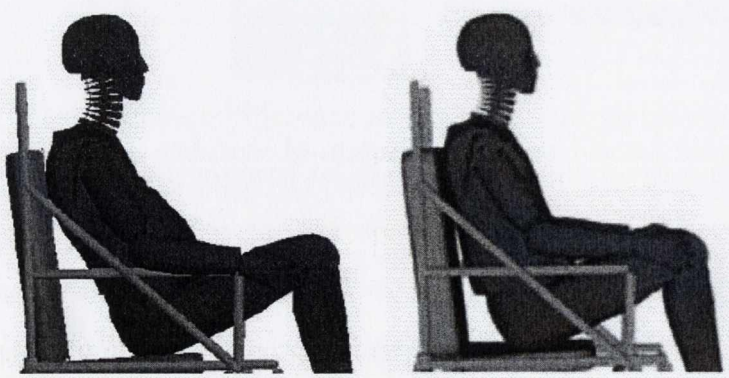
in a point loading effect on the torso. This point loading results in a greater movement of the vertebral joints in the thoracic region about the local coordinate system. There is also a larger degree of movement in parts of the lumbar region. This is again due to direct contact with the seatback as the occupant moves rearward in the seatback.

Outside of these contact zones there is a reduction in the movement of the vertebrae in the global coordinate system. The movement of these vertebrae is due to indirect loading as the spine straightens. However due to the displaced axis of rotation the scoliotic occupant is unable to uncurl its spine to the same extent as the baseline and this results in restricted movement. This reduced movement in the global coordinate system was found in the upper thoracic and lumbar regions which are not directly loaded by contact with the seatback.

Therefore it is the combination of point loading and the altered orientation of the vertebrae which causes the altered kinematics of the scoliotic occupant as compared to the non-scoliotic occupant. These two processes are further investigated to quantify their individual influence in a crash.

7.3 Point loading effect

To single out the effect of point loading the curvature of the scoliotic spine in the sagittal plane was applied to the baseline occupant. This curvature created the exaggerated kyphosis as found in the scoliosis cases which results in point loading. The altered curvature of the spine that was introduced increased the sitting length of the occupant, as distance between the back and the buttocks was increased and so its position within the wheelchair was altered to accommodate this. This resulted in the occupant with the sagittal curvature from the moderate case of scoliosis as shown in figure 7.6, which is compared to the original occupant.



(a) Baseline with Kyphosis (b) Baseline

Figure 7.6: Baseline Model with Kyphosis of Scoliosis Introduced and Original Baseline Occupant

The effect of this on the range of motion of the vertebrae in the local coordinate system is to increase the value in all of the joints of the model with the altered spine. There was an average increase of 46% in the spine with the curvature of the moderate case of scoliosis compared to the baseline case, see table 7.3. The average for the curvature of the mild, moderate and severe cases of scoliosis is 38%.

Joint	Baseline	Baseline with altered spine	Percentage Difference
T2T1	6	6	0
T3T2	5	6	20
T4T3	5	6	20
T5T4	5	5	0
T6T5	4	4	0
T7T6	3	4	33
T8T7	3	4	33
T9T8	3	5	66
T10T9	3	6	100
T11T10	3	7	133
T12T11	4	8	100
L1T12	5	7	40
L2L1	8	10	25
L3L2	7	12	71
L4L3	8	10	25
L5L4	7	12	71

Table 7.3: Range of Motion of Vertebral Joints of Baseline and Baseline with increased Ksyphosis in Local Coordinates

In the global coordinates the range of motion of the baseline model with the altered spine was increased by an average of 19% compared to one which had not been altered. An increased motion was found in each region of the spine except at the area of contact with the seatback in the mid-thoracic region, see table 7.4.

Joint	Baseline	Baseline with increased kyphosis	Percentage Difference
T1	21	23	10
T2	19	20	5
T3	17	15	-12
T4	15	11	-27
T5	12	9	-25
T6	10	7	-30
T7	10	6	-40
T8	11	9	-18
T9	13	13	0
T10	15	18	20
T11	16	22	38
T12	16	26	63
L1	16	30	88
L2	14	33	136
L3	19	35	84
L4	24	31	29
L5	21	22	5

Table 7.4: Range of Motion of Vertebral Joints of Baseline and Baseline with increased kyphosis in Global Coordinates

The increased motion of the upper and lower thoracic and lumbar region is a direct consequence of the point loading. The mid thoracic region which contacts the seatback is seen to have a reduced range of motion as it is restrained by the rest of the spine as shown by the arrows in the animation stills from the crash event, figure 7.7. The same pattern was found in all levels of scoliosis.

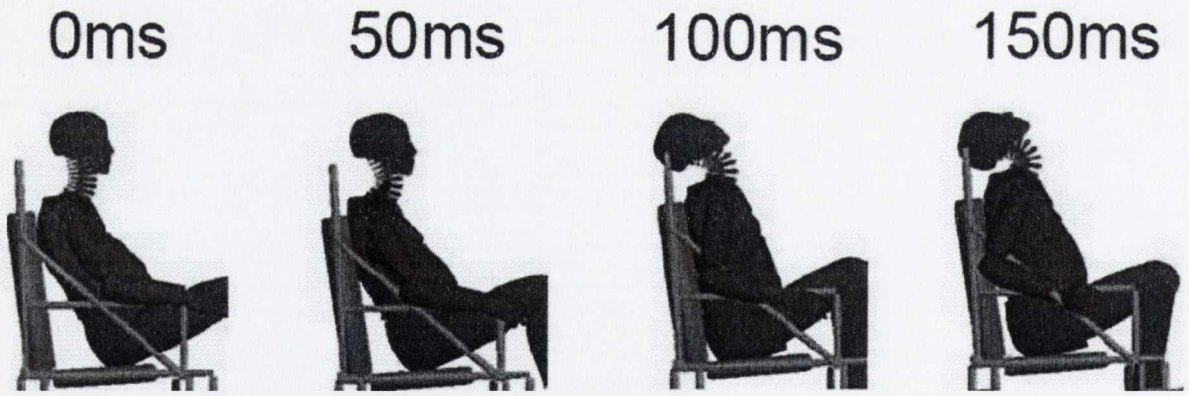


Figure 7.7: Snapshots of baseline model with Scoliosis Kyphosis

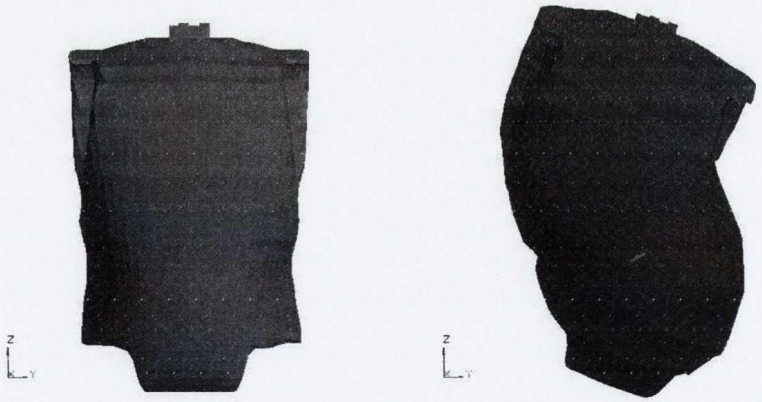
The point loading introduced was also found to have an effect on the forces on the spine. An evaluation of the forces in the joints of the spine showed an average increase in the forces in the whole spine of 30%. This is a substantial increase in the forces on the occupant and so the forces in the scoliosis models were investigated.

7.4 The Scoliotic Spine

To understand the effect of scoliosis on the loading on the spine for the three models the 3D orientation of each of the vertebrae were determined, this is presented in Appendix H.

7.4.1 Quantification of the Effect of Scoliosis

To investigate the effect that scoliosis has on the spine and torso they were investigated in isolation, see figure 7.8, and the resulting kinematics were compared. The differences found between the response of both spines in this simplified form shows the direct effect that having a scoliosis has on the movement and associated loading on the spinal column. The non-scoliotic and moderate scoliosis spine were secured to the reference space using a bracket joint which does not allow any movement. The models were not restricted from moving in any other areas. A small quasi-static anterior load (75N) was applied at the first thoracic vertebra (T1) of the baseline and the scoliotic torso and the response of the two spines was investigated. The 75N load was chosen as a small load that would not damage the spine but would be sufficient to cause motion of the entire spine and torso from the upper thoracic region down to the lumbar region. The differences in the responses were then investigated to determine the altered loading pattern introduced by a scoliosis when subjected to the same loading conditions as a non-scoliotic spine.



(a) Baseline (b) Moderate Scoliosis

Figure 7.8: Torso of Baseline and Moderate Scoliosis used for Isolating and Testing the Effect of Scoliosis

In the local coordinate system the motion of some joints of the moderate scoliosis case was found to increase, however it reduced in others as shown in table 7.5.

Joint	Baseline	Moderate Scoliosis	Percentage Difference
T2T1	1.1	1.1	0
T3T2	1.2	1.1	-8
T4T3	1.3	1.2	-8
T5T4	1.5	1.3	-13
T6T5	1.5	1.4	-7
T7T6	1.4	1.4	0
T8T7	1.2	1.5	25
T9T8	1.2	2.1	75
T10T9	2.0	2.2	10
T11T10	2.0	2.2	10
T12T11	2.9	2.6	10
L1T12	3.0	3.0	0
L2L1	4.2	4.4	5
L3L2	4.5	4.9	9
L4L3	4.8	5.2	8
L5L4	5.3	5.7	8

Table 7.5: Range of Motion in Local Coordinate System of Vertebrae Joints of Baseline and Moderate Scoliosis reduced to Torso

The kinematics of the spine showed a reduced range of motion for the scoliosis model compared to the baseline case, except in the lower lumbar vertebrae, see table 7.6

Joint	Baseline	Moderate Scoliosis	Percentage Difference
T1	31	30	-3
T2	32	31	-3
T3	33	32	-3
T4	34	30	-12
T5	35	33	-6
T6	35	33	-6
T7	36	35	-3
T8	36	35	-3
T9	35	32	-9
T10	33	28	-15
T11	30	24	-20
T12	27	22	-19
L1	24	20	-17
L2	20	19	-5
L3	15	16	7
L4	11	11	0
L5	5	6	20

Table 7.6: Range of Motion in Global Coordinate System of Vertebrae Joints of Baseline and Moderate Scoliosis reduced to Torso

This altered motion in both coordinate systems for the moderate case of scoliosis is as expected. The effect of scoliosis was found again to restrict the movement of the spine. This effect was also found in the mild and severe cases of scoliosis.

The introduction of scoliosis to the spine resulted in an altered motion pattern which would affect the forces that are transmitted through the spine. Therefore this was investigated and the force in all three directions were determined.

7.4.2 Local X Direction Forces

In the direction of the force application (X) the forces in the upper part of the spine resulted in R values of 1.0 as the force is due to the applied force, see figure 7.9. However lower in the thoracic and in the lumbar region this value was larger than 1. The forces in the scoliosis model increased on average by 20%.

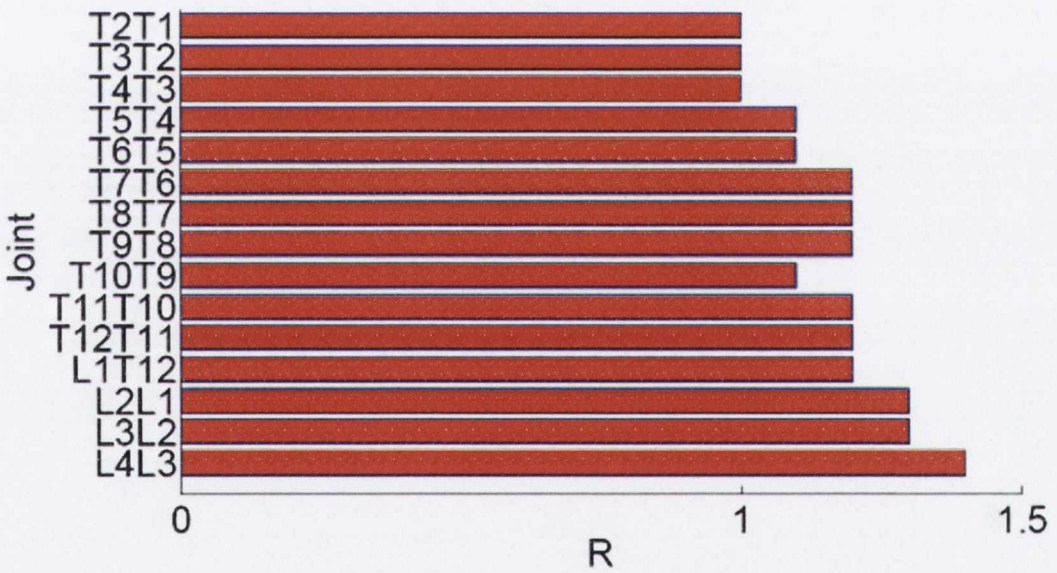


Figure 7.9: R Values of Local X Direction Force for Moderate Torso Compared to Baseline

The initial forces in this lower region of the spine is zero as there is no applied load, it is as the spine moves due to the applied force that the forces on the joints are increased. This is shown by the typical example of joint T10T9 in figure 7.10. This graph shows that the increase in force as the joint moves is greater in the moderate scoliosis case than in the baseline case.

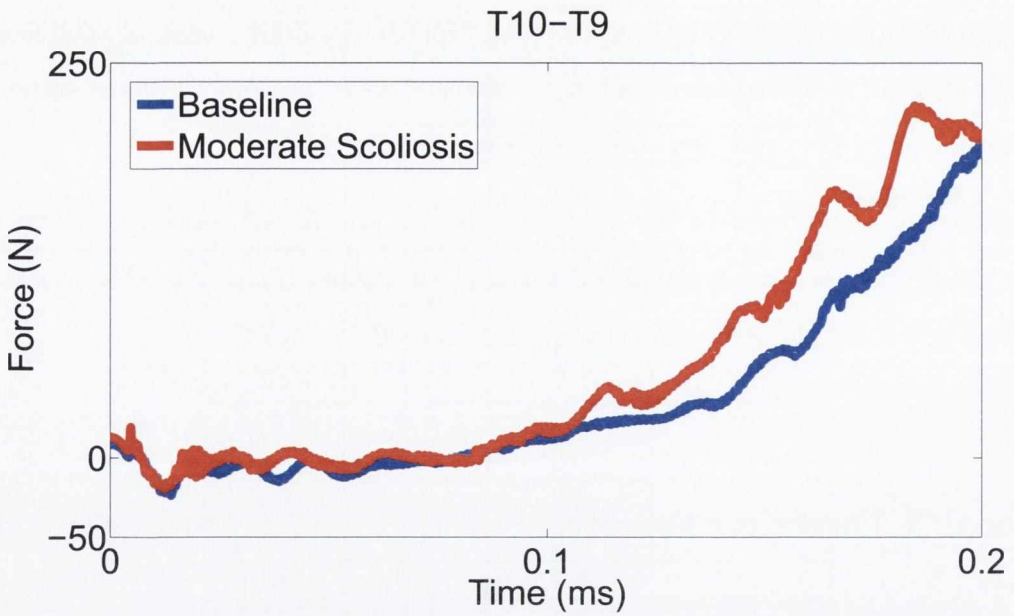


Figure 7.10: Local X Direction Force on T10-T9 Joint

Local Y Direction Forces

The forces in the lateral direction of the spine show a much different pattern for the scoliosis model compared to the baseline case. The forces in the lateral direction for the baseline case are zero as the joints move solely in the sagittal plane due to the application of the single X-direction force. However for the scoliosis case, the effect of the altered shape of the spine is to introduce a load in the lateral direction. The peak forces in this direction are shown in figure 7.11. The largest forces are found in the lower region of the spine for each case of scoliosis.

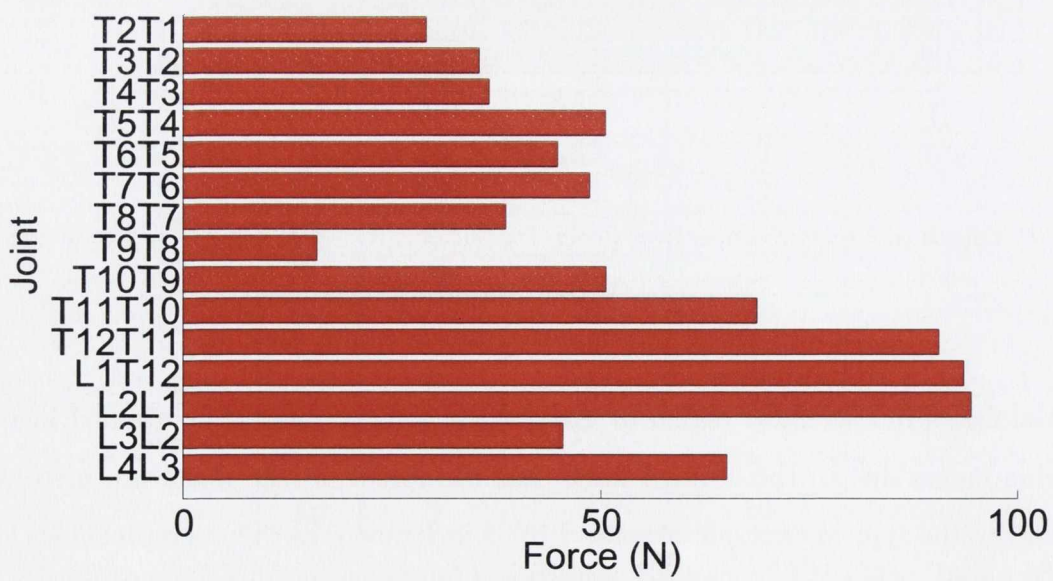


Figure 7.11: Local Y Direction Force for Moderate Torso Compared to Baseline

Z Direction Forces

For this direction of force the joints are subjected to both tensile and compressive loads. Initially the joints are subjected to compressive loads however as the spine moves and flexes these become tensile loads.

In the scoliosis models the joints of the spine experience a lower compressive load than the baseline case. The compressive forces in the scoliosis case do not reach the same level as those found in the baseline case and is reflected in the R values are an average of 0.7, see figure 7.12. This is due to the fact that the scoliotic torso is initially in a more flexed position, figure 7.13, and so its motion is to flex forward when the load is applied. However the initial position of the non-scoliotic spine, figure 7.13, causes the spine to translate forward before flexing when the load is applied. This linear motion causes an increase in the compressive force.

As both spines flex this causes an altered loading pattern as the body is subjected to tensile loading. The tensile forces in the scoliotic spine increase to a greater extent in the upper half of the spine. Figure 7.14 shows joint T6-T5 which typifies this behavior. However in the two lower half of the spine the tensile forces of the baseline case are greater, this is also shown in figure 7.14 of L2-L1 which again is typical of this pattern of behavior. This is due to the restricted motion associated with scoliosis which prevents the lower joints from moving to the same extent as the baseline.

These results show that movement of the spine causes an increase in the forces in the Z-direction. This is due to the increased stiffness of the scoliotic spine. This effect was also found for the shear loading on the spine.

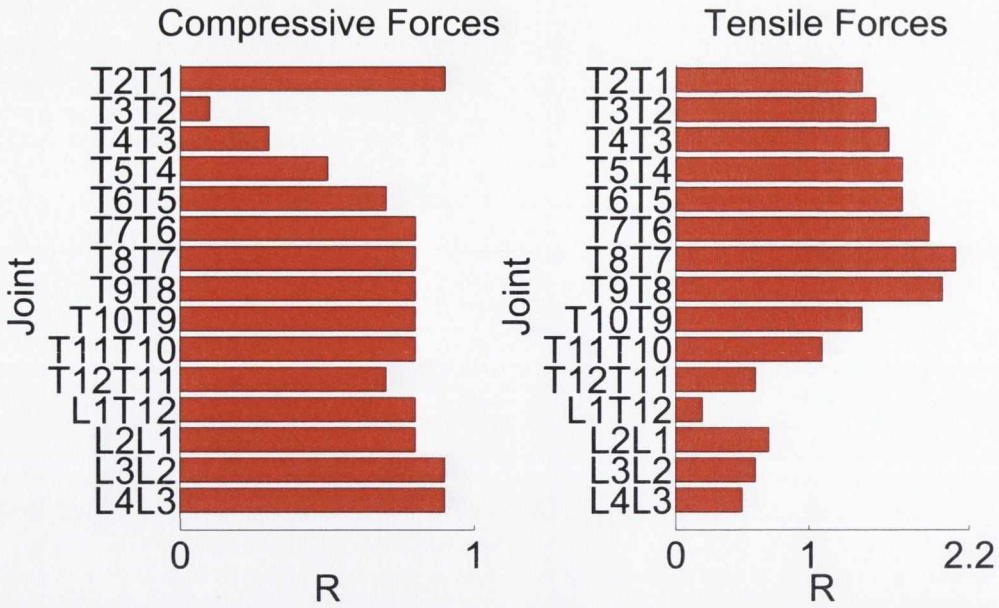


Figure 7.12: R Values of Local Z Direction Force for Moderate Scoliosis Torso Compared to Baseline

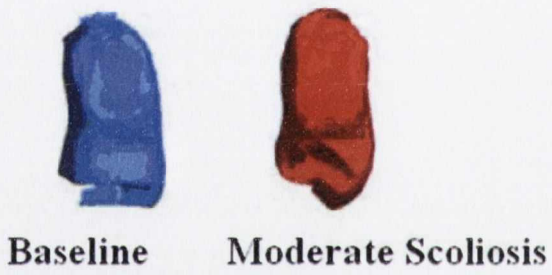


Figure 7.13: Comparison of Baseline Spine and Scoliotic Spine

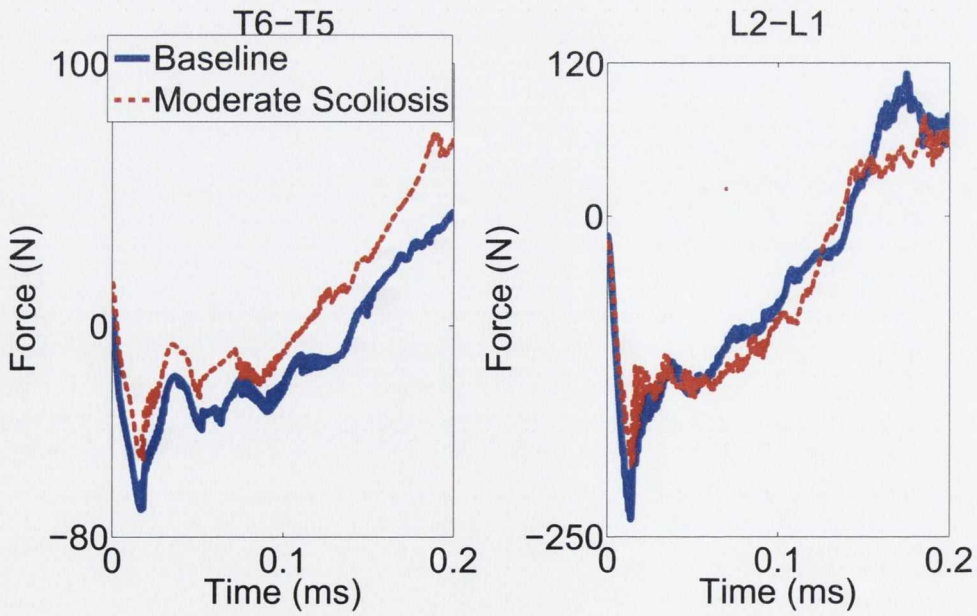


Figure 7.14: Local Z Direction Force on T5-T6 and L2-L1 Joint

7.4.3 Resultant Forces

The resultant forces were found to increase for the scoliosis case, as shown in figure 7.4.3. The average increase in force for the entire spine is 20% which is of significance and may lead to increased injury with an increase in the applied load.

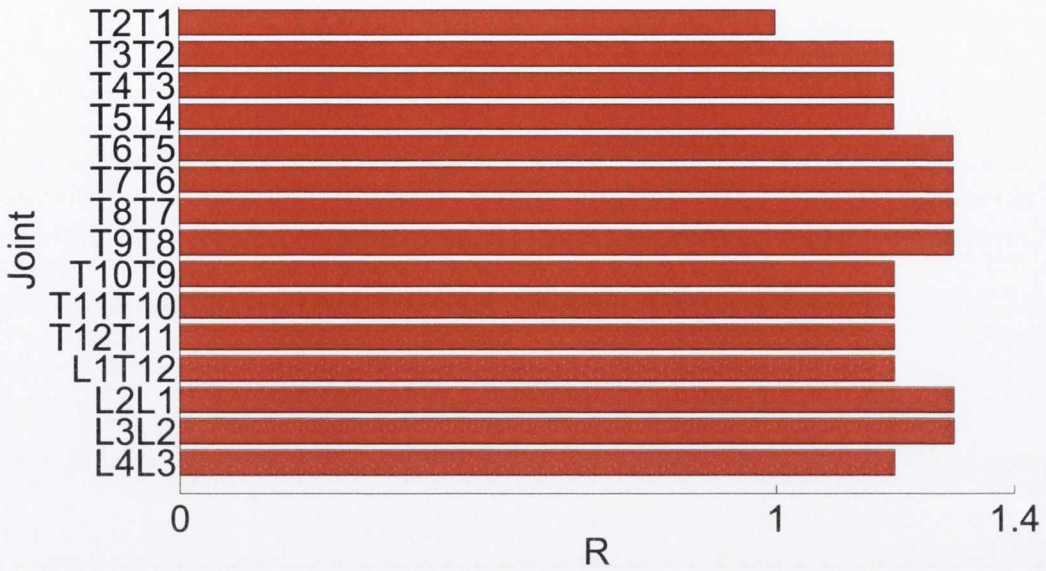


Figure 7.15: R Values of Resultant Force for Moderate Torso Compared to Baseline

7.5 Summary

Scoliosis was found to have two effects on the behaviour of the models. Scoliosis increases the loading on the spine due to the altered shape of the occupant's torso which alters the interaction with the wheelchair - point loading. Scoliosis also reduces the movement of the spine as the joints rotate about an altered axis. When tested in isolation this altered movement has been found to increase the loading on the spine by up to 20%.

7.6 Forces on the Vertebral Joints of Crash Simulation

The forces in the vertebral joints in the three sections of the spine (cervical, thoracic and lumbar) were investigated and are presented here. The findings are compared to the results from the baseline case and the R values were calculated. A distinct pattern in the results was found for all levels of scoliosis and therefore only the results for the moderate case is presented here. The mild and moderate results are shown in Appendix G.

The key area of investigation is the forces in the X direction which is the direction of the crash and is therefore the principal loading direction. Research on destructive testing of human lumbar vertebrae has found a value of 2.8kN to cause breakages to the structures

and this value is used to predict damage to the the spine in this work [108]. The global Y-direction for these models is found to be composed of noise which does not reach any significant levels for injury. The spinal column has been found to be quite resilient to loading in the Z direction [69], and the compressive loads that are found in these models are generally below values which cause injury, however where they are found to be of significance they are presented here.

7.6.1 Contact Forces on the Spine

The contact force on the torso of the spine due to its interaction with the seatback was determined and is presented for the baseline and moderate case of scoliosis in figure 7.16. In this figure the peak forces on the scoliotic spine occur later due to the motion of the restricted spine which takes longer to make full contact with the seatback than the baseline case, see figures 7.18 and 7.17. This altered interaction also shows that there is three distinct loading stages on the scoliotic spine. Initially contact is made with the thoracic kyphosis which then straightens to allow contact with the lower thoracic region and then finally contact with the lumbar region occurs. This is compared to the much smoother contact interaction of the baseline occupant with the seatback, figure 7.16. In the baseline occupant the spine is not restricted and so the kyphosis straightens to allow full contact with the wheelchair. Therefore in the scoliosis cases the area that this load is applied over is reduced. This leads to a point loading effect on the spine. The peak value for moderate case of scoliosis is lower than that of the baseline as the occupant with scoliosis does not move rearwards with the same acceleration as the baseline occupant.

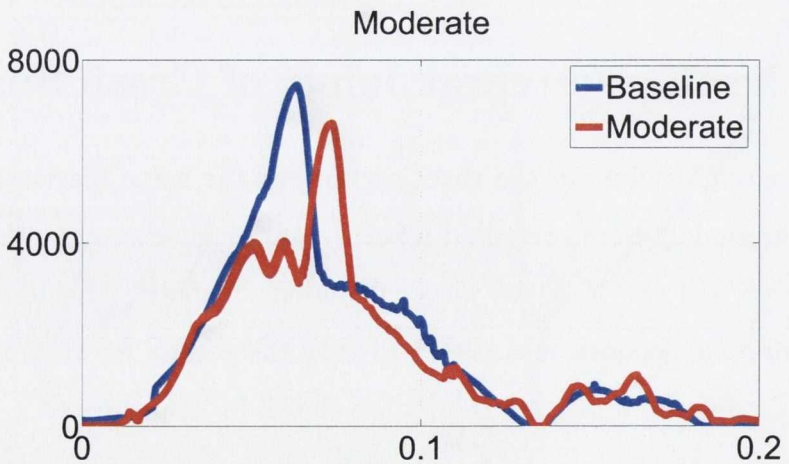


Figure 7.16: Contact Forces Between Occupant and Seatback for Moderate Scoliosis and Baseline Models

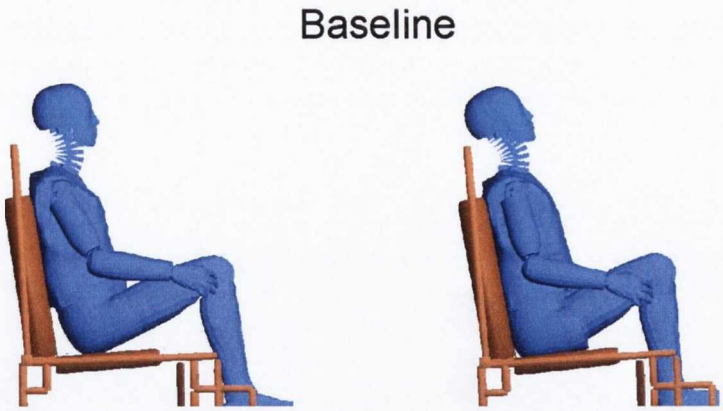


Figure 7.17: Interaction of Baseline Occupant and Wheelchair

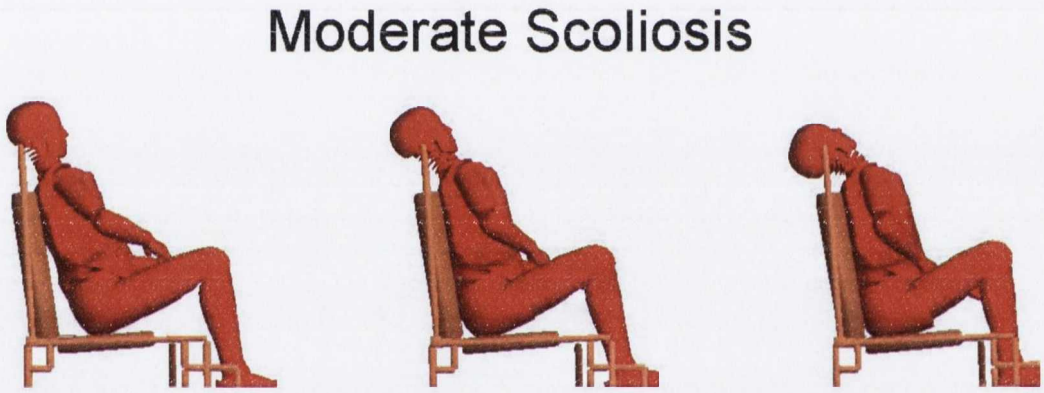


Figure 7.18: Interaction of Moderate Scoliosis Occupant and Wheelchair

7.6.2 Cervical

The cervical region of the scoliotic spine was found to produce similar results to those of the baseline case. The time history plots of force on the joints in the neck for the baseline and moderate case is shown in figure 7.19. This graph also shows that the peak forces in the cervical spine are reached in the scoliosis cases before those of the baseline case. The relative increase in forces, R value, was therefore found to be approximately 1, see figure 7.20.

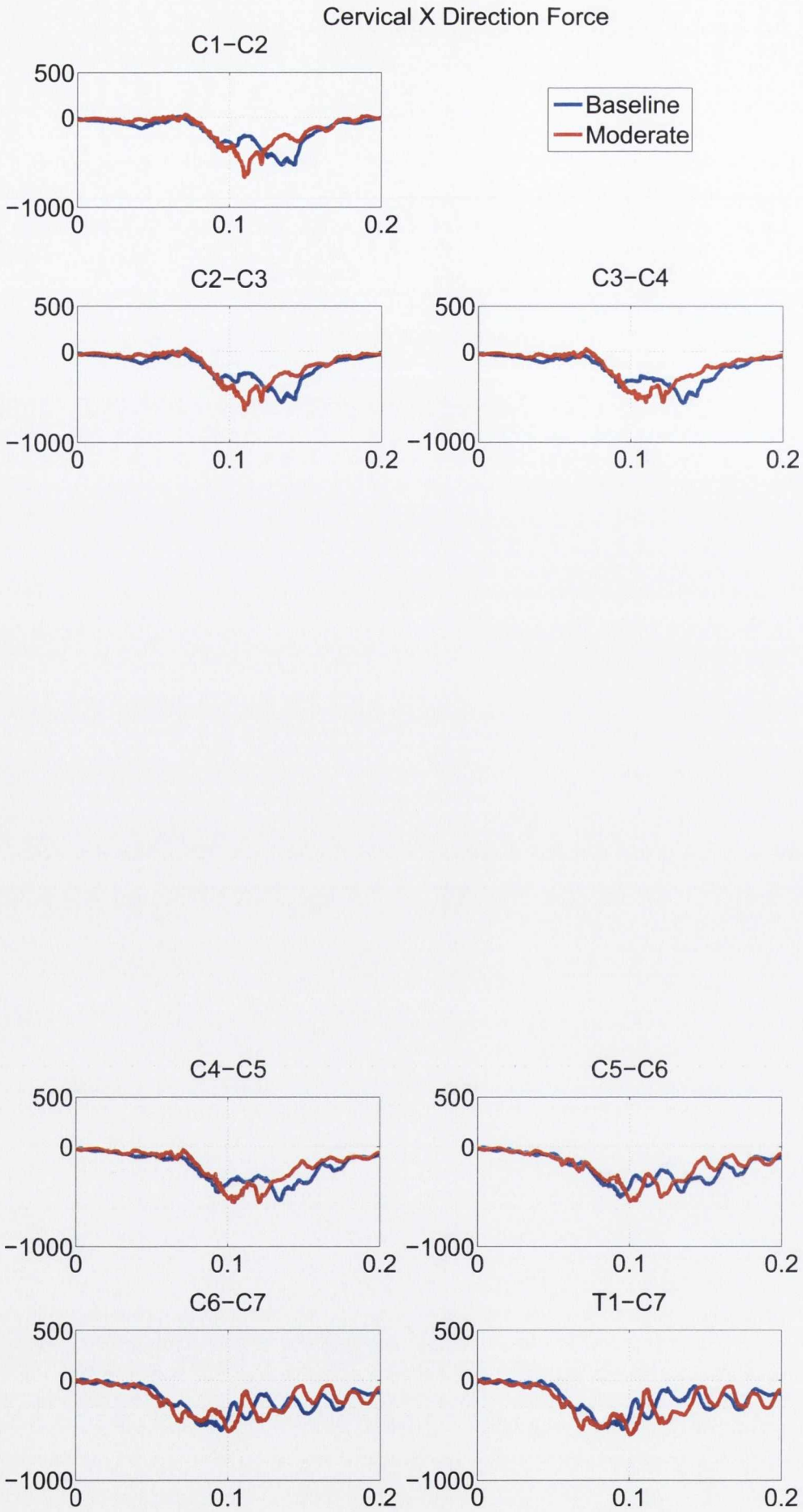


Figure 7.19: Time History Graphs of X-Direction Force in Cervical Joints for Baseline and Moderate Case of Scoliosis

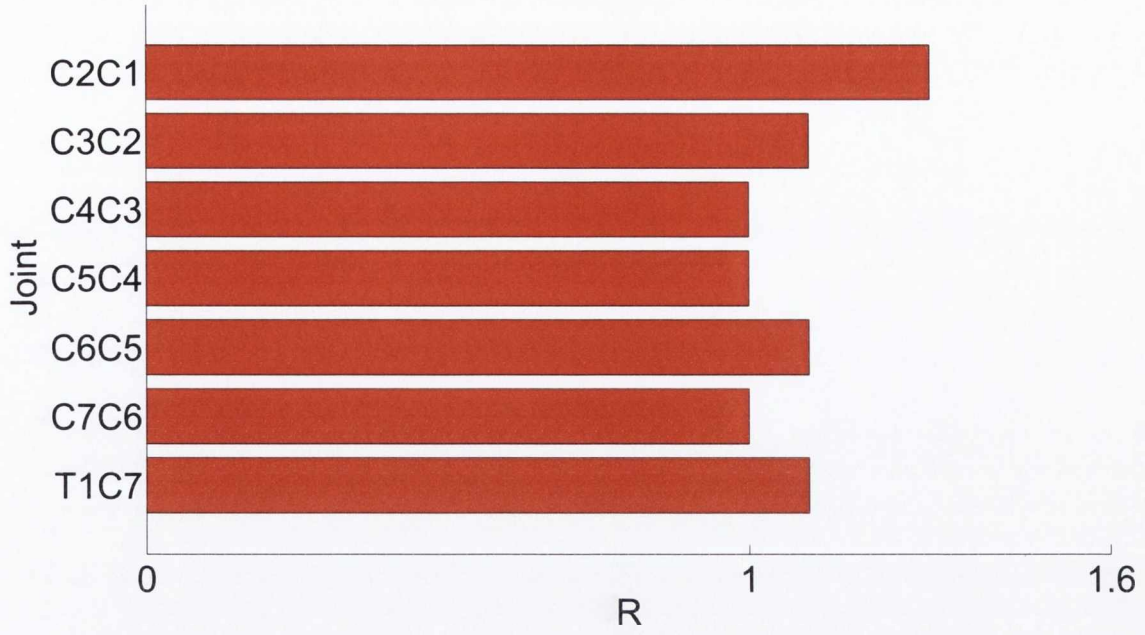


Figure 7.20: R Values for Moderate Scoliosis in Cervical Region

7.6.3 Thoracic

The thoracic region of the scoliotic spine shows an increase in the forces exerted on the vertebral joints. The forces on each of the joints of the moderate case of scoliosis over the duration of the crash are presented in figure 7.21. The largest R value, figure 7.22, for the moderate case is 2.1 however this is not a true reflection of the differences between an occupant with and without scoliosis as it does not compare the same event in both cases. This inflated figure is due to a reduced sitting height that is created due to the deformity of the spine. This alters which sections of the spine are loaded due to contact with the seatback and which are loaded due to rearward motion of the head and neck. Therefore there is a difference in the level at which the joints are loaded in the positive and negative direction. This change in the loading pattern is shown in figure 7.21 as the shift from positive to negative loading on the T5T6 joint for the baseline case and joint T4T5 for the moderate scoliosis case. Therefore when comparing the forces on the joints of the spine it is important not to compare the results at this area of shifting between the different loading conditions as it does not represent the same loading condition on the spine. The magnitude of the results at these joints are not the largest in the spine it is however the relative difference between the baseline and scoliosis models which exaggerates the values. This was also found for the mild and severe cases, see Appendix G. The real R value increases in forces for each level of scoliosis are presented in table 7.7.

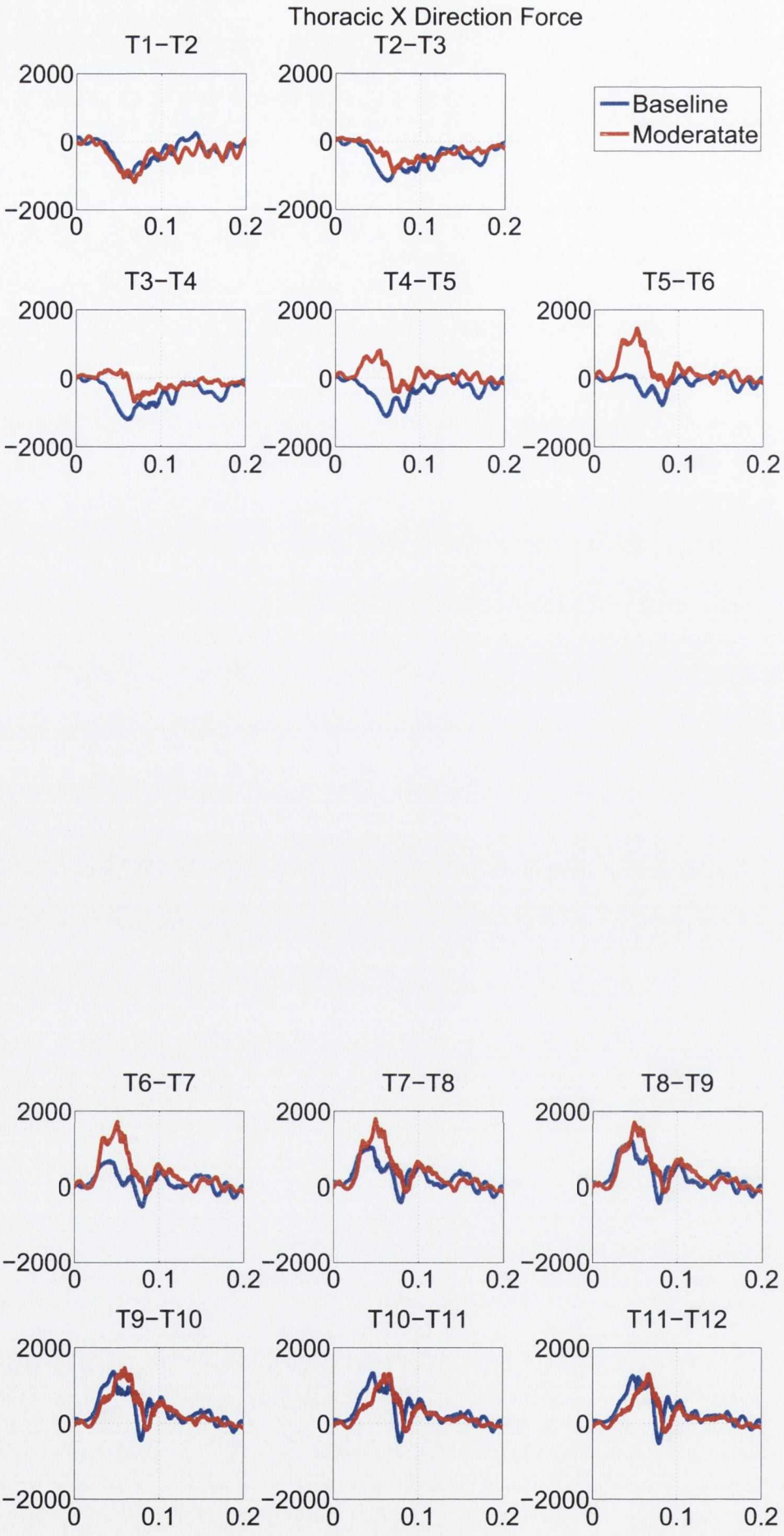


Figure 7.21: Time History Graphs of X-Direction Forces in Thoracic Joints for Baseline and Moderate Case of Scoliosis

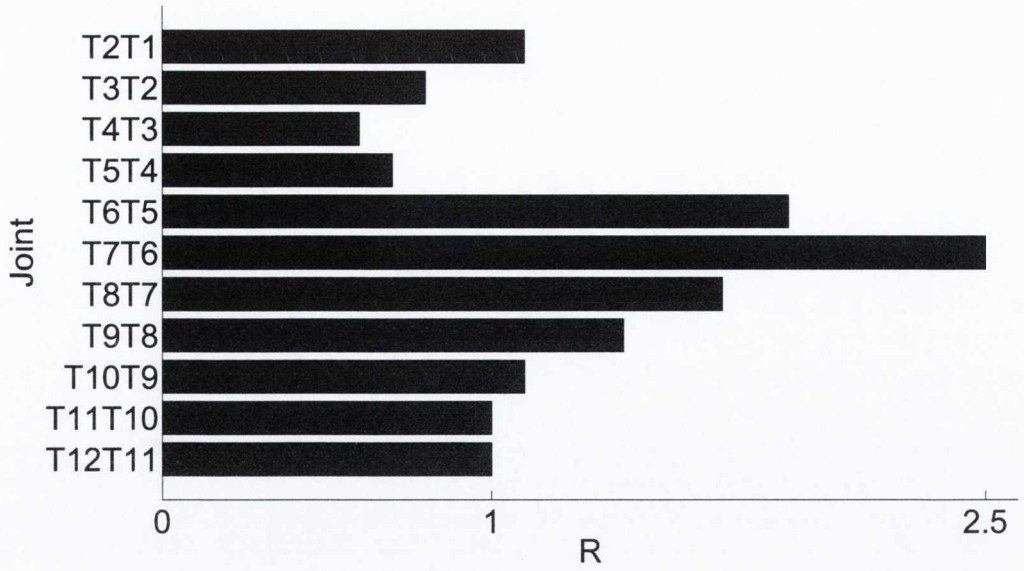


Figure 7.22: R Values for Moderate Scoliosis in the Thoracic Region

	R Value
Mild Scoliosis	1.2
Moderate Scoliosis	1.4
Severe Scoliosis	1.9

Table 7.7: True Peak R Valeus for Mild, Moderate and Severe Case of Scoliosis

Anterior and Posterior Forces

This section further analyses the different shear forces on the spine in the thoracic region. As mentioned previously when scoliosis is introduced to the occupant the deformity of the spine reduces its sitting height in the wheelchair. This resulted in a different loading pattern on the spine of the occupant. The spine is subjected to both posterior and anterior shear loads depending on the interaction with the seatback. In the upper thoracic region the spine is indirectly loaded in the posterior direction (negative shear) due to the inertial motion of the head and neck which pulls the upper part of the spine with it. However the mid and lower thoracic region experiences anterior loading (positive) as these sections are directly loaded due to impact with the seatback. The portion of the spine which is subjected to these posterior and anterior loads differs for the scoliosis models depending on their level of deformity and related seated height.

A relationship between the level of scoliosis and reduced seated height has been established and a rear view of the occupants in their wheelchairs is shown in figure 7.23. The reduced sitting height correlates with the reduced portion of the upper thoracic spine which is loaded posteriorly. This is shown in the graphs of the peak forces on the joints of each of

the spines. The peak forces exerted on the joints of each of the models is shown in figure 7.24. The different joints at which these forces switch from positive to negative is clearly demonstrated. These graphs also show that at this point of switching from positive to negative forces the peak values on the joints are reduced.

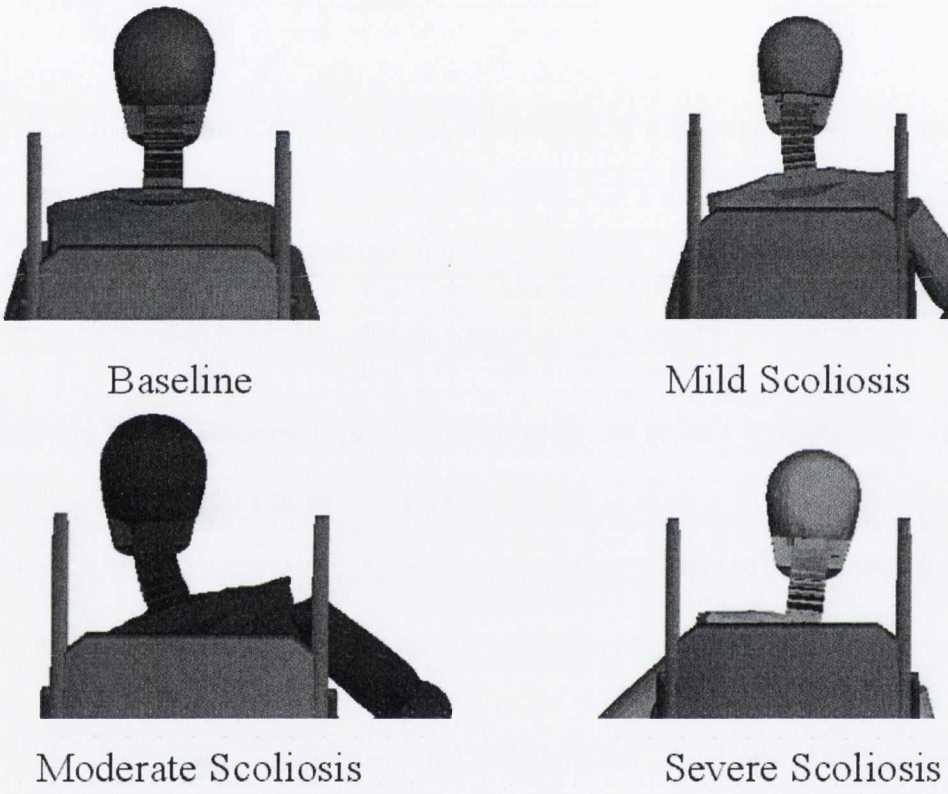


Figure 7.23: Seatback Height Relative to Torso for Baseline and Scoliosis Models

For the mild and moderate cases the change in the forces is based on the seatback height relative to the occupant's torso. However for the severe case of scoliosis this is not the case as its increased deformity means that there is much less contact between the occupant and the seatback.

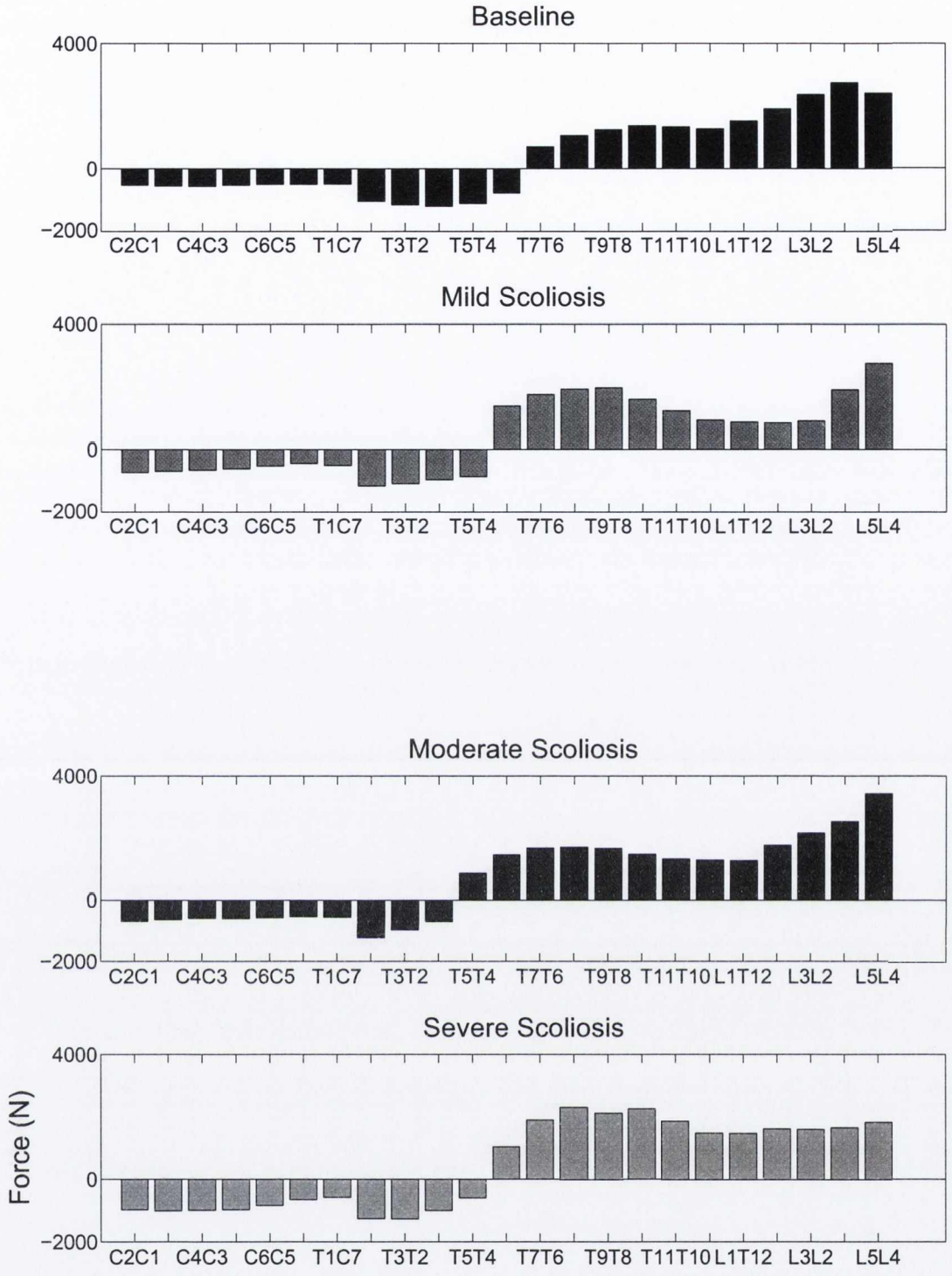


Figure 7.24: Postive and Negative Shear Forces on the Spine

The initial orientation of the upper thoracic region is more pronounced than in the other cases, see figure 7.25. This upper region is therefore less in contact with the seatback and it is the initial orientation of these vertebrae which is responsible for the direction of loading. Therefore the upper thoracic region of this much deformed model does not move through the same rearward pattern as found in the other models. The images from the animation of the crash show this for both the whole torso and at the vertebral level, figure 7.25.

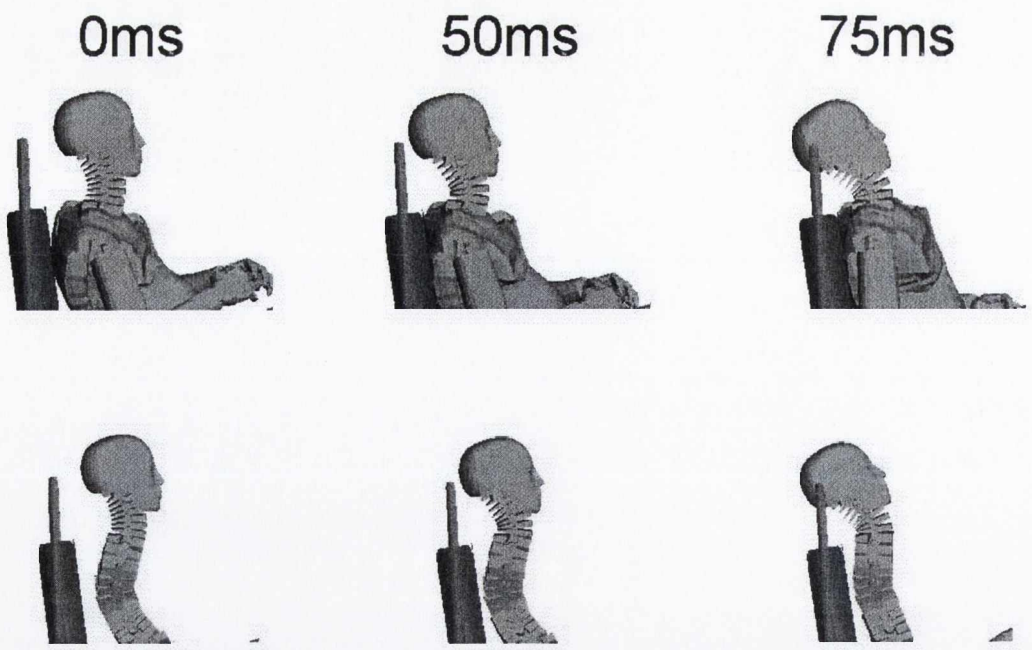


Figure 7.25: Shear Forces on Severe Scoliosis - Effect of Initial Orientation of Upper Throacic Spine

Apex of the curve

The largest force in the joints of the thoracic region is seen to directly correspond to the apex of the scoliotic curve as seen on the frontal x-ray of the moderate case of scoliosis, see figure 7.26. This was found for all cases of scoliosis. This has particular clinical relevance as it highlights the area of greatest risk of injury, as the values are closer to levels known to cause damage to the vertebrae. The largest force in this region of the spine is found in the severe case of scoliosis with a peak value of 2kN on the T7-T8 joint which is at the apex of the spine. This region is the most deformed as determined previously and so the effect of scoliosis which increases the forces in the joints is found to be at its greatest in this region of the spine.

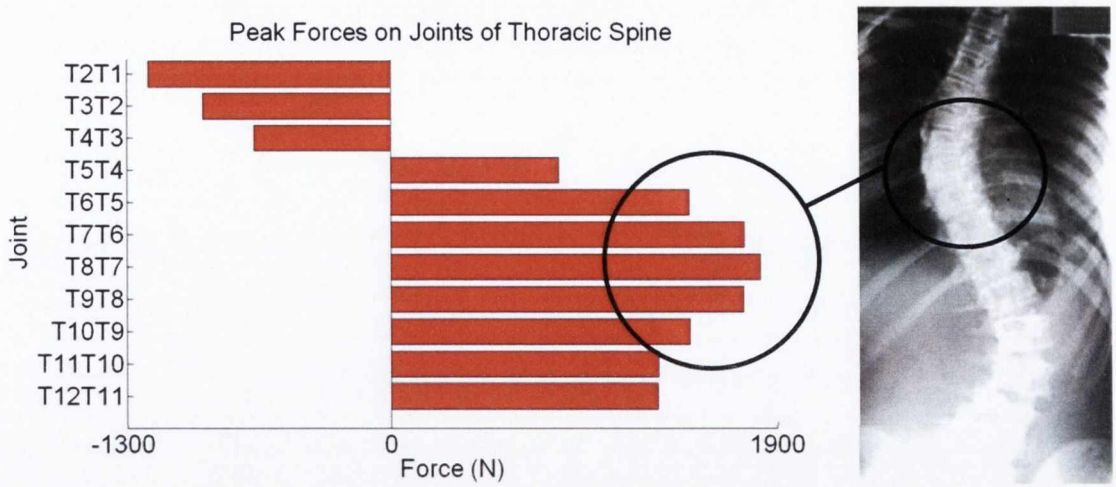


Figure 7.26: R Values in the Thoracic Spine of Moderate Scoliosis and the Corresponding X-ray

The apex of the curve was found to have the highest force since the thoracic region is the area of maximum deformity and is subjected to the highest contact force. This is due to the combined effect of point loading and scoliosis as detailed previously both of which are at maximum levels in this area.

7.6.4 Lumbar

The forces on the lumbar region for the baseline case are the largest in the spine. This increased value is due to the rearward momentum of the pelvis towards the seatback which causes the increased contact force. It has previously been shown that the contact between the lumbar region of the spine and the seatback is shown as a peak in the contact forces as shown in figure 7.16. The peak contact force for the moderate scoliosis model occurs later due to the less flexible scoliotic spine which cannot straighten against the seatback in the same manner as the baseline model. The forces in the lumbar region of the scoliosis models were found to be lower than those of the baseline case, see figure 7.27 with an average R value of 0.9, figure 7.28. The notable exception to this is the lowermost joint L4L5 which has a higher force.

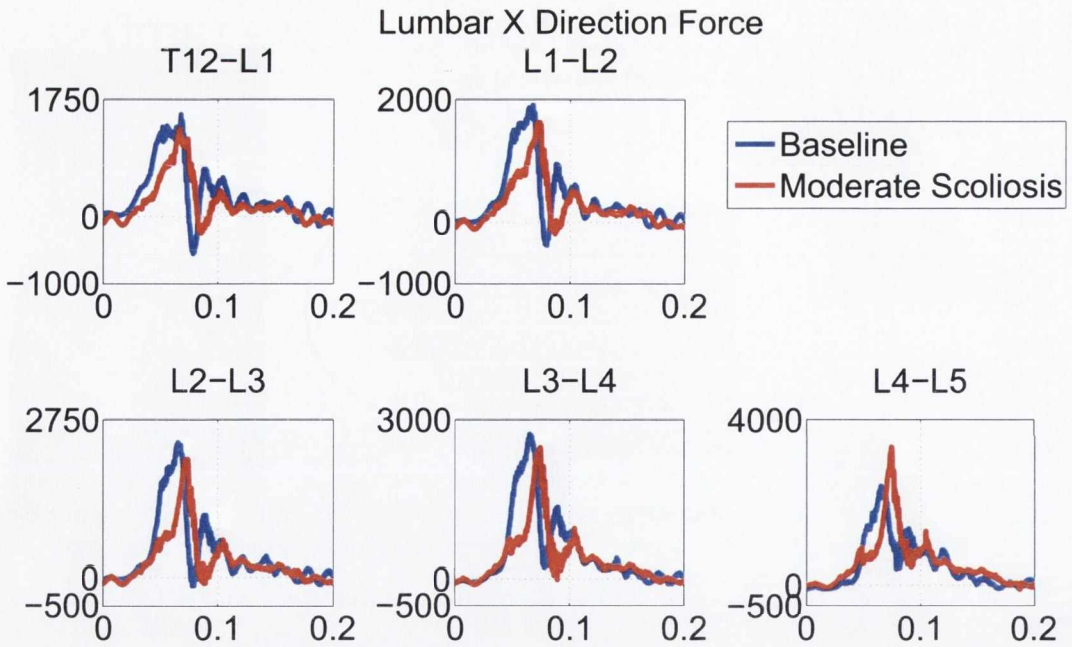


Figure 7.27: Time History Graphs of X-Direction Forces in Lumbar Joints for Baseline and Moderate Case of Scoliosis

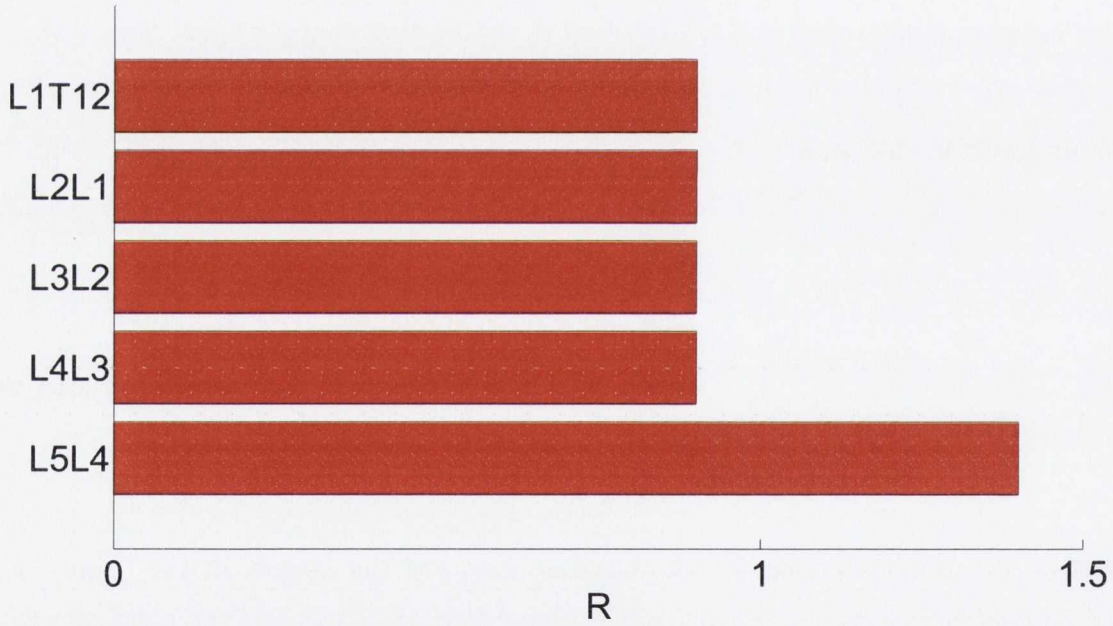


Figure 7.28: R Values for Moderate Scoliosis

The reduced forces on the lumbar spine are due to the restricted motion of the scoliotic vertebrae which reduces the rearward motion of the pelvis towards the seatback. The larger lordosis of the scoliosis does not straighten to the same extent as the baseline case and therefore the lumbar joints do not contact the seatback with the same force. The lowermost (L4-L5) joint and the pelvis are however subjected to point loading due to the curved shape of the spine which leads to a large impact between the occupant and the wheelchair at this

level. This is most clearly shown for the mild case of scoliosis which has the most exaggerated level of lorodosis, see figure 7.29. This altered interaction with the seatback results in the different response as found in the force time history plots in figure 7.30. This is found for both the mild and moderate cases of scoliosis. However an exception to this is the severe case of scoliosis.

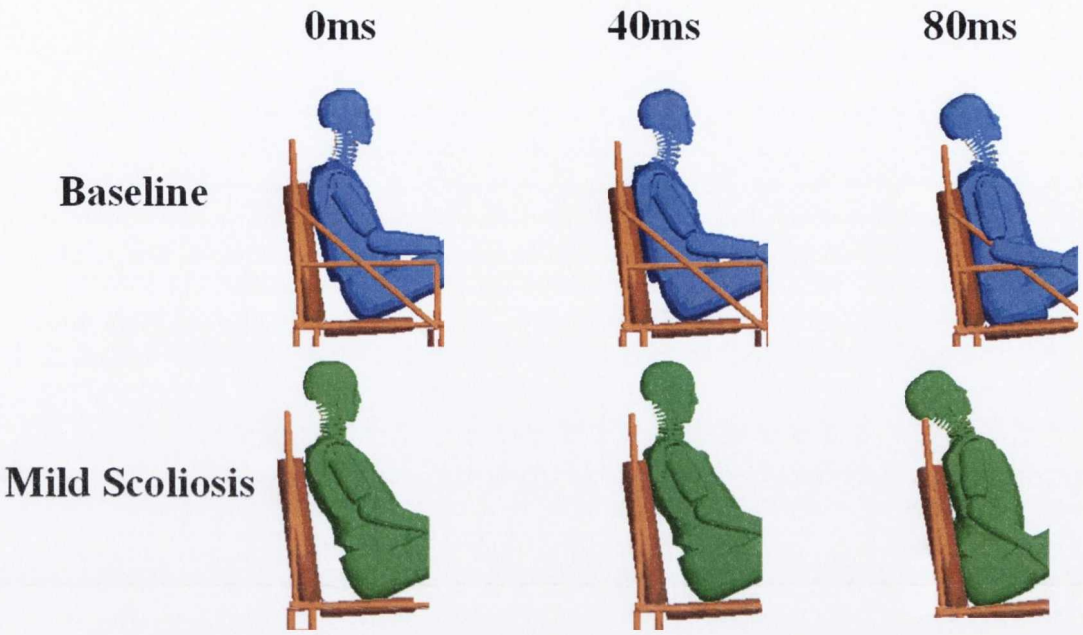


Figure 7.29: Side View of Baseline and Mild Scoliosis Lumbar Regions at 40ms Intervals

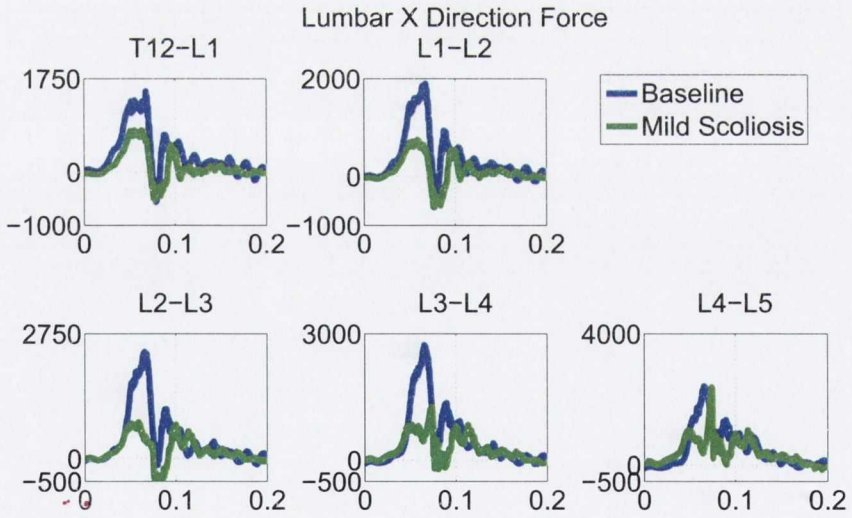


Figure 7.30: Time History Graphs of X-Direction Forces in Lumbar Joints for Baseline and Mild Case of Scoliosis

The severe case of scoliosis does have a lordosis present in the lumbar region of the spine as shown in the x-ray image, figure 7.31. While lordosis is present in the spine of the dummy the height of the vertebrae and the finite element jacket which is wrapped around the spine of the dummy results in the spine as shown in figure 7.32.



Figure 7.31: Lateral X-Ray of Severe Case of Scoliosis

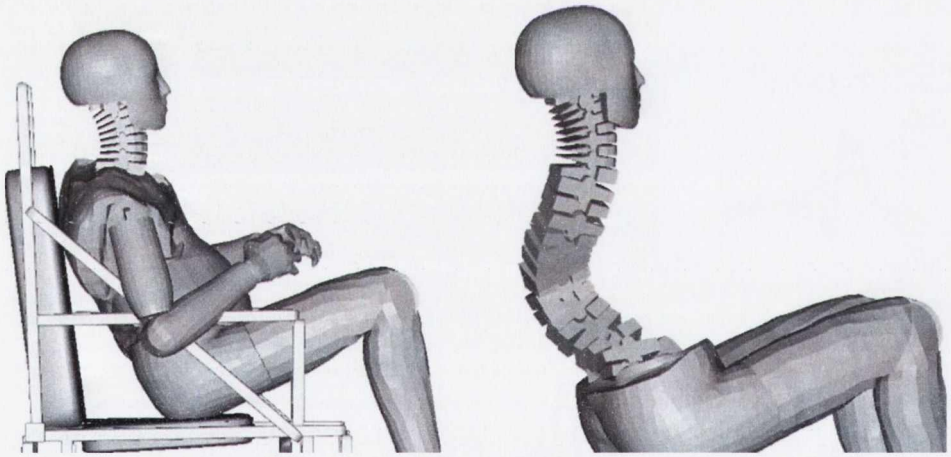


Figure 7.32: Severe Case of Scoliosis in Wheelchair and Spine Joints of Severe Case of Scoliosis

The forces on the spine are much reduced as shown in figure 7.33. This has an altered loading pattern which is more similar in behavior to that of the baseline case as shown in the 40ms snapshots of figure 7.34.

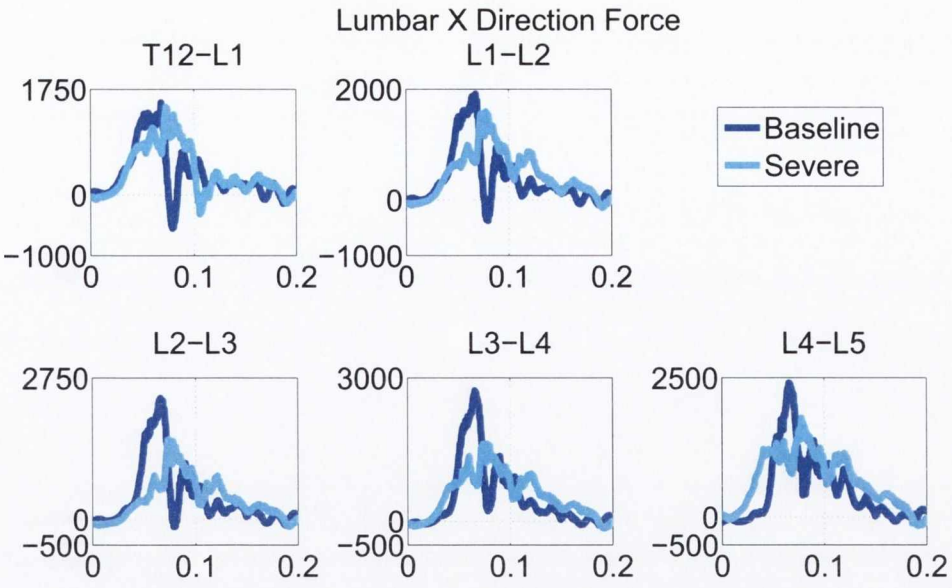


Figure 7.33: Forces in Lumbar Spine of Mild Scoliosis

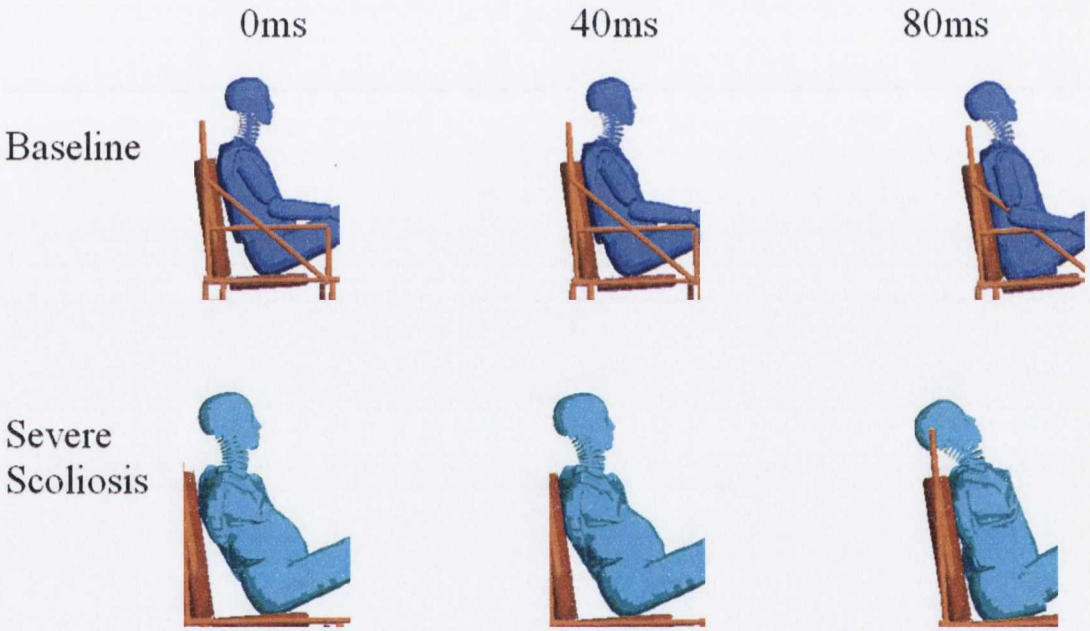


Figure 7.34: Side View of Baseline and Severe Scoliosis Lumbar Regions at 40ms Intervals

7.7 Injury Criteria

Injury Criteria predict the level of injury due to a rear impact. The development, validition and the use of such equations is detailed in Chapter 2. Using these criteria the outputs from the models with scoliosis were used to predict injury levels in the neck. These predicted injury scores were assessed with reference to the baseline case and the results are presented here. The trends that were found and typify the response due to the introduction of scoliosis are also presented.

For the moderate case of scoliosis it was found to produce a higher *NIC* score than that of the baseline case, see figure 7.35, due to the increase in the acceleration of the first thoracic vertebra (T1), see figure 7.36. This increase in the acceleration of the torso is caused by the effect of point loading on the occupant due to the altered shape of the back.

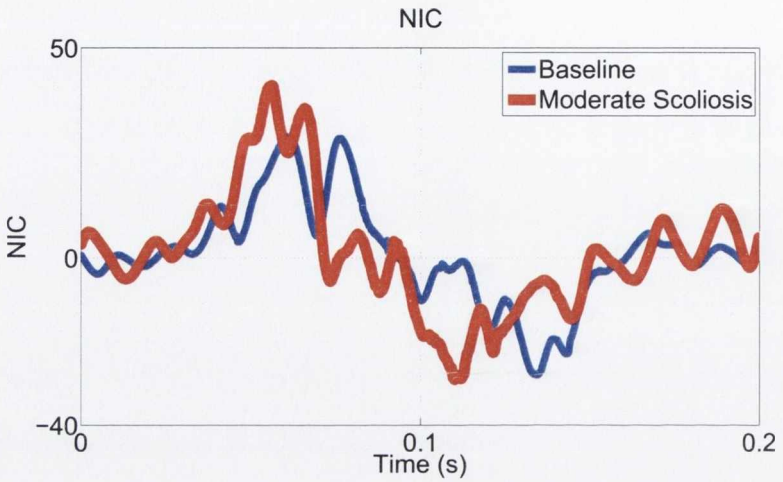


Figure 7.35: Predicted *NIC* values for Baseline and Moderate Scoliosis

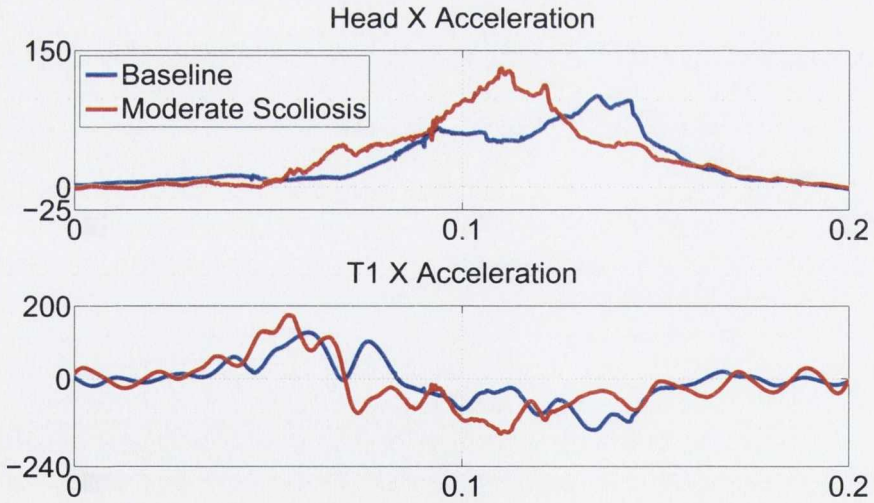


Figure 7.36: Acceleration of Head and First Thoracic Vertebra in X direction

The same pattern was found for the mild case of scoliosis, see figure 7.37.

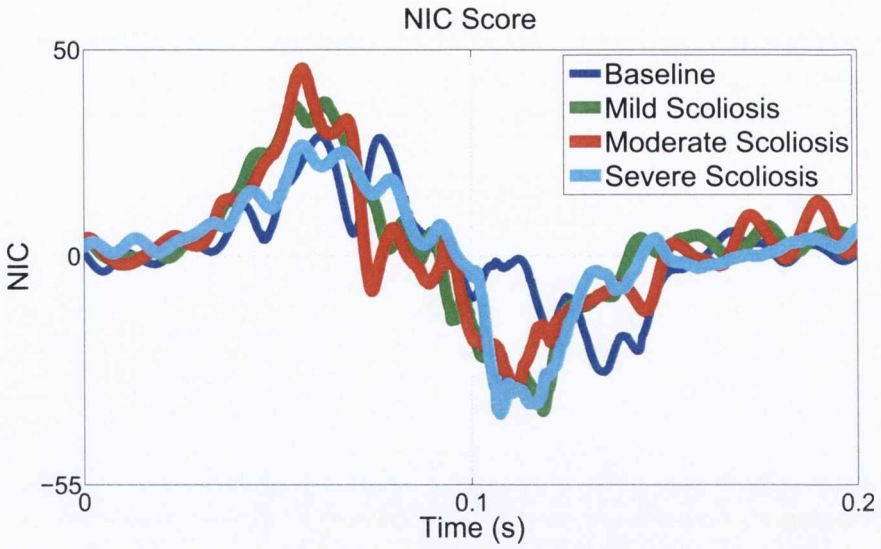


Figure 7.37: Predicted *NIC* values for Baseline, Mild, Moderate and Severe Cases of Scoliosis

However a lower *NIC* score was found for the severe case of scoliosis which is also presented in figure 7.37. This lower *NIC* score is due to the much more deformed upper thoracic spine which restricts the motion of the T1 vertebra to a greater degree than the other cases of scoliosis. This occupant also has a much reduced sitting height which prevents the upwards and rearwards motion that is associated with rear impact, see Chapter 2. These two effects combine to produce a much reduced X direction acceleration of the torso compared to the other scoliosis models which have an increased acceleration due to the point loading on the occupant. This is illustrated in figure 7.38 which compares the motion of the severe and moderate crash test dummies. The T1 of the severe case of scoliosis is much more restricted than that of the moderate case of scoliosis. This results in a much lower T1 X direction acceleration as shown in figure 7.39.

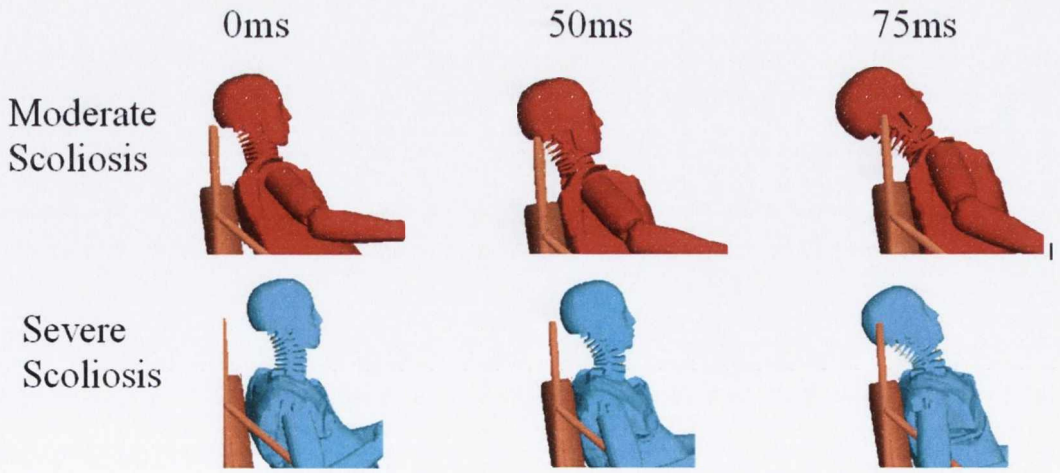


Figure 7.38: Comparison of the Acceleration of the Occupant with Moderate and Severe Scoliosis

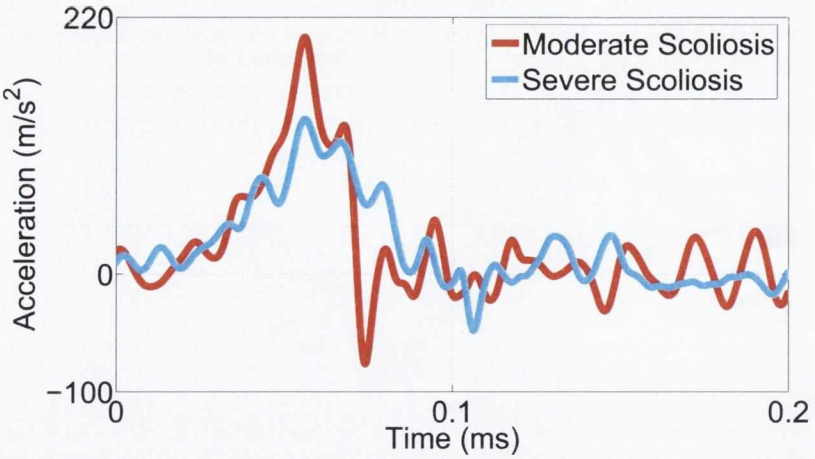


Figure 7.39: X-Direction Acceleration of T1 Vertebra in Moderate and Severe Scoliosis

The peak values for each case of scoliosis is presented in table 7.8. The moderate case of scoliosis shows the largest increase in this injury criterion of 50%.

	NIC (m^2/s^2)	Percentage Difference Compared to Baseline
Baseline	29	
Mild Scoliosis	39	34
Moderate Scoliosis	45	55
Severe Scoliosis	26	-10

Table 7.8: *NIC* peak Values for Baseline, Mild, Moderate and Severe Case of Scoliosis

Nkm

The *Nkm* results shows a marked increase in the values when scoliosis is introduced. For the moderate case the forces and the moments on the neck are seen to increase, see figure 7.40. The upper neck bending moment is the dominant component of the criterion and any changes in this have a direct influence on the injury score. This moderate case of scoliosis has an *Nkm* score of 1.8 which is more than 50% greater than the baseline, see figure 7.41. A similar level of increase was found in each of the scoliosis cases 7.42. The increased score is due to the increased acceleration of the head caused by the point loading effect of the altered curvature of the spine. In the neck the motion of the vertebrae is not restricted by the presence of scoliosis in the same manner as the rest of the torso. As detailed in Chapter 2, the neck does not have scoliosis only a correcting reflex to reposition the head horizontaly to aid vision.

The mild and severe cases of scoliosis therefore also display the same pattern, see figure 7.42. The peak *Nkm* values are presented in table **??**. The percentage increase of these compared to the baseline is also presented, with the largest increase of 68%.

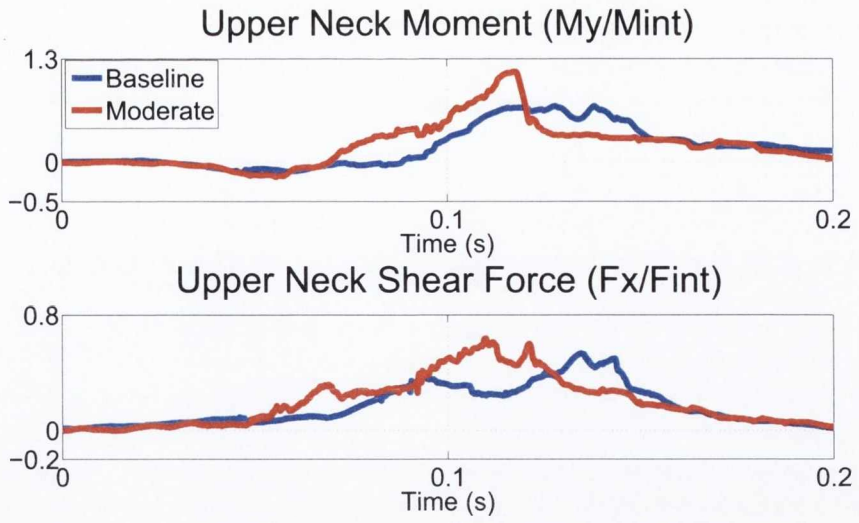


Figure 7.40: Components of *Nkm* for Moderate Scoliosis

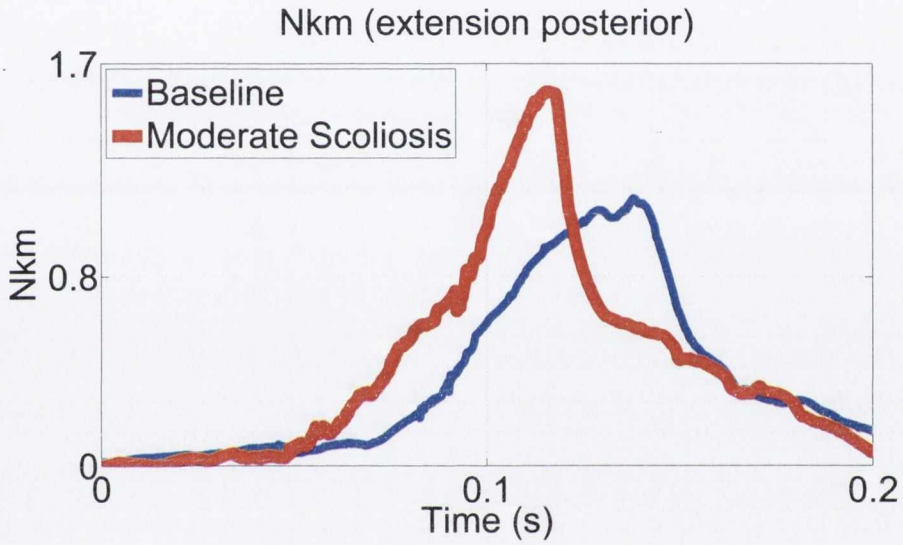


Figure 7.41: *Nkm* for Baseline and Moderate Scoliosis

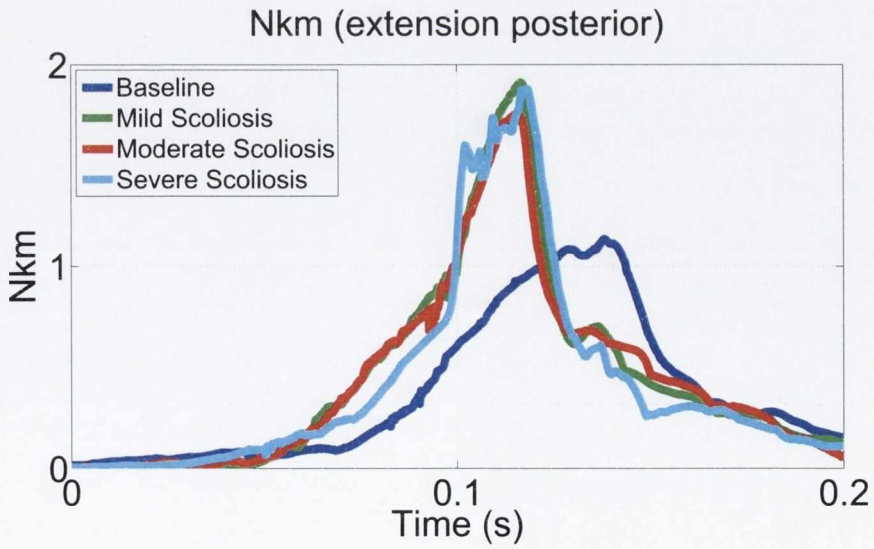


Figure 7.42: *Nkm* scores for Baseline, Mild, Moderate and Severe Cases of Scoliosis

	Nkm	Increase Compared to Baseline
Baseline	1.14	
Mild Scoliosis	1.78	56
Moderate Scoliosis	1.76	54
Severe Scoliosis	1.85	63

Table 7.9: *Nkm* peak Values for Baseline, Mild, Moderate and Severe Case of Scoliosis

7.8 Summary of Investigation into Effect of Scoliosis

The aim of this section of the analysis was to determine the influence of scoliosis in a rear impact and whether this had a substantial effect on the results. To achieve this many approaches were used to assess and define scoliosis in order to characterise it and its effects.

The results from this analysis reveals an increase in loading on the models with scoliosis due its two effects - point loading and increased sagittal stiffness. These combine to have a large effect on - the range of motion that the spine passes through, the forces on the body and the acceleration that the body moves at - and therefore the predicted risk of injury. The influence of scoliosis is shown to be greater with larger levels of deformity, as the R values of the loads on the joints of the scoliosis models compared to the baseline case were found to increase as the degree of scoliosis increased.

The sitting height of the occupant relative to the seatback was shown to have a significant effect on the shear loading conditions. While the forces in the cervical region are not greatly altered by the introduction of scoliosis, there are large increases found in the thoracic region. The peak forces in the thoracic region are near injurious levels. Damage to the vertebrae soft tissue can occur at approximately 1.5kN [77]. The forces on the joints in the spine increase with increased level of kyphosis as well as increased levels of lordosis. This is due to the altered interaction with the seatback that an altered spine shape causes. Therefore the wheelchair will be adapted to better fit each of the scoliosis models. The wheelchair height will be positioned at the same relative height to the spine in the scoliosis cases as found in the baseline, this work is presented in Chapter 9. This will have significance to clinical practice as the wheelchair height can be adapted to the sitting height of the occupant.

Similarly the position of the occupant within the wheelchair was found to have an influence on the loading on the spine and the predicted injury levels. The horizontal distance between the lumbar spine and seatback was found to have an influence on the loading on the spine as the rearward acceleration increased the contact force on the spine. This has clinical relevance for seating clinics which provide adapted seating solutions to their many clients.

This includes the addition of supports to accommodate the altered posture of the occupant which removes any gaps between the occupant and the seatback and will be investigated in Chapter 9.

The true R values that were determined for each level of scoliosis showed an increase with the level of scoliosis. However, this increase did not correspond to the relative increase in the Cobb Angles. The Cobb Angle of each of the scoliotic spines were defined by a clinician in the scoliosis clinic that provided the x-rays. The values were 25^o, 56^o and 94^o and while there is an almost 4 times increase in the level of scoliosis this did not correspond to a 4 times increase in the peak forces or R values on the spine.

The injury criteria show an altered response when scoliosis is introduced. The *NIC* suggests a general increase in risk of injury for scoliosis cases. However the influence of the much greater level of deformity of the upper thoracic spine in the severe case reduces the risk. This region of the body is restricted from moving in the X direction however its acceleration in the Z direction is increased. This is also found in the Z component of forces which is much increased. The forces in this upper thoracic and lower cervical region are increased and are close to levels known to cause damage to the vertebrae. Testing of the vertebrae has found that forces of about 3kN cause breakages in compression [70]. The severe case of scoliosis has values of about 2.7kN which is close to this injurious level. Therefore there is an increased risk of injury for the scoliotic occupants. The *Nkm* value is increased in all cases as the head is accelerated to a greater extent due to the larger impulse passed upwards from the thoracic region due to point loading. The motion of the neck is therefore increased as it is not restricted by the presence of a scoliosis.

For each of the assessments the validity of the result was upheld as it was greater than the discrepancy found in the validation process of the baseline model. Therefore in accordance with the validation tree that was established these values were all above the 10% error of the model, and therefore we can accept the hypothesis that scoliosis has a significant effect on the results. Therefore in accordance with the validation process we accept the given hypothesis.

7.9 Torques on the Body

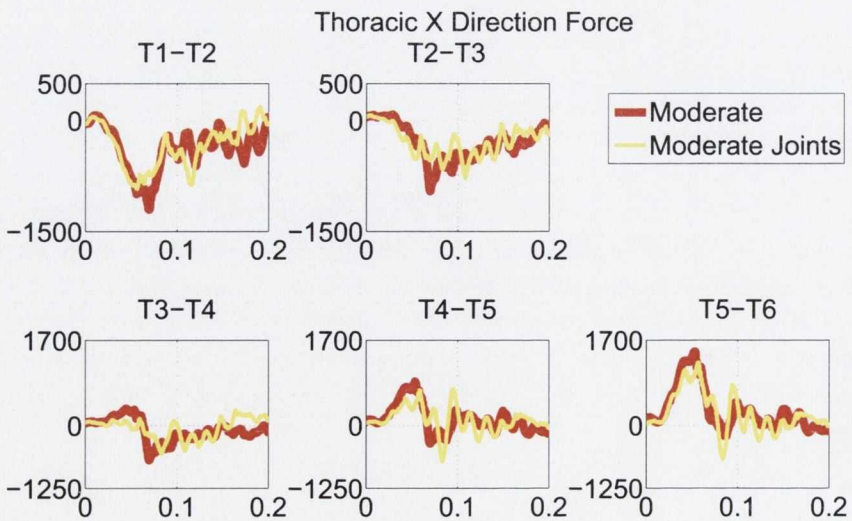
Scoliosis is a 3D deformation of the spinal column, however the model used in this analysis allows motion about the sagittal plane only. Therefore the axial or lateral torques that are experienced in these models are not accounted for. Therefore to better understand the effect of scoliosis on the spine the joints have been altered from a joint which allows rotation about

a single axis to one which allows 3 degrees of freedom, therefore allowing rotation about all three principle axes. The details of this are provided in Chapter 6 which details the process of changing from one type of joint to the other as well as the torque-angle characteristics used in the joints for this analysis. The motion of these joints is controlled by the characteristic determined by Panjabi et al [109] [106] [107]. The characteristics for the lateral and axial motion of the joints of the cervical, thoracic and lumbar regions are each assigned to the baseline and scoliosis models. The output from these models were assessed by looking at the forces as well as the torques that are experienced in a rear impact simulation.

7.9.1 Forces

A comparison of the baseline occupant with the two different types of joint shows that the forces on the spine are not greatly altered. This is due to the fact that the occupant still moves through the same motion pattern of a rearwards and upwards displacement that is characteristic of a rear impact. The single direction loading that is applied in this impact means that the occupant is only loaded in one direction and so this is the only impetus for movement. Therefore it is the shear forces and compression forces which still dominate the loading on the model whether scoliosis is present or not.

For the scoliosis models with the two different joints the X direction forces are not greatly changed by the introduction of the different joints as the X direction loading dominates the reaction and movement of the spine. Figure 7.43 shows this for the X-direction forces in the moderate case of scoliosis for the two different joint types . In each of the scoliosis models the shear (X direction) forces were found to still have the greatest value as it is in the direction of the crash.



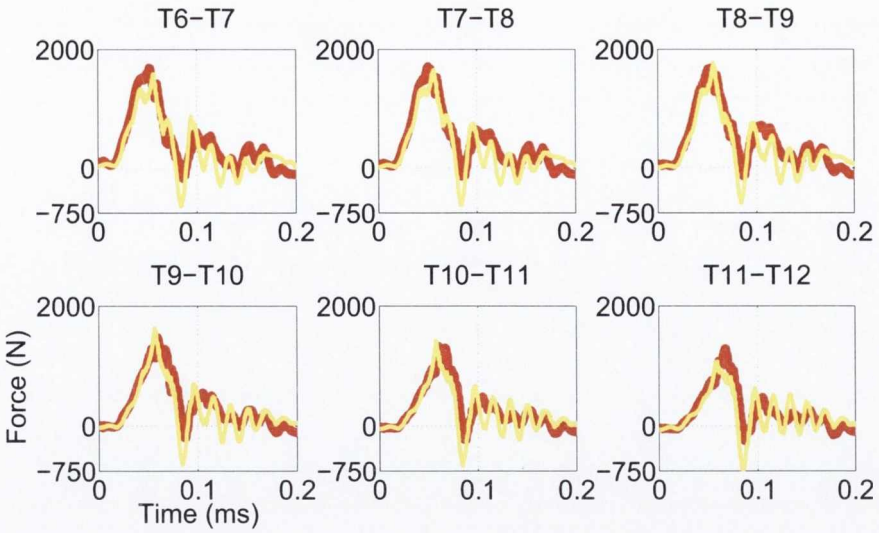
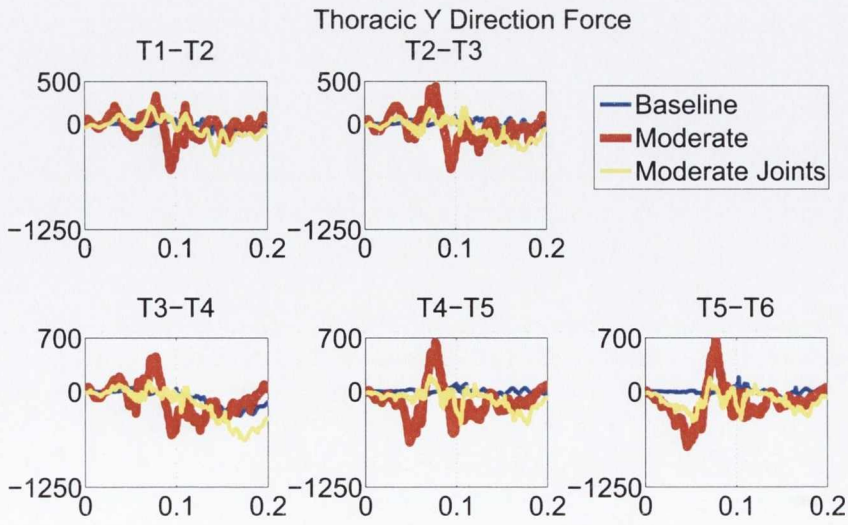


Figure 7.43: Local X Direction Forces on Thoracic Spine

In the lateral direction (Y) the forces again are not greatly altered with the new joints for the baseline case. The scoliosis models have reduced forces in this direction when the new joints are added, as large forces are no longer required to constrain movement in this direction. However a comparison of the baseline and scoliosis forces in this direction show that the baseline are still much less as there is no lateral deviation in the spine, see figure 7.44.



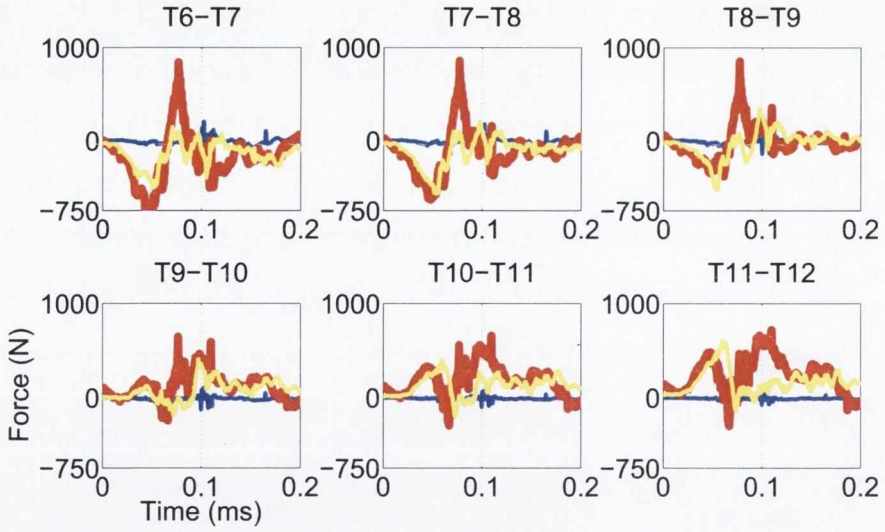
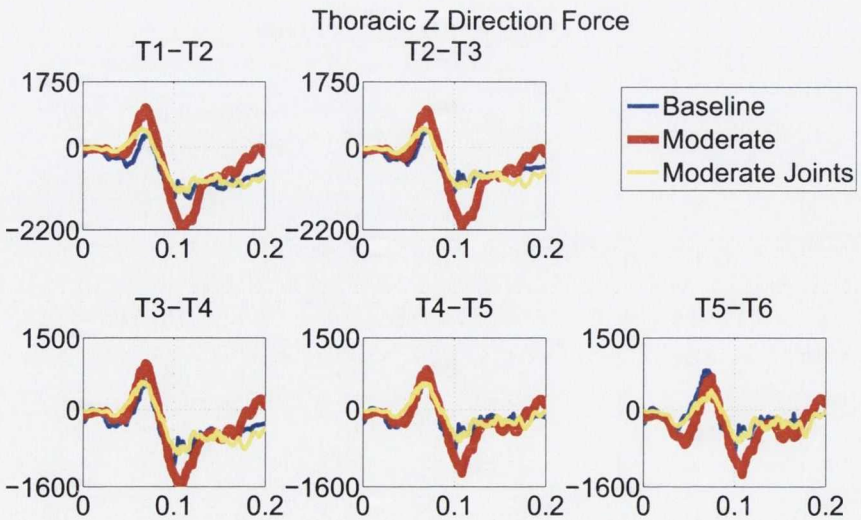


Figure 7.44: Local Y Direction Forces on Thoracic Spine

When the compression/extension (Z direction) forces were compared for the different joint types in the baseline and scoliosis models similar results were found. The loading in this direction is dominated by the characteristic upwards and rearwards motion of an occupant and so the same pattern of results was found regardless of the type of joint used, see figure 7.45.



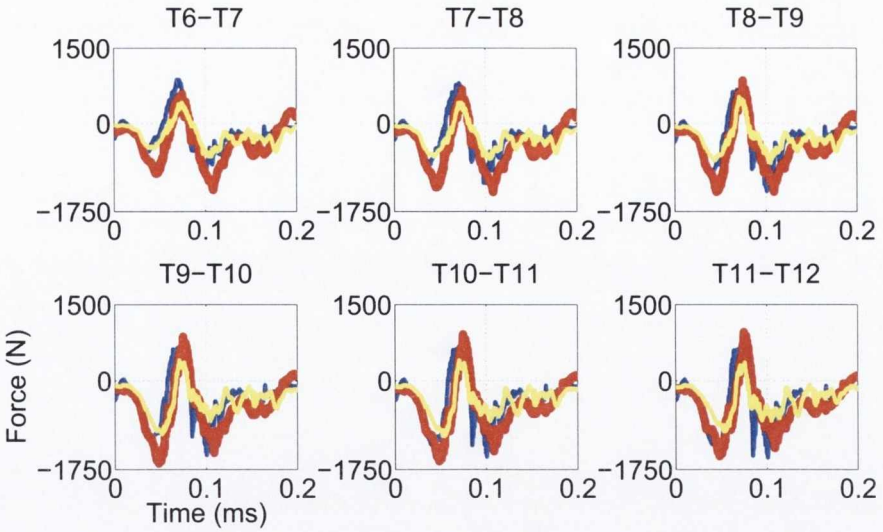
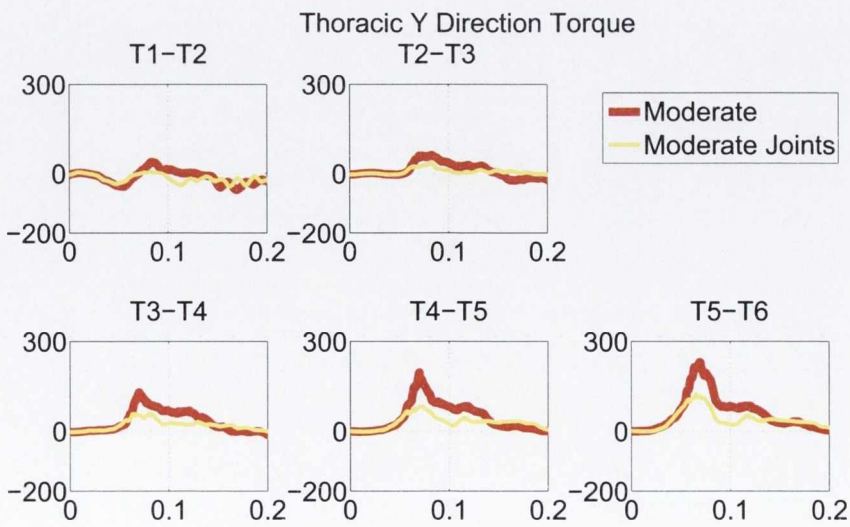


Figure 7.45: Local Z Direction Forces on Thoracic Spine

7.9.2 Torques

The torques on the body are much altered when the new joints are introduced in both the baseline and scoliosis models. The revolute (single axis rotation) joint has increased torques values on the constrained axes as they are required to prevent movement about these axes. This also results in increased values for rotation about the sagittal plane, see figure 7.46. The torques on the spherical joints (3 axes of rotation) are therefore more realistic values of what would be found in real life cases.



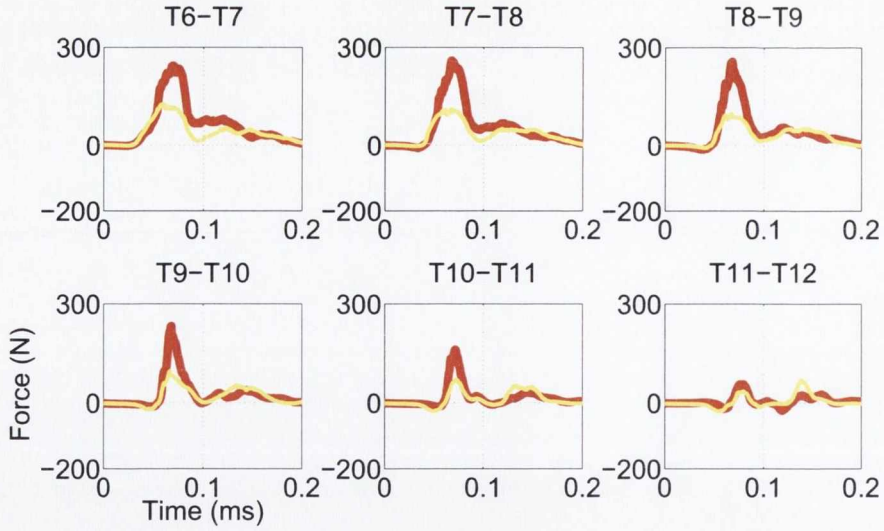


Figure 7.46: Local Y Axis Torques on Thoracic Spine

The models with the new joints in place show that the torques on the scoliosis models are greater than those of the baseline case for all three principal directions. The moments about the sagittal plane are increased by an average of 63% for the scoliosis models compared to the baseline case.

In the lateral direction the movement of the baseline compared to each of the scoliosis models shows a distinct pattern. In both the thoracic and lumbar region the torques are increased above the baseline case. The values for the lumbar region are generally much greater than those of the baseline case as this area of the scoliotic spine has a greater lateral bend than the compensatory thoracic curve, see figure 7.47.

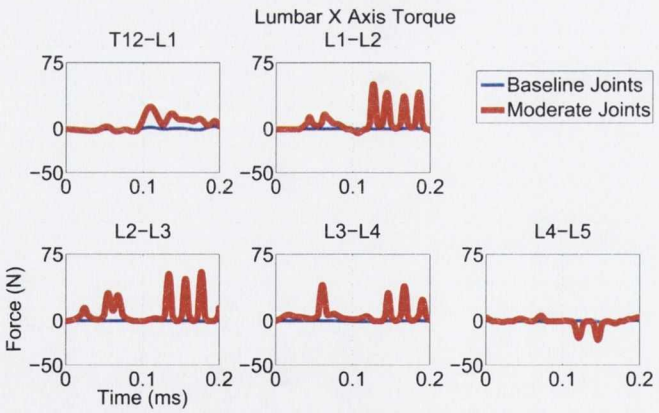


Figure 7.47: Local X Axis Torques on Lumbar Spine

The models with the new joints also allow movement in the transverse plane, which is much increased in the scoliosis models compared to the baseline due to the torsion found in the scoliosis models only, see figure 7.48.

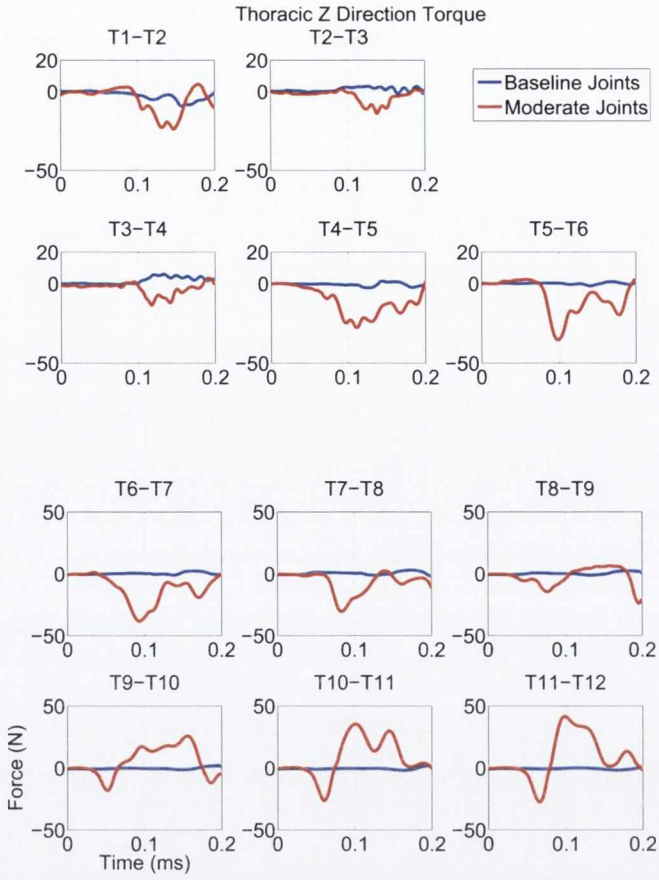


Figure 7.48: Local Z Axis Torques on Thoracic Spine

7.10 Summary of Investigation into Torques on the Body

While research on the effect of such torques on the body is lacking, the much increased values in the scoliosis cases compared to the baseline cases suggests a greater risk of injury. The characteristic implemented to control the movement of the spine is based on testing of vertebral pairs without the surrounding soft tissue structures in place which would alter the range of motion of the spine. However more representative data on the reaction of the spine to an applied loading was not available. Therefore it is the relative increase of the scoliosis cases compared to the baseline cases which is of importance rather than absolute values of torque predicted.

This study therefore illustrates that a comparison of the forces of the baseline and the scoliosis models shows that the relative values between the two are, as expected, not greatly changed with the different types of joints in place. The moments however are altered. This is especially seen in the lateral and axial directions which are much greater for the scoliosis models compared to the baseline. While the characteristics assigned to the scoliosis models may not be applicable, as the stiffness of a scoliotic spine is unknown, the relative increase in the predicted levels of torque on the scoliotic occupant's spine suggests that the occupant's spine is at greater risk of injury than one without scoliosis.

7.11 90-90-90 Seated Position

The results from the investigation into the effect of scoliosis found that the models have different seated heights and this affects the loading on the occupant. This highlights the influence that the position of the occupant in the wheelchair has on the risk of injury. To further investigate this the position of the scoliosis models in the wheelchair will be altered.

The sled tests of the baseline model were conducted with the occupant orientated at 26^o, as this is the validated posture of the BioRID II. However for a wheelchair occupant the 90-90-90 seated posture is the idealised position of the occupant in a wheelchair [1]. This seated posture is referred to as the 90-90-90 position as the hips, knees and ankles should all ideally be at right angles. The pelvis is positioned so that it is as far back in the wheelchair seat as possible. However, this is the ideal and it is not always possible to get the occupant in this position due to their disability.

This idealised position also deviates from the validated posture of the BioRID II occupant. Therefore, the quantitative results predicted for the loading on the spine or the injury criteria score may not be reliable and it is the trends in the results that is most important.

The models have been adapted to be in this position while keeping their scoliotic spine true to the shape found in the x-rays. The simulation files for these models are provided as part of the appendices and are detailed in Appendix C. The effect of this seated posture on the results is examined in this section.

7.11.1 Baseline Model

The baseline model is adapted to be seated in this position first to determine its influence in a crash without the added complexity of an altered posture. Then the scoliosis models are altered and investigated. When the baseline model is altered to be in the 90-90-90 seated position the pattern of results is changed. The full contact between the occupant and the wheelchair alters the interaction between the two. This is seen in the still shots of the animation, figure 7.49, which are taken at 40ms intervals.

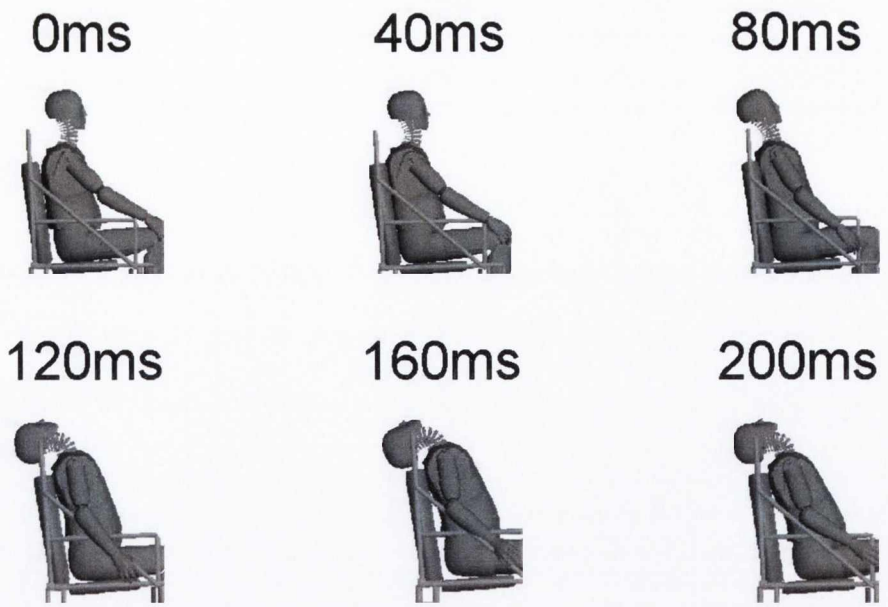


Figure 7.49: 40 millisecond Snapshots from Animation of Baseline Model Positioned at 90 degrees

The contact forces between the occupant and the seatback are shown in figure 7.50 for the validated baseline and the baseline seated at 90^o. The occupant seated at 90-90-90 is subjected to much lower forces due to its proximity to the seatback. The peak forces are also found to occur at an earlier time in the simulation for the occupant seated at 90-90-90 again due to its initial position.

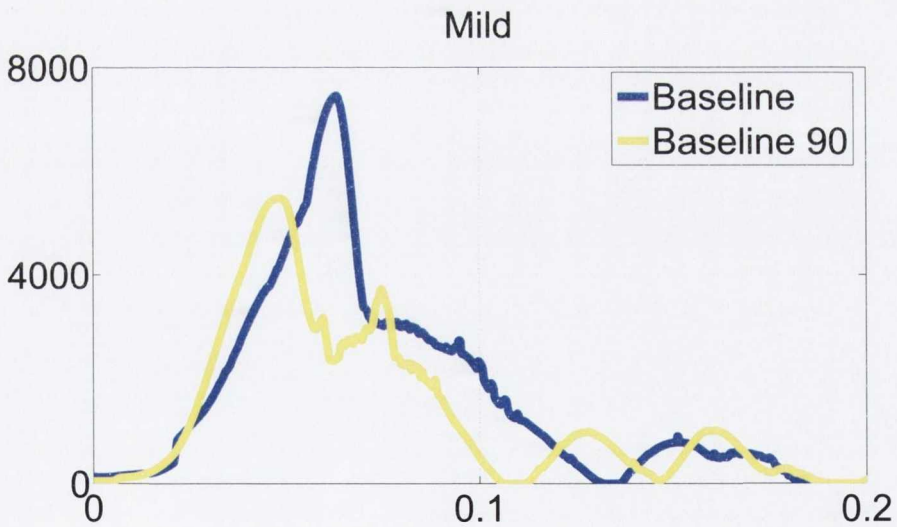


Figure 7.50: Contact Forces between Occupant and Seatback for Baseline and Baseline Seated at 90-90-90

7.11.2 Cervical Region

The forces on the cervical joints are shown in figure 7.51, and these are seen to be similar for both seated positions. The R values show an average of 0.9, see figure 7.52.

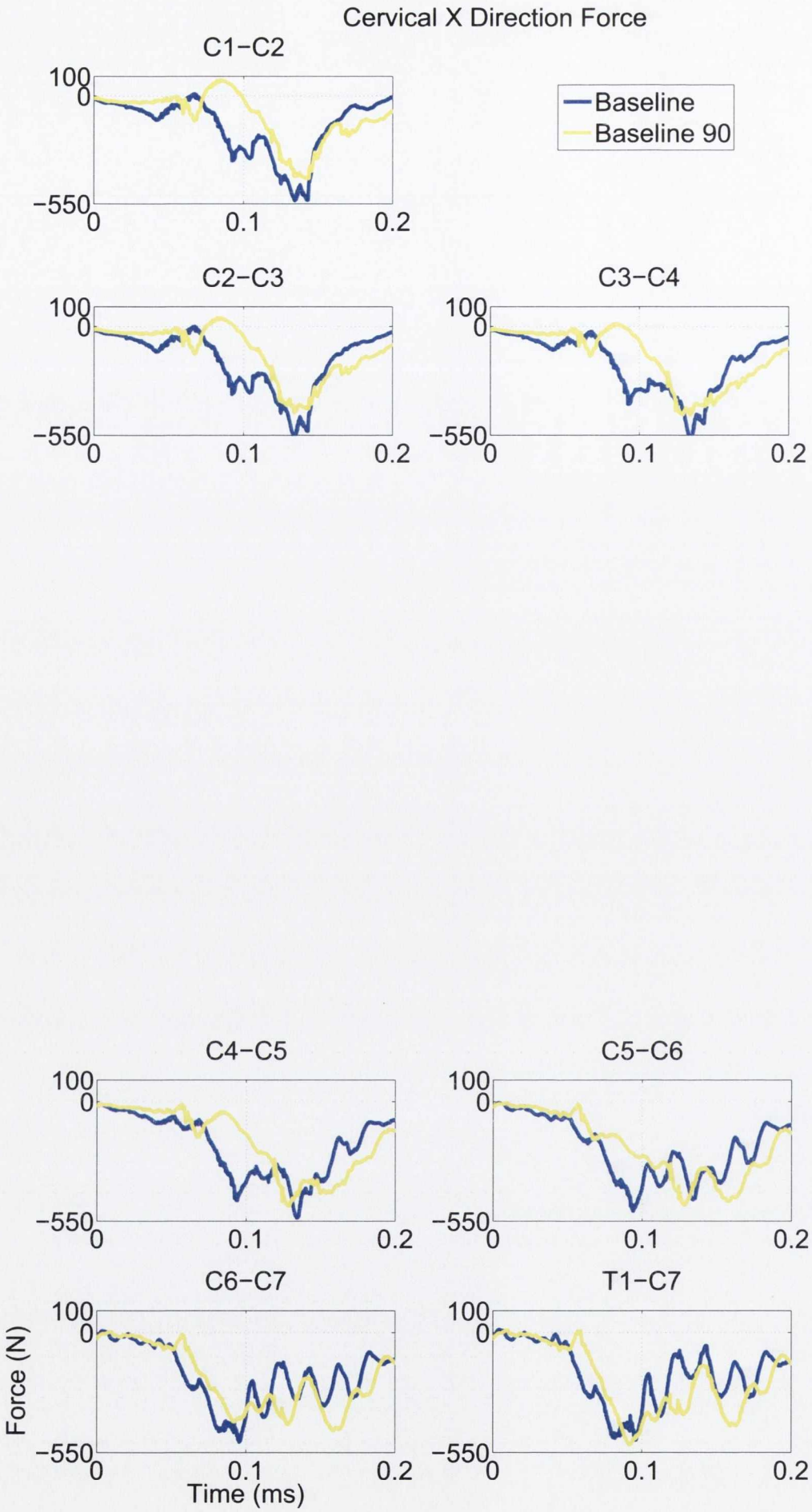


Figure 7.51: Time History Plots of Forces on Cervical Spine of Validated Baseline and Baseline at 90 Degrees

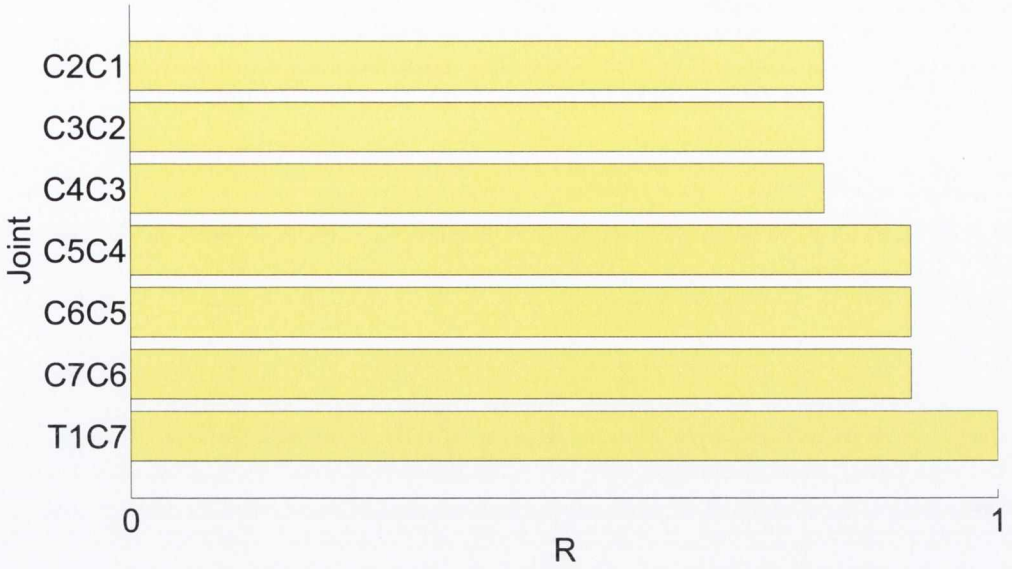
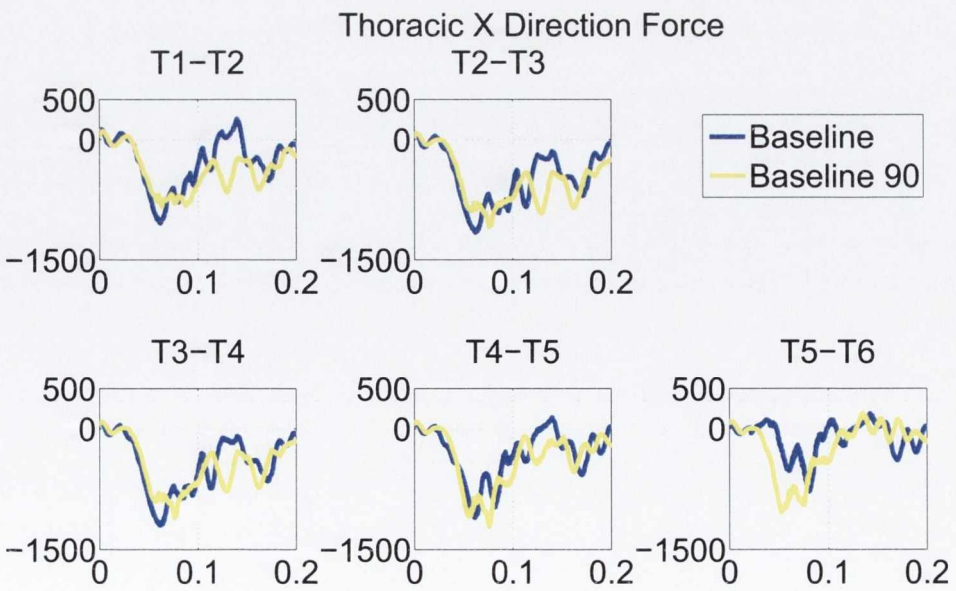


Figure 7.52: R Values for Cervical Spine of Baseline at 90 Degrees and Validated Baseline

7.11.3 Thoracic Region

In the thoracic region the peak forces on the joints are reduced as shown in figure 7.53. This produces an average R value of 0.8 when compared to the occupant positioned in the 26^o, see figure 7.54. The values in this bar chart that are above 1 for joints T5-T4, T6-T5 and T7-T6 represent different loading conditions in the spine as in the 90-90-90 seated posture these joints are loaded posteriorly rather than anteriorly as they are in the 26^o seated posture. This is also shown in the corresponding time history plots and so these values are not representative of the effect of the altered seated position.



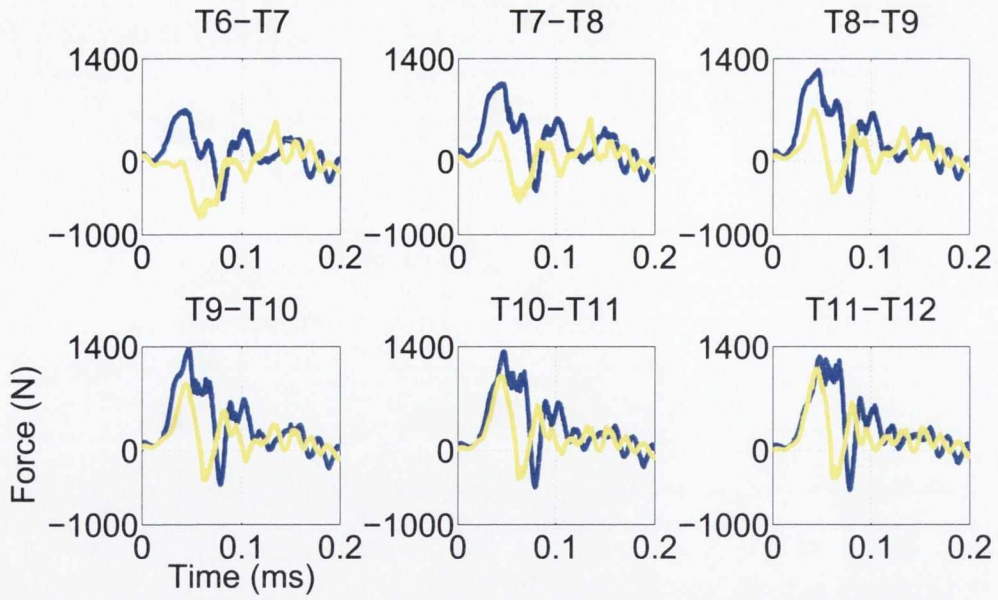


Figure 7.53: Time History Plots of Forces on Thoracic Spine of Baseline and Baseline at 90 Degrees

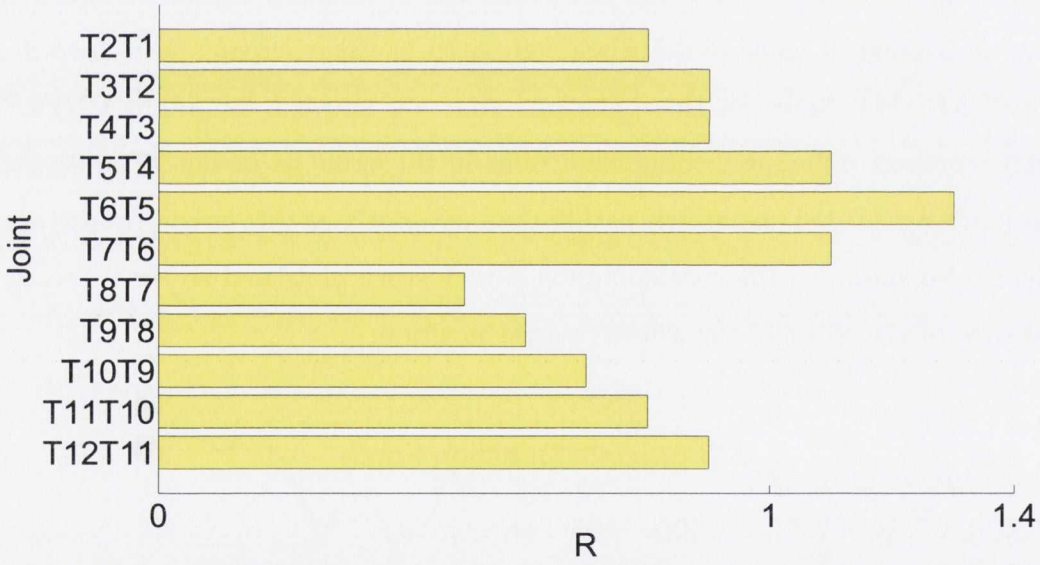


Figure 7.54: R Values for Thoracic Spine of Validated Baseline and Baseline at 90 Degrees

7.11.4 Lumbar Region

This region of the spine shows the most significant reduction in forces on the spine, as shown in figure 7.55. The peak forces on the spine are much reduced in this region of the spine with an average R value of 0.7, see figure 7.56.

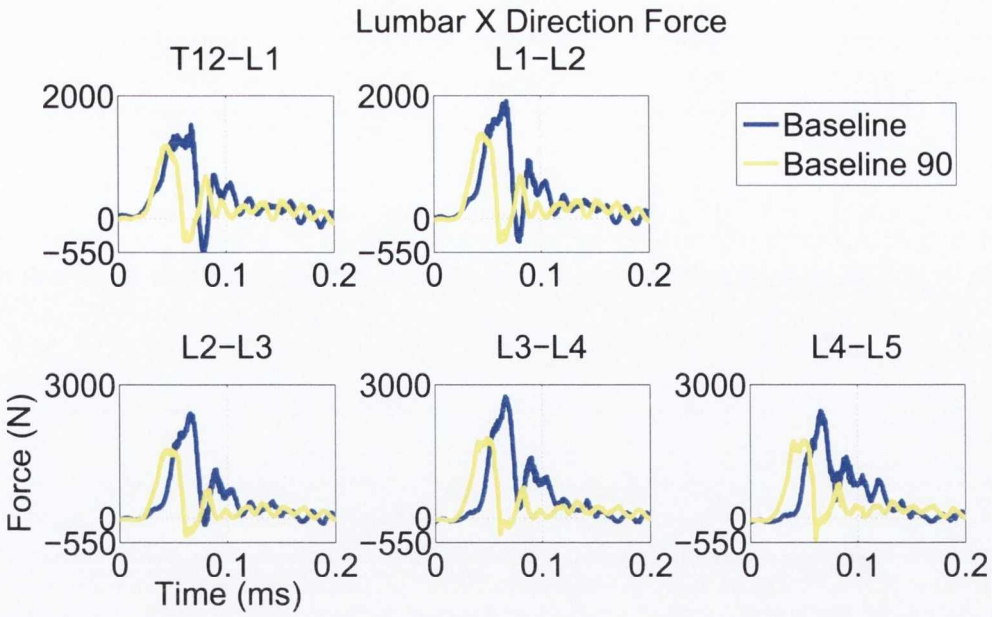


Figure 7.55: Time History Plots of Forces on Lumbar Spine of Baseline and Baseline at 90 Degrees

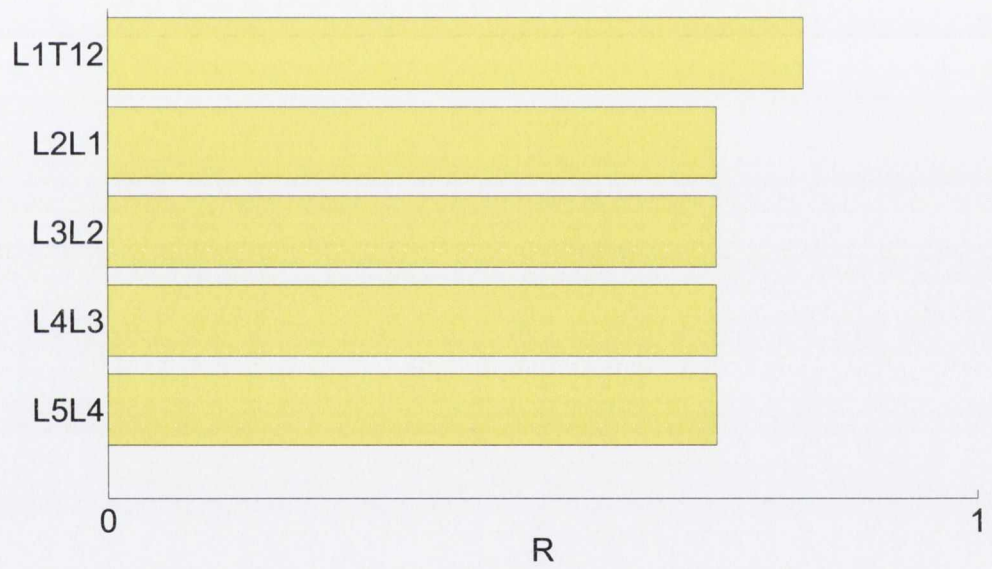
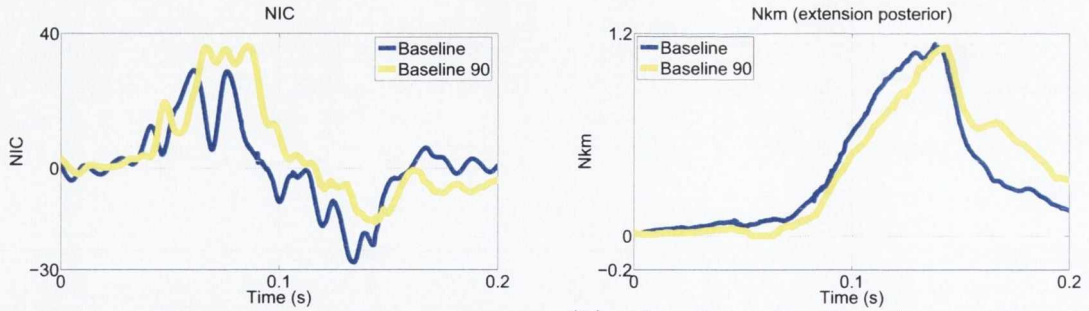


Figure 7.56: R Values for Lumbar Spine of Validated Baseline and Baseline at 90 Degrees

7.11.5 Injury Criteria

The *NIC* is increased when the occupant is placed in the 90-90-90 position, 7.57(a). The altered shape of this curve is due to the interaction of the torso with the seatback. The fluctuating peak of the *NIC* score is due to the contact of the pelvis with the seatback being slightly delayed compared to the interaction of the torso with the seatback which then has an effect in the upper torso. The *Nkm* was found to be equivalent when the occupant was seated in the 90 degree orientation, as shown in figure 7.57(b).



(a) *NIC* for Baseline at 26 and 90 Degree Positions

(b) *Nkm* Score for Baseline at 26 and 90 Degree Positions

Figure 7.57: Injury Criteria

7.11.6 Scoliosis Models at 90-90-90

To investigate the influence of this seated posture on the scoliotic occupant the following models were created, see figure 7.58.

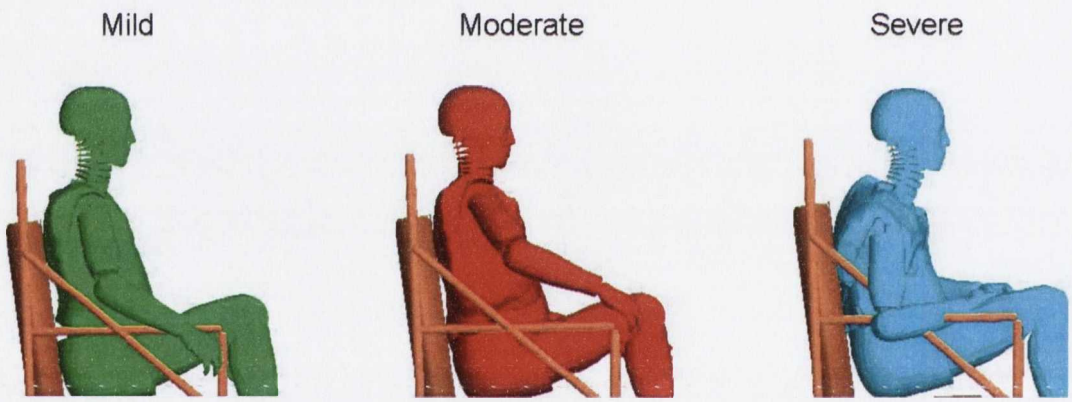


Figure 7.58: Mild, Moderate and Severe Cases of Scoliosis in 90-90-90 Seated Position

The outputs from these altered models were compared to the the original scoliotic occupant seated in the 26^o posture.

7.11.7 Cervical Region Forces

A comparison of the forces in the cervical region shows that the forces are reduced when placed in this 90-90-90 position when compared to the original placement at 26^o, see figure 7.59.

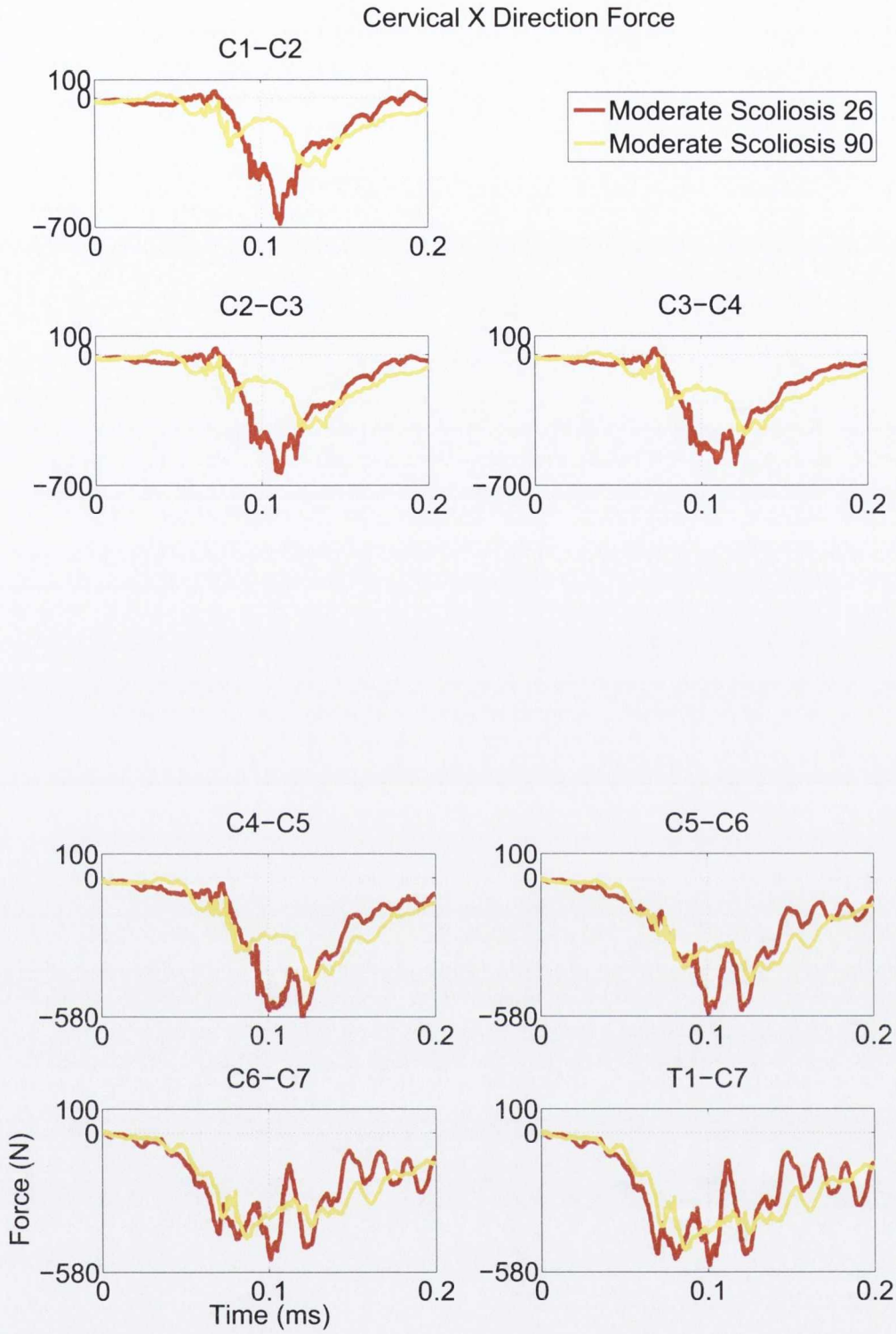


Figure 7.59: Forces on Cervical Region for Moderate Scoliosis Case Seated at 26 and 90 Degrees Orientation

The R values comparing the outputs for the moderate case of scoliosis seated at the two different postures shows a reduced force for the occupant seated at 90-90-90. The R values are on average of 0.8 for all levels of scoliosis, which is a 20% reduction in the forces on the occupant, see figure 7.60

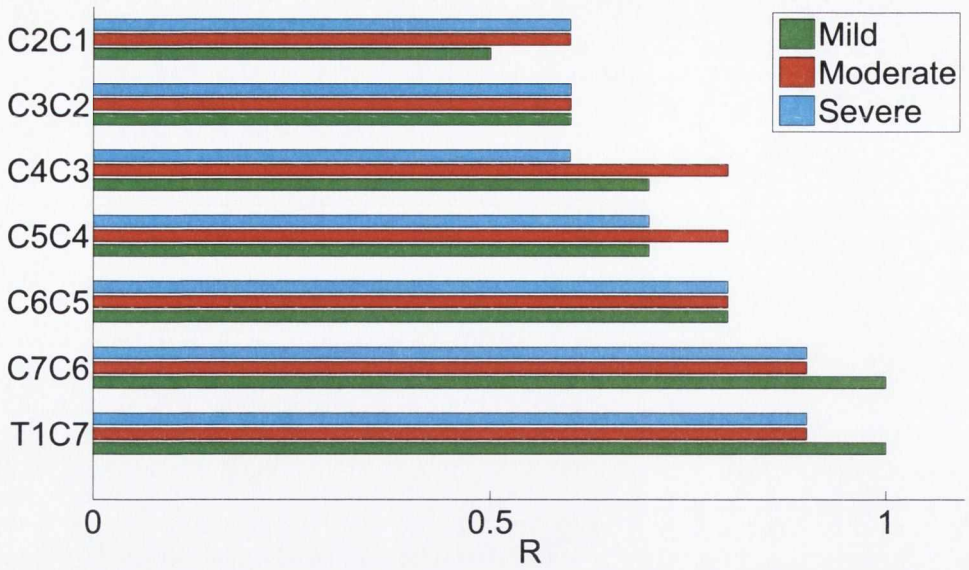
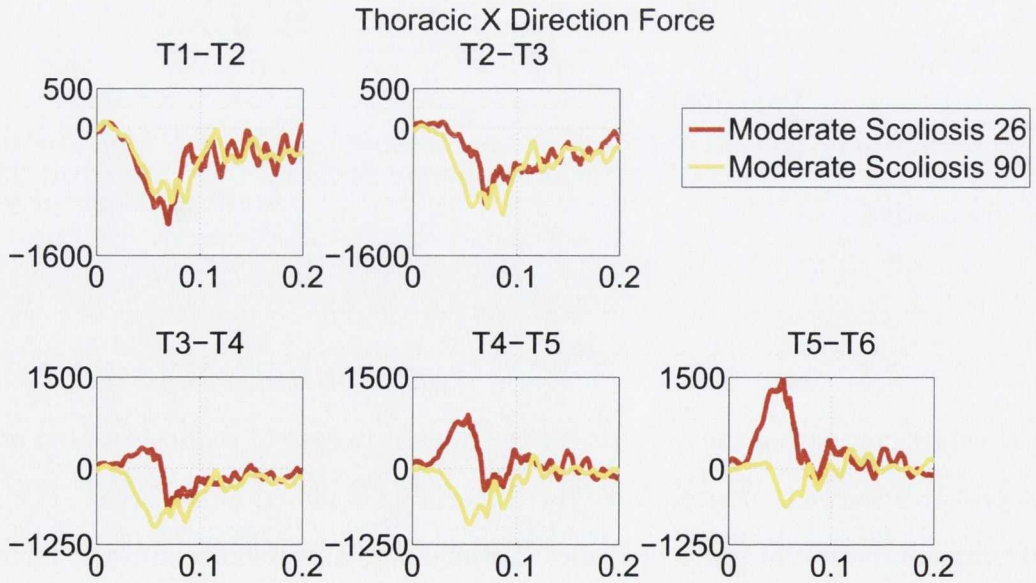


Figure 7.60: R Values for Moderate Scoliosis Case Seated at 26 and 90 Degrees Orientation in Cervical Region

7.11.8 Thoracic Region

In the thoracic region the forces on the moderate case of scoliosis seated at 90-90-90 is much reduced compared to the moderate case at 26^o, see figure 7.61.



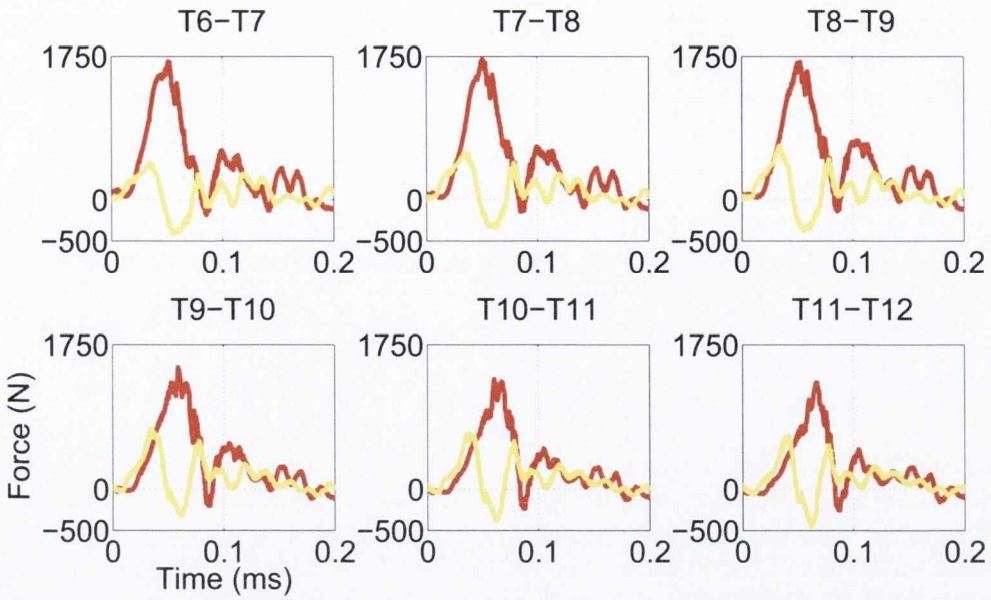


Figure 7.61: Forces on Thoracic Region for Moderate Scoliosis Case Seated at 26 and 90 Degrees Orientation

The R values for each level of scoliosis in this region of the body again reflects the reduction in the forces on the spine. An average R of 0.7 was determined for the thoracic region for all levels of scoliosis. The large peak values in the severe case of scoliosis is due to the different loading conditions on the spine as the height of the occupant with respect to the seatback is much altered in this position, see the previous images in figure 7.58.

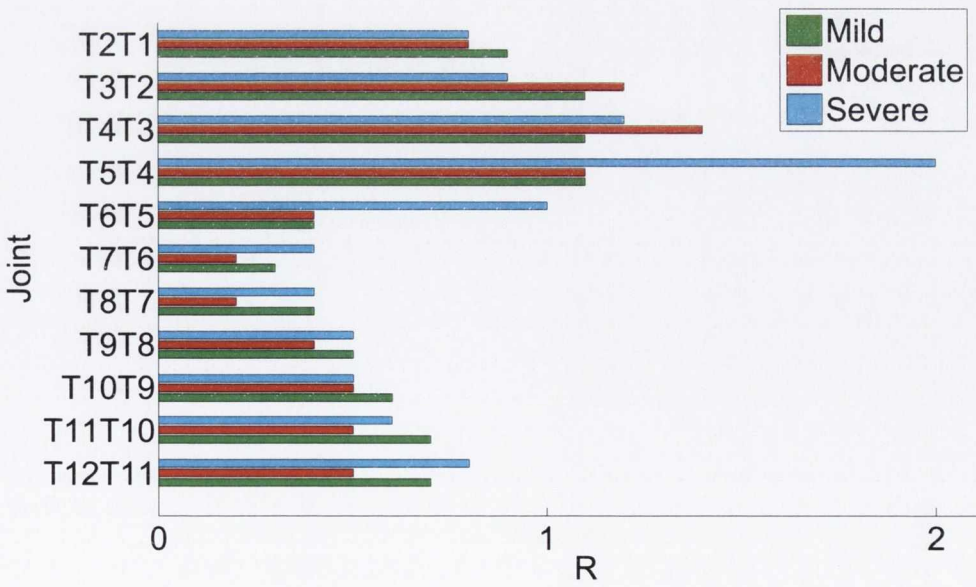


Figure 7.62: R Values for Moderate Scoliosis Case Seated at 26 and 90 Degrees Orientation in Thoracic Region

7.11.9 Lumbar Region

In the lumbar region the effect of having the occupant closer to the seatback is clearly demonstrated, as the forces in this region are much reduced. The peak forces are also seen to occur earlier in the simulation when placed at the 90-90-90 seated position, see figure 7.63.

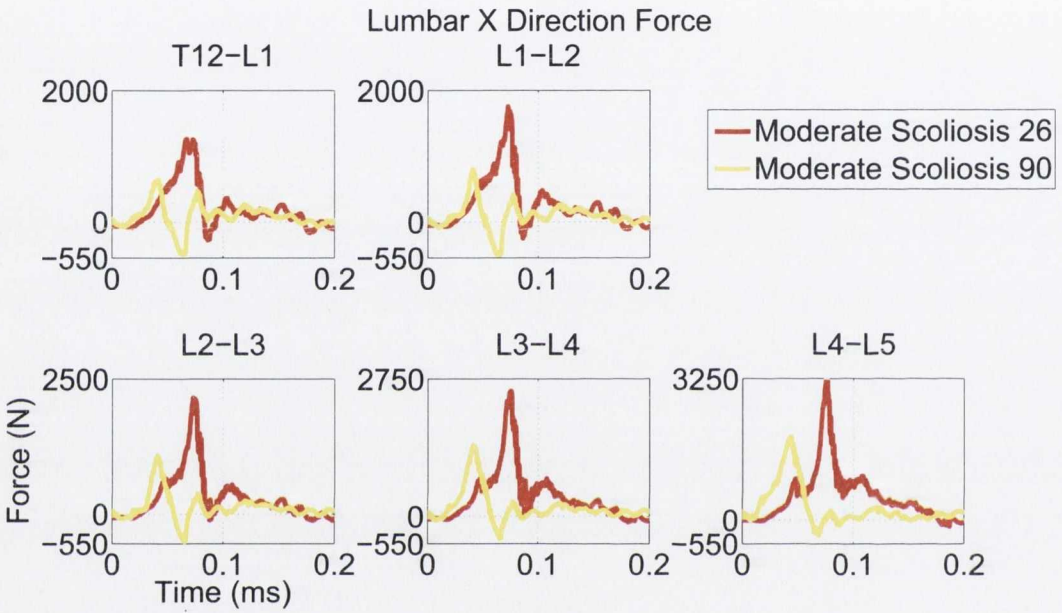


Figure 7.63: Forces on Lumbar Region for Moderate Scoliosis Case Seated at 26 and 90 Degrees Orientation

The lumbar region shows the greatest reduction in the forces on the spine, with an average R value of 0.6. The R values for this region in the mild, moderate and severe case positioned at 26^o and 90^o is shown in figure 7.64. This graph highlights that the greatest reductions are in the mild and moderate cases as they have the greatest lordosis of the spine and so the reduced distance between the occupant and seatback has the greatest influence. The severe case however does not have such a pronounced level of lordosis and so the reduction in the forces is not as great.

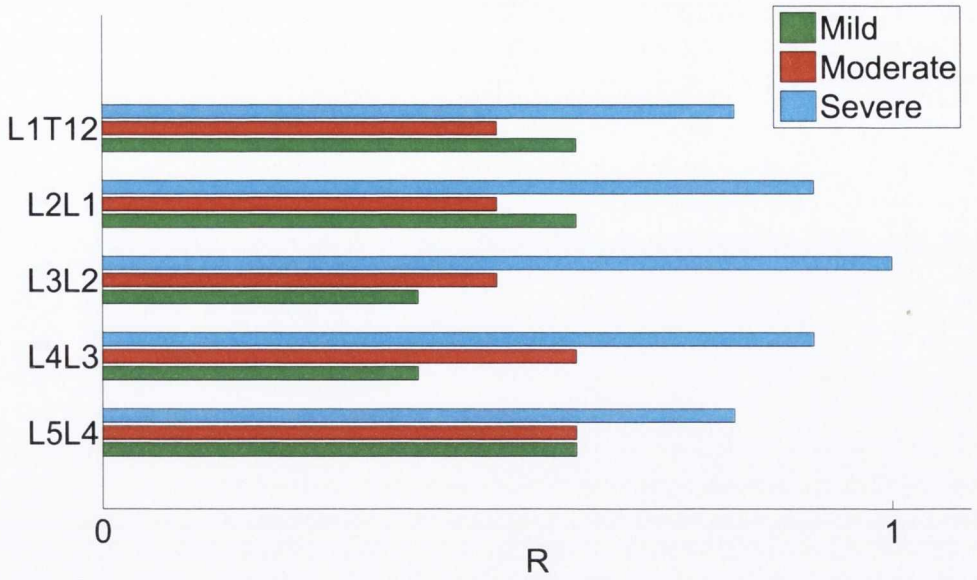


Figure 7.64: R Values for Moderate Scoliosis Case Seated at 26 and 90 Degrees Orientation in Lumbar Region

7.12 Injury Criteria - *NIC* and *Nkm*

The *NIC* and *Nkm* score was both found to reduce for the scoliosis models positioned at this 90-90-90 posture. The average reduction for the three levels of scoliosis was 17%. The *Nkm* also shows a reduction of 32% when the models are changed to be at the 90-90-90 posture. In both incidences this is due to the removal of the point loading on the spine.

7.12.1 Comparison of Baseline and Scoliosis Models at 90-90-90

A comparison of the baseline occupant and scoliosis occupants seated at the 90-90-90 posture shows similar results for each. The time history graphs for each region of the spine are presented in figures 7.65, 7.66 and 7.67. It is seen in these graphs that in the lower thoracic region and the lumbar region that the peak forces on the scoliosis models are less than those of the baseline case.

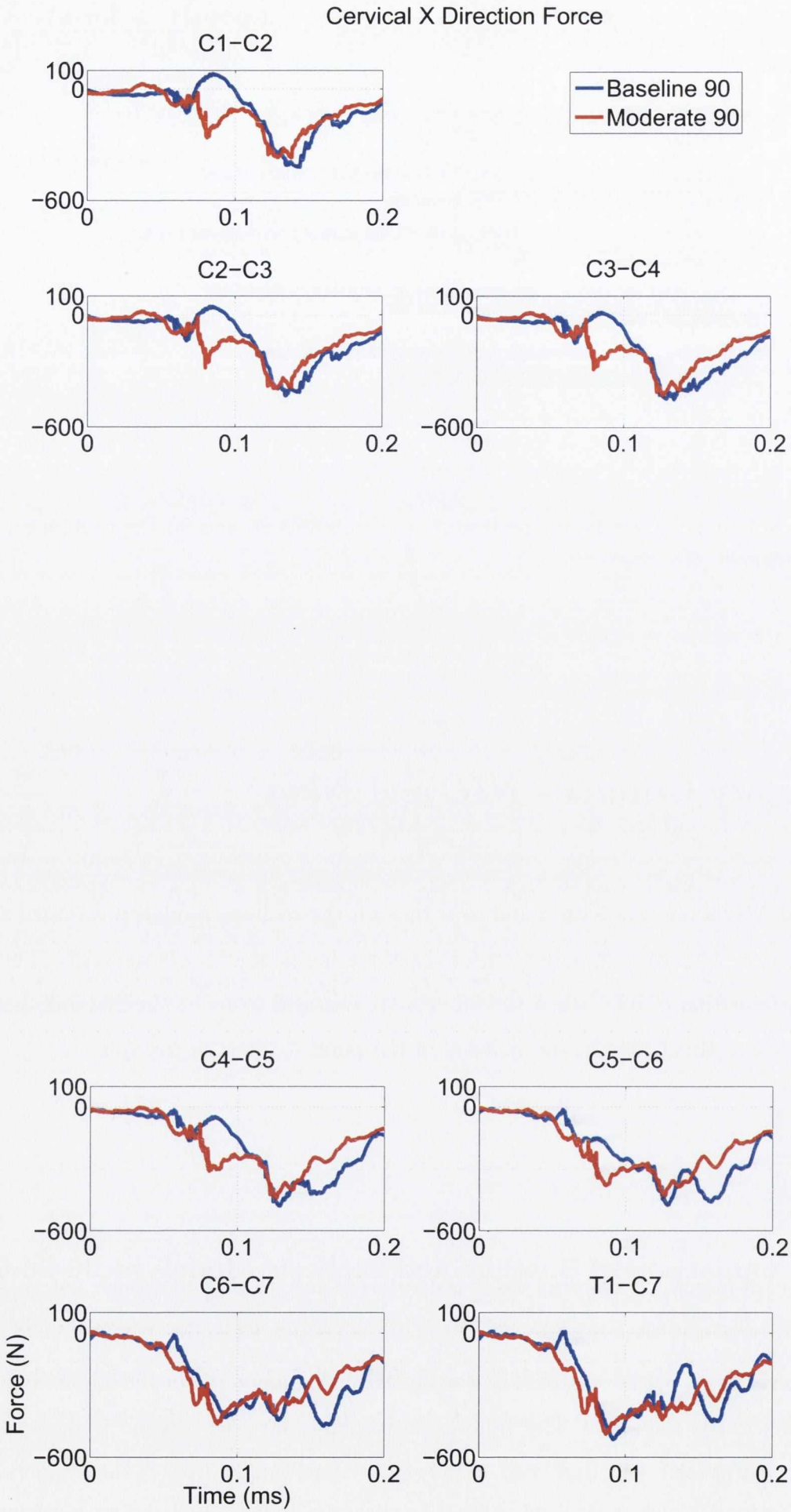


Figure 7.65: Local X Direction Forces for Baseline and Moderate Scoliosis in Cervical Region

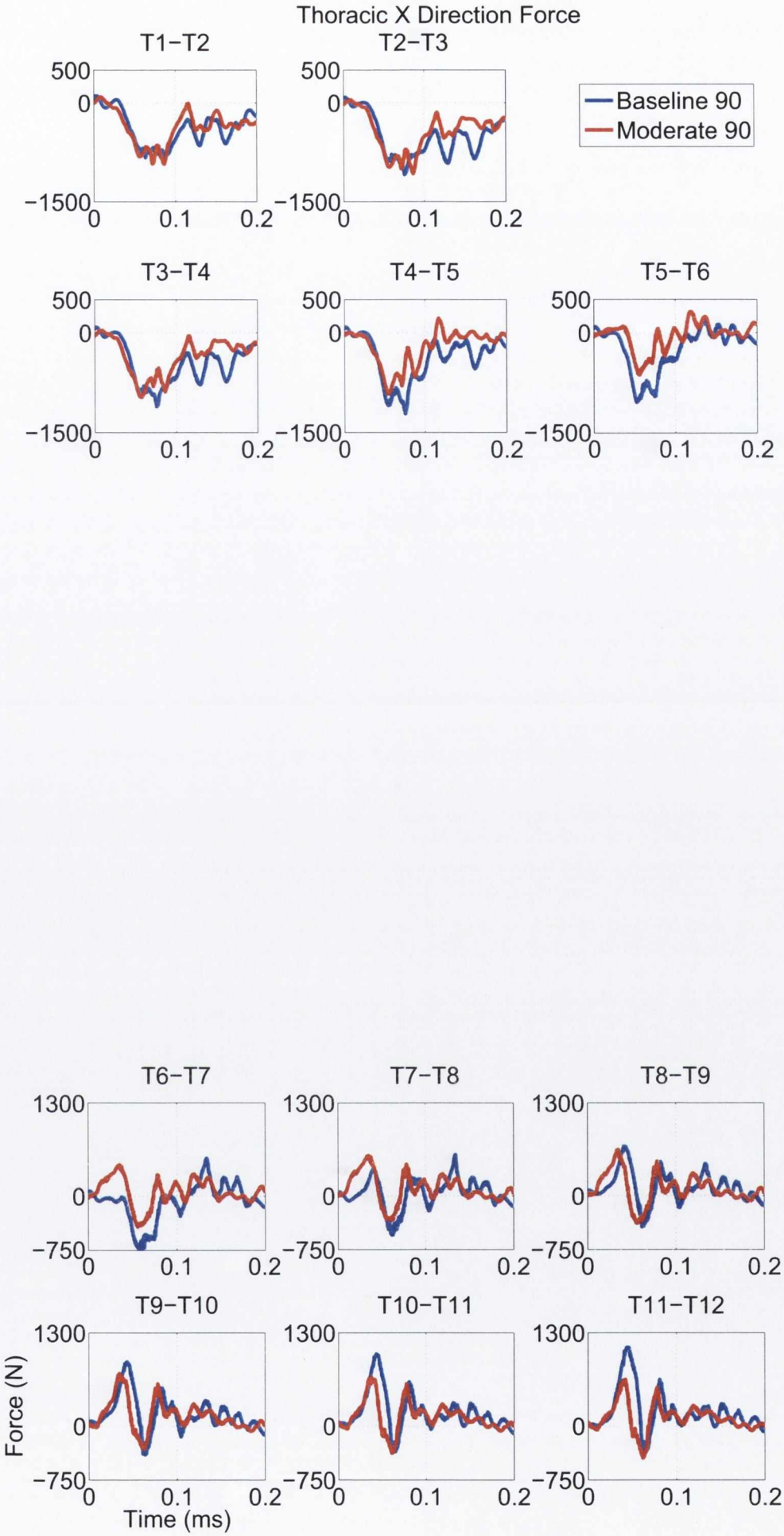


Figure 7.66: Local X Direction Forces for Baseline and Moderate Scoliosis in Thoracic Region

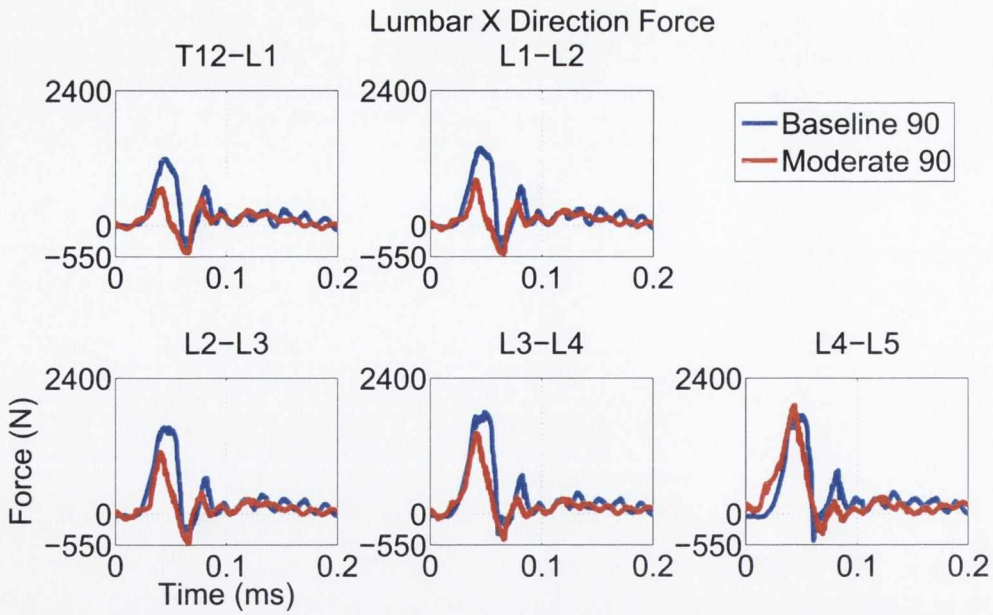


Figure 7.67: Local X Direction Forces for Baseline and Moderate Scoliosis in Lumbar Region

7.13 Summary of Investigation in Occupants Seated at 90-90-90

The BioRID II occupant model seated at 90-90-90 deviates from the validated configuration and therefore it is the trends in the results that are the focus of this investigation. The occupants seated at 90-90-90 with scoliosis were found to be subjected to lower levels of loading and therefore are at a lower risk of injury than the scoliosis models seated at 26^o. The effect of this seated posture is to have more of the occupant's torso in contact with the seatback and this greatly reduces the point loading on the spine compared to the occupant seated at 26^o. This effect has previously been found to increase the forces on the spine by up to 30%. The initial contact of this idealised posture also results in less movement of the occupant's spine and therefore the effect of scoliosis and the increase in forces associated with this is reduced.

In the cervical region the 20% reduction in the forces is due to the removal of this point loading effect. In the thoracic region the largest reduction in the forces for all of the scoliosis models was at the lower thoracic region. This is due to the initial closer contact with the seatback which reduces the forces on the spine. In the upper thoracic region the forces are equivalent as they are still subjected to the same loading as the head and neck rotate backwards causing the rearwards motion of the upper thoracic region. The lumbar region has the greatest area of reduced forces on the spine for the mild and moderate case due to the reduced distance between the occupant and seatback. The effect in the severe case is

not as apparent due to the lower level of lordosis which does not increase the level of forces on this region of the spine.

For the comparison between the models seated at 26^o and 90^o the increase in the risk of injury when looking at the forces and predicted injury criteria scores is greater than the discrepancy of the model. Therefore in accordance with the established validation procedure we can accept the hypothesis that this 90-90-90 position has a significant effect on the results.

A comparison of the loading of the baseline and scoliosis occupants seated at this 90-90-90 posture shows the peak forces are similar. Some differences are found between the models based on the curvature of the spine which prevents the initial proximity to the seatback from being established. These results show that for an occupant seated in close initial contact with the wheelchair the loading is reduced regardless of the presence of scoliosis or not. This has implications for clinic practice which will be discussed in Chapter 10.

From this investigation the influence of seated posture within the wheelchair on occupant loading is evident. However for an occupant with scoliosis a posture which allows initial contact with the seatback is not always possible and so the wheelchair must be adapted to the occupant. The effect of this will be established in Chapter 9.

Chapter 8

Methods 4: Alterations to Wheelchair Model

8.1 Introduction

This chapter details the alterations that were carried out to the wheelchair to investigate the influence they have on the results. Firstly the wheelchair model was adapted to better fit the occupant and these alterations reflect commonly carried out procedures in seating clinics, such as our collaborator, Enable Ireland. Secondly, the process of adding a cushioned layer on the surface of these surfaces and on the wheelchair is detailed.

8.2 Postural Supports

The addition of postural supports to wheelchairs is common practice as the factory finished wheelchair does not always suit the requirements of the occupant. The functional needs of the wheelchair user may require additional supports added to the wheelchair to position and support the occupant. However, under current legislation this is seen to be tampering with the crash tested wheelchair and so it is no longer certified as being safe for transport. However it is essential for the occupant for this process to be carried out.

The type of adaptation that will be modelled in this work is creating a custom contoured seating system for the occupant. There is a large variation in the methods that are used to create such a contoured wheelchair. In some cases a mould of the occupant is taken and a foam cast is made of this shape and secured to the wheelchair on a plywood board, see figure 8.1. Adjustable back supports are also widely used which can be altered to obtain the best fit for the occupant by adjusting the sections to fit the contours of the occupant's torso, see figure 8.2.

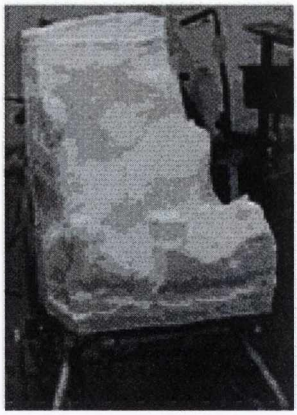
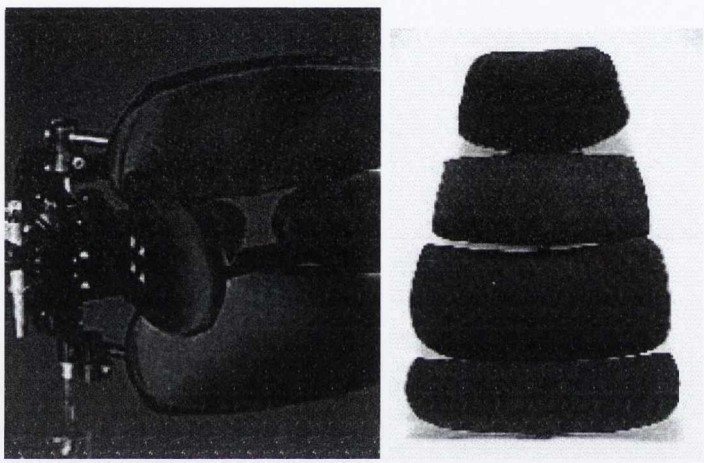


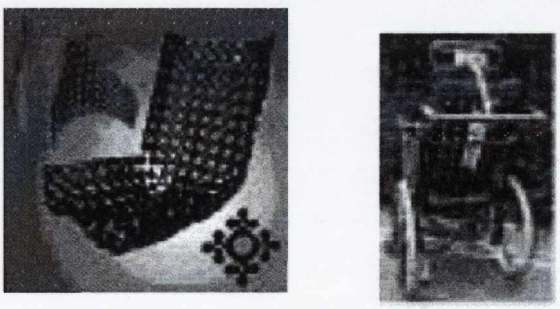
Figure 8.1: Molded Seat



(a) (b)

Figure 8.2: Adjustable Back Supports

More recently a system of links have been developed by different companies which again can be moulded to fit the contours of the occupant's body and these are then covered with a foam layer, see figure 8.3 (a) and (b).



(a)Link System (b)Link System with cushioning

Figure 8.3: Link System of Contoured Wheelchair

8.2.1 Implementation into Model

To recreate this in the numerical model a series of planes were used to contour around the torso of the occupant. These effectively closed the gaps that are introduced between the occupant and the wheelchair due to its deformed shape. A similar seating system was also added to the baseline model to investigate the effect of the seating for a non-scoliotic occupant. For both the scoliotic and non-scolitic occupants an individualised wheeclahir was created.

The altered shape of the spine for each of the scoliosis models in shown in figure 8.4, as compared to the baseline case. The level of deformity for each case of scoliosis is unique and therefore the wheelchair is created for each occupant seperately.

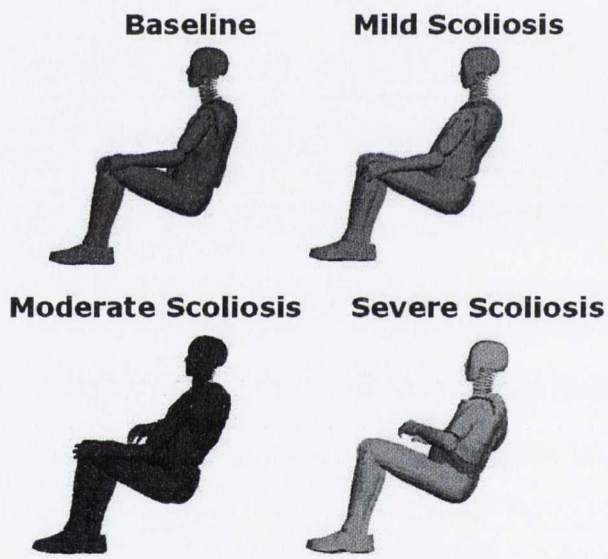


Figure 8.4: Deformed Surface of Occupants Torso

Surface planes were created to fit around the shape of the occupant's spine, see figure 8.5. These surfaces therefore created an occupant and wheelchair model which did not have large gaps between the occupant and the surface of the wheelchair. The effect that this has on the results is determined in the following chapter.

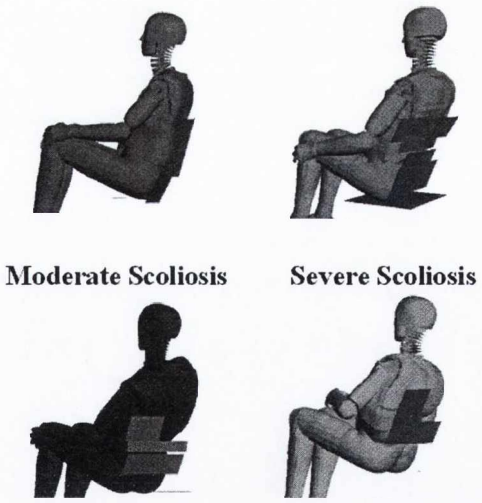


Figure 8.5: Moulded Seating System of Adapted Wheelchair

The surface of these supports are covered with foam and this is also modelled in this work.

8.3 Cushioning

The most commonly used padding in the seating clinic of our collaborator Enable Ireland is Sunmate^{TM}. As part of a parallel project this padding has been tested to determine its force-penetration characteristic [110], see figure 8.6. This cushion was tested in an Instron using the human headform that is penetrated into the cushion and the force-penetration characteristic associated with this was recorded 8.7. The curvature of the headform is not very dissimilar to the thoracic curve and pelvis which contact the wheelchair surfaces and so can be used for this analysis.

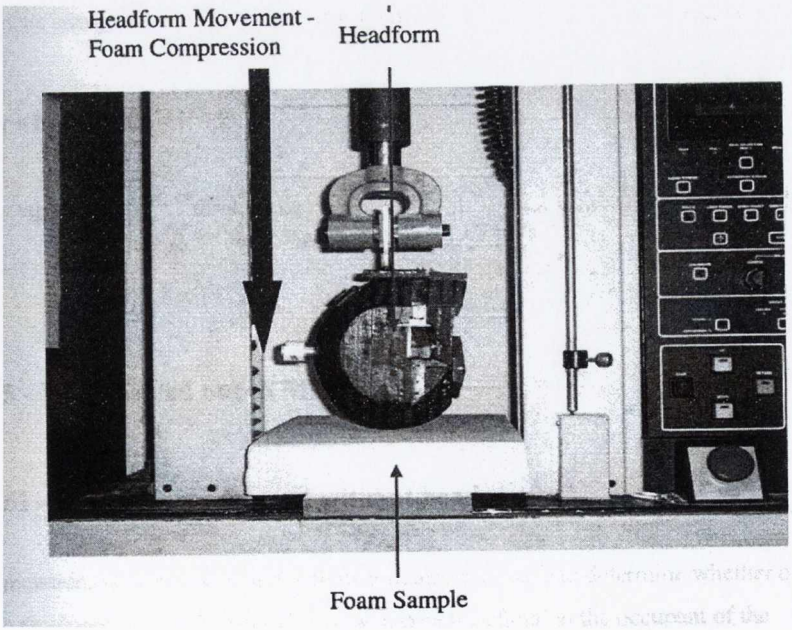


Figure 8.6: Headform Tested on Foam [110]

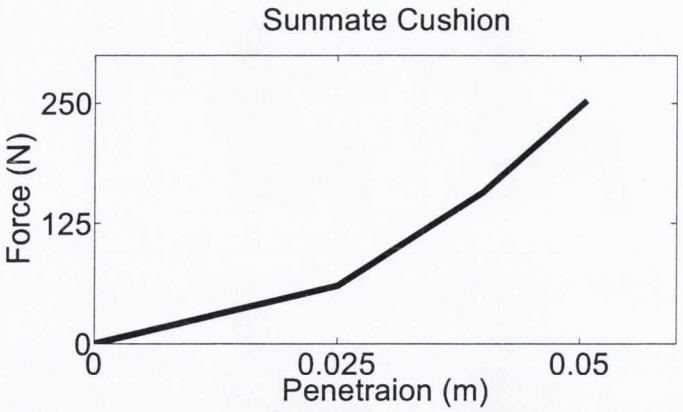


Figure 8.7: Force Penetration Characteristic of Sunmate Foam

This was then combined with the characteristic that was determined for the seatback of the surrogate wheelchair, so that the characteristic represented a 2inch thick padded surface that is used in the Enable Ireland seating clinic with a plywood board beneath it. This combined characteristic is shown in figure 8.8. This relationship was assigned to the seatback for each of the models.

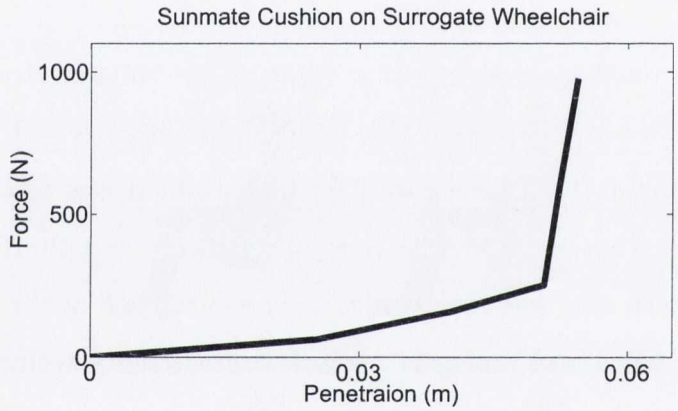


Figure 8.8: Force Penetration Characteristic of Sunmate Foam on the Surrogate Wheelchair

The MADYMO simulation models created using these methods are provided as part of the appendices. A description of each of the models is provided in Appendix C. These models were then used to investigate the effect of adaptations to a wheelchair in a rear impact, which is detailed in the following chapter.

Chapter 9

Results 3: Alterations to Wheelchair

9.1 Introduction

This section details investigations into the influence of altering the wheelchair. These are commonly conducted alterations which are carried out in seating clinics such at Enable Ireland [1]. The same methods of analysis was used as that for the Chapter 7 investigating the effect of altering the occupant. This involves determining the loading on the occupant and the injury level predicted from this based on injury criteria (*NIC* and *Nkm*). The significance of any finding was also related back to the validity of the model and analysed.

The altered wheelchair is tested with the four occupant models - baseline, mild scoliosis, moderate scoliosis and severe scoliosis. The results often show a similar pattern for all levels of scoliosis and therefore the moderate case is presented as a representative model. The results for rear impact of the mild and severe case are provided in Appendix I. However, any deviation from the pattern is presented and analysed in this chapter so that the complex relationship between the occupant and altered wheelchair can be established.

9.2 Postural supports

The addition of postural supports is common practice carried out in seating clinics world-wide [1]. The aim of such supports is to obtain and maintain the best possible posture for the occupant to allow an improved functional ability.

This adapted seating system results in full and close contact between the occupant and the wheelchair. In effect this closes the gaps between the occupant and the contacting surface that are introduced by the curvature of the occupant's torso. Due to the X-direction crash pulse that is applied and the single axis of rotation of the occupants any lateral postural supports were found not to have an influence on the kinematics of the occupant and so did not form part of this investigation. The creation of the supports is detailed in Chapter 8.

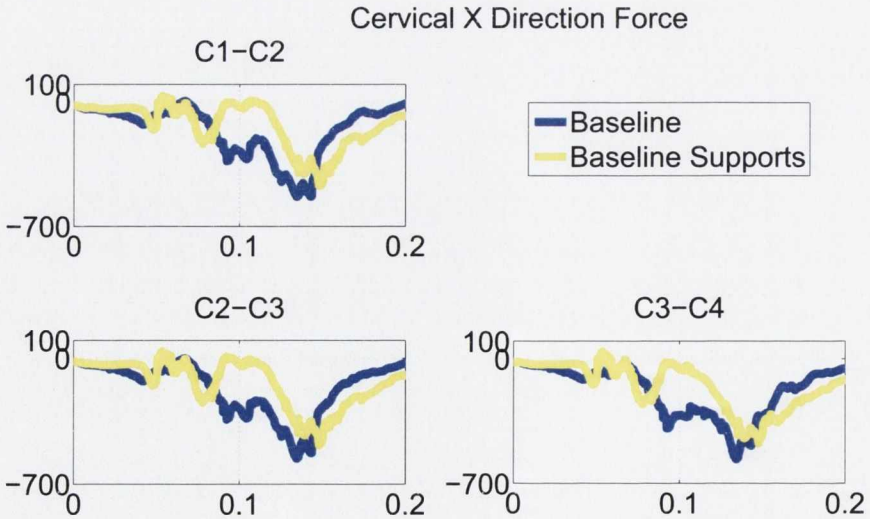
To determine the influence of the supports introduced here they are first added to the baseline case and assessed. The supports are then added to the scoliosis case and comparisons are made between the results.

9.3 Postural Supports added to Baseline Model

The baseline model of the BioRID II seated at the validated 26^o orientation results in gaps between the occupant and the seatback. The addition of postural supports removes these gaps and instead there is full contact between the occupant and the surfaces of the wheelchair. The loading on the spine when the occupant is placed in a wheelchair with such supports is presented in this section.

9.3.1 Cervical Region

The addition of postural supports was not found to greatly influence the peak forces in the neck of the occupant. The forces on the joints are slightly reduced to an average of 90% of the values of the baseline without the supports. The time history plots of the forces as shown in figure 9.1.



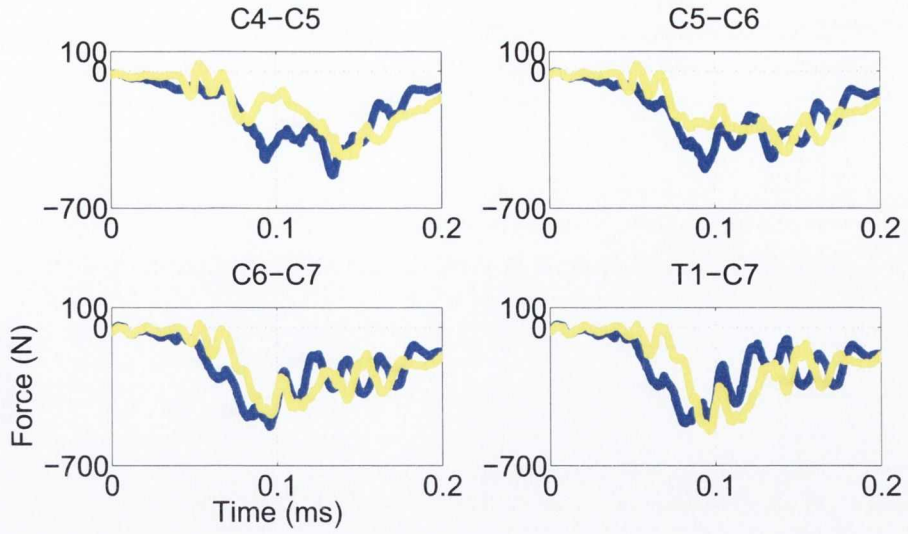
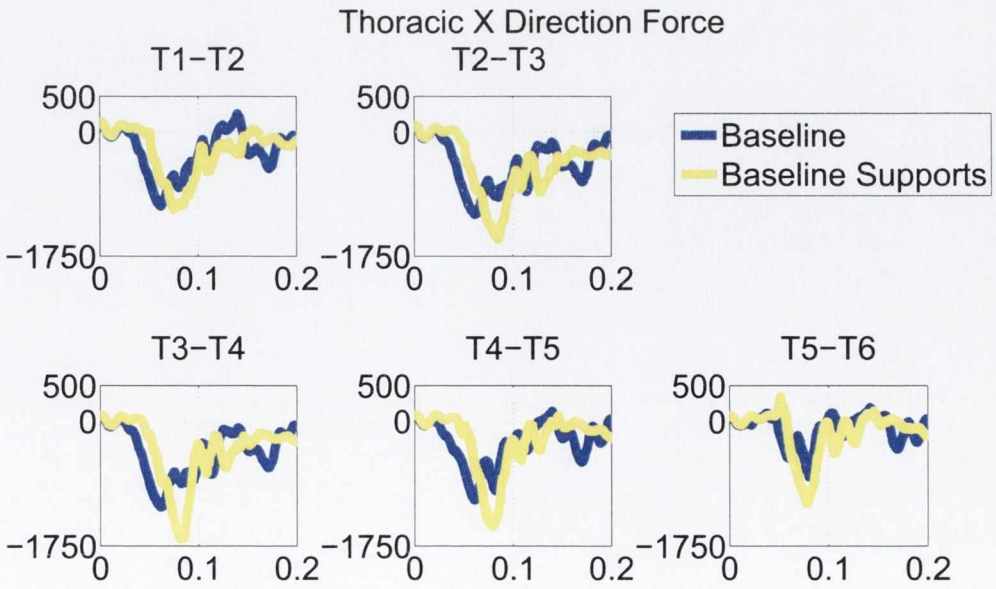


Figure 9.1: Forces in the Cervical Region for Baseline Occupant in Original Wheelchair and with Postural Supports

9.3.2 Thoracic Region

In the thoracic region of the spine the forces on the joints are increased by 30% when supports are added. In a similiar manner when a cushion is added to the surface of the wheelchair there is a delay in reaching the peak forces when the wheelchair is adapted in this manner, see figure 9.2.



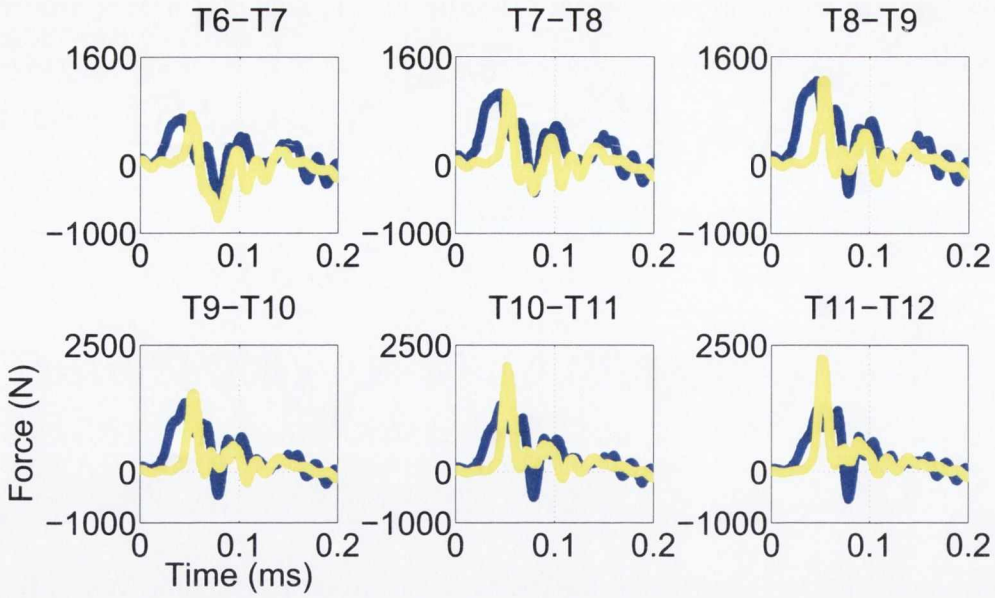


Figure 9.2: Forces in the Thoracic Region for Baseline Occupant in Original Wheelchair and with Postural Supports

9.3.3 Lumbar Region

The peak forces in the lumbar region are also elevated (20% greater) when the wheelchair is adapted. However in this region of the spine the peak forces are reached at an earlier time in the simulation. This is due to reduced gap found between the occupant and the seatback with the supports in place. However the characteristic quick ramping up to peak forces is seen in this case due to bottoming out of the cushion followed by contact with the hard plywood seatback.

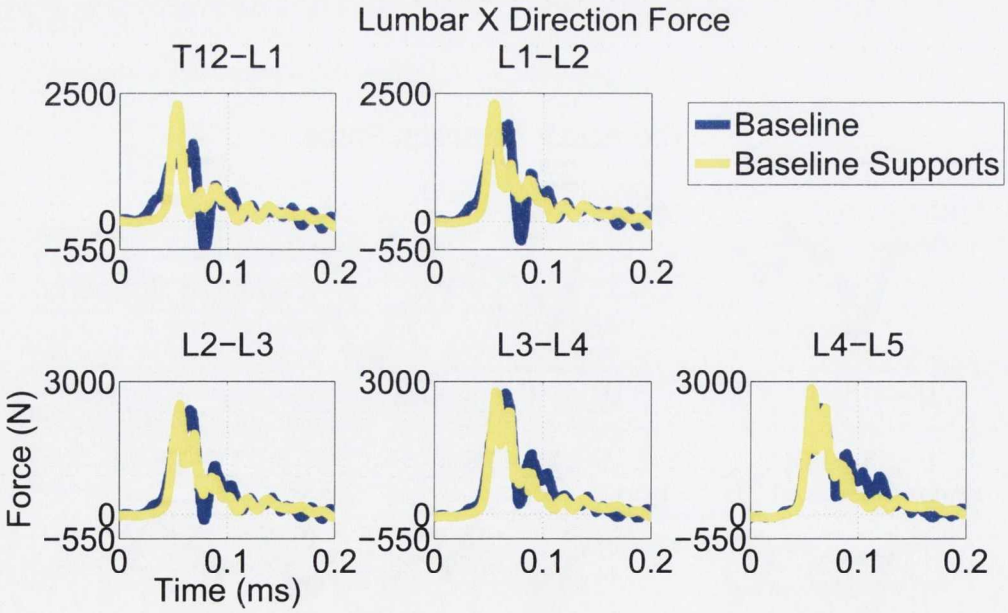
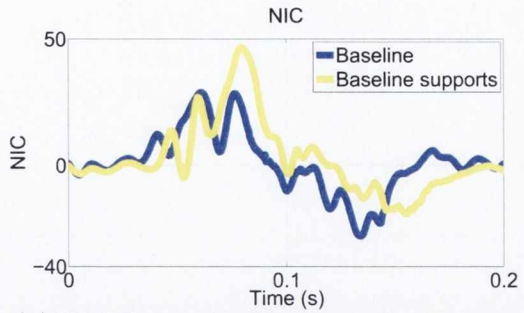


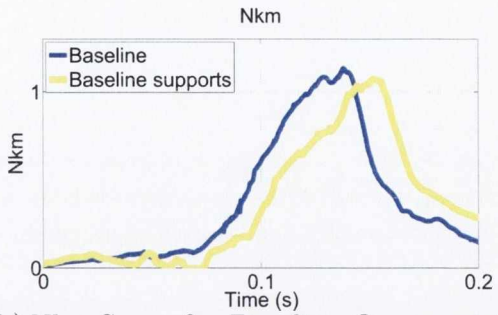
Figure 9.3: Forces in the Lumbar Region for Baseline Occupant in Original Wheelchair and with Postural Supports

9.3.4 Injury Criteria

The *NIC* score for this combination of occupant and wheelchair was increased as shown in figure 9.4(a). The *Nkm* was slightly reduced as expected as the forces in the cervical region were found to decrease. This is shown in figure 9.4(b).



(a) *NIC* Score for Baseline Occupant in Original Wheelchair and in Wheelchair with Supports



(b) *Nkm* Score for Baseline Occupant in Original Wheelchair and in Wheelchair with Supports

Figure 9.4: Mild Scoliosis X-rays

9.4 Postural Supports added to Scoliosis Models

The altered curvature of the spine of the scoliosis models results in an altered shape of the surface of the torso of the occupant. This results in gaps between the occupant's pelvis and lumbar spine and wheelchair as found for the baseline case. For the scoliosis models there is also an associated exaggerated kyphosis in the thoracic region which leads to less surface contact between the occupant and the wheelchair. As detailed in Chapter 7 this results in increased loading on the occupant as the increased kyphosis of the spine leads to a point loading effect against the rigid seatback. The addition of postural supports removes this effect as the gaps between the occupant and the wheelchair are greatly reduced. The outputs from the models with postural supports are compared to the scoliosis cases without the supports in place.

9.4.1 Forces on the Cervical Spine

The peak values in the cervical region is not greatly altered by the introduction of the postural supports, while there is a delay in reaching the peak forces the peak values are equivalent. The time history graphs of the moderate case of scoliosis without the postural supports compared to the case with the supports in place is shown in figure 9.5.

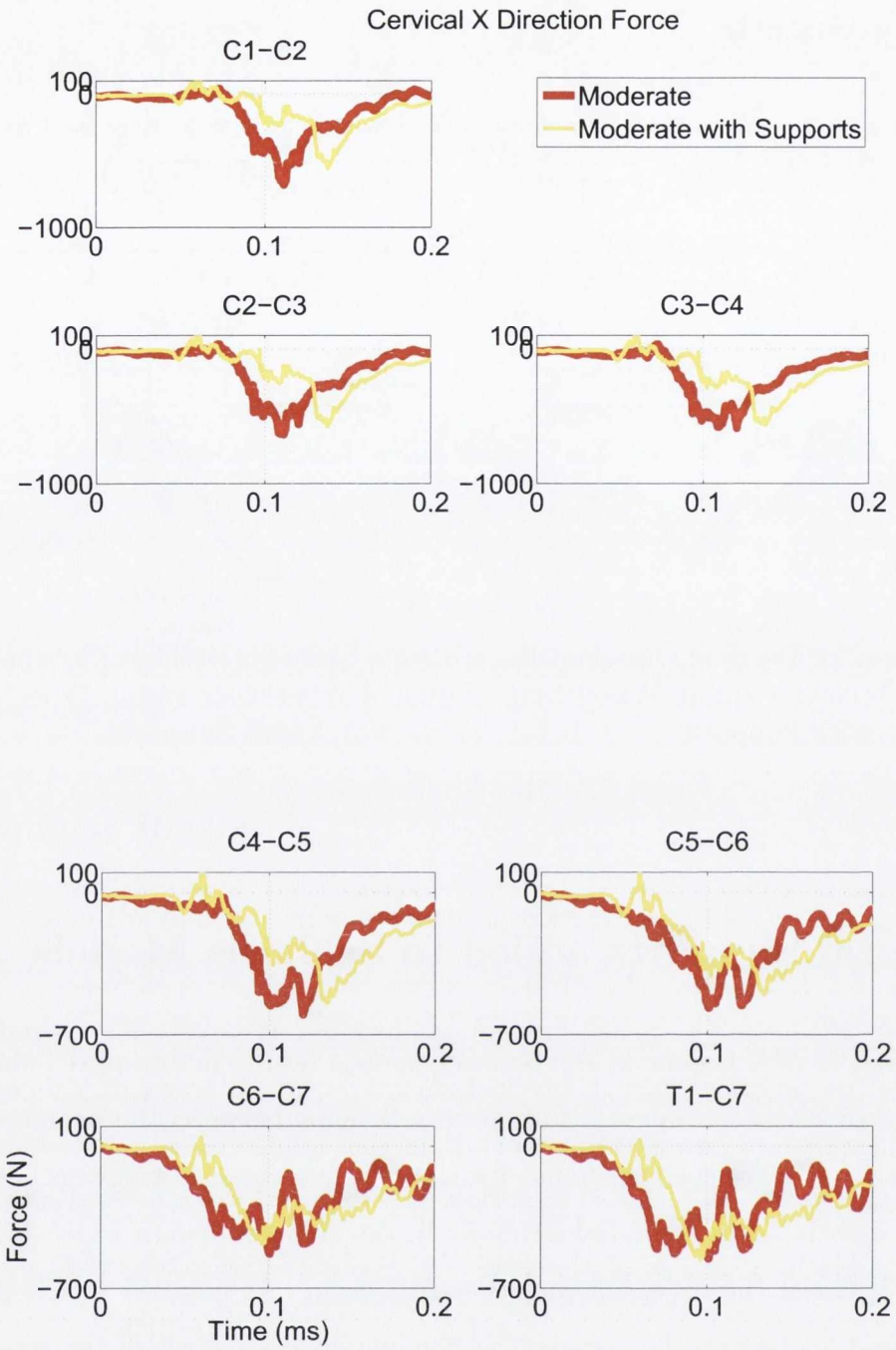


Figure 9.5: Forces on Cervical Region for Moderate Scoliosis Occupant with and without Postural Supports

9.4.2 Forces on the Thoracic Spine

The comparison of the loads in the thoracic region between the case with and without the postural supports shows that the peak forces are similar. However the rate at which they ramp up to this maximum is increased for the case with the postural support in place, see figure 9.6.

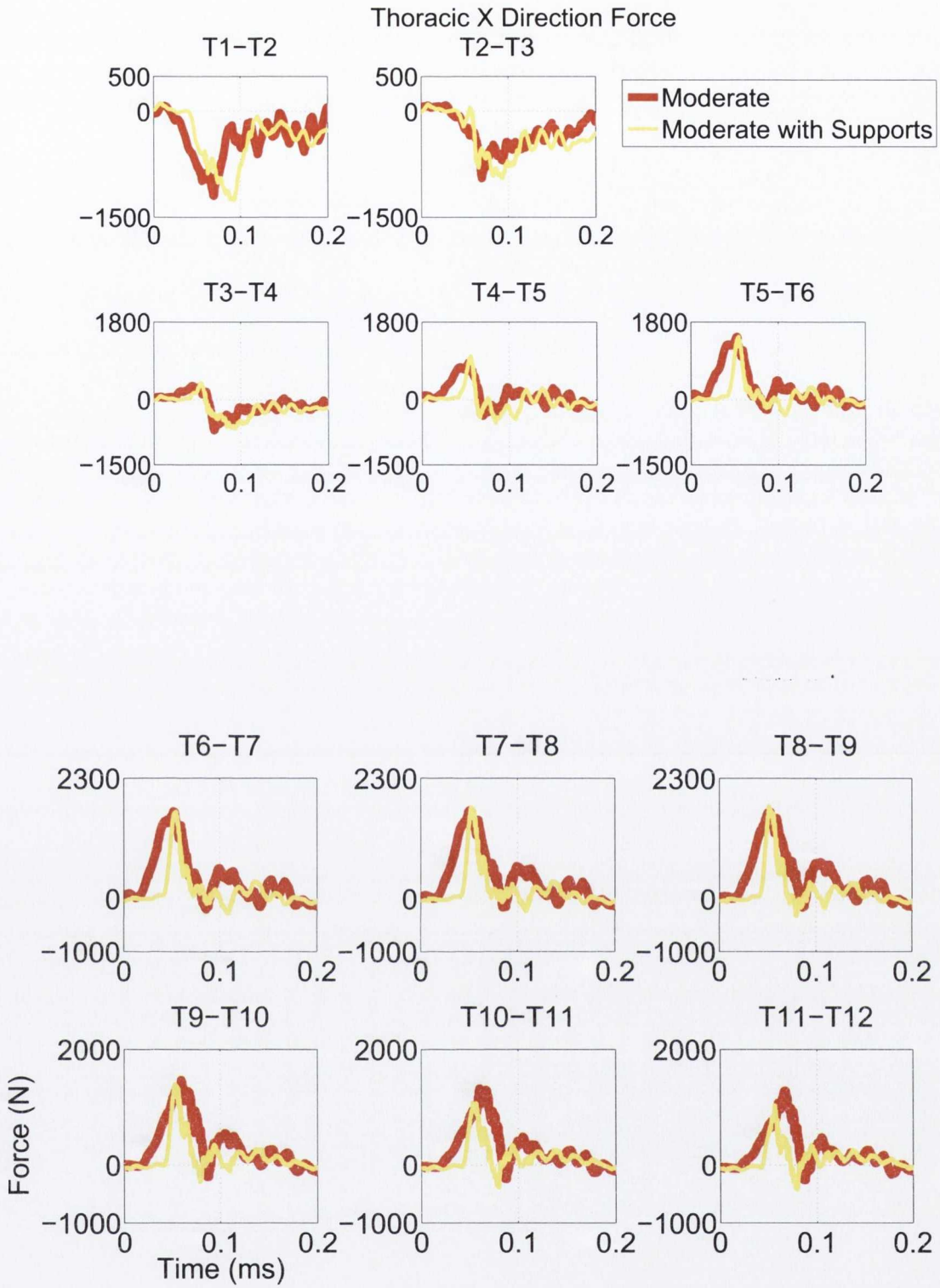


Figure 9.6: Forces on Thoracic Region for Moderate Scoliosis Occupant with and without Postural Supports

9.4.3 Forces on the Lumbar Spine

The lumbar region shows that the peak forces occur at an earlier time when the supports are in place than in the simulation without the postural supports, see figure 9.7.

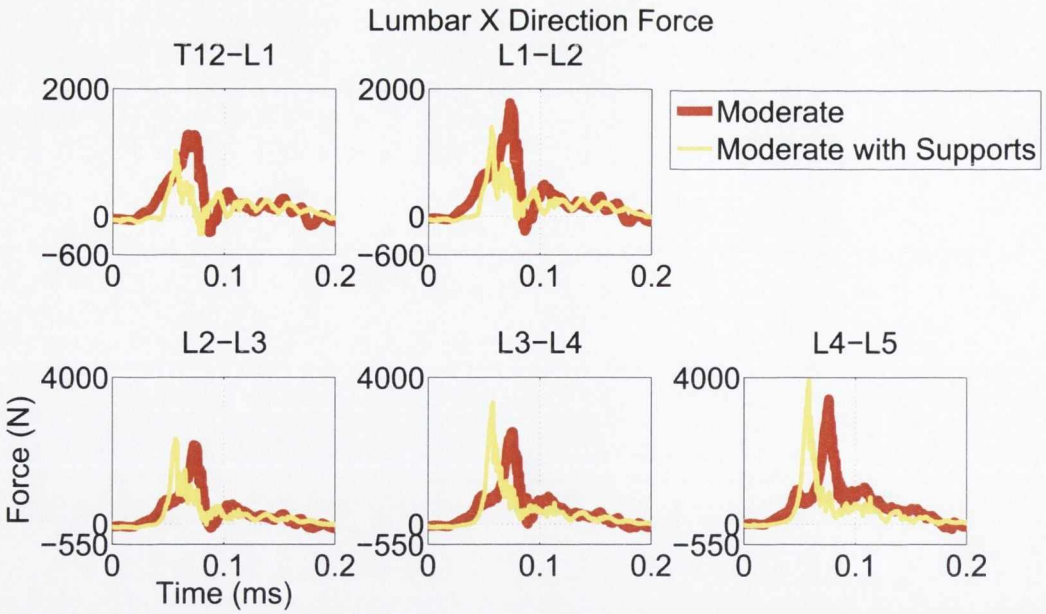


Figure 9.7: Forces on Lumbar Region for Moderate Scoliosis Occupant with and without Postural Supports

9.5 Summary

The addition of postural supports to the baseline and scoliosis models alters the loading on the occupant. The forces on the joints are seen to be dealyed in reaching their peak value and then ramp up quickly. In the baseline case the peak forces are slightly higher when the supports are added to the wheelchair. This results in higher predicted levels of injury. The peak values in each of the scoliotic spines shows an average R value of 1.0 when compared to the model without the postural supports in place. This also results in the injury scores being equivalent for the model with and without postural supports, except they occur at a later time when the supports are in place. This suggests that while the timing of these results is altered the peak forces are similar to those of the scoliosis models in a wheelchair without postural supports added to it.

However the underlying reason for the increase in forces is altered by the introduction of postural supports. The effect of the supports is to reduce the two effects of scoliosis - point loading and increased sagittal stiffness. The point loading is reduced as there is a increased contact surface between the occupant and the wheelchair. Also the occupant is more constrained in the wheelchair with the supports and so it cannot move a great deal. It has previously been found that relative motion between the joints of the scoliotic spine increases the forces on the spine (Chapter 7) and so for the constrained occupant this increase in force is no longer seen. Therefore the beneficial effects of the postural supports is to remove these two effects.

Another important effect that is found when cushioned postural supports are added is the loading on the spine when the cushion bottoms out and contact is made with the rigid plywood surface underneath. This effect accounts for the delay in reaching the peak force followed by a rapid increase in the force. This "bottoming-out" of the foam material on the surface of the supports is highlighted on the force-penetration characteristic assigned to the cushioned surfaces, see figure 9.8.

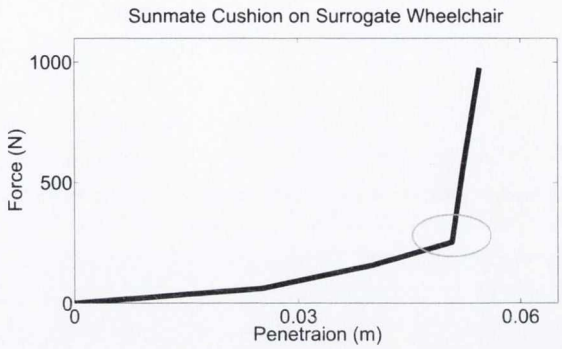


Figure 9.8: Force Penetration Characteristic of Wheelchair with Cushioned Surface

The effect of a cushioned surface on the unaltered wheelchair was also investigated by adding the cushioned surface to it. The same pattern in the forces on the spine was found for the baseline and scoliosis occupants when placed in this wheelchair, due to the bottoming-out of the foam.

The results from both the original and adapted wheelchair with the cushioned surface are greater than the discrepancy in the model and therefore the hypothesis can be accepted as holding true. It can therefore be said that the altered surface of the wheelchair as introduced here has a significant effect on the results of a rear impact.

This has clinical relevance to the practice of adding postural supports such as those modelled in this section of the analysis, and will be further discussed in Chapter 10. The overall effect of the cushioning is to increase the rate of loading on the spine as the cushion bottoms out. This suggests that this combination of Sunmate^{TM} foam and plywood seatback may not be the most appropriate for rear impact protection. However this is a complex issues and will be discussed in Chapter 10 based on all of the findings from this body of work.

9.6 Postural Supports without Cushioning

The behaviour of the foam under impact loading was found to increase the loading on the spine. A comparison of the loading on the occupant in the original wheelchair and in the wheelchair with cushioning in place reveals lower loading when cushioning was not added. Therefore the effect of removing the cushioning on the postural supports was investigated.

While these supports are not representative of real cases they can indicate the influence of cushioning on the outputs. This will first be applied to the baseline case and then to scoliosis models.

9.6.1 Baseline Model

The cushioning layer was removed from the surface of the postural supports with the non-scolioitic occupant. The effect of this will be investigated by looking at the forces and injury criteria predicted for the model. This provides information about these rigid postural supports without the added complexity of scoliosis.

Cervical Region

The forces in this region of the spine are reduce for the case with rigid supports, see figure 9.9. This produces an average of 30% less force on the neck.

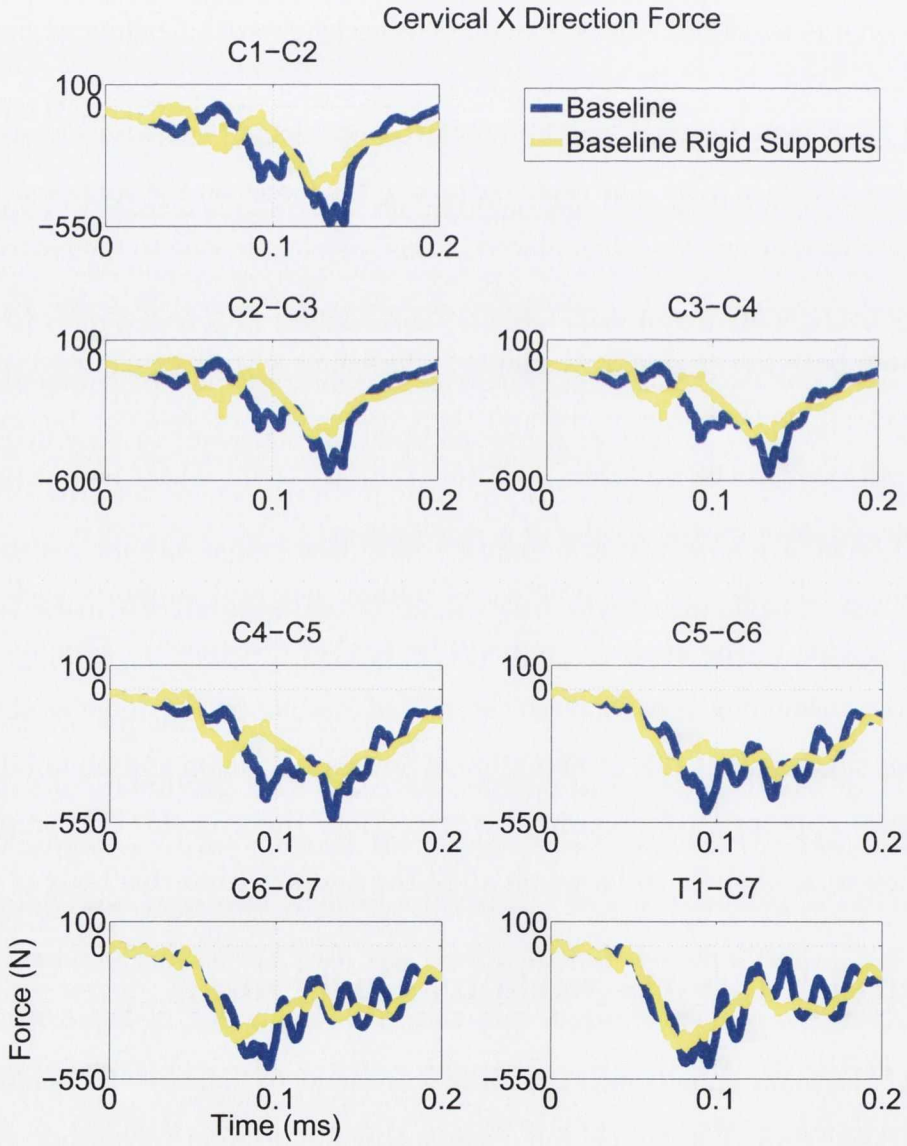


Figure 9.9: Forces on Cervical Region of Spine in Wheelchair without Supports and Wheelchair with Rigid Supports

Thoracic Region

The supports are added from the mid thoracic region downwards and so there is a different response in the lower regions of the thoracic spine for the two different models. In the lower thoracic region the loading is reduced, this is shown in figure 9.10. The forces in this region are reduced when compared to the baseline occupant in the standard wheelchair model by an average of 20%. However the loading in the upper thoracic region is increased due to the increased acceleration passed to the occupant by the larger surface contact area.

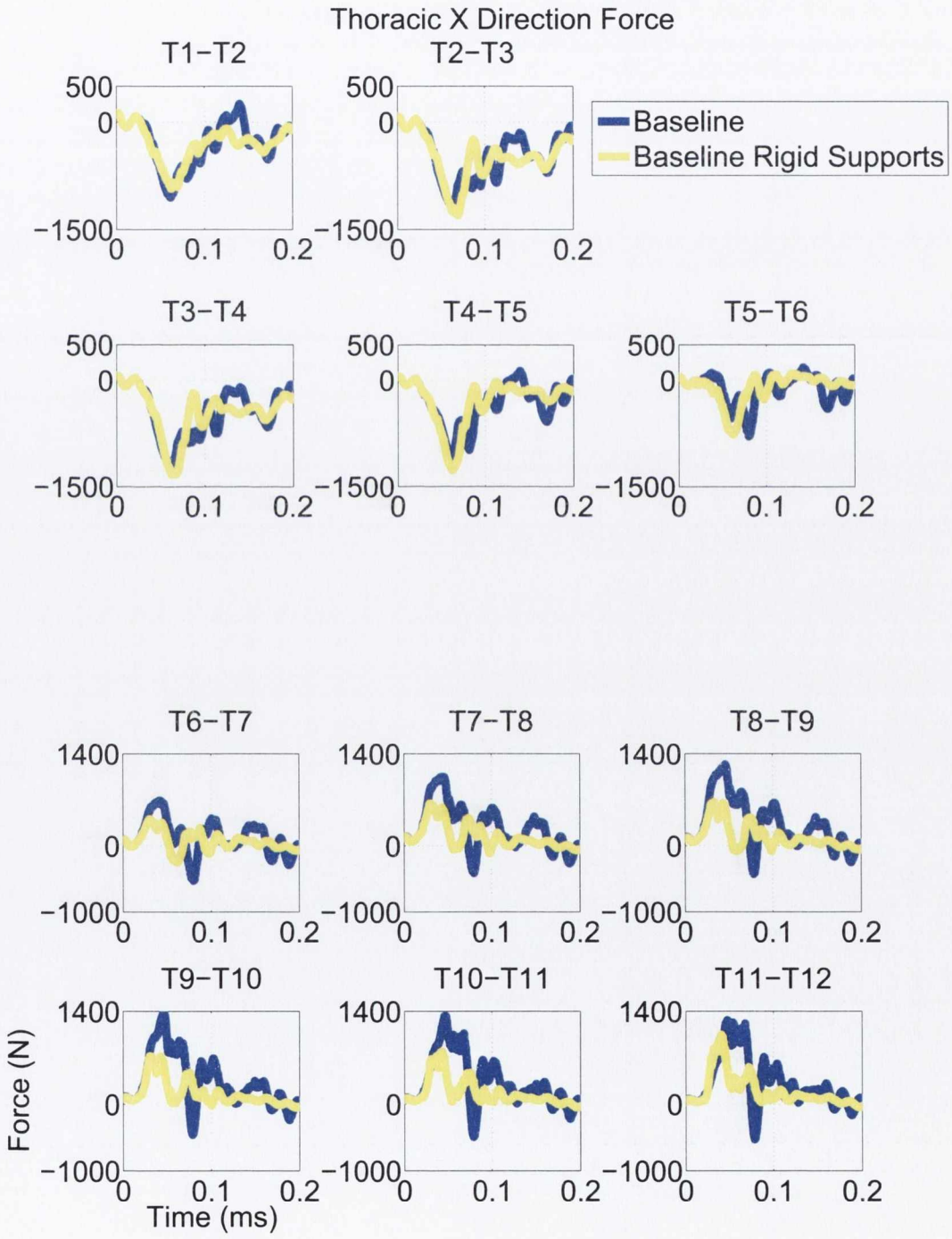


Figure 9.10: Forces on Thoracic Region of Spine in Wheelchair without Supports and Wheelchair with Rigid Supports

Lumbar Region

The effect of the supports is also clearly evident in the lumbar region of the spine. As illustrated in figure 9.11 the forces on the spine are reduced by an average of 30% when rigid postural supports are added.

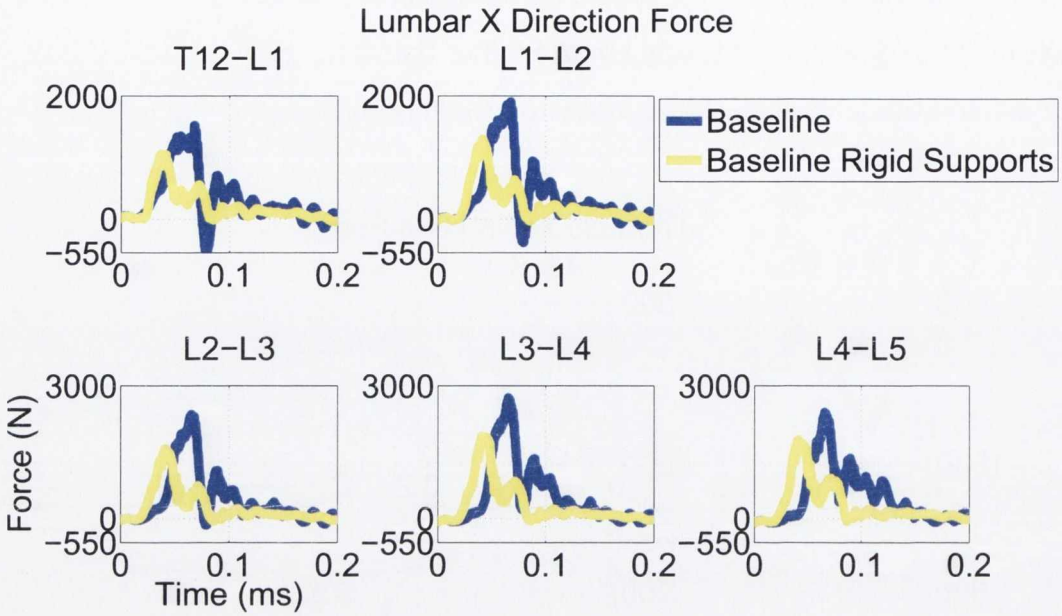
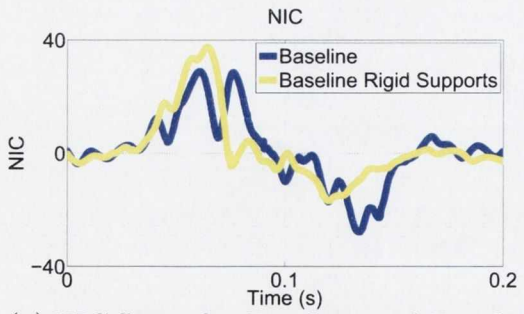


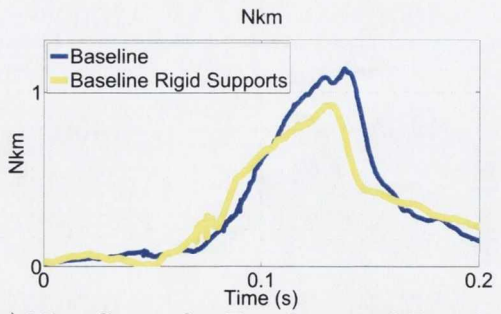
Figure 9.11: Forces on Lumbar Region of Spine in Wheelchair without Supports and Wheelchair with Rigid Supports

9.7 Injury Criteria

With the rigid supports in place this alters the results of the predicted injury level. The *NIC* is elevated compared to the model without the supports in place, figure 9.12(a). This is due to the elevated acceleration of the T1 vertebra in the upper thoracic region. Whereas the *Nkm* is reduced as the loading on the cervical spine is reduced, figure 9.12(b).



(a) *NIC* Score for Baseline and Baseline in Wheelchair with Rigid Postural Supports



(b) *Nkm* Score for Baseline and Baseline in Wheelchair with Rigid Postural Supports

Figure 9.12: Mild Scoliosis X-rays

9.7.1 Scoliosis Models

The loading on the occupant was assessed by investigating the forces on the spine and determining the predicted injury levels. The outputs from this model are compared to the outputs from the scoliosis models seated in the original wheelchair.

Cervical Forces

In the neck of the spine the forces were reduced by an average of 30% for each level of scoliosis. This is shown for the moderate case of scoliosis presented in figure 9.13.

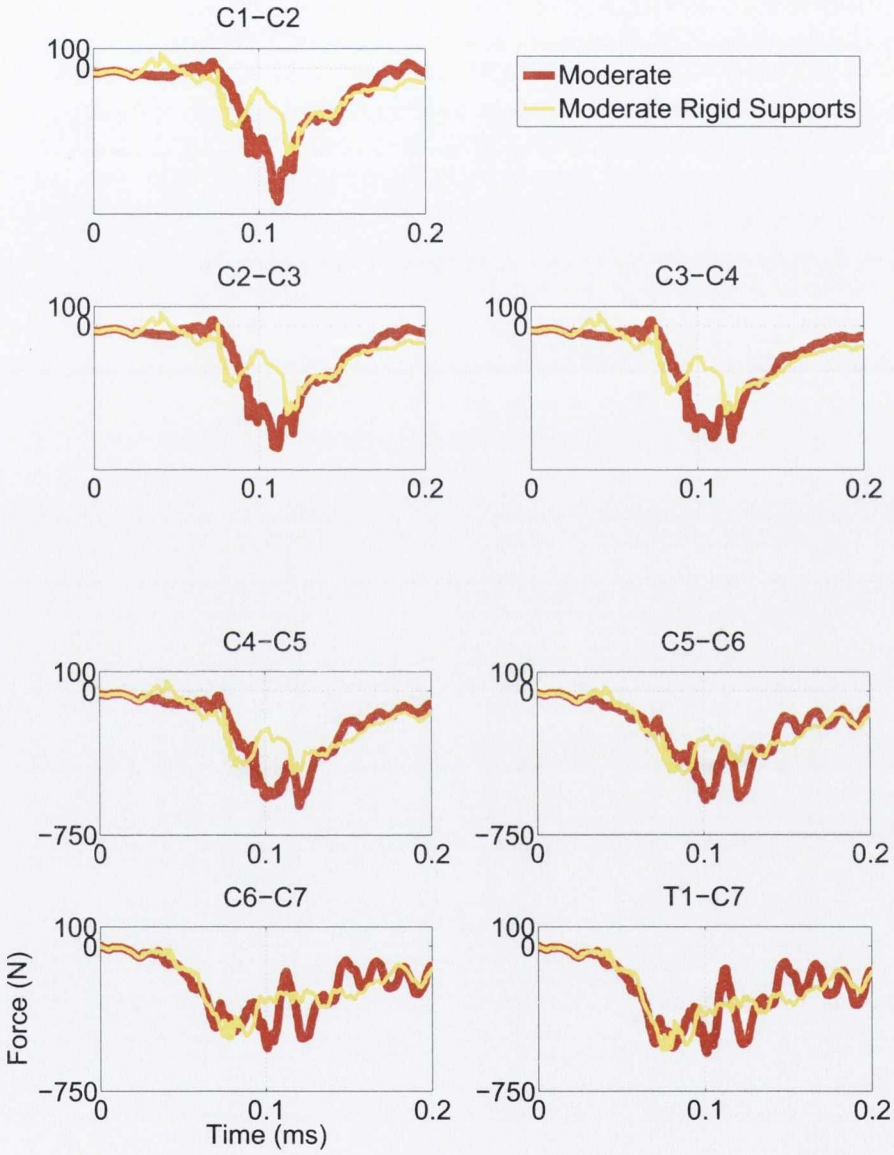


Figure 9.13: Forces in the Cervical Region of the Spine for Moderate Scoliosis in Standard Wheelchair and in one with Rigid Postural Supports

Thoracic Forces

This region of the spine highlights the large difference that the addition of these rigid supports made to the models. The lower thoracic region shows much reduced forces on the spine with

an average of 30%, as seen in joints T4-T5 down towards the lumbar region. For the moderate case of scoliosis the average reduction is 50% in the forces on the spine, see figure 9.14.

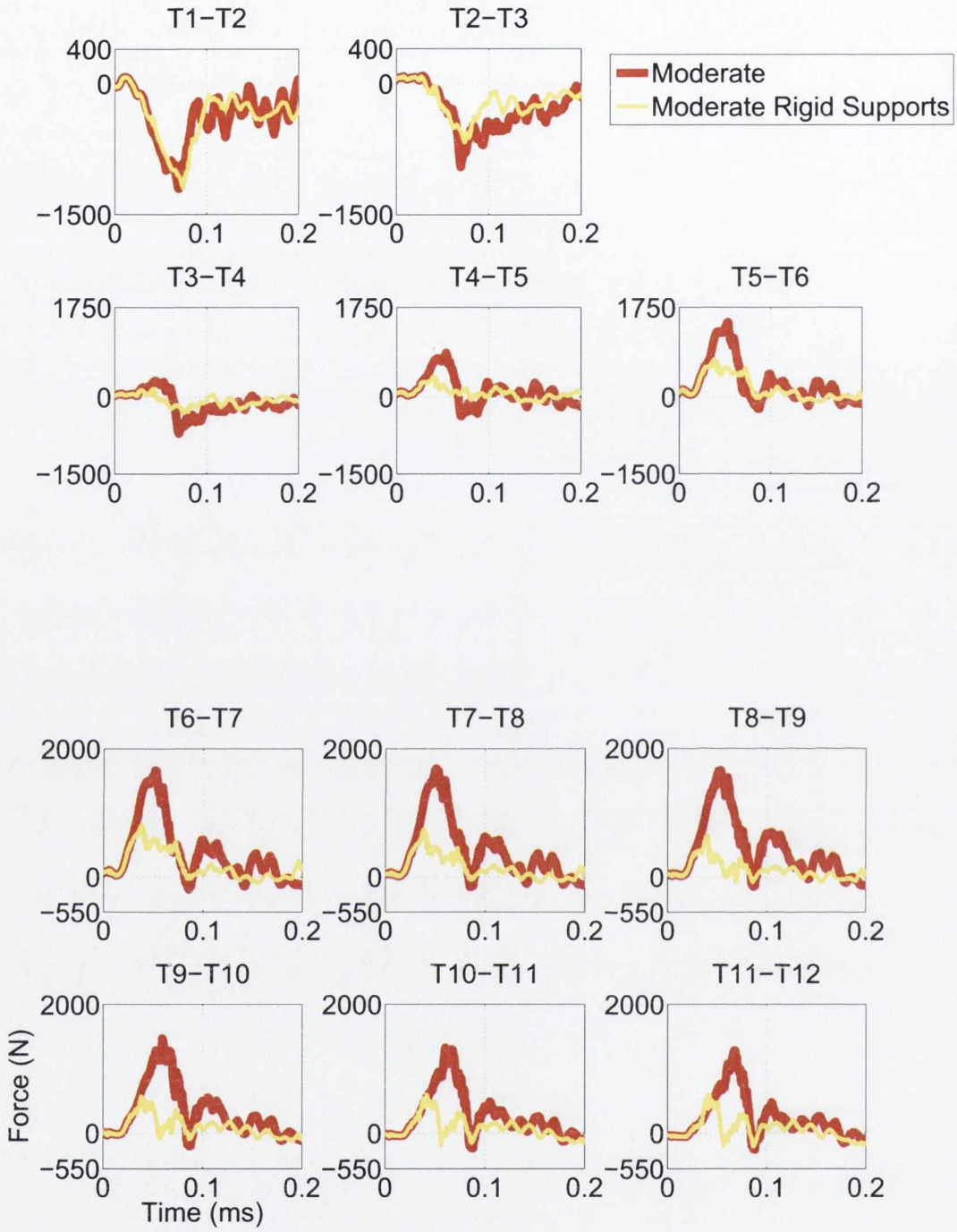


Figure 9.14: Forces in the Thoracic Region of the Spine for Moderate Scoliosis in Standard Wheelchair and in one with Rigid Postural Supports

Lumbar Forces

The forces in this lower most region of the spine again shows the positive influence of the effect of the rigid contacting surface. The reduced forces on the spine are shown in figure 9.15.

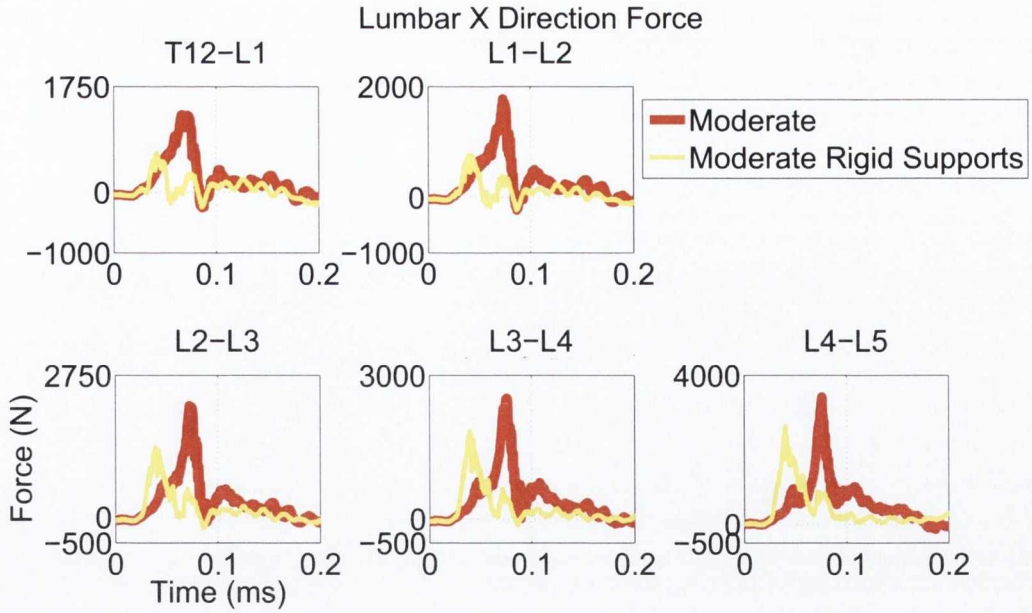


Figure 9.15: Forces in the Lumbar Region of the Spine for Moderate Scoliosis in Standard Wheelchair and in one with Rigid Postural Supports

9.8 Injury Criteria

The predicted *NIC* score for each of the scoliosis models is slightly higher with the rigid supports in place which follows the trend established in the baseline. This is caused by the increased acceleration passed to the first thoracic vertebra (T1) due to the increase surface area of contact. The average increase is 26%. The *Nkm* values are also reduced which again was found in the baseline case.

9.9 Summary

The models in this work found that a stiffer surface reduced the loading on the spine by an average of 30% when placed in direct initial contact with the occupant. The stiff supports prevent the additional rearward movement that is allowed when cushioning is placed on the surface of the supports. The stiff supports also reduce the influence of the the two main modes of increasing the loading on the occupant - point loading and scoliosis effect - as detailed in Chapter 7. Point loading is reduced as the contact surface between the occupant and the seatback is increased, leading to a more distributed loading over the torso of the occupant. The effect of scoliosis is also greatly reduced as the occupant's spine is unable to move and flex and therefore the increase in forces associated with the increased sagittal stiffnesss is not seen.

The predicted risk of injury is also altered by the introduction of these rigid postural supports. The *NIC* is increased due to the increased acceleration of the torso. The *Nkm* however is reduced as the loading on the neck is reduced.

Therefore although these stiffer supports are not representative of actual cases they do highlight the importance of the characteristic of the surface material. This is also applicable for the normal surfaces of the wheelchair and has an important clinical relevance which is discussed in Chapter 10.

9.10 Seatback Height

The analysis of the scoliosis models in Chapter 7 revealed an altered sitting height which reduced as the level of scoliosis increased. The sections of the spine which are loaded anteriorly and posteriorly are therefore altered depending on whether they are supported by the seatback or not. Briefly, it was found that the upper thoracic spine is loaded posteriorly as it is pulled rearwards due to the weight of the head and neck as they move backwards relative to the wheelchair. However, the mid and lower thoracic regions of the spine are loaded anteriorly due to contact with the seatback. The point at which the joints switch from posterior to anterior shear forces was found to be at a different level for each degree of scoliosis, as shown in the sitting heights of the modelsin figure 9.16.

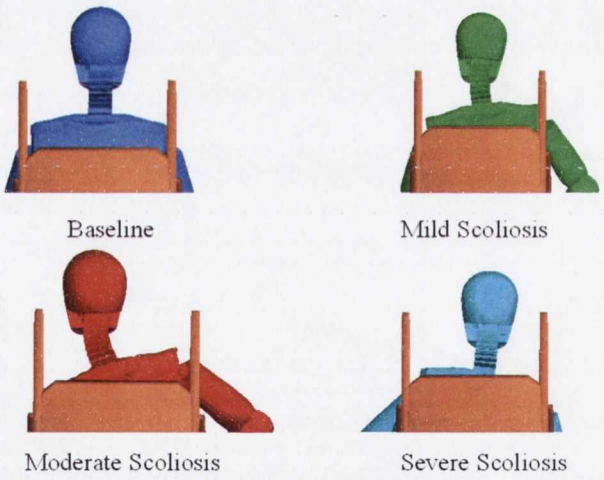


Figure 9.16: Seatback Height Relative to Torso for Baseline and Scoliosis Models

To investigate this the seatback height was created to be at the same height relative to the torso for each level of scoliosis as that of the baseline case. Therefore the seatback height for each case was adjusted to be at the T5-T4 joint, see figure 9.17. In this image each of the scoliosis cases are stripped down to their spine and the T5-T4 joint is highlighted in black and is the marker for the new height of the seatback.



Figure 9.17: Rear View of Models with Seatback Height at T5-T4 Joint

These models were subjected to a computational rear impact and the same methods of analysis was conducted, the results of which are presented here.

9.10.1 Forces on the Spine

The forces on the spine were analysed with particular focus on the thoracic region of the spine as this is where the greatest changes would be expected. The loading on the cervical and lumbar regions show that the forces are only slightly changed, an average of 10%. An analysis of the peak forces and time of occurance in these regions shows that there is no great difference in the results when the seatback height is lowered.

The R values for the thoracic region of the spine of the mild, moderate and severe case of scoliosis in the shorter seatback height compared to the occupant in the original wheelchair reveal that the R values are generally 1.0. The noticeable exception being around the T5-T4 joint, see figure 9.18 .

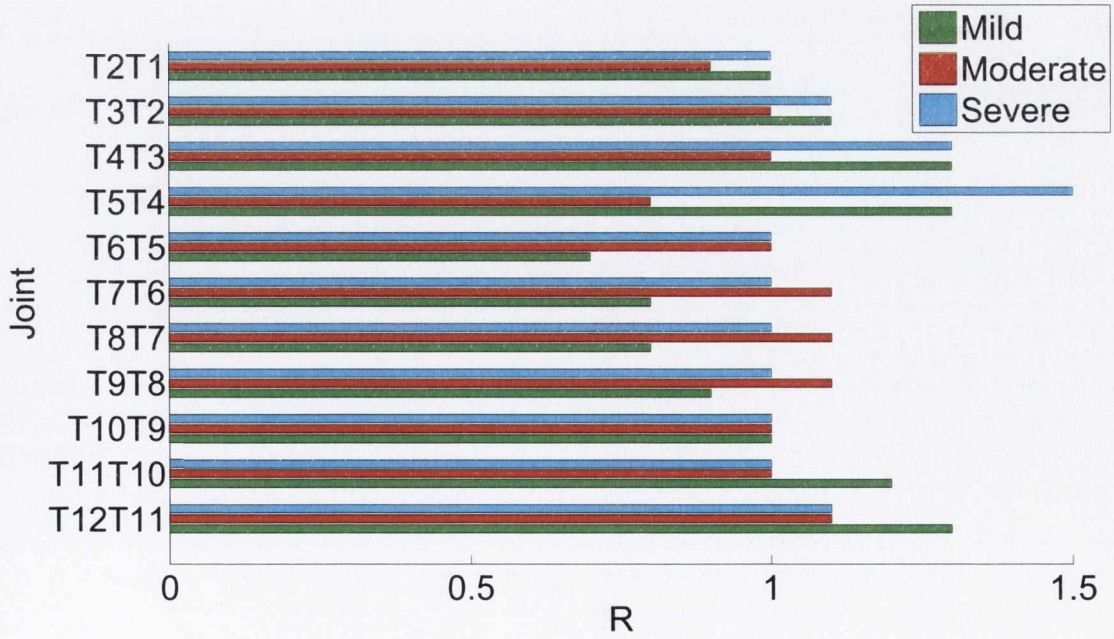


Figure 9.18: R Values for Mild, Moderate and Severe Scoliosis in Short Wheelchair Compared to Original

The forces on the joints in this region for each of the scoliosis models are shown in figure 9.19. This shows that the forces on the joints for the models with the altered seatback height are slightly reduced when compared to the case with the original seatback height. This figure shows the forces for the original seatback height and the forces for the reduced seatback height.

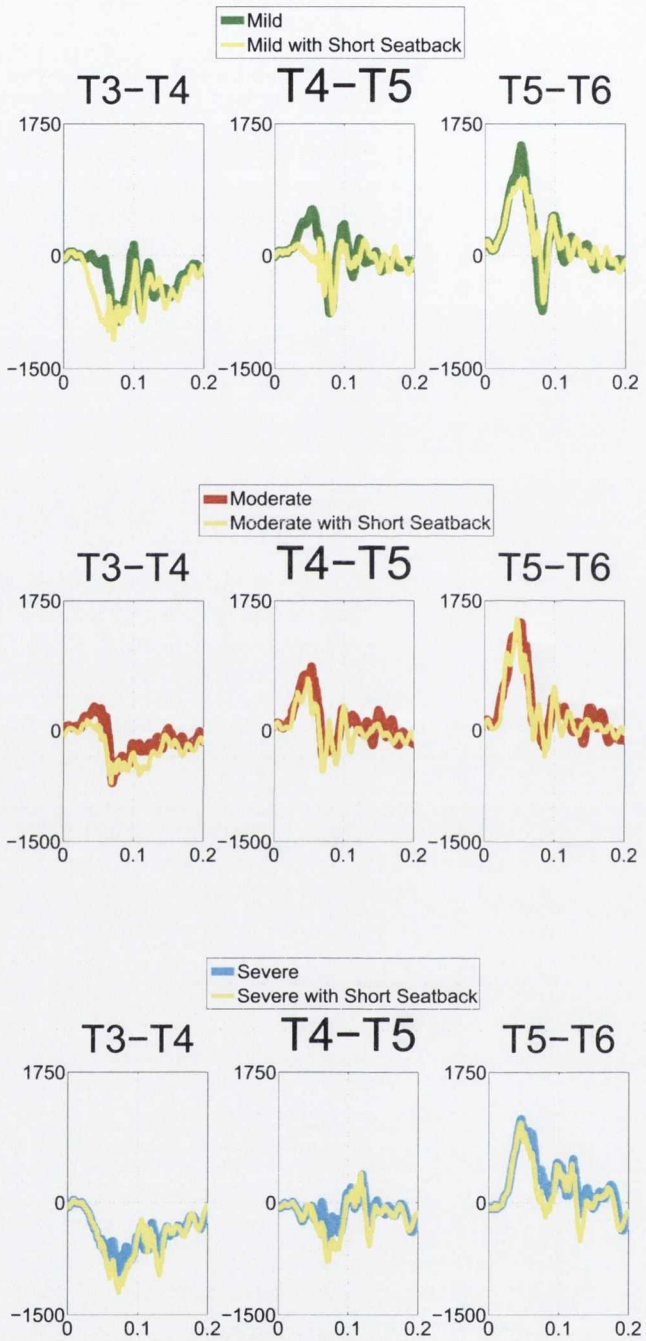


Figure 9.19: Time History Plots of Force on Mild, Moderate and Severe Scoliosis Models in Normal Wheelchair and Reduced Seatback Height

9.10.2 Injury Criteria

The injury criteria for the model in the wheelchair with the reduced seatback height do not show substantial differences in the result compared to the model in the wheelchair of the

original seatback height. The *NIC* values for each case of scoliosis is presented in figure 9.20. The *Nkm* is also shown for each level of scoliosis in figure 9.21. The peak values for each level of scoliosis in both wheelchairs seatback heights are presented in table 9.1

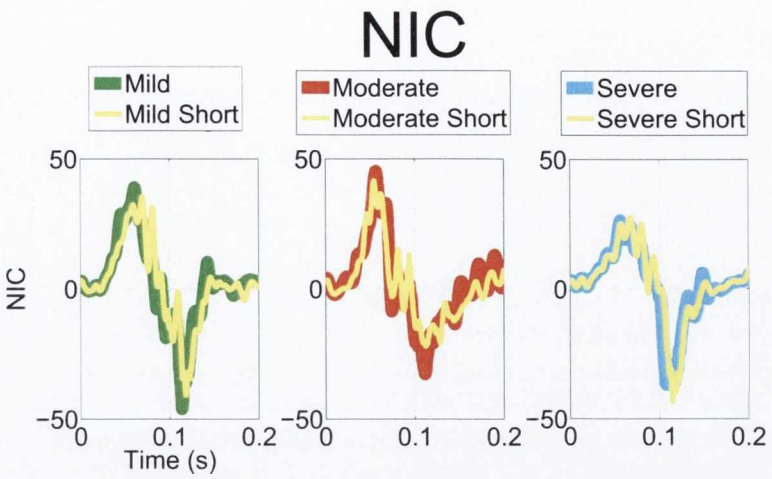


Figure 9.20: *NIC* for Mild, Moderate and Severe Case of Scoliosis in Wheelchair with Original Seatback Height and Reduced Height

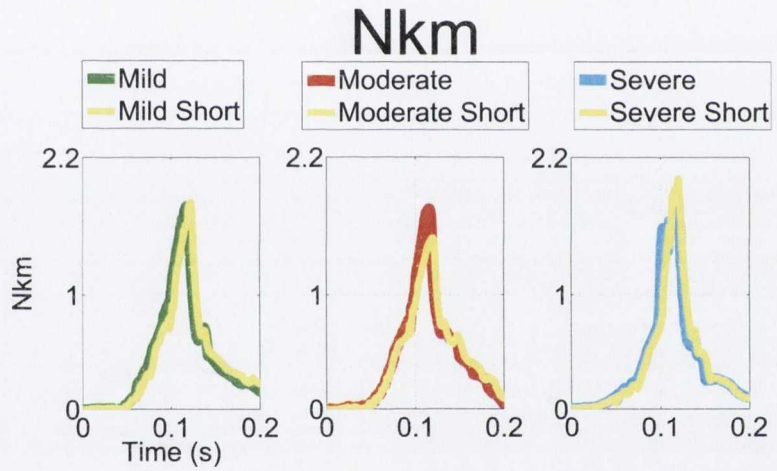


Figure 9.21: *Nkm* for Mild, Moderate and Severe Case of Scoliosis in Wheelchair with Original Seatback Height and Reduced Height

Model	Seatback of Original Height	Seatback of Reduced Height	Percentage Difference
NIC			
Mild	39	36	-8
Moderate	45	42	-7
Severe	26	28	+8
Nkm			
Mild	1.77	1.81	+3
Moderate	1.76	1.5	-15
Severe	1.85	2.02	+9

Table 9.1: Injury Criteria for Wheelchair Seatback at Original Height and at Reduced Seatback Height

9.11 Summary

The point at which these values switch is based on not only the seatback height but the deformity of the spine. The deformity of the spine results in an altered orientation of the body with respect to the seatback and so there is an altered interaction with the seatback. The results found in this section of analysis found that the effect of the seatback height resulted in values that were very similar to those of the unaltered seatback height. The effect of scoliosis is therefore greater than that of adjusting the seatback height. These values were lower than the discrepancy found in the validation of the model and therefore are said not to have a substantial effect on the results.

The investigations carried out in this chapter show the effect of alterations to the wheelchair has in the case of a rear impact. The relevance this has to occupant protection and for wheelchair adaptation in a clinical setting will be discussed in the following chapter.

Chapter 10

Discussion

This chapter brings together the results from the analysis of the baseline model, the scoliosis models and the adapted wheelchair models. The main issues are highlighted and discussed. Clinically relevant findings are also discussed as they provide a scientific basis for many best-practice procedures that are carried out in seating clinics.

Research to date has aimed to improve wheelchair occupant crash safety by restraining the wheelchair and occupant using a WTORS system. The work presented in this thesis focuses on rear impact investigations as this has not been as extensively investigated as frontal impact. Work to date has also focused on the 50^{th} percentile occupant which is not always a good surrogate for wheelchair occupants who may have a postural deformity such as scoliosis. Therefore scoliosis was introduced into the computational model of the occupant. Wheelchairs are often adapted for occupants with these types of postural deformities and the effect of altering the occupant and the wheelchair in a rear impact was investigated using numerical modelling. Occupant loading in these models was also investigated, which again has not been extensively investigated to date.

10.1 Limitations

For the work in this thesis there are some limitations and assumptions which must be acknowledged and their influence on the results must also be evaluated.

Numerical Modelling

The validation data for the numerical model was based on the output data from the BioRID II occupant. The data from wheelchair and WTORS was not provided by the testing facility due to a malfunction and not having the required facilities. However, the wheelchair displacement and the tiedown system in the numerical model were visually checked to ensure correspondence with the sled test. The occupant restraint was not considered as it does not play a role in the first 200ms of a rear impact. The validation of the model was conducted

with these parameters checked visually, however, having the output data would have added weight to the validation.

The validation of the numerical model was based on a single physical test, due to the limitation imposed by the testing facility to prevent hyper-extension of the neck of the BioRID II in all three tests. In using only a single test any inherit variation due to parameters such as the test set-up would not be accounted for. Also any anomaly in the single test may not be identified. However, the numerical model was compared to the corridor of results up to the time of head contact with the restraint (in Tests 2 and 3) and good correlation was found with the sled tests up to that point. The comparison of the numerical model and the single test in which full extension of the neck of the neck occurred (Test 1) found good correlation, with some differences.

The differences found between the physical and numerical results in this work are similar to levels found in other computational models [47] [48] [51] [105]. The best correlation between the tests and the computer model were found in the X direction which is the direction of the applied loading. The injury criteria which predict injury are based on the loading in this direction and therefore these are the most important parameters to consider when evaluating the model.

The BioRID II occupant model used in this work was developed by MADYMO. While extensive work has gone into the creation of this model there are some limitations associated with it, mainly that the model was validated against a single sled test. Another limitation of the BioRID II occupant model is the joints of the spine. These are represented a lumped mass system with a single characteristic describing the behaviour of the soft and hard tissues of the spine, however this is quite a complex relationship. Also these joints allow for motion in a single plane which is not wholly realistic. However, the BioRID II was developed for use in a zero offset rear impact in which there would be limited out of plane movement.

The model developed in this work provides a baseline computational model which can be altered to assess the influence of altering the occupant and the wheelchair on spinal loading in an impact. The acceptance or rejection of the hypothesis that such alterations to the occupant and wheelchair are significant is based on whether the difference they cause in the model are greater than or less than the discrepancy in the model. The acceptance/rejection of the hypothesis is therefore a function of how well the model is validated. To reduce the influence of this circular argument the model was only considered valid once the discrepancies were reduced to a minimum. The validation was also only accepted once the level of discrepancy was less than established upper limits of acceptable difference based on other published models.

Use of Rigid Wheelchair

The use of the ISO surrogate wheelchair which has a rigid seatback was chosen for testing as it has been extensively used for frontal impact evaluation and has been used to guide the design of the wheelchair tiedown and occupant restraint system (WTORS) [46] [48] [101]. The same approach was used for the validation of the BioRID II dummy comparing its response to that of volunteers [19]. Rigid seats have also been used to investigate injury and the kinematics of a vehicle seated occupant subjected to a rear impact [20] and in the evaluation of wheelchair headrests [6]. A headrest was not used for the tests conducted here as it is not mandatory for transport, and many wheelchair users do not use one while in transit. The performance of these headrests in a rear impact has been evaluated in a parallel study [62].

The seat and seatback of the wheelchair used in this study were constructed of plywood with a firm foam placed on the seatback. The rigidity of the seatback leads to increased loading on the spine [111] [112]. However, as the long term goal was to establish the influence of postural deformities on spinal loading, the confounding effects of wheelchair cushioning and structural deformation were avoided through the use of a rigid wheelchair. An alternative wheelchair design may have produced significantly different results. A less rigid seat back may have lead to catastrophic failure as found by Manary [50] and Senin [61].

Scoliosis Implementation

Scoliosis is a 3D deformation of the spine however the BioRID II has a spinal articulation in the sagittal plane only. The dummy replicates the behaviour of the human spine under uni-direction applied loading. The single axis of rotation is assumed to model the reaction of the body due to such loading in a non-oblique collision. The vertebral joints in the model are revolute joints with an axis of rotation initially parallel to the global y-axis with all other degrees of freedom constrained. Therefore, when scoliosis is applied using the X-ray data, the joint axis of rotation of each vertebral pair is altered.

However, to evaluate the influence of allowing rotation about all three axes, the joints were altered to create this type of spine. The findings showed that, while axial and lateral rotation were found in the scoliosis models, rotation about the sagittal plane was still the dominant feature of the response of the spine due to the large acceleration in this direction.

Neck Correction

In creating the scoliotic occupants, the position of the head was also based on assumptions. An ocular reflex corrects the head and neck orientation so that the eyes are positioned

horizontally [65] [66]. This means any lateral deviation in the lumbar and thoracic region is compensated for at the base of the neck. The X-ray data was limited to the lowermost cervical region, and therefore the model head orientation was based on a study of clinical cases. However different methods of correcting the head were used and did not produce any significant difference in the results.

Initial Posture of Occupant

The 26^o orientation of the occupant seated in the wheelchair is the validated position of the BioRID II and was therefore used to create a valid baseline model. However this is not an ideal representation of the position of an occupant in a wheelchair. The idealised position of the occupant is upright and with the pelvis as far back in the seat as possible, while this is the ideal it is not always possible or comfortable for the occupant. Throughout the day for comfort and for alleviation of pressure the occupant may move position in the seat and therefore the altered position as found in these models is not wholely unrealistic. The idealised 90-90-90 position was also investigated in order to have a full understanding of the effect of this. The same trends were found as that of the occupant seated at 26^o but to a smaller magnitude, and it is trends in the results which is most important for the work conducted here.

Despite these assumptions and limitations, the numerical models created provide the first robust means to investigate rear impact of wheelchair occupants.

10.2 Baseline Rear Impact

The baseline used in this work comprised of the BioRID II occupant and the ISO surrogate wheelchair which was subjected to a rear impact. Due to the large variation in occupant and wheelchair, these representative models have been created. This occupant model and surrogate wheelchair had not previously been combined to determine the risk of injury to a wheelchair occupant in a rear impact. The work presented here therefore investigated this using a combined physical and numerical approach. The numerical model was created and validated against a physical test and while some discrepancies were found, they were deemed to be acceptable. Using the data from the numerical model, the risk of injury due to a rear impact was evaluated.

10.2.1 Baseline Evaluation - Injury Criteria

The most common region of the body where injury is found due to a rear impact is in the neck and so the predicted level of neck injury for the baseline occupant was determined using

two injury criteria the *NIC* and *Nkm*. The *NIC* criterion is based on the relative acceleration of the the torso and head. The *Nkm* criterion is based on the forces and moments of the upper neck. These criteria are commonly used to assess the level of injury due to a rear impact.

High levels of injury were predicted when the *NIC* and *Nkm* injury criteria were evaluated. The peak injury scores were determined and are presented in table 10.1 as well as the cut-off values above which injury is expected.

Injury Criterion	Baseline Peak	Cut-off Value
NIC	29	15
Nkm	1.14	1.0

Table 10.1: Injury Criteria for Baseline Model

These values are much greater than levels which predict injury of $15m^2/s^2$ for the *NIC* and 1 for the *Nkm*. However, a limitation of the use of the *NIC* and *Nkm* is the single threshold level predicting the occurrence or non-occurrence of injury. It is more appropriate to consider risk probabilities due to the inherent variability in injury risk for different individuals. Therefore the risk probabilities associated with neck injuries with symptoms lasting more than one month and the calculated NIC and Nkm scores derived by Kullgren et al [39] from accident reconstructions are used for the assessment of whiplash injury risk for adult wheelchair users, see figure 10.1.

The values predicted for the baseline occupant in this work correspond to a respective risk probability of 90% and 40% of sustaining neck injuries with symptoms lasting more than one month, see figure 10.1.

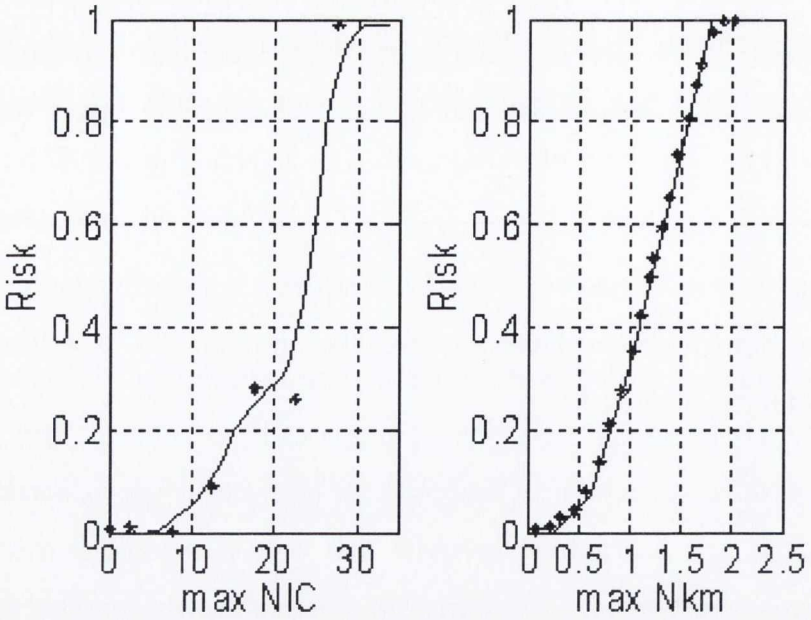


Figure 10.1: Risk Probability of Injuries with Symptoms Lasting More Than One Month Associated with *NIC* and *Nkm* Scores [39]

The high level of injury predicted for the occupant is as expected as the dummy was tested in a rigid wheelchair without a headrest. The use of a headrest in transit is not mandatory, however investigations into headrests used on wheelchairs have been conducted as part of a parallel project. The findings have shown that a properly designed and positioned headrest can substantially reduce the risk of injury to an adult occupant in a rear impact [62]. This mimics the work conducted into rear impact of child occupants [35], which also found reduced risk of injury with a headrest in place. This important safety feature is therefore sometimes lacking for wheelchair occupants in transit and would significantly improve the safety level.

10.2.2 Baseline Rear Impact Evaluation - Spinal Loading

The greatest forces on the spine of the baseline model were found in the lumbar region due to the rearward motion of the occupant and large contact force with the seatback. The forces are close to levels that can cause damage to the vertebrae. The largest peak force in this region was 2.7kN in the X-direction. Fractures of hard tissues such as the facet joints of lumbar vertebrae have been found due to a shear load of 2.8kN [77]. This indicates that there is a high probability of damage to the vertebrae in a rear impact. There may also be damage to the surrounding soft tissue of the spinal column, however, the focus of this work is on vertebral joints and damage due to loading on the bony tissues.

10.3 Scoliosis

When scoliosis was introduced in the spine three main effects were found, these are

- Asymmetrical movement
- Point Loading
- Increased sagittal stiffness

Each of these have a significant effect on the resulting loads on the occupant. These are detailed in the following sections.

Asymmetrical movement

Scoliosis introduces asymmetry to the movement of the dummy which alters the kinematic response. This is shown in the comparison of the baseline and moderate scoliotic occupant in a rear impact (see Chapter 7). The reaction of the spine was analysed and detailed from the gross motion of the torso down to the individual vertebrae. This altered movement of the spine was evident at each level of investigation into the spine.

The altered movement of the spine was attributed to the displaced axis of rotation that is introduced by scoliosis. The individual vertebrae were seen to rotate about their local Y axis, however due to the introduction of scoliosis, this was no longer the global Y axis, see figure 10.2. This resulted in a reduced motion of the scoliotic dummy in the global coordinate system as the vertebral joints were rotating about this shifted axis. This was found for all levels of scoliosis.

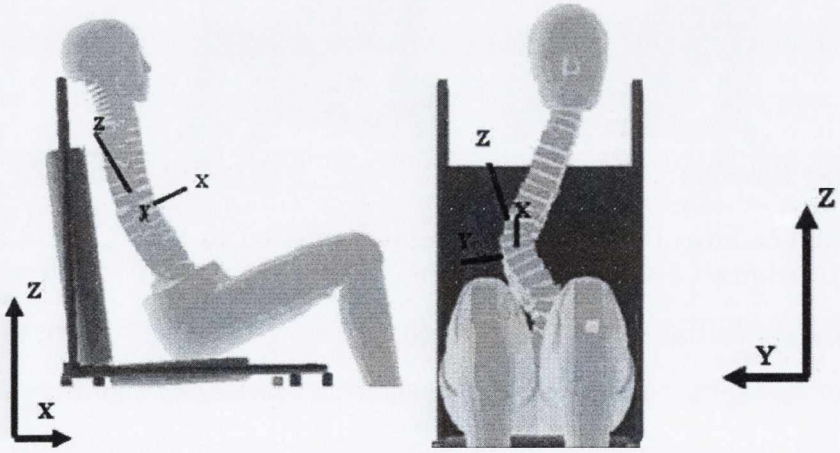


Figure 10.2: Displaced Axis of Rotation of Vertebra Compared to Global Coordinate System

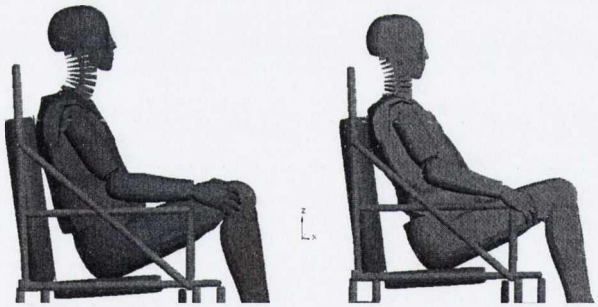
The altered response of the scoliotic occupant reflects that of real life cases [97]. For scoliotic occupants it is important to note that, due to the many classification of scoliosis (Type

I degenerative, Type II idiopathic, Type III neuromuscular [113]) there may be many different reasons for an altered kinematics of the spine which is mimicked in these computational models. In some cases of scoliosis there is degradation of the articular cartilage between the vertebrae and this would produce an altered spinal movment [114]. Degradation of the vertebral bone is also found and can result in bony prominences on the articulating surfaces which would effect the movement of the vertebrae passing over each other. Similarly, the musculature of the spine may not allow the range of motion normally associated with the spine due to an increase or decrease in the muscle tone. In the case of idiopathic scoliosis there can be an associated altered interaction of the facet joints which play an important role in the biomechanics of the spine [115]. Other researchers have found that in cases of idiopathic scoliosis there exists a coupling between ventral flexion or extension and axial rotation which is not found in spines without scoliosis [80].

This altered movement of the spine is replicated in the models created for this work, and is an important factor in the altered loading on the scoliotic occupant.

Point Loading and Increased Sagittal Stiffness

The altered shape of the scoliotic occupants results in an altered interaction with the seatback. This altered shape has an exaggerated kyphosis which creates a point loading effect on the spine, see figure 10.3. This figure compares the baseline to the mild scoliosis occupant in the wheelchair.



(a) Baseline (b) Mild Scoliosis

Figure 10.3: Point Loading of Baseline Occupant Compared to Mild Case of Scoliosis

The stiffness of the spine is also greatly increased in the sagittal plane due to the displaced axes of movement of the spine. In the work presented in this thesis the increased sagittal stiffness was found to increase the forces in the joints of the spine when subjected to loading in this plane.

This result mirrors the reduced flexibility found in patients with idiopathic scoliosis which found that every 10^o increase in Cobb Angle over 40^o results in a 10% decrease in side-bending flexibility [97]. Some cases of idiopathic scoliosis have also found that the posterior elements

of the vertebrae on the neural arch are deformed so that the facets on the concave side are out of alignment with those on the convex side. This has been found to produce locking of the vertebrae in an altered posture [81].

The effect that each of these factors have on spinal loading was determined separately - point loading and increased sagittal stiffness were found to create an average of 30% and 20% increase respectively in the forces on the spine. However, their combined effect is not a simple matter of addition as their interaction is more complex. At each vertebral joint, the effect of these two factors is based on the degree of deviation from the normal curvature of the spine and the interaction with the seatback. Therefore, the increased loading is unique to each spinal curve.

10.3.1 Loading on the Scoliotic Spine

While the neck is the traditional area of injury due to a rear impact [26], and high levels of injury are predicted in the baseline and scoliosis cases, there is also an increased risk of injury in the thoracic region when scoliosis is introduced. The forces on the joints in this region are increased by up to 30% with the peak value of 2.3kN. This value is close to forces found to cause fracture of the lumbar vertebra, 2.8kN, when tested in shear [77]. While data on the response of the thoracic vertebrae to shear loading is limited, the compressive strength has been established [69] and found to be less than that of the vertebrae in the lumbar region. This reduced strength has been atributed to the reduced size of the throacic vertebrae. Therefore it is logical to suggest that the shear strength of the thoracic vertebrea would also be less than that of the vertebrae in the lumbar region.

The direction of the shear loading on the lumbar spine has been found to be an important factor as the spine has been shown to be stiffer when shear loads are applied in the anterior direction rather than in the posterior direction [108]. The same can also be hypothesised about the thoracic region and therefore loading due to contact with the seatback would be expected to be less injurious.

Investigations into crash injuries have found that a case of a compressive fracture in the thoracic spine occurred due to a rear impact [17]. While the full details of the crash event are not provided, this study shows that such injuries can occur. This investigation also shows that when the spine is straight and upright it is better able to resist crash loading, as a higher risk of injury was associated with an non-upright posture. The paper also states that the "spine can sustain higher loads in a straight posture rather than when curved or rotated", therefore the effect of scoliosis may be to reduce the ability of the spine to resist the high loads associated with a crash [17].

The soft tissues of the spine can also be injured in a crash. Long term injuries in the lumbar region have previously been found after rear impact and have been attributed to damage to the soft tissues of the joints [67]. In scoliotic spines the articulating cartilage has been found to be degenerated, and therefore the risk of injury may be greater. This can be further complicated by the fact that in some cases there is more degeneration in the concave side than in the convex side at the apical vertebra [114], which could lead to a higher risk of injury. However, this cannot be evaluated with the current results.

Research into the response of vertebrae to shear loading has found fractures of immature vertebral bone at both the facet joints and at the endplates [76]. The 6 month old porcine test specimens showed that fractures at the endplates occurred at higher loading rates and also when the vertebrae were in a flexed position. This has possible consequences for children with cerebral palsy, who may have an associated scoliosis [89], as they have been found to have skeletal immaturity compared to children of the same age [116], [117].

Compression fractures of vertebrae were found to occur at substantially lower, 25%, values when the load is applied eccentrically to the vertebrae compared to when a purely axial load is applied [71]. This may have a siginificant influence on a scoliotic spine in which the shape is altered substantially. The presence of wedged vertebrae may lead to eccentric loading and so may effect the response of the vertebrae under compression loading. This may esepcially be true for the apex of the curve which is the most deformed area.

Apex of the Curve

For all levels of scoliosis, the greatest increase in forces on the joints was in the area around the apex of the curve. The peak force for the severe case of scoliosis in this region was found to have approximately a 200% increase when compared to the baseline value. This large increase is due to the point loading on the scoliotic spine as well as the increased deformity in this region.

In this region of the spine with the greatest deformity, a rib hump may be found. This deformity is due to the torsion of the vertebral bodies which causes the deformed shape of the attached ribs [118].

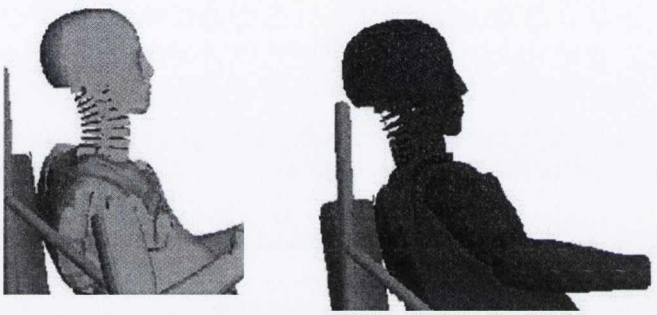
From the work conducted in this thesis this region of the spine has been found to be at greatest risk of injury due to increased loading.

10.4 Injury Criteria

The injury criteria were determined based on these outputs from the scoliotic dummy and were compared to the level predicted for the baseline case.

10.4.1 *NIC*

When scoliosis was applied the effect of point loading was to increase the loading on the dummy. For the mild and moderate case of scoliosis, this caused a much greater acceleration of the uppermost thoracic vertebra (T1) than in the baseline case. However the severe case did not continue this pattern as the T1 vertebra was accelerated at a lower rate than the baseline. This is due to the much increased deformity of the spine at the upper thoracic level. This increased deformity causes a greater restriction of the motion of this region of the spine than in the mild and moderate cases. The increased deformity is shown in figure 10.4 and is compared to that of the moderate case of scoliosis. The increased deformity in this region therefore has a direct influence on reducing the *NIC* score, see table 10.2.



(a)Severe Scoliosis Model (b)Moderate Scoliosis Model

Figure 10.4: Severe Scoliosis Case and Moderate Scoliosis Case

	NIC (m^2/s^2)	Percentage Difference Compared to Baseline
Baseline	29	
Mild Scoliosis	39	34
Moderate Scoliosis	45	55
Severe Scoliosis	26	-10

Table 10.2: *NIC* peak Values for Baseline, Mild, Moderate and Severe Case of Scoliosis

10.4.2 *Nkm*

The *Nkm* was found to increase when scoliosis was applied. This increase is because this criterion focuses solely on the upper neck which is subjected to increased loading due to the point loading introduced by the altered shape of spine. The neck, however, did not have scoliosis and so the head was not restricted in its motion. This increases the forces and moments in this region as the head and neck move freely about the normal global Y axis. The peak values for the baseline and each of the scoliosis models is given in table 10.3.

	Nkm	Increase Compared to Baseline
Baseline	1.14	
Mild Scoliosis	1.78	56
Moderate Scoliosis	1.76	54
Severe Scoliosis	1.85	63

Table 10.3: *Nkm* peak Values for Baseline, Mild, Moderate and Severe Case of Scoliosis

The altered injury levels predicted for the scoliotic occupants are therefore due to the interaction of the occupant and the wheelchair as well as the level of deformity.

The probability of injuries with symptoms lasting more than one month are also substantially increased for the scoliotic occupants. For both the *NIC* and *Nkm* criteria the increased values have an associated 100% probability risk of such injuries. This likelihood of injury is much increased compared to the baseline case [39].

10.5 More Vulnerable Occupants

In 2000, it was noted by Bertocci et al that commonly used injury criteria thresholds are typically based on values at which 25% of the general population would experience serious injury, but stated that "levels of risk associated with the use of able-body population based injury criteria may actually result in higher risk in the disabled population" [11]. This, combined with Temming's findings that gender, age, height and weight all influence the risk of injury [12], helped developed our hypothesis that a disability and associated postural deformities will also significantly influence injury likelihood. The increased spinal loading and predicted levels of injury found in the work presented here raise significant safety issues for scoliotic wheelchair occupants.

For the scoliotic occupants the underlying disability of the occupant may also play a key role in injury. A scoliotic curve can result from osteoporosis [113] and therefore the vertebrae of the spine would be more vulnerable, when loaded, due to their lower strength.

Scoliosis is also strongly associated with Cerebral Palsy (CP) and often people with CP are wheelchair bound. Also associated with CP is a lack of skeletal growth and lower bone density [116], [117], which suggests that the vertebrae may be more likely to break under crash loading.

A lower bone density is also commonly associated with Duchenne Muscular Dystrophy (DMD) and 90% of these individuals also have scoliosis. Due to the progressive nature of this muscular degenerative disease, all end up in a wheelchair. This again would lead to the wheelchair occupant being more vulnerable if involved in a rear impact while in transit.

For people with DMD there is also a correlation of 4% loss in pulmonary function with every degree of scoliosis [119]. This, coupled with clinical observations, would suggest that a wheelchair occupant may be more vulnerable in a rear impact.

Deterioration of cardiopulmonary function is also associated with scoliosis caused by CP due to the degenerative nature and severe degree of curvature that is found. If subjected to a rear impact, these wheelchair users may also be more vulnerable than other scoliotic wheelchair occupants. This is because pain is often associated with this type of scoliosis and secondary osteoarthritis is often found in more severe cases. In more acute cases of CP, it has been found that the degree of scoliotic deformation is a reflection of the severity of total body involvement as the abnormal muscle tone that is associated with Cerebral Palsy is found in more areas of the body [120]. Research has also found that after spinal fusion surgery, the presence of a severe preoperative kyphosis adversely effected survival rates. This suggests that those with a greater level of scoliosis are at a greater risk than those with lower levels [121].

The evidence presented in this section indicates that scoliotic wheelchair occupants are more vulnerable if involved in a rear impact.

10.6 Cobb Angle

Cobb Angle is used to define the degree of curvature of the scoliotic spine. While the largest forces on the spine was found in the severe case, the Cobb angle did not correlate well with the forces on the spinal column. So that while there was a 30% increase in the degree of scoliosis from the mild to severe case, this did not correspond to an equivalent increase in the forces on the spine.

The risk of neck injury, calculated using the *NIC* and *Nkm* also did not display a relative increase in score with greater levels of scoliosis. In fact the *NIC* showed a non-linear relationship as the severe case of scoliosis had the lowest *NIC* score. This is due to the much increased deformity of the upper thoracic region which was detailed previously (Chapter 7).

The Cobb Angle is a measure of the deformation of the spine in a single plane (frontal) and therefore does not take into account the level of kyphosis or lordosis that is introduced by scoliosis. It is the altered shape of the spine in this sagittal plane which affects the movement of the spine in a rear impact as well as the interaction between it and the seatback that has the greatest influence on the results.

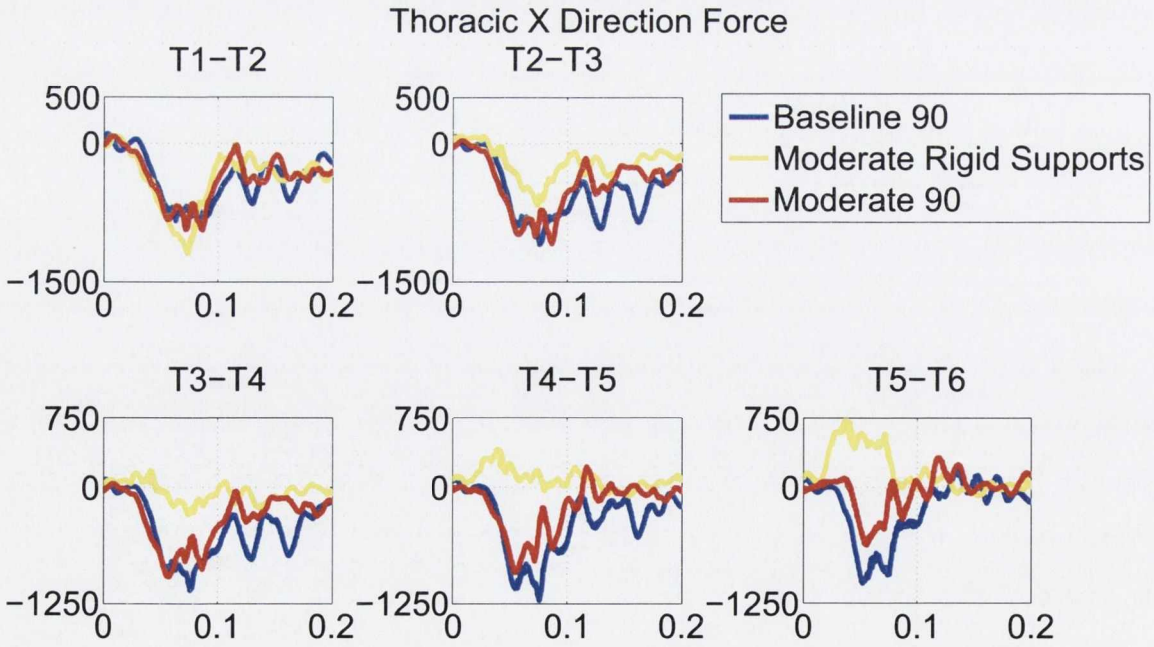
Therefore the degree of deformity as quantified using this method is not an accurate predictor of the level of risk to the occupant.

10.7 Clinical Implications

The results from the work in this thesis can be used to guide clinical practice in seating clinics such as at Enable Ireland. The findings support many practices that are conducted while also providing extra information about the consequences of different adaptations in a rear impact.

10.7.1 Occupant Positioning

The position of the occupant in the wheelchair was found to affect the resulting loads. The interaction of the occupant with the wheelchair was found to be altered depending on its initial position relative to the wheelchair structure. Significantly different results were found when the occupant was placed in the idealised 90-90-90 seated position and also when rigid postural supports were added. In both these cases the loading on the spine was reduced significantly for the occupants and in both cases the underlying reasons for such a reduction were the same - removal of point loading and restricting the movement of the spine. This is evident in the comparison of the loading on the thoracic spine for the baseline occupant seated at 90-90-90, the moderate case of scoliosis in the 90-90-90 seated position and with the moderate case of scoliosis seated in the wheelchair with rigid postural supports, see figure 10.5.



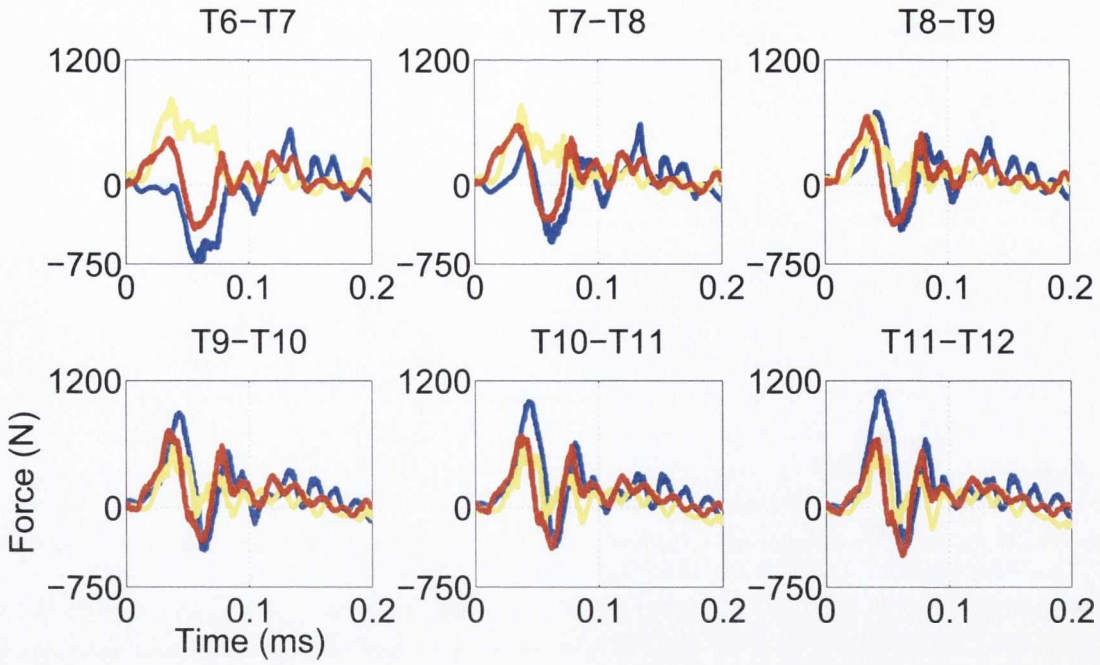


Figure 10.5: Time History of Forces in Thoracic Spine of Baseline at 90-90-90, Moderate Scoliosis Model with Rigid Supports and Moderate Scoliosis Model with at 90-90-90

The much reduced loading on the spine is clearly shown in these graphs. The baseline occupant seated at the 90-90-90 posture was found to have the lowest levels of loading for the baseline case. It can be seen that at some joints in the thoracic spine the values for the scoliosis cases are equivalent to, or in some cases are less than, those of the baseline. These joints, where the scoliosis models have the lowest force, represent the area of the baseline model in which it was not possible to have full contact between the occupant and the seatback due to the shape of the torso. This highlights the importance of having reduced gaps between the occupant and the wheelchair in all regions of the spine.

This is most clearly seen in the lumbar region as the forces are greatly reduced when the pelvis is positioned closer to the wheelchair such as for the 90-90-90 seated posture rather than the 26° position.

Therefore reducing the gaps between the occupant and the wheelchair reduces loading on the spine. The injury criteria are also reduced due to this close contact between occupant and the wheelchair as the torso, head and neck are no longer accelerated at an increased rate due to point loading.

10.7.2 Wheelchair Seating Surface

The occupant loading is greatly influenced by the addition or removal of a cushioned surface. When cushioning is added to the surfaces, this alters the response of the model. The time of the peak forces is delayed, as the cushioned surface delays contact with the stiffer surface

beneath. In some cases the peak forces are increased due to the cushion bottoming-out and subsequently the contacting force between the occupant and plywood backing is increased. This pattern of response was found when cushioning was added to the wheelchair surface and to postural supports.

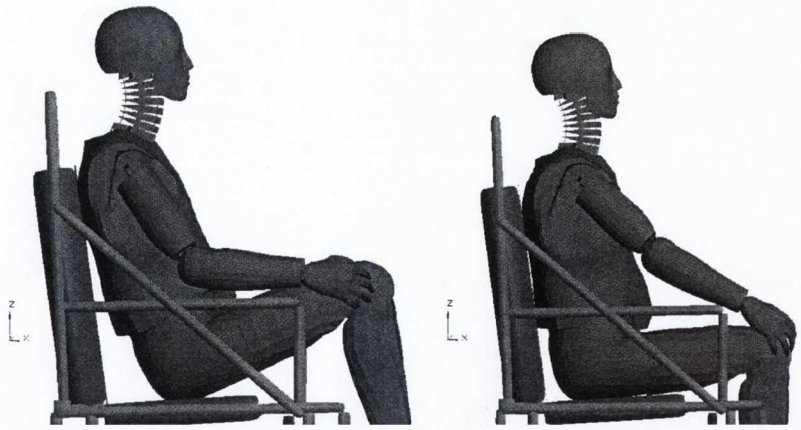
However, a stiffer contacting surface was found to be more beneficial and improved the level of protection offered to the occupant. Therefore the cushion that is added to the surface of the seatback plays a role in protecting the thoracic and lumbar spine. A more appropriate material, which could absorb more of the crash energy and not bottom out, would protect the occupant from the sharp increase in contact force with the plywood backing. A combination of layers of cushioning materials that control the motion of the occupant may be required, as simply increasing the thickness of the foam may not be practical. This layered material would also allow the other functions of the seating surface - comfort and pressure distribution - to be fulfilled while protecting the occupant in the case of a rear impact. The layered material would also aid frontal impact crash safety because the occupant rebounds into the seatback due to the action of the occupant restraints.

The material selection for such supports should also be evaluated as this may reduce the loading on the occupant if it can give sufficient support in normal loading conditions but can yield under the increased loading of a crash.

These types of adaptations to the wheelchair are commonly carried out in seating clinics and need to be investigated. The need for extra research into the viability of defining what is permissible in the "design and testing requirements for such after-market seating systems" [58] is supported by the findings here.

10.7.3 Seatback Height

The results from this section of the analysis found that the influence of seatback height was outweighed by the effect of the scoliosis of the occupant. However, for the baseline case the direction of the peak forces on the spine were seen to be influenced by the seated height of the occupant. The model seated at 26^o and at 90^o shows an altered seated height as shown in figure 10.6. The altered forces and position of switching from positive to negative values associated with this are seen in figure 10.7.



(a)Baseline at 26^o (b)Baseline at 90^o

Figure 10.6: Baseline Occupant Seated at Validated 26^o and 90^o Orientation

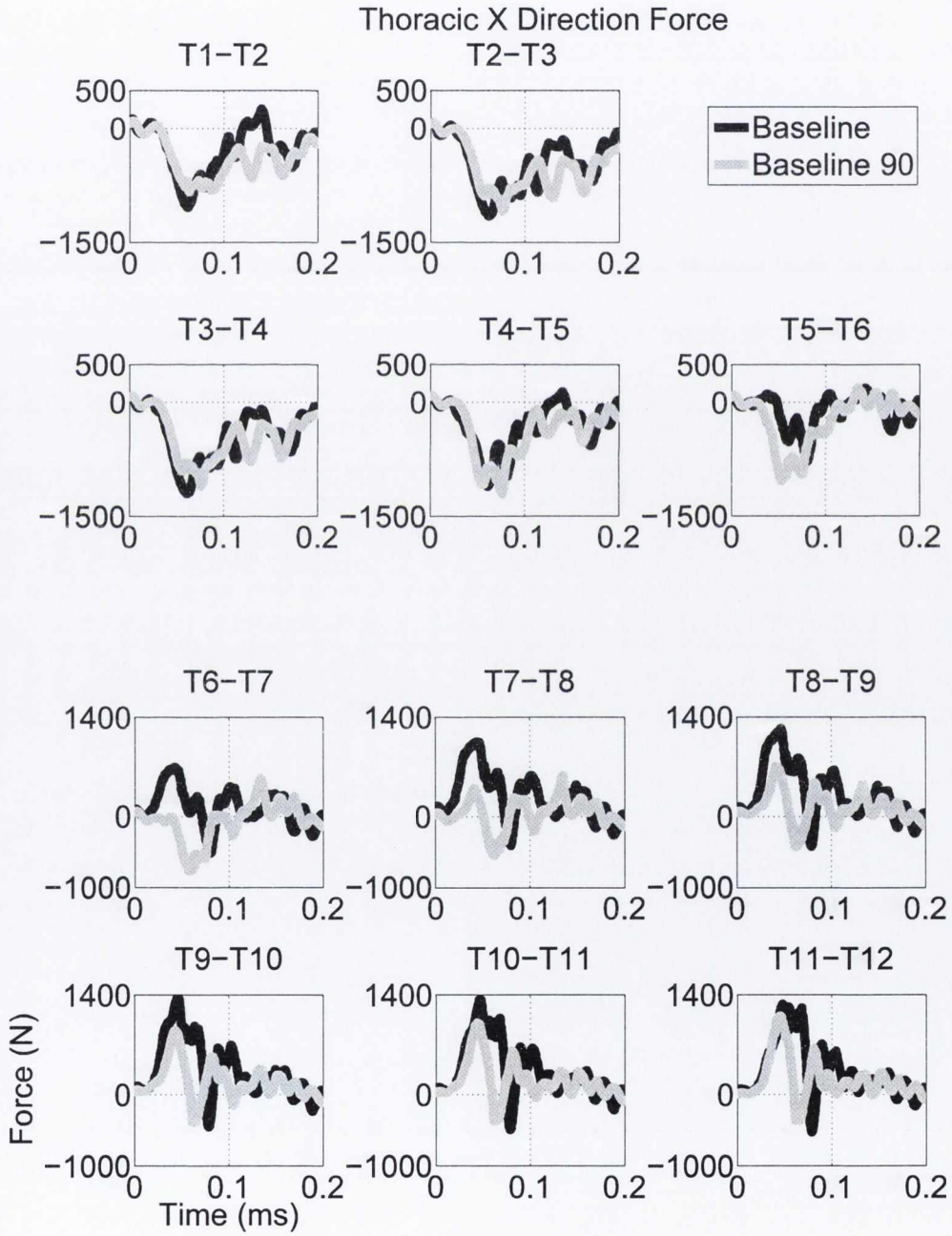


Figure 10.7: Forces in Thoracic Region of Spine for Baseline and Baseline in 90-90-90 Seated Posture

Therefore when there is no scoliosis in the spine a higher seatback provides more protection to the thoracic spine through anterior loading, which vertebrae are better able to withstand. However, there is an inherent trade-off with increased risk of neck injury as the increased surface area may increase the forward acceleration of the T1 vertebra. This could lead to an increased risk of injury that is predicted using the *NIC*. However, with the addition of an appropriate head restraint, this will also accelerate the head forward in conjunction with the torso and so reduce its relative rearward acceleration and keep the head and T1 in alignment which reduces the risk of injury.

Chapter 11

Conclusion

In this chapter the main conclusions are defined and the optimal protection for a wheelchair occupant is determined. Future work leading on from the results of this thesis is also presented.

11.1 Conclusion - Idealised Wheelchair and Occupant Interaction

Based on the work conducted, the idealised wheelchair and occupant set up, whether scoliosis is present or not, can be established. These fundamental principles can be applied to wheelchair users and incorporated into the guidelines for occupant positioning and wheelchair adaptation. For rear impact protection the important factors are:

- Straight upright spine with pelvis as far back in the seat as possible
- Close initial contact between the occupant and wheelchair over the entire torso
- Firm contacting surface

The application of these guidelines however may vary depending on the occupant. While the straight upright spine and rearwards position may be easily obtained for an occupant without a postural deformity this may not be possible for an occupant with an altered posture. This would prevent full contact between the occupant's torso and the seatback. The addition of postural supports or a moulded seat would therefore artificially create this interaction. In this situation the result is to remove the point loading due to the altered shape of the spine and to reduce the influence of the stiffness introduced by the movement of a scoliotic spine. The stiffness of the material used on the surface of these supports was found to improve the safety afforded to the occupant, with stiffer surfaces offering greater protection. However, stiffer surfaces have a negative effect on the comfort of the occupant

and could lead to other pressure related problems (pressure sores). Therefore, a balance needs to be struck for the optimised material on the seating surfaces.

The right combination of these measures would help improve the safety of a wheelchair occupant.

11.2 Future Work

The baseline numerical model created and validated in this work can be used to investigate the influence of alterations to other parameters of the occupant and/or the wheelchair. This model can be used to determine the influence of other disabilities that are found among wheelchair users. Different disabilities require different adaptations of the wheelchair. The influence of these alterations in a rear impact warrants further investigation using the computational model created as part of this work.

The scoliosis models created in this work have been altered only in terms of shape, as an idiopathic scoliosis was introduced. There is also often a change in muscle tone that is commonly found in wheelchair users with scoliosis due to Cerebral Palsy (CP) or Duchenne Muscular Dystrophy (DMD). The level of altered tone associated with CP varies greatly from person to person with increased stiffness or weakness or a combination of both [122], [123]. Research to date has focused on the causes of this altered tone with no corresponding research into the levels found. However, the model can be easily updated to reflect altered stiffness levels, if known.

The effect of an altered muscle tone in a rear impact is unknown. It is known that the active response of muscles would be too slow to have an effect on the outcome, as it is estimated that a response would take 200ms. This would be after the injury has occurred [26]. However, sled testing of occupants who were aware of an impending crash found that the precontracted neck musculature acted as a bracing system in a rear impact [124]. For an occupant with an increased muscle tone, the same bracing mechanism may be found and could be assessed using the model produced in this work.

The effect of having an amputee occupant in a wheelchair may also produce some interesting results as the centre of gravity of the occupant is greatly altered in such cases.

The adaptations that are conducted in seating clinics and the influence of each of these can be determined using the numerical model created for this study. Among these adaptations are seat and seatback tilt, seat length as well as footrest height and tilt.

11.3 Concluding Statements

The work conducted here fulfilled the aims and objectives that were established at the outset. These were:

- To create and validate a baseline computational model of a rear impact sled test of a wheelchair and occupant. This model can then be used as an analysis tool to investigate the effect of alterations to the model.
- To create and investigate more realistic representations of wheelchair occupants by implementing scoliosis in the computational model.
- To investigate the influence that postural supports have in a rear impact.
- To determine occupant loading levels and predict the likelihood of injury for the baseline and altered models.

Each of these lead to the central hypothesis that alterations to the baseline wheelchair and occupant model have a significant effect on occupant loading in a rear impact. This hypothesis was assessed by comparing the results of the altered models to those of the baseline case. The differences between these models had to be greater than the discrepancy of the model (identified during the validation process) to be considered significant. The 50^{th} percentile occupant model was adapted by introducing scoliosis and the effect of the position of the occupant within the wheelchair was also investigated. The surrogate wheelchair was adapted by adding cushioning, postural supports and altering the height of the seatback. The results from these investigations corroborated the hypothesis that alterations to the baseline occupant and wheelchair models have a significant effect on the results. The trends of the results and the underlying causes in each case was also determined.

11.3.1 Recommendations for future standards

This research combines the many complex issues of wheelchair user seating and transport using automotive crash research methods. These methods form the basis to provide information and guidelines to improve occupant safety.

This work coupled with that investigating the performance of commercial wheelchairs [23] [50] [60] highlights the lack of data and information in rear impact crash protection. The work presented in this thesis focuses on the loading experienced by the occupant and this, combined with the design requirements that will be developed from the work

of Manaray et al and Salipur et al, can lead to improved safety for all wheelchair occupants. The recommendations from this work for future safety standards are:

- To explicitly address rear impact safety in the standards.
- To include cut off values for injury criteria in any rear impact standard that is developed, as the current approach of providing excursion limits is not applicable in a rear impact.
- To give special consideration to postural supports, as this work highlights that their true effect may be to improve the safety of the occupant

Consequently, this information can then be used to develop ISO standards on rear impact protection. This will improve rear impact safety and will ultimately help to increase the level of protection afforded a wheelchair seated occupant to that of a vehicle seated occupant.

Bibliography

[1] J.Tiernan Senior Clinical Engineer. Enable ireland. *Personal Communication*, 2006.

[2] ISO 10542 Technical systems and aids for disabled or handicapped persons – Wheelchair tiedown and occupant-restraint systems , 2001.

[3] ISO 7176-19 Wheelchairs – Part 19: Wheeled mobility devices for use in motor vehicles , 2001.

[4] Wheelchairs Volume 1 Section 19 - Wheelchairs used as seats in motor vehicles, 1998.

[5] SAE J2249 Wheelchair tiedown and occupant restraint systems for use in motor vehicles, 1999.

[6] P. Karg and S. Sprigle. Development of test methodologies for determining the safety of wheelchair headrest systems during vehicle transport. *Journal of Rehabilitation Research and Development*, 33(3):290–304, 1996.

[7] Viano. *Role of the Seat in Rear Crash Safety.* SAE International, 2002.

[8] L. van Roosmalen, G. E. Bertocci, D. A. Hobson, and P. Karg. Preliminary evaluation of wheelchair occupant restraint system usage in motor vehicles. *Journal of Rehabilitation Research and Development*, 39(1):83–93, 2002.

[9] Federal motor vehicle safety standards 202: Head restraints.

[10] Federal motor vehicle safety standards 208: Occupant crash protection.

[11] G. E. Bertocci, D. A. Hobson, and K. H. Digges. Development of a wheelchair occupant injury risk assessment method and its application in the investigation of wheelchair securement point influence on frontal crash safety. *IEEE Transactions on Rehabilitation Engineering*, 8(1):126–39, 2000.

[12] J Temming and R Zobel. Frequency and risk of cervical spine distortion injuries in passenger car accidents: significance of human factors data. In *IRCOBI* , pages 219–233, Goteborg, Sweeden, 1998.

[13] National Highway Traffic Safety Administration. Buckle Up America, 1997.

[14] M. Huang. *Vehicle crash mechanics.* Society of Automotive Engineers ; American Technical, Warrendale, Pa. Hitchin, 2002. Matthew Huang. ill. ; 27cm.

[15] O. Bostrom, M.Y. Svensson, B Aldman, H.A. Hansson, Y Haland, P Lovsund, T Seeman, A Suneson, A Saljo, and T Ortengren. A new neck injury criterion candidate based on injury findings in the cervical spinal ganglia after experimental neck extension trauma. In *IRCOBI*, 1996.

[16] J Davidsson, M.Y. Svensson, A. Flogard, Y Haland, L. Jakobsson, A. Linder, P Lovsund, and K. Wiklund. BioRID I - A new biofidelic rear impact dummy. In *IRCOBI*, pages 377 – 390, Goteborg, 1998.

[17] L. Jakobsson, T. Bergman, and L. Johansson. Identifying thoracic and lumbar spinal injuries in car accidents. In *IRCOBI*, pages 61–71, Madrid, Spain, 2006.

[18] http://www.carsp.ca, 2006.

[19] J Davidsson, P Lovsund, K. Ono, M.Y. Svensson, and S. Inami. A comparison between volunteer, BioRID P3 and Hybrid III performance in rear impacts. In *IRCOBI*, pages 165–178, Stiges, Spain, 1999.

[20] M. Yaguchi, K. Ono, M. Kubota, and F. Matsuoka. Biofidelic responses to rear impact of the head/neck/torso among human volunteers, PMHS and dummies, 2006.

[21] *MADYMO Instruction Manuals.*

[22] D. Ha, G. Bertocci, and R. Jategaonkar. Development and validation of a frontal impact 6-year-old occupant and wheelchair computer model. *Assistive Technology*, 19(4):223–38, 2007.

[23] Z. Salipur and G. Bertocci. Development and validation of rear impact computer simulation model of an adult manual transit wheelchair with a seated occupant. In *RESNA*, 2008.

[24] R. Dsouza and G. Bertocci. Development and validation of a computer crash simulation model of an occupied adult manual wheelchiar subjected to a frontal impact. In *RESNA*, 2008.

[25] M. Van Loocke, C. G. Lyons, and C. K. Simms. Viscoelastic properties of passive skeletal muscle in compression: stress-relaxation behaviour and constitutive modelling. *Journal of Biomechanics*, 41(7):1555–66.

[26] M Panjabi, J Cholewicki, K Nibu, J Grauer, L Babat, and J Dvorak. Mechanism of whiplash injury. *Clinical Biomechanics*, 13:239–249, 1998.

[27] K. U. Schmitt, M.H. Muser, and P. Niederer. A new neck injury criterion candidate for rear-end collisions taking into account shear forces and bending moments. In *Enhanced Safety of Vehicles*, Amsterdam, 2001.

[28] K. Ono, S. Inami, K. Kaneoka, T. Gotou, Y. Kisanuki, S. Sakuma, and K. Miki. Relationship between localized spine deformation and cervical vertebral motions for low speed rear impacts using human volunteers. In *IRCOBI*, pages 149–164, Stiges, Spain, 1999.

[29] K. Kaneoka, K. Ono, S. Inami, and K. Hayashi. Motion analysis of cervical vertebrae during whiplash loading. *Spine*, 24(8):763–9; discussion 770.

[30] K. Ono and K. Kaneoka. Motion analysis of human cervical vertebrae during low-speed rear impacts by the simulated sled. *Journal of Crash Prevention and Injury Control*, 1(2):87–99, 1998.

[31] M.Y. Svensson, B Aldman, H.A. Hansson, P Lovsund, T Seeman, A Suneson, and T Ortengren. Pressure Effects in the Spinal Canal during Whiplash Extension Motion: A Possible Cause of Injury to the Cervical Spinal Ganglia. In *IRCOBI*, Eindhoven, Netherlands, 1993.

[32] J Davidsson, C. Deutscher, H. Wolfram, P Lovsund, and M.Y. Svensson. Human volunteer kinematics in rear end sled collisions. *Traffic Injury Prevention*, 2(4):319–333, 2001.

[33] I. Macnab. Acceleration injuries of the cervical spine. *Journal of Bone and Joint Surgery American Edition*, 46:1797–9, 1964.

[34] B. Squires, M. F. Gargan, and G. C. Bannister. Soft-tissue injuries of the cervical spine. 15-year follow-up. *Journal of Bone and Joint Surgery British Edition*, 78(6):955–7.

[35] S.I. Fuhrman, P. Karg, and G. Bertocci. Effect of wheelchair headrest use during rear impact on pediatric head and neck injury risk outcomes. 2007.

[36] A Eichberger, H Steffan, B Geigl, M. Y. Svensson, O. Bostrom, P Leinzinger, and M Darok. Evaluation of the Applicability of the Neck Injury Criterion (NIC) in Rear End Impacts on the Basis of Human Subject Tests. In *IRCOBI*, Goteborg, Sweeden, 1998.

[37] A. King. 'Fundamentals of impact biomechanics: Part 1 - Biomechanics of the head, Neck and Thorax.

[38] K. U. Schmitt and M.H. Muser. How to calculate the Nkm. Technical report, 2003.

[39] A. Kullgren, L. Eriksson, O. Bostrom, and M. Krafft. Validation of neck injury criteria using reconstructed real-life rear-end crashes with recorded crash pulses. In *Experimental Safety Vehicles*, Japan, 2003.

[40] A Eichberger, M Darok, H Steffan, P Leinzinger, O. Bostrom, and M.Y. Svensson. Pressure measurements in the spinal canal of post-mortem human subjects during rear-end impact and correlation of results to the neck injury criterion. *Accident Analysis and Prevention*, 32:251–260, 2000.

[41] M. Kleinberger, E. Sun, R. Eppinger, S. Kuppa, and R. Saul. Development of improved injury criteria for the assessment of advanced automotive restraint systems, 1998.

[42] J Davidsson. BioRID II final report. Technical report, Crash Safety Division, Department of Machine and Vehicle Design, Chalmers University of Technology, 1999.

[43] L. VanRoosmalen, G. E. Bertocci, D. Ha, and P. Karg. Wheelchair integrated occupant restraints: feasibility in frontal impact. *Medical Engineering and Physics*, 23(10):687–98, 2001.

[44] G. E. Bertocci and J. Evans. Injury risk assessment of wheelchair occupant restraint systems in a frontal crash: a case for integrated restraints. *Journal of Rehabilitation Research and Development*, 37(5):573–89, 2000.

[45] The Victorian Harness Safety Industry Working Group. Promoting airway safety when prescribing harness for wheelchairs and other seating devices. Technical report.

[46] G. E. Bertocci, D. A. Hobson, and K. H. Digges. Development of transportable wheelchair design criteria using computer crash simulation. *IEEE Transactions on Rehabilitation Engineering*, 4(3):171–81, 1996.

[47] G. E. Bertocci, S. Szobota, D. A. Hobson, and K. Digges. Computer simulation and sled test validation of a powerbase wheelchair and occupant subjected to frontal crash conditions. *IEEE Transactions on Rehabilitation Engineering*, 7(2):234–44, 1999.

[48] W. Kang and W. D. Pilkey. Crash simulations of wheelchair-occupant systems in transport. *Journal of Rehabilitation Research and Development*, 35(1):73–84, 1998.

[49] G. Bertocci, A. L. Souza, and S. Szobota. The effects of wheelchair-seating stiffness and energy absorption on occupant frontal impact kinematics and submarining risk using computer simulation. *Journal of Rehabilitation Research and Development*, 40(2):125–30, 2003.

[50] M. Manary, B. Bezaire, G. Bertocci, S Zdravko, and L. Schneider. Crashworthiness of forward-facing wheelchairs under rear impact conditions. 2007.

[51] D. Ha and G. Bertocci. Injury risk of a 6-year-old wheelchair-seated occupant in a frontal motor vehicle impact–'ANSI/RESNA WC-19' sled testing analysis. *Medical Engineering and Physics*, 29(7):729–38, 2007.

[52] D. Ha, G. Bertocci, E. Deemer, L. van Roosmalen, and P. Karg. Evaluation of wheelchair back support crashworthiness: combination wheelchair back support surfaces and attachment hardware. *Journal of Rehabilitation Research and Development*, 37(5):555–63, 2000.

[53] G. Bertocci, D. Ha, E. Deemer, and P. Karg. Evaluation of wheelchair seating system crashworthiness: "drop hook"-type seat attachment hardware. *Archives of Physics and Medical Rehabilitation*, 82(4):534–40, 2001.

[54] G. Bertocci, D. Ha, L. van Roosmalen, P. Karg, and E. Deemer. Evaluation of wheelchair drop seat crashworthiness. *Medical Engineering and Physics*, 23(4):249–57, 2001.

[55] L. van Roosmalen, G. Bertocci, D. R. Ha, P. Karg, and S. Szobota. Proposed test method for and evaluation of wheelchair seating system (WCSS) crashworthiness. *Journal of Rehabilitation Research and Development*, 37(5):543–53, 2000.

[56] D. Ha, G. Bertocci, P. Karg, and E. Deemer. Evaluation of wheelchair sling seat and sling back crashworthiness. *Medical Engineering and Physics*, 24(6):441–8, 2002.

[57] M. Manary and L. Schneider. Wheelchair seatback loads and deflections in rear impacts. In *RESNA Annual Conference*, Orlando, Florida, 2004.

[58] G. E. Bertocci, S. Szobota, D. R. Ha, and L. van Roosmalen. Development of frontal impact crashworthy wheelchair seating design criteria using computer simulation. *Journal of Rehabilitation Research and Development*, 37(5):565–72, 2000.

[59] S.I. Fuhrman, P. Karg, and G. Bertocci. Characterization of pediatric wheelchair kinematics and wtors loading during rear impact. In *RESNA*, Atlanta, Georgia, 2006.

[60] Z. Salipur, G. Bertocci, M. Manary, and N. Ritchie. Wheelchair tiedown and occupant restraint system associated with an adult manual ansi wc19 transit wheelchair with a seated 50th percentile atd exposed to a rear impact. 2007.

[61] A. R. Senin, L. M. Saez, and T. V. Corral. Experimental evaluation of the wheelchair occupant protection under different impact conditions using commercial wheelchairs. *International Journal of Crashworthiness*, 11(5):425–441, 2006.

[62] C. Simms, B. Madden, J. Tiernan, and D. FitzPatrick. Development of a wheelchair headrest for rear impact protection. In *IRCOBI*, pages 425–428, Bern, Switzerland, 2008.

[63] Richard L. Drake, Wayne Vogl, Adam W. M. Mitchell, and Henry Gray. *Gray's anatomy for students.* Elsevier/Churchill Livingstone, Philadelphia ; London, 2005.

[64] I. A. Stokes, L. C. Bigalow, and M. S. Moreland. Three-dimensional spinal curvature in idiopathic scoliosis. *Journal of Orthopedic Research*, 5(1):102–13.

[65] David S. Bradford. *Moe's textbook of scoliosis and other spinal deformities.* W.B. Saunders, Philadelphia ; London, 2nd. edition, 1987.

[66] J. I. P. James. *Scoliosis.* Livingstone, Edinburgh ; London, 1967.

[67] A. Fast, J Sosner, P.C. Begeman, MA Thomas, and T Chiu. Lumbar spinal strains associated with whiplash injury. *American Journal of Physical Medicine and Rehabilitation*, 81(9):645–650, 2002.

[68] H. S. Lin, Y. K. Liu, and K. H. Adams. Mechanical response of the lumbar intervertebral joint under physiological (complex) loading. *Journal of Bone and Joint Surgery American Edition*, 60(1):41–55, 1978.

[69] K. Singer, S. Edmondston, R. Day, P. Breidahl, and R. Price. Prediction of thoracic and lumbar vertebral body compressive strength: Correlations with bone mineral density and vertebral region. *Bone*, 17(2):167–174, 1995.

[70] F Pintar, N Yoganandan, L. Voo, J Cusick, D. Maiman, and A Sances. Dynamic characteristics of the human cervical spine. Technical report, Society of Automotive Engineers, 1995.

[71] A. Baranto, L. Ekstrom, M. Hellstrom, O. Lundin, S. Holm, and L. Sward. Fracture patterns of the adolescent porcine spine: an experimental loading study in bending-compression. *Spine*, 30(1):75–82.

[72] W. W. Lu, K. D. Luk, A. D. Holmes, K. M. Cheung, and J. C. Leong. Pure shear properties of lumbar spinal joints and the effect of tissue sectioning on load sharing. *Spine*, 30(8):E204–9, 2005.

[73] H. Frei, T. R. Oxland, and L. P. Nolte. Thoracolumbar spine mechanics contrasted under compression and shear loading. *Journal of Orthopedic Research*, 20(6):1333–8, 2002.

[74] K. L. Markolf. Deformation of the thoracolumbar intervertebral joints in response to external loads: a biomechanical study using autopsy material. *Journal of Bone and Joint Surgery American Edition*, 54(3):511–33, 1972.

[75] J. H. van Dieen, A. van der Veen, B. J. van Royen, and I. Kingma. Fatigue failure in shear loading of porcine lumbar spine segments. *Spine*, 31(15):E494–8.

[76] V. R. Yingling and S. M. McGill. Anterior shear of spinal motion segments. kinematics, kinetics, and resultant injuries observed in a porcine model. *Spine*, 24(18):1882–9, 1999.

[77] P.C. Begeman, H. Visarius, L.P. Nolte, and P. Prasad. Visocelastic shear responses of the cadaver and Hybrid III lumbar spine. Technical report.

[78] B. M. Cyron, W. C. Hutton, and J. D. Troup. Spondylolytic fractures. *Journal of Bone and Joint Surgery British Editiion*, 58-B(4):462–6, 1976.

[79] 3rd White, A. A. Kinematics of the normal spine as related to scoliosis. *Journal of Biomechanics*, 4(5):405–11, 1971.

[80] A. G. Veldhuizen and P. J. Scholten. Kinematics of the scoliotic spine as related to the normal spine. *Spine*, 12(9):852–8, 1987.

[81] Harry N. Herkowitz, Richard H. Rothman, and Frederick A. Simeone. *The Spine*. W.B. Saunders, Philadelphia, Pa ; London, 3rd ed, editorial board: Harry N. Herkowitz edition, 1992.

[82] Bernard Sarai Epstein. *The spine: a radiological text and atlas.* Lea and Febiger ; Distributed by Kimpton, Philadelphia London, 4th edition, 1976.

[83] R. F. Closkey and A. B. Schultz. Rib cage deformities in scoliosis: spine morphology, rib cage stiffness, and tomography imaging. *Journal of Orthopedic Research*, 11(5):730–7.

[84] C. J. Adam, G. N. Askin, and M. J. Pearcy. Gravity-induced torque and intravertebral rotation in idiopathic scoliosis. *Spine*, 33(2):E30–7.

[85] http://www.rad.washington.edu/mskbook/scoliosis.html.

[86] L. M. Stern and B. E. Clark. Investigation of scoliosis in Duchenne dystrophy using computerized tomography. *Muscle and Nerve*, 11(7):775–83, 1988.

[87] J. Jeppesen, A. Green, B.F. Steffensen, and J. Rahbek. The Duchenne muscular dystrophy population in Denmark, 1977-2001: prevalence, incidence and survival in relation to the introduction of ventilator use. *Neuromuscular Disorders*, 13:804–812, 2003.

[88] S. Winter, A. Autry, C. Boyle, and M. Yeargin-Allsopp. Trends in the prevalence of cerebral palsy in a population-based study. *Pediatrics*, 110(6):1220–1225, 2002.

[89] G. A. Balmer and G. D. MacEwen. The incidence and treatment of scoliosis in cerebral palsy. *Journal of Bone and Joint Surgery*, 52(1):134–7, 1970.

[90] B. Heidari, D. FitzPatrick, K. Synnott, and D. McCormack. Modelling of annulus fibrosus imbalance as an aetiological factor in adolescent idiopathic scoliosis. *Clinical Biomechanics*, 19(3):217–24, 2004.

[91] B. Heidari, D. Fitzpatrick, D. McCormack, and K. Synnott. Correlation of an induced rotation model with the clinical categorisation of scoliotic deformity–a possible platform for prediction of scoliosis progression. *Stud Health Technology Information*, 123:169–75, 2006.

[92] I. A. Stokes and M. Gardner-Morse. Analysis of the interaction between vertebral lateral deviation and axial rotation in scoliosis. *Journal of Biomechanics*, 24(8):753–9, 1991.

[93] A. M. Huynh, C. E. Aubin, T. Rajwani, K. M. Bagnall, and I. Villemure. Pedicle growth asymmetry as a cause of adolescent idiopathic scoliosis: a biomechanical study. *European Spine Journal*, 16(4):523–9.

[94] I. A. Stokes, H. Spence, D. D. Aronsson, and N. Kilmer. Mechanical modulation of vertebral body growth. implications for scoliosis progression. *Spine*, 21(10):1162–7.

[95] I. A. Stokes. Axial rotation component of thoracic scoliosis. *Journal of Orthopedic Research*, 7(5):702–8.

[96] I. A. Stokes, J. G. Armstrong, and M. S. Moreland. Spinal deformity and back surface asymmetry in idiopathic scoliosis. *Journal of Orthopedic Research*, 6(1):129–37.

[97] V. Deviren, S. Berven, F. Kleinstueck, J. Antinnes, J. A. Smith, and S. S. Hu. Predictors of flexibility and pain patterns in thoracolumbar and lumbar idiopathic scoliosis. *Spine*, 27(21).

[98] D.A. Entrekin. On the geometric characterization of the lenke classification scheme for idiopathic scoliosis, 2004.

[99] http://www.aafp.org/afp/20020501/1817.html.

[100] G. Bertocci, M. Manary, and D. Ha. Wheelchairs used as motor vehicle seats: seat loading in frontal impact sled testing. *Medical Engineering and Physics*, 23(10):679–85, 2001.

[101] G. Bertocci, K. Digges, and D. Hobson. Shoulder belt anchor location influences on wheelchair occupant crash protection. *Journal of Rehabilitation Research and Development*, 33(3):279–89, 1996.

[102] IIWPG Protocol for the Dynamic Testing of Motor Vehicle Seats for Neck Injury Prevention, 2005.

[103] M. M. Verver, R. de Lange, J. van Hoof, and J. S. Wismans. Aspects of seat modelling for seating comfort analysis. *Applied Ergonomics*, 36(1):33–42, 2005.

[104] T. Deter. Validation of a seat-dummy simulation model for rear impact. Technical report, German Insurance Association - Accident Research.

[105] V. Cormarkovic and A. Hasler. Effect of head restraint system on risk for whiplash injury in low speed rear impact and correlation of BioRID II test results using LS-DYNA/MADYMO coupling. In *IRCOBI*, Madrid, Spain, 2006.

[106] M. M. Panjabi, J. J. Crisco, A. Vasavada, T. Oda, J. Cholewicki, K. Nibu, and E. Shin. Mechanical properties of the human cervical spine as shown by three-dimensional load-displacement curves. *Spine*, 26(24):2692–700.

[107] M. M. Panjabi, T. R. Oxland, I. Yamamoto, and J. J. Crisco. Mechanical behavior of the human lumbar and lumbosacral spine as shown by three-dimensional load-displacement curves. *Journal of Bone and Joint Surgery American Edition*, 76(3):413–24.

[108] P.C. Begeman, H. Visarius, L.P. Nolte, and P. Prasad. Viscoelastic Shear Responses of the Cadaver and Hybrid III Lumbar Spine. In *Stapp Car Crash Conference*, Fort Lauderdale, FLorida, USA, 1994. Society of Automotive Engineers.

[109] M. M. Panjabi, Jr. Brand, R. A., and 3rd White, A. A. Mechanical properties of the human thoracic spine as shown by three-dimensional load-displacement curves. *Journal of Bone and Joint Surgery American Edition*, 58(5).

[110] T.J. Normoyle. *Development of a multi-body model of an anti-whiplash wheelchair headrest to represent an experimental crash test procedure under development.* Masters, Trinity College, 2006.

[111] C. Strother and M. James. Evaluation of seatback strength and seatbelt effectiveness and rear end impact. In *Society of Automotive Engineers Conference*, pages 225–243, 1987.

[112] S. Parkin, M. Mackay, AM. Hassan, and R. Graham. Rear end collisions and seat performance - to yield or not to yield. In *AAAM*, pages 231–244, 1995.

[113] M. Aebi. The adult scoliosis. *European Spine Journal*, 14(10):925–48, 2005.

[114] N. Kita. Ultrastructural studies of articular cartilaginous degeneration in the facet joints in spinal scoliosis. *Nippon Seikeigeka Gakkai Zasshi*, 68(4):184–95, 1994.

[115] Y. Petit, J. Dansereau, H. Labelle, and J. A. de Guise. Estimation of 3D location and orientation of human vertebral facet joints from standing digital radiographs. *Medical and biological engineering and computing*, 36(4):389–94, 1998.

[116] D. Y. Ihkkan and E. Yalcin. Changes in skeletal maturation and mineralization in children with cerebral palsy and evaluation of related factors. *Journal of Child Neurology*, 16(6):425–30, 2001.

[117] R. C. Henderson, S. R. Gilbert, M. E. Clement, A. Abbas, G. Worley, and R. D. Stevenson. Altered skeletal maturation in moderate to severe cerebral palsy. *Developmental Medicine and Child Neurology*, 47(4):229–36, 2005.

[118] T. Thulbourne and R. Gillespie. The rib hump in idiopathic scoliosis. Measurement, analysis and response to treatment. *Journal of Bone and Joint Surgery*, 58(1):64–71, 1976.

[119] L. T. Kurz, S. J. Mubarak, P. Schultz, S. M. Park, and J. Leach. Correlation of scoliosis and pulmonary function in duchenne muscular dystrophy. *Journal of Pediatric Orthopedics*, 3(3):347–53, 1983.

[120] C. Bonnett, J. C. Brown, and T. Grow. Thoracolumbar scoliosis in cerebral palsy. Results of surgical treatment. *Journal of Bone and Joint Surgery*, 58(3):328–36, 1976.

[121] A. I. Tsirikos, W. N. Chang, K. W. Dabney, F. Miller, and J. Glutting. Life expectancy in pediatric patients with cerebral palsy and neuromuscular scoliosis who underwent spinal fusion. *Developmental medicine and child neurology*, 45(10):677–82, 2003.

[122] S Delp. What causes increased muscle stiffness in cerebral palsy. *Muscle and Nerve*, 27:131–132, 2003.

[123] G Elder, J. Kirk, G Stewart, K Cook, D Weir, A Marshall, and L Leahey. Contributing factors to muscle weakness in children with cerebral palsy. *Developmental medicine and child neurology*, 45:542–550, 2003.

[124] B Stemper, N Yoganandan, J Cusick, and F Pintar. Stabilizing effect of precontracted neck musculature in whiplash. *Spine*, 31(20):E733–č738, 2006.